

UNIVERSITY OF NOVA GORICA
GRADUATE SCHOOL

Nina MALI

**CHARACTERIZATION OF TRANSPORT PROCESSES IN
THE UNSATURATED ZONE OF A GRAVEL AQUIFER BY
NATURAL AND ARTIFICIAL TRACERS**

DISSERTATION

Nova Gorica, August 2006

Table of Contents

1	INTRODUCTION.....	1
2	THEORY	4
2.1	Occurrence and movement of groundwater.....	4
2.1.1	Forces acting on groundwater.....	4
2.2	Unsaturated flow system	5
2.2.1	Unsaturated flow.....	5
2.2.2	Hydrodynamic dispersion.....	7
2.2.3	Preferential flow.....	8
2.3	Isotope hydrology.....	8
2.3.1	Stable isotopes.....	9
2.4	Evolution of carbon in groundwater.....	11
2.4.1	Carbon-13 in the carbonate system.....	12
2.5	Lumped-parameter models.....	13
2.6	Tracing techniques.....	16
2.6.1	Tracers.....	17
2.6.2	Evaluation and interpretation of tracing tests.....	17
2.7	Hydrograph separation	20
3	SITE DESCRIPTION.....	22
3.1	Geographical description	22
3.2	Geological and hydrogeological description.....	22
3.3	Lysimeter location.....	24
3.4	Detailed site characterization.....	25
3.4.1	Lithology and petrography.....	25
3.4.2	Pedological investigations.....	26
3.4.3	Hydraulic properties.....	29
3.4.3.1	Methods for characterizing hydraulic properties.....	29
3.4.3.2	Site hydraulic properties.....	31
4	METHODOLOGY	33
4.1	Research plan	33
4.1.1	Experimental site characterization.....	33
4.1.2	Isotope and geochemical investigations.....	34
4.1.3	Tracing experiment.....	34
4.2	Experimental set-up.....	36
4.2.1	Lysimeter construction.....	36
4.2.2	Evaluation of experimental set-up.....	40
4.3	Sampling	40
4.4	Measurements	42
4.4.1	Field measurements.....	42
4.4.2	Stable isotope analysis.....	43
4.4.3	Chemical analyses.....	44
4.4.4	Tracers.....	44
4.4.5	Overview of chemical and isotope analyses.....	45
4.5	Chemical data presentation	45
4.5.1	Water typology determination.....	45
4.5.2	Statistics.....	46

5	RESULTS AND DISCUSSION	48
5.1	In- situ measurements.....	48
5.2	Geochemical characteristics of the unsaturated water.....	55
5.2.1	Geochemical processes in the unsaturated zone	60
5.3	Isotope composition results of the long term monitoring.....	61
5.3.1	Seasonal oscillation of $\delta^{18}\text{O}$ isotope composition.....	63
5.3.2	Depth profiles of $\delta^{18}\text{O}$ signal - groundwater dynamics based on $\delta^{18}\text{O}$ signal	65
5.3.3	Lumped parameter modelling	66
5.4	Combined uranine and deuterium tracing experiment.....	70
5.4.1	Results of deuterium tracing experiment	70
5.4.2	Results of uranine tracer	74
5.4.3	Comparison of deuterium and uranine tracer.....	76
5.4.4	Evaluation of tracing method (tracing experiment).....	77
5.5	Analyses of precipitation events	77
5.5.1	Snow melting 2004	77
5.5.2	Summer storm events.....	81
5.5.3	Preferential flows	82
5.6	Water dynamics in a coarse gravel unsaturated zone	83
6	CONCLUSIONS	85
6.1	Results summary	85
6.2	Research conclusions	88
7	REFERENCES.....	91

List of Tables

<i>Table 1: The stable environmental isotopes (Clark and Fritz, 2000)</i>	10
<i>Table 2: Review of tracing test terms (Kass, 1998)</i>	18
<i>Table 3: Site characterization methods</i>	25
<i>Table 4: Results of pedological analysis</i>	28
<i>Table 5: Hydraulic property parameters</i>	31
<i>Table 6: List of sampling and measuring points</i>	33
<i>Table 7: In-situ measurement instruments</i>	42
<i>Table 8: Analysed parameters with the measuring period</i>	45
<i>Table 9: Statistics of p_{CO_2} measurements</i>	50
<i>Table 10: Statistics of soil and unsaturated zone temperature measurements</i>	52
<i>Table 11: Statistics of pH, temperature and conductivity measurements</i>	54
<i>Table 12: Mean values of chemical analyses results</i>	55
<i>Table 13: Percentage of cations and anions</i>	57
<i>Table 14: Correlation coefficients of principal water components and conductivity</i>	58
<i>Table 15: Mean values of geochemical measurements in the period 2004-2005</i>	58
<i>Table 16: Correlations between conductivity, CO_2 and temperature</i>	61
<i>Table 17: Statistics of $\delta^{18}O$ and δ^2H isotope composition results of the monthly sampled water</i>	62
<i>Table 18: Mean values of $\delta^{18}O$ isotope composition by particular year</i>	64
<i>Table 19: Correlation coefficient of the precipitation</i>	67
<i>Table 20: Average percentage of infiltration used in input functions</i>	68
<i>Table 21: Mean values of MRT modelled by different models and compared with results of the tracing experiment (MRT is expressed in months)</i>	69
<i>Table 22: Average MRT and estimated flow velocities</i>	69
<i>Table 23: Calculated fastest, dominant and mean flow velocities of deuterium tracer</i>	73
<i>Table 24: Cumulative outflow water volume and recovery amount of deuterium tracer</i>	74
<i>Table 25: Calculated dominant, mean flow velocity and retardation factor of uranine</i>	76
<i>Table 26: $\delta^{18}O$ values of unsaturated water in time of snow melting</i>	78
<i>Table 27: $\delta^{18}O$ statistics of unsaturated water at the time of snow melting</i>	79
<i>Table 28: Water discharge in time of snow melting observation</i>	80
<i>Table 29: Matrix flow shares in discharge water</i>	80
<i>Table 30: Comparison of LPM and CDM modelling results</i>	83
<i>Table 31: Estimation of MRT of the water in the coarse gravel unsaturated zone in Selniška Dobrava</i>	84

List of Figures

<i>Figure 1: Subsurface distribution of water (How groundwater occurs, 2003).</i>	4
<i>Figure 2: Moisture retention curves (Unsaturated zone flow ..., 2001).</i>	6
<i>Figure 3: Characteristic curves for fine sand with wetting and drying cycles (Fitts, 2002).</i>	6
<i>Figure 4: The ratio of conductivity to saturated hydraulic conductivity, as a function of water (Fitts, 2002).</i>	7
<i>Figure 5: Example of oxygen isotope ^{18}O.</i>	8
<i>Figure 6: The meteoric relationship for ^{18}O and ^2H in precipitation (Clark and Fritz, 2000).</i>	10
<i>Figure 7: Ranges for ^{13}C values in selected natural compounds (Clark and Fritz, 2000).</i>	12
<i>Figure 8: Schematic of fractionation of ^{13}C during equilibrium exchange of carbon between CO_2, DIC and calcite at 25°C (Clark and Fritz, 2000).</i>	13
<i>Figure 9: Ideal concentration curve from a tracing test (Kass, 1998).</i>	18
<i>Figure 10: Storm hydrograph separation for a two-component system using $\delta^{18}\text{O}$ (Clark and Fritz, 2000).</i>	21
<i>Figure 11: Geological map (Mioč and Žnidarčič, 1976).</i>	23
<i>Figure 12: Hydrogeological map (Mali, 1996).</i>	24
<i>Figure 13: Study area – Location of the lysimeter Selniška Dobrava.</i>	25
<i>Figure 14: Unsaturated zone profile</i>	27
<i>Figure 15: Pedological profile</i>	28
<i>Figure 16: Set-up of double ring measurements</i>	30
<i>Figure 17: Coarse gravel at the Selniška Dobrava lysimeter location.</i>	32
<i>Figure 18: Research sampling plan</i>	35
<i>Figure 19: Lysimeter cross-section; Locations of sampling points from JV-1 to JV-10.</i>	36
<i>Figure 20: Lysimeter construction</i>	37
<i>Figure 21: Entrance and the inside of lysimeter</i>	37
<i>Figure 22: Sampling point set-up</i>	38
<i>Figure 23: Soil measurement system</i>	39
<i>Figure 24: CO_2 carbon ($\delta^{13}\text{C}$) sampling</i>	41
<i>Figure 25: Principal water types in D'Amore plots (D'Amore e tal., 1983)</i>	46
<i>Figure 26: Boxplot presentation</i>	46
<i>Figure 27: Moisture content by the time</i>	48
<i>Figure 28: Boxplot of p_{CO_2} measurements</i>	49
<i>Figure 29: Time plot of p_{CO_2} measurements</i>	49
<i>Figure 30: Profiles of p_{CO_2} measurements</i>	50
<i>Figure 31: Boxplot of soil and unsaturated zone temperature measurements</i>	51
<i>Figure 32: Profiles of soil and unsaturated zone temperature</i>	51
<i>Figure 33: Time plot of soil and unsaturated zone temperature measurements</i>	52
<i>Figure 34: Results of in-situ measurements of pH</i>	53
<i>Figure 35: Results of in-situ water temperature measurements</i>	53
<i>Figure 36: In-situ water conductivity and temperature measurement</i>	53

Figure 37: Results of in-situ conductivity measurements.....	55
Figure 38: Piper plot	56
Figure 39: D'Amore plot.....	56
Figure 40: Bar plots of principal cations and anions.....	57
Figure 41: Mean values of geochemical parameters in unsaturated zone	58
Figure 42: Profiles of mean values of geochemical measurements in the period 2004-2005 ...	59
Figure 43: Regressions among Ca^{2+} , HCO_3^- and conductivity.....	60
Figure 44: $\delta^{18}\text{O}$ isotope composition results of the monthly sampled water	61
Figure 45: $\delta^2\text{H}$ isotope composition results of the monthly sampled water.....	62
Figure 46: $\delta^{18}\text{O}$ isotope composition for JV-5	63
Figure 47: $\delta^{18}\text{O}$ isotope composition for the year 2002.....	64
Figure 48: Average values of $\delta^{18}\text{O}$ isotope composition of the monthly sampled water.....	65
Figure 49: The profile of $\delta^{18}\text{O}$ values by the depth at the typical seasons	66
Figure 50: Comparison of the $\delta^{18}\text{O}$ isotope composition of Selnica, Ljubljana and Klagenfurt precipitation with GMWL.....	67
Figure 51: $\delta^{18}\text{O}$ values of Ljubljana, Selniška Dobrava and Klagenfurt precipitation	68
Figure 52: Observed and fitted $\delta^{18}\text{O}$ output functions for sampling point JV-5 (model numbers present MRT in months)	69
Figure 53: Tracing experiment.....	70
Figure 54: Deuterium breakthrough curves and precipitations during the tracing experiment ..	71
Figure 55: Vertical reviews of $\delta^2\text{H}$ values of water in unsaturated zone	72
Figure 56: Best fit curves for deuterium concentrations by convection-dispersion model for all sampling points in lysimeter	73
Figure 57: Comparison of deuterium and uranine breakthrough curves.....	75
Figure 58: Maximum, minimum and mean day temperature for Maribor meteorological station .	78
Figure 59: $\delta^{18}\text{O}$ values at the time of snow melting.....	79
Figure 60: Discharge of the water in unsaturated zone in time of snow melting.....	80
Figure 61: Snow melting component.....	81
Figure 62: Thunderstorm precipitation	81
Figure 63: Diagrams of typical reaction of conductivity, precipitation amount and discharge on storm event.....	82

List of Annexes

- Annex A: Granulometric analyses of a coarse gravel in Selniška Dobrava*
- Annex B: Soil and unsaturated zone moisture, temperature and pCO₂ measurements*
- Annex C: Water conductivity, temperature and pH measurements*
- Annex D: Plots of water conductivity and temperature measurements*
- Annex E: Chemical analyses*
- Annex F: Stiff plots*
- Annex G: Diagrams of relations between conductivity and principal chemical components*
- Annex H: Geochemical measurements*
- Annex I: $\delta^2\text{H}$ and $\delta^{18}\text{O}$ isotope composition data in the monthly sampled water*
- Annex J: $\delta^{18}\text{O}$ isotope composition plots of the monthly sampled water*
- Annex K: Results of lumped parameter modelling*
- Annex L: Hydrograph separation*
- Annex M: Measurements of precipitations, conductivity and discharge for events in July and August 2005*

Abbreviations and Symbols

α_i	- infiltration coefficient
δ_{in}	- precipitation input function
θ	-volumetric water content
λ	- decay constant
ψ	- matric potential
A	- cross-section of flow
B	- empirical coefficient (800-1200 for pure and homogeneous sand and 400-800 for unhomogenous, loam sand) used in Hazen empirical equation
C	- tracer concentration
D	- dispersion coefficient
$d_{ef (10,20)}$	- effective grain size diameter (the contents of which in the sample is lower than 10, 20%)
$g(t)$	- weighting function
h	- hydraulic head
h_p	- pressure head
k	- hydraulic conductivity
M	- total mass of the injected tracer
P_D	- dispersion parameter $P_D = \frac{D}{v x}$
p	- fluid pressure, pore water pressure
Q	- discharge, flow rate
q	- flow rate
R	- rate of new and old water by hydrograph separation
R_d	- retardation factor
V	- volume rate
v	- fluid velocity
x	- distance between injection and observation point
z	- elevation above datum
CDM	- convection-dispersion model
DM	- dispersion model
EM	- exponential model
EPM	- exponential-piston-flow model
LM	- linear model
LP	- lumped parameter models
LPM	- linear-piston- flow model
MRT	- mean residence time
PFM	- piston flow model
SEC	- conductivity

1 INTRODUCTION

The interest of hydrogeological investigations in recent years has shifted from the problems of water supply to water quality issues. Contamination of aquifers is a growing and demanding problem. The vulnerability of an aquifer to pollution is directly linked to the hydraulic characteristics of its upper unsaturated and lower saturated zone. In situ characterization of the hydraulic properties of materials within the unsaturated zone has become increasingly important over the past several years. One of the major problems is how to fully characterize the unsaturated zone. The implementation of measurements in a high-permeable gravel unsaturated zone is quite difficult. Sometimes it is almost impossible to measure in-situ parameters which define unsaturated zone characteristics, and also pore water sampling is difficult.

Classical hydraulic methods to calculate seepage flow are based on the hydraulic functions. Mualem (1976) and Van Genuchten (1980) developed empirical relations to determine these hydraulic functions using basic parameters of soil and sediments. To solve these equations measurements of suction and water content under undisturbed conditions in the field are needed. In most conceptual models to simulate seepage, it is presumed that fluxes are homogeneous within small compartments and mostly vertical: both these boundary conditions can hardly be controlled by means of statistical evaluations of suction and water content measurements and therefore often remain theoretical. To reduce this, tracer methods (artificial as well as environmental tracers) are applied to support and improve hydraulic evaluations (Seiler and Zojer, 2001). Both methods, however, only develop optimal results in combination with numerical simulations and with an appropriate conceptual model, which may be deduced also from tracer experiments.

Models for flow and transport in the subsurface, especially in the unsaturated zone have been developing at a rapid pace since the late seventies of the 20th century. There are different ideas and personal views of what models are and what they are presumed to be. In general, it is assumed that such models are research tools, and that they can ultimately be scaled up to represent the significant features or reality (Maloszewski et al., 1982; 1985; 1996; Nutzman and Stichler, 2001; Schoen et al., 1999).

The water flow and solute transport in the unsaturated zone has been the topic of many investigations. Articles and surveys have pointed out the importance of preferential flow in the unsaturated zone (Schoen et al., 1999; Van der Hoven et al. 2002). Dye as a tracer is a useful tool for revealing spatial flow patterns, and has been used by soil scientists for years (Kung et al., 2000; Yasuda et al., 2001; Öhrström et al., 2004). The adsorption of the dye differs between soil types; soils with high clay content and low content of organic carbon tend to adsorb more dye than others (Ketelen and Meyer-Windel, 1999). Bromide has been used as a tracer to investigate the flow, solute transport processes and determine preferential flow in various experiments (Jabro et al., 1994; Fank and Berg, 2001). Measurements of salt tracer concentration have been widely used to determine transport parameters like velocity and dispersion (Wild and Babiker, 1976; Jury, 1982). Also natural isotopes like deuterium, tritium (T) and ^{18}O have been used to study water flow (Maciejewski et al., 2006; Maloszewski et al., 2006; Rank et al., 2001). Different tracers have also been combined in the same solution with for example, chloride and nitrate (Biggar and Nielsen, 1976), different fluorescent tracers (Aeby et al., 2001), bromide and deuterium (Nutzmann and Stichler, 2001; Schoen et al., 1999), and chloride, bromide, dye and colloidal tracer (Mortensen et al., 2004). Simultaneous application of the dye Brilliant Blue and bromide was conducted by Flury and Fluhler (1995). Environmental tracers (^3H , ^{85}Kr , ^{39}Ar , ^{14}C and stable noble gases) have been combined with chemical signatures to investigate the groundwater age distribution and mixing processes in the Fontainebleau sands aquifer (Corcho et al., 2004).

Several studies of solute transport in the unsaturated zone of fractured and karstified rocks have been performed in Slovenia. The uranine fluorescence and some selected geochemical parameters (discharge, pH, conductivity, carbonates, calcium, magnesium, chloride, nitrate, sulphate, and phosphate) were used to study the flux and non-reactive contamination transport through the unsaturated zone in Postonjska Jama (Kogovšek and Šebela, 2004). The flow and

solute transport in fractured and karstified rocks, above all in the unsaturated zone and its epikarstic zone, were investigated at experimental field site Sinji Vrh (Veselič and Čenčur-Curk, 2001, Veselič et al., 2001). The multitracer experiment of longer duration was conducted with the use of several tracers (uranine, NaCl, KCl, MnCl₂, CuSO₄·5H₂O, NiSO₄·6H₂O) to define the impact of rock structure on transport processes in the unsaturated zone. The long-term and short-term observation periods have been used. The hydraulic behaviour of the unsaturated zone in karst aquifer in the Hubelj spring catchment area has been studied also by using an indirect research method based on natural tracers (Trček et al., 2003). The results produced information on the aquifer recharge, storage and discharge processes, as well as on mechanisms that affected them.

Natural tracers and tracing experiments are important tools for studying the flow and the solute transport from the recharge area through the upper unsaturated zone and saturated to the outflow. Irrespective of many tracing studies in the unsaturated zone, according to the author's knowledge, high-permeable gravel unsaturated zone was not studied before.

The processes in coarse gravel unsaturated zone develop quite differently from those in aquifers with finer granulation. The aim of this study was to describe transport processes in a high-permeable coarse gravel unsaturated zone by means of isotope methods and a tracing experiment using a lysimeter in the Selniška Dobrava aquifer. The lysimeter was designed on the basis of previous hydrogeological investigations of the area where fast vertical and horizontal flow of groundwater had been reported. The aquifer of Selniška Dobrava, 20 km west from Maribor, has been investigated since 1993. Investigation results have confirmed that this aquifer is a suitable alternative water resource for the supply of Maribor and its surroundings (Mali and Janža, 2005). In few years the Selniška Dobrava gravel aquifer will become an important water resource. Its effective protection requires the knowledge of unsaturated zone properties, on the basis of which land use restrictions can be proposed. An evaluation of a coarse gravel aquifer's vulnerability with regard to the protective function of the unsaturated zone also requires a detailed knowledge of possible transport mechanisms through the aquifer.

The dissertation was formulated to investigate the characteristics, groundwater flow and transport in the unsaturated zone of a coarse gravel aquifer. Water flow and transport processes were estimated by experimental work in the lysimeter. The research was focused on the development and application of a successfully designed unsaturated zone monitoring network and lysimeter construction in a high-permeable aquifer. Special attention was given to the selection of monitoring equipment and its testing, and to the implementation of an in-situ measuring of some unsaturated zone characteristics. Beside flow and transport processes also geochemical processes were studied. It was established that carbon cycle plays an important role in unsaturated zone processes and one of the aims was the determination of these processes. Hydrogeological processes and solute transport in the unsaturated zone were evaluated by tracing and isotope techniques.

The presented study of processes in the coarse gravel unsaturated zone had the following objectives:

- construction and equipment of experimental field laboratory - lysimeter with improvement of field measurement methodology in a high-permeable gravel unsaturated zone
- investigation of flow and transport processes in coarse gravel unsaturated zone by isotope and tracing methods
- evaluation of experimental work by modelling to predict percolation, travelling times of groundwater flow in high-permeable unsaturated zone

The following parameters were measured to reach investigation objectives:

- in-situ measurements (water - temperature, conductivity, pH, water discharge; unsaturated zone - temperature, moisture and pCO₂)
- natural isotopes (water – deuterium, oxygen-18, carbon-13 DIC, carbon-13 – CO_{2(gas)})
- chemical composition – major ions (K⁺, Na⁺, Ca²⁺, Mg²⁺, HCO₃⁻, SO₄²⁻, Cl⁻)
- artificial tracers (deuterium, uranine)

The isotope and geochemical investigations are classified in two groups, long-term investigations and short-term investigations. Long-term investigations were performed to define characteristic behaviors of the unsaturated zone processes which can not be determined in one hydrological period or with a single sampling. Short-term investigations were used to precisely identify the reaction of the system of coarse gravel unsaturated zone to special events like snow melting and storm events. At that time of soil and gravel saturation, the preferential flow occurs.

To supplement the conclusion of isotope and geochemical investigations also a combined tracing experiment was performed using both deuterated water and uranine. Conservative tracers are necessary to obtain groundwater transport properties. Deuterated water is known as an effective tracer for this purpose (Becker and Coplen, 2001) due to its chemical stability, non-reactivity, ease of handling and sampling, and reasonable price. Compared to other groundwater tracers, deuterium shows the highest degree of conservativeness (Leis and Benischke, 2004). Fluorescent dyes react readily with subsurface materials, particularly in groundwaters of neutral and lower pH values, so their transport is often retarded with respect to water movement (Kasnavia et al., 1999). For this reason deuterium was chosen to study water movement; while uranine with its sorption capacity was used as an indicator of pollution movement through the unsaturated zone.

The research will contribute significantly to our knowledge about water flow and transport processes in a coarse gravel unsaturated zone. Lysimeter design and setting up of a monitoring system with measuring equipment in a coarse gravel unsaturated zone is the first such described experimental field and presents a base for other experimental research of processes in porous media unsaturated zone. The use of different methodologies (isotope modelling, tracing) enabled the evaluation of applicability of used tools to study transport processes in a coarse gravel unsaturated zone. The results of the flow and transport processes study in coarse gravel unsaturated zone could be used to determine measures for groundwater protection of water resources, such as Selniška Dobrava aquifer.

The research was carried out within the project Urban Hydrogeology – The impact of Infrastructures on Groundwater, financed by Ministry of Higher Education, Science and Technology of Republic Slovenia (project no. L-1-6670-0215). Research has been performed in cooperation with Institute of Water Resources Management, Hydrogeology and Geophysics, Joanneum Research Forschungsgesellschaft mbH from Graz (Austria).

2 THEORY

This chapter presents basic principles of groundwater movement in the unsaturated zone. In this research also isotope and tracing methods were used and they are summarized in short. Although isotope studies are part of tracing studies, they are described separately because in my research the isotope and tracing investigations are treated separately as well. The principles of lumped parameter modelling and evolution of carbon in groundwater are explained at the end.

2.1 Occurrence and movement of groundwater

The occurrence and movement of groundwater are related to physical forces acting in the subsurface and the geological environment in which they occur. Groundwater flow is part of a complex dynamic hydrological cycle. Saturated formations below the surface act as mediums for the transmission of groundwater, and as reservoirs for its storage.

An aquifer is a geological unit that can store and transmit water. Groundwater occurs in the subsurface in two broad zones: the unsaturated zone and the saturated zone (*Figure 1*). The unsaturated zone, also known as the vadose zone, consists of soil pores that are filled to a varying degree with air and water. The zone of saturation consists of water-filled pores that are assumed to be at hydrostatic pressure.

Unsaturated zone. The unsaturated zone serves as a large reservoir which, when recharged, typically discharges water to the saturated zone for a relatively long period after the cessation of surface input. The unsaturated zone commonly consists of three sub-zones: root zone, intermediate zone, and capillary fringe.

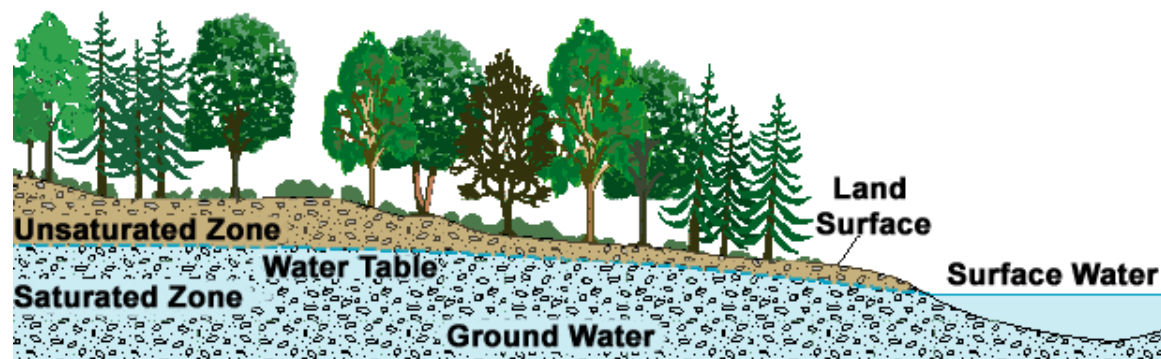


Figure 1: Subsurface distribution of water (How groundwater occurs, 2003).

Saturated zone. In the zone of saturation, all communicating voids are filled with water under hydrostatic pressure. Water in the saturated zone is known as groundwater or phreatic water.

A more detailed theory about groundwater movement can be found in Fitts (2002), Bear and Verruijt (1992), de Marsily (1986), How groundwater occurs (2003), etc.

2.1.1 Forces acting on groundwater

External forces which act on water in the subsurface include gravity, pressure from the atmosphere and overlying water, and molecular attraction between solids and water. In the saturated zone, groundwater flows through interconnected voids in response to the difference

in fluid pressure and elevation. The driving force is measured in terms of hydraulic head. Hydraulic head (or potentiometric head) is defined by Bernoulli's equation:

$$h = z + \frac{p}{\rho g} + \frac{v^2}{2g} \quad (1)$$

where

h - hydraulic head

z - elevation above datum

p - fluid pressure with constant density ρ

g - acceleration due to gravity

v - fluid velocity

Pressure head (or fluid pressure) h_p is defined as:

$$h_p = \frac{p}{\rho g} \quad (2)$$

By convention, pressure head is expressed in units above atmospheric pressure. In the unsaturated zone, water is held in tension and pressure head is smaller than atmospheric pressure ($h_p < 0$). Below the water table, in the saturated zone, pressure head is greater than atmospheric pressure ($h_p > 0$). Because groundwater velocities are usually very low, the velocity component of hydraulic head can be neglected. Thus, hydraulic head can usually be expressed as:

$$h = z + h_p \quad (3)$$

2.2 Unsaturated flow system

The theory of unsaturated flow system was summarized by Fitts (2002), Seiler and Zojer; Fank et. al. in Berg et al. (2001), Fetter (1993), Stephens (1996) and Unsaturated zone (2003), Unsaturated zone flow...(2001).

2.2.1 Unsaturated flow

The discussion of flow is usually focused on the saturated zone where there is only water in pore spaces. In the unsaturated zone water flows under the same physical principles that have been outlined for saturated flow. The concepts of hydraulic head and Darcy's law are generally the same as for saturated flow. The most important difference about the unsaturated zone flow is that the hydraulic conductivity k is not a material constant like it is in the saturated zone; it is variable, depending on the volumetric water content θ . The pore water pressure p also varies with θ . These differences make the analysis of unsaturated flow more complex than the analysis of saturated flow.

The most basic measure of the water in an unsaturated medium is water content or wetness (θ), defined as the volume of water per bulk volume of the medium. Water is held in an unsaturated medium by forces whose effect is expressed by pressure of the water. Various types of pressure may be relevant in unsaturated hydrology, but one called the matric pressure or matric potential. Matric potential (commonly symbolized Ψ) is the pressure of the water in a pore of the medium relative to the pressure of the air. When a medium is unsaturated, the water generally is at lower pressure than the air, so the matric potential is negative. Greater water content goes with greater matric potential. Zero matric potential is associated with high (saturated or nearly saturated) water content. As matric potential decreases the water content

decreases, but in a way that is nonlinear and hysteretic. The relation between matric potential and water content, called a retention curve (*Figure 2*), is a characteristic of a porous medium that depends on the nature of its pores. This relation strongly influences the movement of water and other substances in unsaturated media.

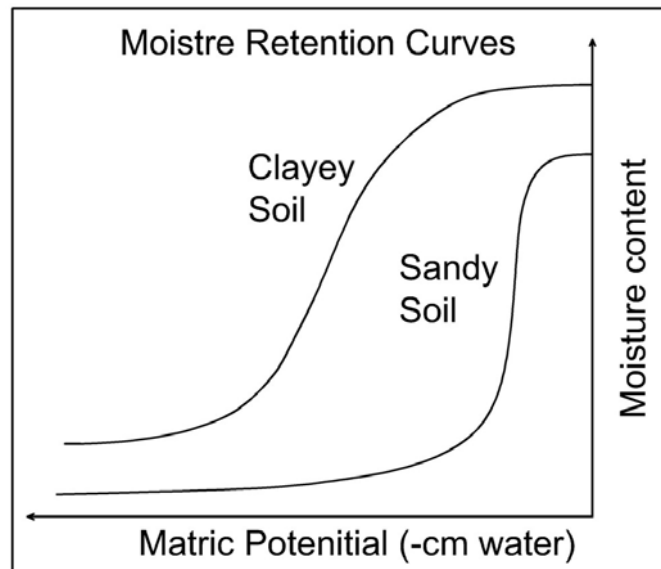


Figure 2: Moisture retention curves (*Unsaturated zone flow ...*, 2001).

The relationship between θ and matric potential as θ increases (wetting) is different than the relationship when θ decreases (drying), as shown in *Figure 3*. This behavior is hysteretic: p depends on the history of θ as well as the current value of θ .

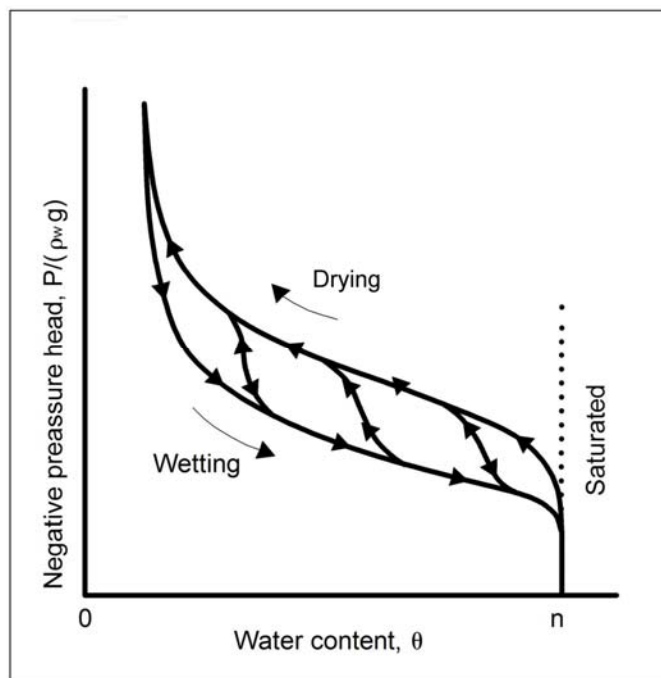


Figure 3: Characteristic curves for fine sand with wetting and drying cycles (*Fitts*, 2002).

The relationship between k and θ for granular material is shown in *Figure 4*. k declines to nearly zero as the material approaches its driest state in which nearly all water is tightly bound to the matrix. The dependence of k upon θ makes the analysis of unsaturated flow more mathemati-

cally complex than analysis of saturated flow. Models must incorporate equations that approximate the nonlinear hysteretic relationship $\theta(\Psi)$, as well as the nonlinear relationship $k(\theta)$.

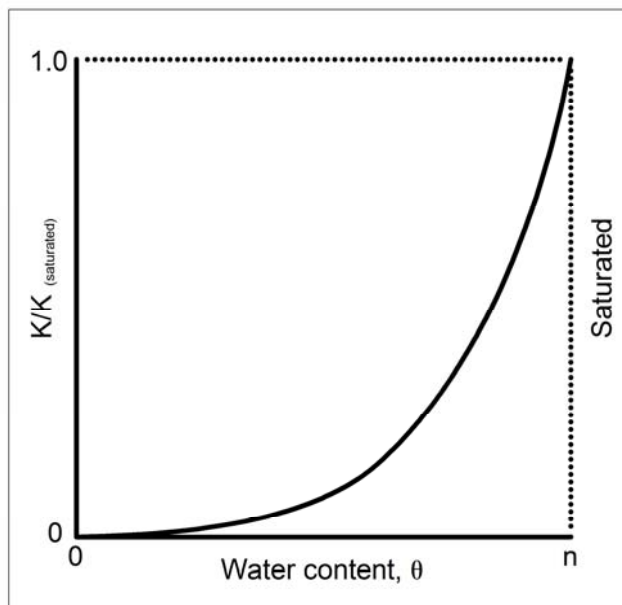


Figure 4: The ratio of conductivity to saturated hydraulic conductivity, as a function of water (Fitts, 2002).

Two transport phenomena in unsaturated zone are important: hydrodynamic dispersion and preferential flow.

2.2.2 Hydrodynamic dispersion

It is becoming increasingly common in the investigation of groundwater flow systems to view the flow regime in terms of its ability to transport dissolved substances. These solutes may be natural constituents, artificial tracers, or contaminants. The process by which solutes are transported by the bulk motion of the flowing groundwater is known as advection. Owing to advection, non-reactive solutes are carried at an average rate equal to the average linear velocity of the water. There is a tendency, for the solute to deviate from the ideal path that it would be expected to follow according to the advective hydrodynamic dispersion.

Mechanical dispersion is most easily viewed as a microscopic process. On the microscopic scale, dispersion is caused by three mechanisms. The first occurs in individual pore channels because the molecules travel at different velocities at different points across the channel due to the drag exerted on the fluid by the roughness of the pore surfaces. The second process is caused by the difference in pore size along the flow paths followed by the water molecules. Because of differences in surface area and roughness relative to the volume of water in individual pore channels, different pore channels have different bulk fluid velocities. The third dispersive process is related to the tortuosity, branching, and interfingering of pore channels. The spreading of the solute in the direction of bulk flow is known as longitudinal dispersion.

Dispersion is a mixing process. For porous media, the concepts of average linear velocity and longitudinal dispersion are closely related. Longitudinal dispersion is the process where some of the water molecules and solute molecules travel more rapidly than the average linear velocity and some travel more slowly along the groundwater water flow direction

When a tracer experiment is set up in the laboratory or in the field, the only dispersion that can be measured is that which is observable at the macroscopic scale. It is assumed that this macroscopic result has been produced by the microscopic processes described above.

2.2.3 Preferential flow

The main characteristic of preferential flow is that some of the water infiltrating into the unsaturated zone bypasses the major part of the matrix and quickly moves downwards. Preferential flow occurs through macropores.

Generally macropores are characterized by the lack or very small impact of capillary potential and therefore are mainly influenced by gravity. G. M. Aubertin (1971; in Berg et al., 2001) describes them as a large pore, cavity, passageway, channel, tunnel or void in the soil, through which water usually drains by gravity.

The formation of macropores is mainly caused by biogenic or geogenic factors: these are the tunnels of animals or the roots of plants; their diameter ranges from 1 mm to > 5 cm and they are concentrated in the upper soil layers. The numbers of macropores connected to the surface decreases with depth, so that the role of macropores generally diminishes with depth over the top 6 m. Root channels and the other structure of the materials have been identified as important by-pass pathways.

Macropores however do not represent a stable system; they are very sensitive to influences of various factors like climate/weather, plants, animals, mankind etc.. Macropores and other structures need to be in contact with a saturated zone or other source of free water to act as preferred pathways. A critical feature of preferential flow is that it allows groundwater and solute to by-pass the matrix of the soil or aquifer with little or no interaction.

2.3 Isotope hydrology

Isotopes are atoms of the same element that have different masses; they have the same number of protons and electrons, but a different number of neutrons (*Figure 5*). The 92 natural elements give rise to more than 1,000 stable and radioactive isotopes. These are often called environmental isotopes.

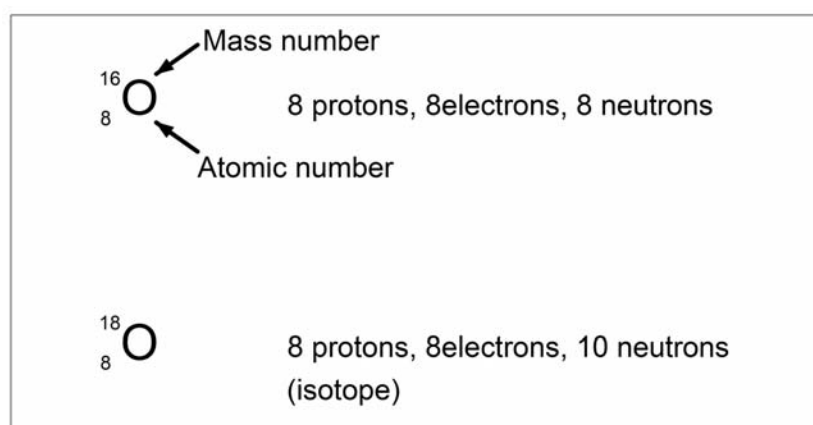


Figure 5: Example of oxygen isotope ^{18}O .

Tracing groundwater by means of environmental isotopes offers unique and supplementary information on the origin and movement of groundwater and its dissolved constituents, on residence time of groundwater in the aquifer, and as well allows a quantitative evaluation of

mixing and other physical processes. References can be found in Moser and Rauert, 1980; IAEA, 1983; Mazor, 1997; Clark and Fritz, 2000.

Environmental isotopes are commonly categorized into two general groups: stable isotopes and unstable (radioactive) isotopes. Stable isotopes are not involved in radioactive decay. Most stable isotopes do not react chemically in the subsurface environment and are of particular use in determining the source of groundwater. Unstable (radioactive) isotopes are involved in radioactive decay and they are of particular use in determining the age of water.

More detailed description of the use of environmental isotopes can be found in Fritz and Fontes (1980), Kendall and McDonnell (1998) and Isotope tracers... (2001).

2.3.1 Stable isotopes

Stable isotopes can serve as natural tracers that move at the average velocity of groundwater, and are of particular use in determining the recharge areas, mixing ratios among waters of different origin, and hydrograph separation. The most common stable isotopes used in hydrologic analysis are oxygen-18 and hydrogen-2 (also known as deuterium or D).

Isotopic fractionation

In lighter elements, such as hydrogen (H) and oxygen (O), the differences in the mass produced by isotopes are significant to the total mass of the atom. Isotopes of the same chemical element have almost identical physical and chemical properties. Because of their small mass differences, they have different reaction rates and different abundances in the two chemical compounds or phases that are in isotopic exchange. Also physical processes such as diffusion, evaporation, condensation, melting, etc. produce isotopic differentiation. All these variations in the isotopic composition, produced by chemical or physical processes, in compounds or phases, taking place in the same system, are called isotopic fractionation. Isotopic fractionation is any process that causes the isotopic ratios in particular phases or regions to differ from one another. For example, the ratio of $^{16}\text{O}/^{18}\text{O}$ in rain is different from the ratio in the oceans.

Isotope concentrations $\delta^2\text{H}$ and $\delta^{18}\text{O}$ are expressed as the difference between the measured ratios of the sample and reference divided by the measured ratio of the reference. This ratio is represented by δ :

$$\delta^2\text{H}_{\text{sample}} = \frac{\left(\frac{^2\text{H}}{\text{H}}\right)_{\text{sample}} - \left(\frac{^2\text{H}}{\text{H}}\right)_{\text{VSMOW}}}{\left(\frac{^2\text{H}}{\text{H}}\right)_{\text{VSMOW}}} \cdot 1000\text{‰VSMOW} \quad (4)$$

$$\delta^{18}\text{O}_{\text{sample}} = \frac{\left(\frac{^{18}\text{O}}{^{16}\text{O}}\right)_{\text{sample}} - \left(\frac{^{18}\text{O}}{^{16}\text{O}}\right)_{\text{VSMOW}}}{\left(\frac{^{18}\text{O}}{^{16}\text{O}}\right)_{\text{VSMOW}}} \cdot 1000\text{‰VSMOW} \quad (5)$$

The IAEA prepared standard water from distilled seawater. This reference is identified as VSMOW (Vienna Standard Mean Ocean Water). VSMOW has been the internationally accepted reference for ^{18}O and ^2H in waters for almost three decades.

For a specific area, the relationship between $\delta^{18}\text{O}$ and $\delta^2\text{H}$ in rainfall is approximately linear and can be plotted on a meteoric water line, an empirically derived relationship for continental precipitation. Monitoring of the stable isotopic composition of precipitation world wide (IAEA Global Network for Isotopes in Precipitation - GNIP) has defined the relationship between ^{18}O

and ^2H in worldwide fresh surface waters as the »global meteoric water line«, shown in *Figure 6*.

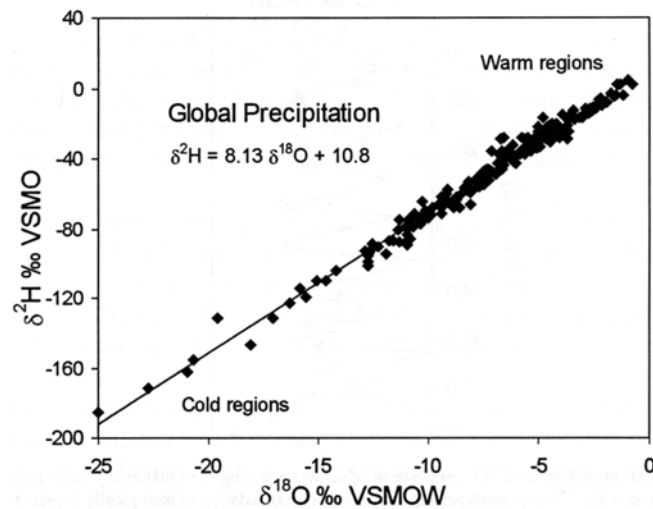


Figure 6: The meteoric relationship for ^{18}O and ^2H in precipitation (Clark and Fritz, 2000).

Isotopic fractionation of $\delta^{18}\text{O}$ and $\delta^2\text{H}$ during phase changes enriches one isotope relative to another. Water that has been subject to evaporation is enriched in $\delta^2\text{H}$ (D) relative to $\delta^{18}\text{O}$ because of its lower atomic weight. Fractionation is temperature-dependent. For example, winter precipitation is depleted in $\delta^{18}\text{O}$ and $\delta^2\text{H}$ compared with summer precipitation. Additionally, precipitation at the beginning of a storm is often higher in $\delta^{18}\text{O}$ and $\delta^2\text{H}$ than at the end of the storm, as the heavier isotopes are selectively removed from the vapor phase. These processes provide water masses with unique signatures that can be used as natural tracers in groundwater studies. Hence, the source areas of different waters, and the mixing patterns between waters can be assessed.

The major stable environmental isotopes used in hydrogeology are presented in *Table 1*.

Table 1: The stable environmental isotopes (Clark and Fritz, 2000).

Isotope	Ratio	% natural abundance	Reference (abundance ratio)	Commonly measured phases
^2H	$^2\text{H}/^1\text{H}$	0.0015	VSMOW ($1.5575 \cdot 10^{-4}$)	H_2O , CH_2O , CH_4 , H_2 , OH^- minerals
^3He	$^3\text{He}/^4\text{He}$	0.000138	Atmospheric He ($1.3 \cdot 10^{-6}$)	He in water or gas, crustal fluids, basalt
^6Li	$^6\text{Li}/^7\text{Li}$	7.5	L-SVEC ($8.32 \cdot 10^{-2}$)	Saline waters, rocks
^{11}B	$^{11}\text{B}/^{10}\text{B}$	80.1	NBS 951 (4.04362)	Saline waters, clays, borate, rocks
^{13}C	$^{13}\text{C}/^{12}\text{C}$	1.11	VPDB ($1.1237 \cdot 10^{-2}$)	CO_2 , carbonate, DIC, CH_4 , organics
^{15}N	$^{15}\text{N}/^{14}\text{N}$	0.366	AIR N_2 ($3.677 \cdot 10^{-3}$)	N_2 , NH_4^+ , NO_3^- , N-organics
^{18}O	$^{18}\text{O}/^{16}\text{O}$	0.204	VSMOW ($2.0052 \cdot 10^{-3}$) VPDB ($2.0672 \cdot 10^{-3}$)	H_2O , CH_2O , CO_2 , sulphates, NO_3^- , Carbonates, silicates, OH^- , minerals
^{34}S	$^{34}\text{S}/^{32}\text{S}$	4.21	CDT ($4.5005 \cdot 10^{-2}$)	Sulphates, sulphides, H_2S , S-organics
^{37}Cl	$^{37}\text{Cl}/^{35}\text{Cl}$	24.23	SMOC (0.324)	Saline waters, rocks, evaporites, solvents
^{81}Br	$^{81}\text{Br}/^{79}\text{Br}$	49.31	SMOB	Developmental for saline waters
^{87}Sr	$^{87}\text{Sr}/^{86}\text{Sr}$	$^{87}\text{Sr}=7.0$ $^{87}\text{Sr}=9.86$	Absolute ratio measured	Water, carbonates, sulphates, feldspar

The carbon isotope ^{13}C is an excellent tracer of carbonat evolution in groundwaters because of large variations. More detail description of the carbon isotope ^{13}C in the carbonate system is in the chapter 2.4.1.

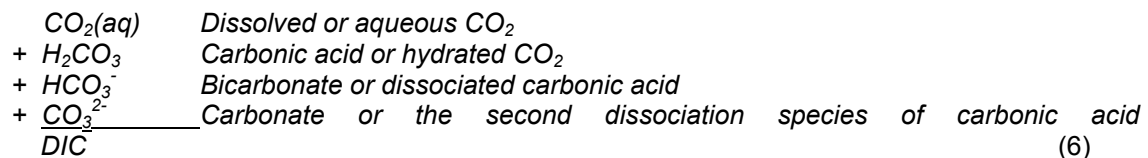
2.4 Evolution of carbon in groundwater

Evolution of carbon in groundwater is described in detail in Clark and Fritz (2000).

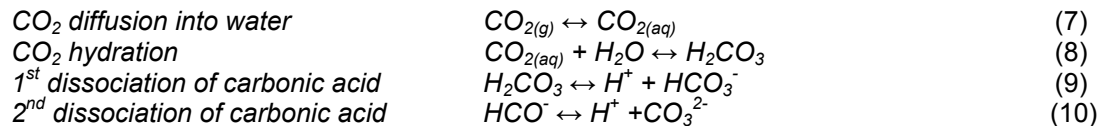
The carbon cycle in groundwaters begins with weathering reactions in the recharge area driven by CO_2 dissolved from the soil. Carbonate reactions dominate the geochemical evolution in shallow groundwaters, and so bicarbonate is generally the dominant anion in fresh water resources. The carbonate system evolves with subsequent organic and inorganic reactions in soils and aquifers. Microbiological activity plays a key role in the degradation of organic compounds and evolution of redox conditions. The chemistry and isotopes of carbon species provide insights into carbonate evolution and carbon cycling in groundwaters.

Fresh groundwaters invariably originate as meteoric waters, in most cases infiltrating through soils and into the geosphere. Along the way, dissolved inorganic carbon (DIC) is gained by dissolution of CO_2 and evolves through the weathering of carbonate and silicate parent material. As carbonate acidity is "consumed" by weathering, the pH rises and the distribution of dissolved inorganic carbonate species shifts towards bicarbonate (HCO_3^-) and carbonate (CO_3^{2-}). At the same time, labile organic matter from the soil can be dissolved. Oxidation of the dissolved organic matter (DOC) will take initially place by aerobic bacteria that use O_2 .

When waters infiltrate to the subsurface, they equilibrate with soil CO_2 . Bacterial oxidation of vegetation in soils and respiration of CO_2 in the root zone maintains CO_2 levels higher than in the air. Dissolution of soil CO_2 produces carbonic acid, which lowers pH and increases the weathering capacity of groundwater. The amount of carbon dioxide that can dissolve will depend on the geochemistry of the recharge environment: the temperature and initial pH of the water, and the partial pressure of soil CO_2 . When $\text{CO}_{2(g)}$ diffuses into water, it forms four main species of dissolved inorganic carbon (DIC).



Their distribution, or relative concentration, is a function of pH. Dissolution of $\text{CO}_{2(g)}$ in water takes place according to the reactions:



The higher the CO_2 concentration in the soil atmosphere, the lower will be the initial groundwater pH. The low pH is then buffered by mineral weathering in the soil and upper bedrock. Calcite dissolution is perhaps the most common and effective buffering reaction. Calcite dissolution can be written as the simple dissociation reaction:



In most groundwater systems, calcite dissolution is enhanced by carbonic acid from soil CO_2 according to the next reaction:



Carbonate dissolution according to this reaction is sensitive to the partial pressure of CO_2 . The higher the CO_2 concentration in the soil, the greater will be the amount of calcite dissolved, and the higher will be the groundwater's DIC. However, another condition must be considered in determining the DIC gained during infiltration: that is the degree of "openness" between the groundwater and soil atmosphere.

Under *open system* conditions, calcite dissolution proceeds with a constant supply of soil CO_2 . Open system conditions are typical of the unsaturated zone where gas and aqueous phases coexist. Much more calcite will be dissolved due to the continual replenishment of CO_2 , and the final equilibrium concentration of DIC will be high. Under *closed system* conditions, the groundwater infiltrates through the soil and reaches the saturated zone before it begins dissolving calcite. Here the groundwater is closed off from the source of soil CO_2 . The fixed concentration of CO_2 gained in the soil is not replenished as carbonate dissolution proceeds, and so the amount of dissolution and the final DIC concentration will be lower. Closed system conditions are typical of recharge areas where infiltration to the water table is fast (e.g. karst) or in saturated soils with little or no carbonate content.

2.4.1 Carbon-13 in the carbonate system

The carbon source and the reactions can be traced also by the Carbon-13 isotope. The groundwater $\delta^{13}\text{C}$ composition gives information on the flow type and solute transport. It provides an insight into the water's geochemical evolution, adjacent rock types in the flow path and conditions in the recharge area (Urbanc, 1989; Pezdič, 1999; Trček, 1997; Trček, 2001). The $\delta^{13}\text{C}$ isotope composition in carbonate rock is 0‰, in the soil CO_2 , which is the product of plant's breathing and decomposing, it is about -25‰, similar as in plants, and in the atmospheric CO_2 it is -7‰ (Kendall and McDonell, 1998; Trček, 2001). The $\delta^{13}\text{C}$ composition varies inversely with alkalinity. In *Figure 7* ranges for $\delta^{13}\text{C}$ values in selected natural compounds are presented.

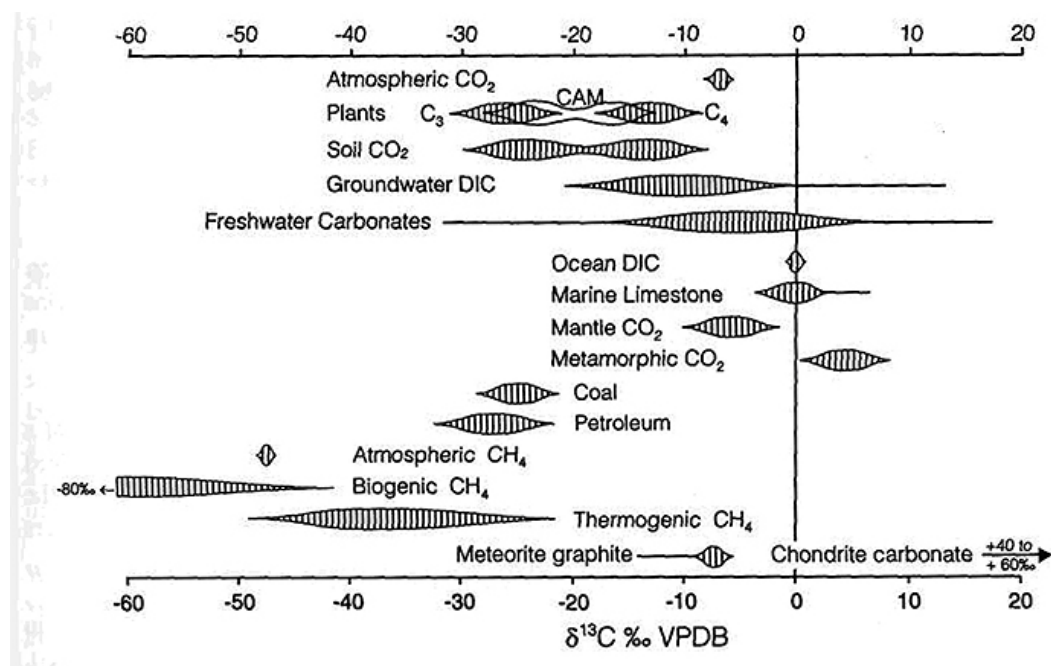


Figure 7: Ranges for ^{13}C values in selected natural compounds (Clark and Fritz, 2000).

A different isotope fractionation factor comes into play between each aqueous species and the soil gas (*Figure 8*). The largest fractionation occurs during CO_2 hydration.

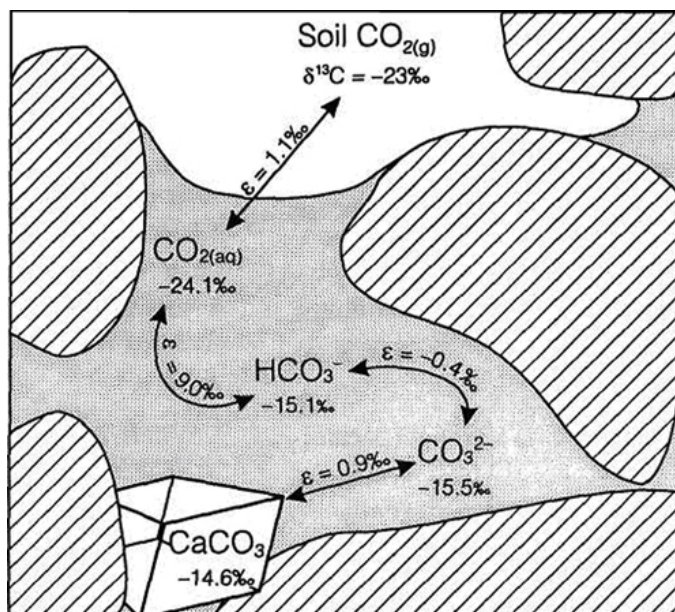


Figure 8: Schematic of fractionation of ^{13}C during equilibrium exchange of carbon between CO_2 , DIC and calcite at 25°C (Clark and Fritz, 2000).

2.5 Lumped-parameter models

One of the potential contributions of isotope methods in the water resources sector is also the estimation of residence time of water in the system. The term residence time refers to the period of time that the groundwater spends in the aquifer (Ozyurt and Bayari, 2003). Because, in many situations, the groundwater is a mixture of past recharges with different residence times, the term **mean residence time** (MRT) is more appropriate to use. Analysis of MRT is important because it provides valuable information on the age distribution of water in the aquifer, which may be used to estimate the spread velocity of contaminants or to identify the groundwater flow characteristics. MRT analysis may be carried out by using the analytical and numerical solution routines that are based on Darcy's Law. However, such solutions require detailed information on the flow system (e.g. boundary conditions, porosity, hydraulic conductivity, geometry of aquifer, etc.), which are mostly not available particularly for large groundwater systems. The **lumped-parameter (LP) models** provide an opportunity to determine and analyze the MRT of aquifers in the absence of such information. Even when sufficient information is available, LP models may still be used as preliminary investigation tools because they are much easier to implement compared to the more sophisticated distributed-parameter models.

LP models appeared initially in the field of chemical reactor engineering (Levenspiel, 1962; Levenspiel, 1999), but have also been used in other disciplines including hydrogeology (Maloszewski and Zuber, 1982; Zuber, 1986a; Zuber, 1986b; Maloszewski, 1996). The computer codes available in the hydrogeology literature for LP modelling are limited in number and scope. The FLOWPC version 3.2 (Maloszewski, 1996), BOXMO-DEL (Zoellmann and Aeschbach-Hertig, 2001) and TRACER (Bayari, 2002) are the public domain codes that can be used in MRT analysis in groundwater systems. These codes include LP models for relatively simple groundwater flow systems that may be simulated by a plug, exponential, serially connected exponential and plug, linear and dispersive flow reservoirs. However, more complicated groundwater flow systems may also include dead water zones, reservoirs connected in parallel with or without cross flow in between, bypass flow skipping over the reservoirs that cannot be effectively treated by simple models. LUMPED (Ozyurt and Bayari, 2003) has been designed to meet these requirements. The code comprises 15 different LP models, each describing a different flow system that operates under steady-state conditions.

Basic articles such as, Nir (1986), Zuber (1986a, b), Maloszewski (1996), Levenspiel (1999), Ozyurt and Bayari (2003) may be referred to for detailed information.

In the lumped-parameter approach, the flow domain (aquifer) is treated as a black-box in which the tracer input concentration (impulse) is converted to tracer output concentration (response) according to the system response function selected. The system response function may be regarded as an overall equation that lumps all the factors affecting the transport of tracer in the aquifer. If the system response function is capable of describing the flow (and transport) characteristics of the reservoir correctly, the theoretical tracer output series will exactly match the temporally observed outputs.

The system response function is also called the **weighting function** because it determines the weight of past impulses on response at any time. The weighting function $g(t)$ can be expressed in a general form by

$$g(t) = \frac{C_{input}(t)}{\int_{t=0}^{t=\infty} C_{input}(t) dt} = \frac{C_{input}(t)Q}{M} \quad (13)$$

Where $C_{input}(t)$ is the tracer input concentration at time t , Q is the flow rate and M is the total mass or activity of the tracer entered into the system (Maloszewski, 1996). As a result, $g(t)$ is the flow averaged weighting function of the tracer concentration.

In a steady-state groundwater system, the tracer output concentration $C_{output}(t)$ at time t is related to the tracer-input concentrations $C_{input}(t')$ of past recharges that occurred at times t' by the following convolution integral:

$$C_{output}(t) = \int_{t'=-\infty}^{t'=0} C_{input}(t') g(t-t') \exp(-\lambda(t-t')) dt' \quad (14)$$

where $(t-t')$ is the respective residence time, $g(t-t')$ is the weight of respective tracer input concentration $C_{input}(t')$ at the time of entry (t'), and λ is the first-order (radioactive or chemical) decay constant of the tracer. Eq. (14) points out that the tracer output concentration at time t is the sum of tracer input concentrations at times $(t-t')$ in the past, multiplied by their respective weights $g(t-t')$ and corrected for the decay (or chemical degradation and sorption) effect for the time elapsed $(t-t')$.

On the other hand, the MRT of tracer (or water) in the flow system can be described as follows:

$$MRT = \frac{\int_{t'=0}^{t'=0} t C_{input}(t) dt}{\int_{t=-\infty}^{t=0} C_{input}(t) dt} \quad (15)$$

In a flow system, where tracer particles move like the water molecules and both the tracer and water masses are conserved, Eq. (15) is identical to

$$MRT = \frac{V}{Q} \quad (16)$$

where V and Q are the volume and flux rate of the flow system. In this case, MRT is also called as the turnover time of the system to refer to the time required for filling up the whole volume V with a flux rate Q .

In each computer program there are several LP models each describing a different flow system that may be simulated by a plug, exponential, serially connected exponential and plug, linear and dispersive flow reservoirs. The models can be also used to determine different flow system parameters. The models included in the FLOWPC 3.1 program (Maloszewski, 1996), which were applied in the study, are:

- piston flow model (PFM)
- exponential model (EM)
- linear model (LM)
- dispersion model (DM)
- exponential-piston-flow model (EPM)
- linear-piston- flow model (LPM)

Detailed description of the models can be found in Maloszewski and Zuber (1982, 1996) and Zuber (1986a).

Piston flow model

In the *piston flow model* (PFM) approximation, the flow lines are assumed to have the same transit time, and the hydrodynamic dispersion and diffusion are negligible. Therefore, the tracer moves from the recharge area as if it was in a can. The response function is given by the well-known Dirac delta function,

$$g(t') = \delta(t' - t_t) \quad (17)$$

which inserted into Eq. 14 yields:

$$C(t) = C_{in}(t - t_t)\exp(-\lambda t_t) \quad (18)$$

The transit time of the tracer (t_t) is the only parameter of the model, and the shape of the input concentration function is followed by the output concentration in the case of a conservative tracer.

Exponential model

In the *exponential model* (EM) approximation, the flow lines are assumed to have the exponential distribution of transit times, i.e., the shortest line has the theoretical transit time equal to zero, and the longest line has the transit time equal to infinity. It is assumed that there is no exchange of tracer between the flow lines, and then the following response function is obtained:

$$g(t') = t_t^{-1} \exp(-t'/t_t) \quad (19)$$

Similarly to the PFM, the mean transit time of tracer is the only parameter of the EM, which unambiguously defines the whole transit time distribution.

Combined exponential-piston flow model

In the *exponential-piston flow model* (EPM) approximation, the aquifer is assumed to consist of two parts in line, one with the exponential distribution of transit times, and another with the distribution approximated by the piston flow. The response function of the EPM is:

$$g(t') = \begin{cases} (\eta/t_t) \exp(-\eta t'/t_t + \eta + 1) & \text{for } t' \geq t_t(1 - \mu^{-1}) \\ = 0 & \text{for } t' < t_t(1 - \mu^{-1}) \end{cases} \quad (20)$$

where η is the ratio of the total volume to the volume with the exponential distribution of transit times, i.e., $\eta = 1$ means the exponential flow model. The response function is independent of the sequence in which EM and EPM are combined. The EPM has two fitting parameters, t_t and η .

Dispersion model

In the *dispersion model* (DM), the following uni-dimensional solution in the flux mode to the dispersion equation for a semi-infinite medium is used as the response function (Kreft and Zuber 1978):

$$g(t') = (4\pi P_D t' / t_t)^{1/2} t'^{-1} \exp\left[-(1 - t'/t_t)^2 / (4P_D t' / t_t)\right] \quad (21)$$

where P_D is the apparent dispersion parameter ($D/v.x$), which is practically unrelated to the common dispersivity (D/v) of groundwater systems, and mainly depends on the distribution of travel times. The higher the value of the dispersion parameter is, the wider and the more asymmetrical are the distributions of the travel times.

Linear and combined linear-piston flow models

The *linear model* (LM) is a simple model and describes an aquifer with linearly increasing thickness and constant hydraulic gradient. When combined with the piston flow model it gives the *linear-piston flow model* (LPM).

The lumped parameter approach is applicable for any tracer with variable input. It is possible to use a constant tracer input or variable tracer input. In this study the variable tracer input was used for MRT estimation. The input data was taken from the local precipitation with the function:

$$\delta_{in}(t) = \bar{\delta} + \left[\alpha_i P_i (\delta_i - \bar{\delta}) \right] / \left(\sum_{i=1}^n \alpha_i P_i / n \right) \quad (22)$$

Where $\bar{\delta}$ is the mean input, n is the number of months and α_i is infiltration coefficients.

2.6 Tracing techniques

Tracing techniques are used in different scientific disciplines: geology, hydrology, chemistry, physics, water management, civil engineering, biology, limnology, etc. A more detailed description of tracing techniques, which covered mostly groundwater, was edited by Kass (1998). The International Atomic Energy Agency (IAEA) published numerous publications, books as well as proceedings, dealing with isotopes in hydrology (IAEA, 2000 a,b).

2.6.1 Tracers

Tracing tests can be carried out by artificial or 'natural' tracers. Artificial tracers are introduced into the water system that is under investigation. Natural tracers are naturally occurring constituents or other properties determined in the water.

A substance is introduced into the water system as artificial tracer that can be recognized and identified at another site. Such substances need to fulfill the following requirements:

- Absent in natural waters or present only in low concentrations,
- Good quantitative analysis with high sensitivity,
- Harmless for man, animals, and plants,
- Good water solubility or dispersion properties,
- Good resistance to chemical, biological or physical attacks; i.e. stable with regards to oxidation, reduction, acidic, or basic reactions, non-biodegradable as well as resistant to light and temperature,
- No interactions with the flow medium; i.e. free from sorption and ion-exchange properties,
- Economical with regard to its purchasing, using and analysis.

The expression natural tracer is not completely correct. Man-introduced unintended tracers also belong to this group. Such cases can happen during accidents. Groundwater pollution due to halogen-hydrocarbons or waste sites and thermal wastes also fall into this category, as well as unintended changes in the microbiological stock of a water body.

However, the most important group of naturally occurring tracers are the water's natural chemical constituents, as well as its isotope content. Important results can be determined from the naturally occurring contents as well as from those changed by civilization.

Artificial and naturally occurring tracers, which are available for tracing in water bodies, can be classified into the following groups:

- **Artificial tracers**

- Water soluble tracers –dyes, salts, surfactants, aromas and other chemicals, radioactive isotopes
- Particulate tracers - club moss (*Lycopodium*) spores, fluorescent microspheres, bacteria, bacteriophages, other particulate tracers;

- **Naturally occurring water constituents** - environmental isotopes, environmental chemicals, environmental organisms, physical environmental influences.

2.6.2 Evaluation and interpretation of tracing tests

The time and space dependent spreading of tracers in the underground is controlled by the temporal changes in concentration at certain observation points. The observed breakthrough curves are the expression of the hydrodynamic processes to which the tracers are subjected along their underground transport path (Bear, 1972; Lenda and Zuber, 1970; MacKay et al., 1986; Shulz, 1998).

The breakthrough curve forms the base for tracing analysis. The results of measured concentration are drawn in the form of time dependent tracer concentration curve (*Figure 9*). Beside the breakthrough curves, the (cumulative) recovery curves also give information for the comparison of tracer behaviour along the transport path.

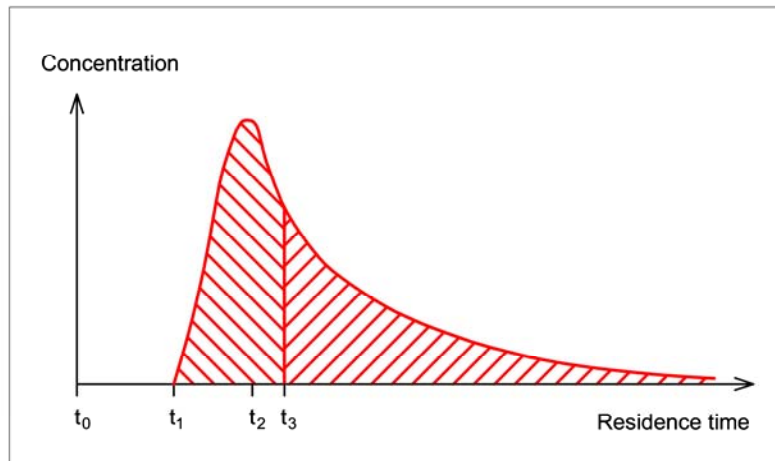


Figure 9: Ideal concentration curve from a tracing test (Kass, 1998).

The definitions for the different passage times are:

t₀: The time of injection. With injections that cover a period of time, t₀ is the beginning of injection (start of tracing experiment).

t₁: The first detection of the tracer. The first proof of the tracer is dependent upon analytical sensitivity and is therefore not identical with the first appearance of the tracer. The actual velocity can be calculated using the length of the flow path. Due to possible confusion with the actual velocity at the concentration maximum, this velocity is not called the maximum velocity, but rather the 'fastest' velocity (v_{al}).

t₃: Half-life time (average velocity, v_a) which is determined from the concentration curve. The half-life time is defined as the time when half of the tracer has reappeared at the sampling sites.

t₄: Last detection time. As with the first detection, this term is critically dependent upon the analytical sensitivity.

The Table 2 provides a review of the above terms:

Table 2: Review of tracing test terms (Kass, 1998)

Point of time	Concentration	Flow velocity
t ₀ input	-	-
t ₁ first detection time	Detection limit (c _E)	Fastest flow velocity (v _{al})
t ₂ highest conc.	Max. Conc. (c _{max})	Dominating f.v. (v _{al dom})
t ₃ half-life time	Half load (c _m)	(Median) flow velocity (v _a)
t ₄ last detection time	Detection limit (c _E)	-

In most cases due to practical reasons tracing tests are generally evaluated with the help of temporal changes in concentration at one site. The evaluation of such concentration-breakthrough curves provides the advection and dispersion parameters. Although, especially the mean flow velocity (v_a) can be more directly derived from the spatial distribution of a tracer cloud at a specific point in time than from the breakthrough curve, the advection and dispersion parameters can be derived from breakthrough curves with sufficient accuracy.

Another method for evaluating breakthrough curves was described by Sauty (1980). This method allows the simultaneous determination of the effective flow velocity and the dispersivity by comparing the normalized breakthrough curve with a calculated type curve. A more detailed description of evaluation and interpretation of the tracing test were described by Kass (1998).

The mathematical evaluation of breakthrough curves from a tracing test is possible using analytical and numerical procedures. Especially the simple explicit form of analytical solutions allows a quick determination of transport parameters. The measured tracer concentrations may

show deviations from theoretical curves. The parameters occurring in the analytical solutions may be determined by best-fit methods. As a theoretical background to analytical solutions, different model assumptions exist. Advection-dispersion models describe only the physical transport conditions. The literature on this topic could be found at references: Bear (1972), Grisack and Pickens (1980), Lege et al. (1996), Maloszewski and Zuber (1993).

The results of tracing experiment in this dissertation were evaluated by analytical best-fit method with computer program TRACI'95 (Käss, 1998). The analytical solution with one-dimensional convection-dispersion-model with standardising values for single porosity was chosen.

$$C_{fN}(x,t) = \frac{C_f(x,t)}{C_N(x,t)} = \sqrt{\left(\frac{t_N}{t}\right)^3} \exp\left[\frac{1 - \frac{t_N}{t}}{4t_N t_0} \left(P_D - \frac{t_N t}{P_D}\right)\right] \quad (23)$$

with boundary conditions:

$$C_f(0,t) = \frac{M}{Q} \delta(t)$$

$$C_f(\infty,t) = 0$$

$$C_f(x,t) = 0$$

Where C_f is tracer concentration in water, C_N normalized concentration, t_0 mean transit time, t time variable, t_N time after injection when normalized concentration was observed, x distance between injection and observation point and P_D is dispersion parameter. Dispersion parameter P_D is related to the dispersion coefficient by:

$$P_D = \frac{D}{v \cdot x} \quad (24)$$

where D is in our case vertical dispersion coefficient and v mean flow velocity.

Our analytical results are presented in ‰ $\delta^2\text{H}$. Because the basis for analytical best-fit model is the concentration of tracer (mg/m^3), the ‰ $\delta^2\text{H}$ values of results had to be converted. The mg/l concentrations of ^2H were calculated from the slightly modified equation published by Becker and Coplen (2001) taking into account the influence of the water density.

$$\text{Deuterium}_{\text{conc}} = 34.721 \left[\frac{1000 + \delta D_{\text{VSMOW}}}{1000} \right] \quad (25)$$

Retardation factor

The calculation of retardation factor for the uranine was made using results of convection-dispersion model for the estimation of mean flow velocity. The retardation factor R_d was calculated by:

$$R_d = \frac{v_{aD}}{v_{au}} \quad (26)$$

where R_d is retardation factor, v_{aD} is mean flow velocity of the deuterium tracer and v_{au} is mean flow velocity of the uranine.

2.7 Hydrograph separation

The recharge, storage and discharge characteristics of a watershed are reflected by its behaviour during rainfall and base flow. Stream hydrograph separation into baseflow and storm runoff components is the basic tool in determining the components of discharge from a catchment. The principle of hydrograph separation using stable isotopes is based on a contrast in the isotopic composition of the basin groundwater and that of a given storm. Oxygen or hydrogen isotopes may be used to separate a hydrograph if the difference in the isotopic compositions of event and pre-event waters is "large" relative to the isotopic variability within each component and the analytical uncertainty associated with the isotopic analyses. In the present study, hydrograph separation was used to determine the contribution of single water components in snow melting and study the possibility of occurrence (or properties) of preferential flow in gravel unsaturated zone.

The two-component separation of a storm hydrograph into storm runoff and prestorm baseflow can be described as mass balance equations. In the simplest form, the mass balance equations are (Van der Hoven et al., 2002)

$$Q_s = Q_n + Q_o \quad (27)$$

and

$$Q_s C_s = Q_n C_n + Q_o C_o \quad (28)$$

where Q is discharge, C is concentration of a tracer, and the subscripts s, n, and o are streamflow, event water, and pre-event water, respectively. In this study, the pre-event water is assumed to be groundwater from the unsaturated zone.

The mass balance Eqs. (27) and (28) can be used to calculate the amount of the new and old water in the stream. By setting:

$$R = \frac{Q_o}{Q_s} \quad (29)$$

And substitution Eq.(29) into Eq.(27), and followed by substitution of Eq.(27) into Eq.(28) yields:

$$R = \frac{(Q_s - Q_n)}{(Q_o - Q_n)} \quad (30)$$

Hydrograph separation techniques, which use mass balance of environmental tracers, require a number of assumptions (Sklash and Farvolden, 1982). They include:

- (1) Groundwater and baseflow can be characterized by a single constant composition.
- (2) Rain or snowmelt can be characterized by a single constant composition. If this is not the case, the variations in composition are documented.
- (3) The composition of rain water is significantly different from that of groundwater/baseflow.
- (4) Contributions from soil water are negligible, or the composition is identical to that of groundwater.
- (5) Contributions from surface water bodies are negligible.

The separation of two-component system on the basis of one parameter is illustrated in *Figure 10*, based on equations above (Clark and Fritz, 2000).

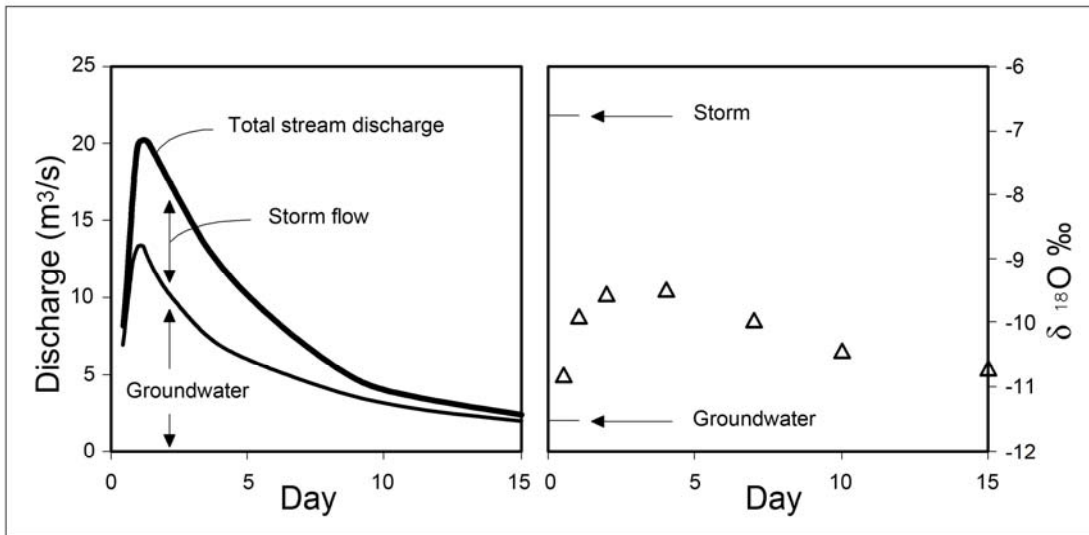


Figure 10: Storm hydrograph separation for a two-component system using $\delta^{18}\text{O}$ (Clark and Fritz, 2000)

3 SITE DESCRIPTION

3.1 Geographical description

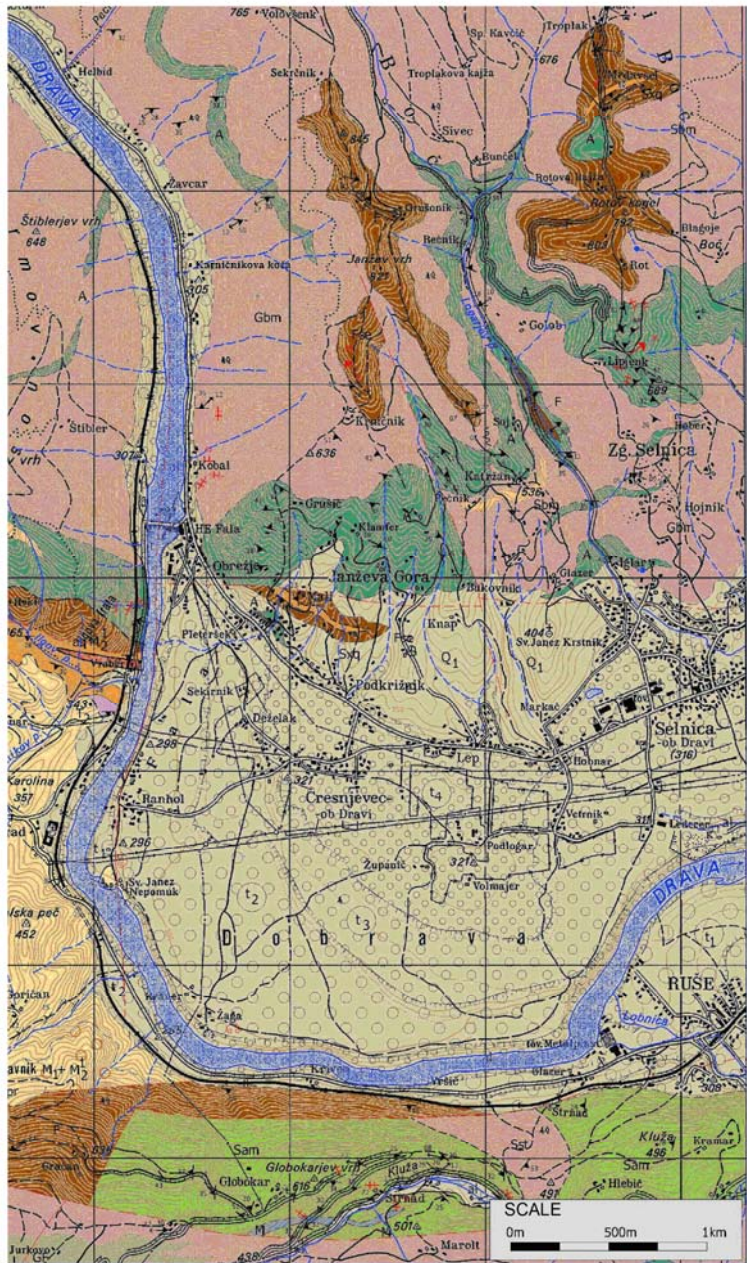
The larger area of Selnica ob Dravi is situated in the north-east of Slovenia. The 15 km² area is defined by geographical coordinates (the Gauß-Krüger coordinate system) x=5158454, y=5534960 in the north-west and x=5154177, y=5538315 south-east. The area is bounded by the Drava in the south and with hilly areas of Spodnji and Zgornji Boč in the north (Mali et al., 2005).

The research area belongs to the moderate continental climate of central Slovenia with a typical continental precipitation regime and an average annual rainfall between 900 and 1200 mm. The average yearly air temperature lies between 8 and 12 °C.

3.2 Geological and hydrogeological description

The Drava valley between Dravograd and Maribor is relatively young and was formed by young neotectonic faults (Mioč and Žnidarčič, 1976). Quaternary sediments of the Drava in Selniška Dobrava are deposited where the Drava flows out of the narrow gorge near Fala (*Figure 11*). Downstream from this point the Drava valley widens to about 2 km up to the Maribor city and then even more in the area of Dravsko polje. Quaternary sediments of Selniška Dobrava are mostly underlain by Miocene conglomerates, built from gravel of metamorphic rocks bonded with grey clay and marl. Quaternary sediments can be divided into older, Pleistocene sediments and younger, Holocene alluvium/deposits. Pleistocene sediments in the north-eastern fringe of Selniška Dobrava between Zgornji Boč and Janževa gora are mainly composed of yellowish-brown to brown sandy and silty clay, which is in some places mixed with gravel. All other alluvial deposits of the Drava belong into the Holocene. They mostly consist of coarse to medium granulation with inserts of large blocks of metamorphic rocks (0.5 to 1 m in diameter), some of which have a volume of over 2m³. Space between gravel and unrounded blocks is filled with coarsely granulated sand. Fine fractions of silt or even clay are practically not found in these deposits. Four terraces were formed in the accumulated material along the valley. The oldest level has the thickest clay cover and the highest elevation above the present river level. It is the least preserved and has lower permeability. Other terraces are mostly built of gravel (70%), sand (20%) and sandy clay (10%).

The area can be classified as an intergranular aquifer of good permeability with unconfined groundwater table (*Figure 12*). The old river bed, which presents the principal aquifer, runs along the present stream of the Drava river. The aquifer is recharged from the Drava, by the infiltration of precipitation and by seepage from the upper terrace aquifer. The thickest coarse gravel deposit is estimated to about 50 m. Groundwater table is at a depth of 25 to 37 m in the average, thus the thickness of the saturated layer along the aquifer axis is estimated to 7-14m, and even more in the deepest sections. The hydraulic conductivity of the coarse gravel aquifer is estimated to 5x10⁻³m/s (Mali, 1996; Mali et al., 2005).



GEOLOGICAL MAP


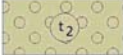


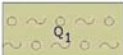
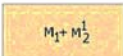
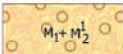
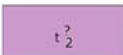
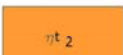
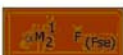

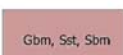


- FAULT
- ==== LITHOLOGICAL BOUNDARY:
COVERED, GRADUAL
-  GRAVEL
-  GRAVEL, SAND, SILT
-  SANDY GRAVEL WITH BOULDERS
-  SANDY GRAVEL WITH BOULDERS
-  CLAY WITH GRAVEL
-  $M_1 + M_2^1$ SANDSTONE AND CONGLOMERATE
-  $M_1 + M_2^2$ CONGLOMERATE
-  $t_2^?$ LIMESTONE
-  kt_2 KERATOPHYRE
-  M_2^1 F (F₅₆) DACITE (RED), PHYLLITE
-  A AMPHIBOLITE
-  Gbm, Sst, Sbm GNEISS AND MICASCHIST
-  Sam CLORITE AMPHIBOL SLATE
-  GF GNEISS AND PHYLLITE

Figure 11: Geological map (Mioč and Žnidarčič, 1976)

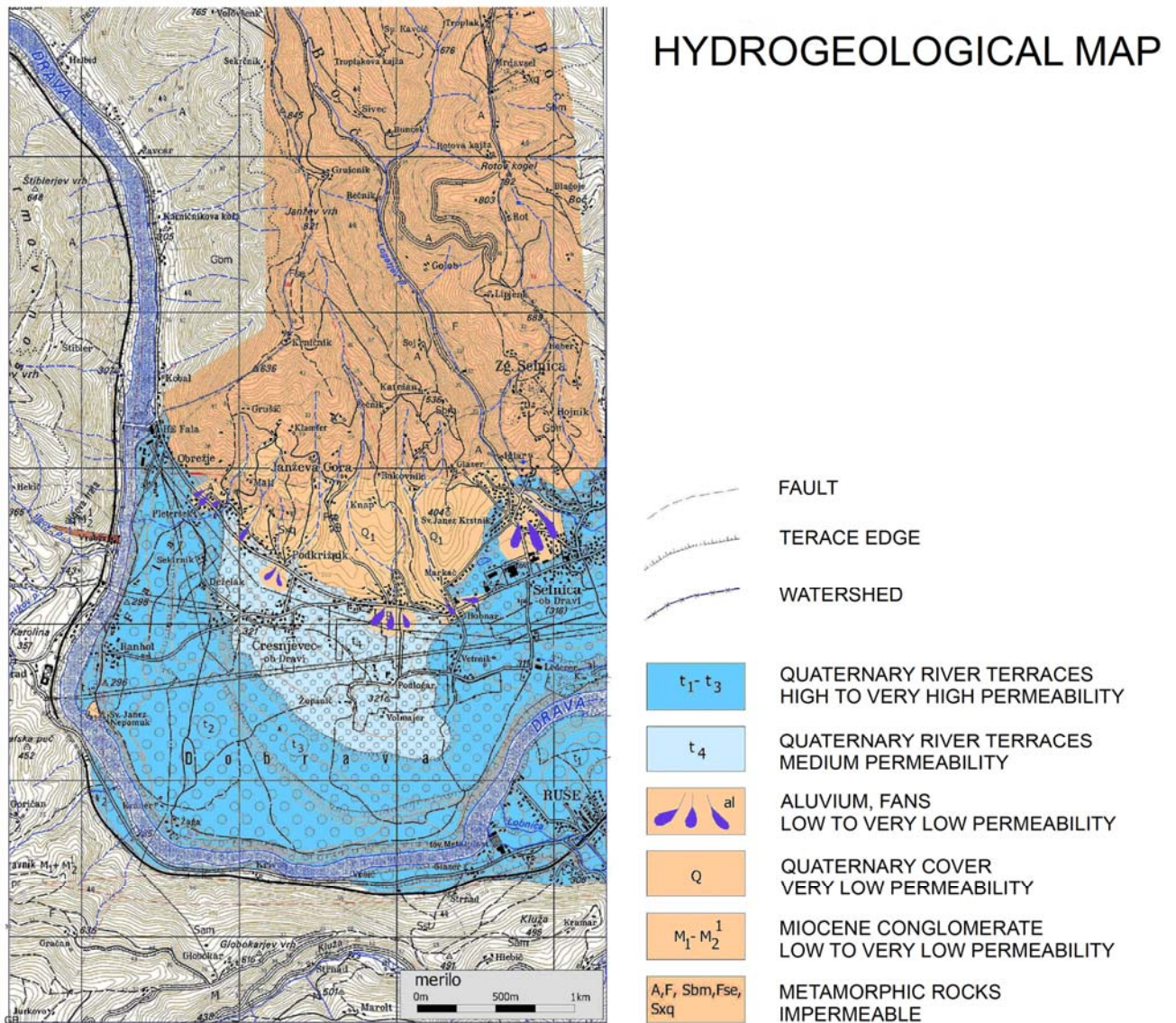


Figure 12: Hydrogeological map (Mali, 1996)

3.3 Lysimeter location

The lysimeter is located in the area of the principal aquifer of Selniška Dobrava downstream from the pumping station GV-1 on coordinates $x=5154641$, $y=5536401$ (according to Gauß-Krüger) at altitude 295 m (Figure 13). The thickness of the gravel deposit in this area is 37.5m, the water table is at 27.5m, and the saturated layer is 10 m thick. The larger area of the lower aquifer is covered by mixed forest. The lysimeter is situated at the piezometer PS-5, which is constructed to the basement and enables measurements of groundwater tables and sampling of groundwater.

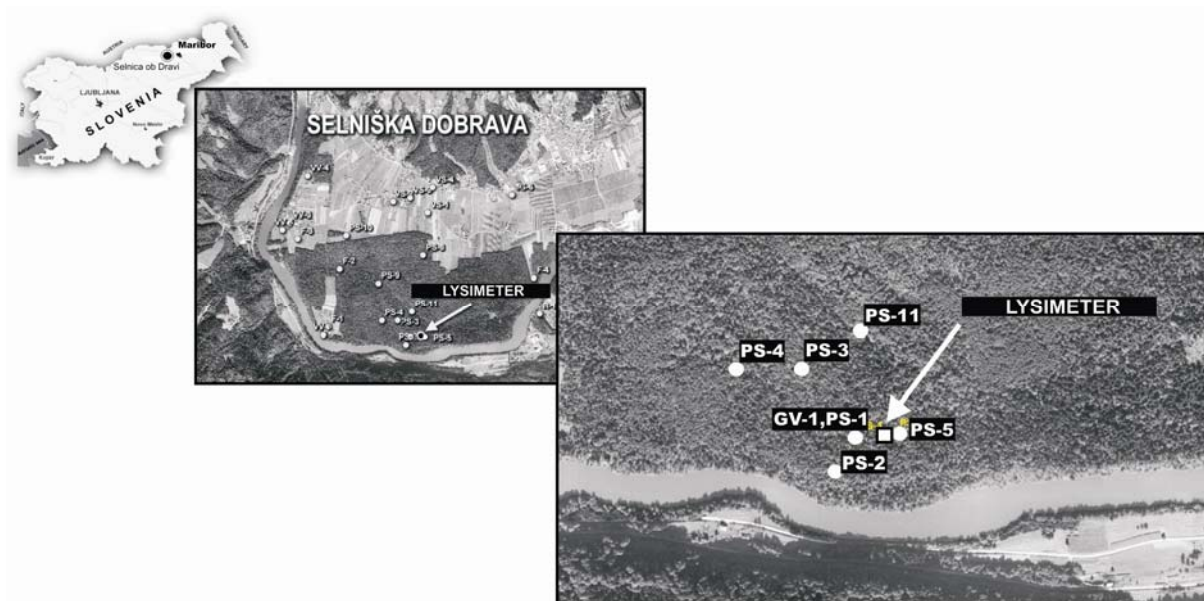


Figure 13: Study area – Location of the lysimeter Selniška Dobrava.

3.4 Detailed site characterization

Before studying the flow and solute transport processes in the lysimeter, the site characteristics should be estimated. At the time of lysimeter construction the samples of gravel for granulometrical and petrographical analyses were taken. At the same time also a pedological list of soil cover was made. The soil was sampled for pedological investigations. To measure the infiltration rate and the saturated hydraulic conductivity of the soil, several infiltration tests by double ring method were performed. *Table 3* contains a list of measuring and calculation methods used in site characterization.

Table 3: Site characterization methods

Method	Determination of	Calculation method	Producer
Pedological characterization			GeoZS; KGZ-MB
Petrographic analysis			GeoZS
Granulometric analyses	Sorting, hydraulic conductivity	USBR, Hazane	Geoinženering d.o.o
Double ring infiltrometer	Infiltration, hydraulic conductivity	Hvorslev	GeoZS

3.4.1 Lithology and petrography

Two samples of gravel for petrographic analyses were taken nearby the lysimeter at 2m depth. The samples were analyzed for their macroscopic petrographic composition in the laboratory of GeoZS (Trajanova, 2004). The amount of carbonate in two fractions was determined by calcimetry.

Two samples of gravel with labels Jazbina and Jazbina- Kraner weighing 35 kg and 46 kg were taken. The samples were screened at sieves with openings 32, 16, 8, 4 and 2 mm. A required amount of the sample was divided by quartered cuts on the screens and weighted percentage was calculated. Fractions 0-2 mm and 2-4mm were analysed for carbonate content by calcimetry. In other fractions the presence of carbonates was defined macroscopically, only the fraction (+2-4mm) was repeated for comparison of both methods.

The results of the lithology and petrography examination of two samples taken in the same profile of the coarse gravel unsaturated zone showed quite different results (Trajanova, 2004). One was sampled at a location where the material was cemented (Jazbina 2), the other (Jazbina 1) was very loose. The sample Jazbina 1 was lithologically classified as material with major metamorphic rock structure. Although the sample Jazbina 2 contained 13-19% of metamorphic rock and to a major part quartzite flint (20-50%), almost half of the material was determined as carbonate rock (gravel). The limestone prevailed (14-42%), followed by marble-sandstone, marble and agglutinated carbonate gravel. Thus different sources of origin are presumed, from the surrounding rocks and the Drava river sediments. Due to a high content of carbonate material, gravel was locally incrustated by calcite.

On the basis of petrography and also of profile survey at the time of construction it was concluded that the lithological structure of gravel at lysimeter location is more similar to sample Jazbina 2 and is mixture of metamorphic rocks to carbonates (limestone, marble-sandstone, marble and agglutinated carbonate gravel). Here and there the gravel is incrustated by calcite.

3.4.2 Pedological investigations

During lysimeter construction the pedological survey (soil list) was carried out. All determined horizons were listed in the field. Each soil horizon (A, A(B), (B), and (B)C) were sampled to determine soil acidity, organic matter content, texture range and saturation with basic cations. The samples were dried at 40 °C in ventilation oven and screened below 2 mm. Laboratory analyses were done in Kmetijsko gozdarski zavod Maribor – KGZ-MB (Agriculture and Forest Survey of Maribor), the pedological evaluation was completed by Gosar (2000) – Geological survey of Slovenia (GeoZS).

The pedological profile on the location of the lysimeter is composed of O₁O_n, A, A, A(B), (B) and (B)C horizons (*Figure 14*). The sketch of profile is presented in *Figure 15*.

Based on the pedological laboratory analysis of soil acidity, organic matter content, texture range and saturation with basic cations of soil horizons (A, A(B), (B), and (B)C) the results in *Table 4* were determined (Gosar, 2000):

The analyzed soil is very acid, pH values in the entire profile are under 5. Soil texture of the whole profile is classified as sandy clay (PI). The most organic matter is found in the upper horizon (6.96%), also in the transitional horizon A(B) it still amounts to 6.28 %, in the deeper parts of the profile the organic matter is under 1.5%. Up to the depth of 56 cm, the degree of saturation with basic cations is under 20%, at 56-140 cm it is 36.4%. Gravel pebbles are present in the entire profile. Gravel quantity increases with the depth and is estimated to 70% at a depth of 56-140 cm. Based on field description and laboratory analyses, the soil on lysimeter location is defined as distric cambisol.

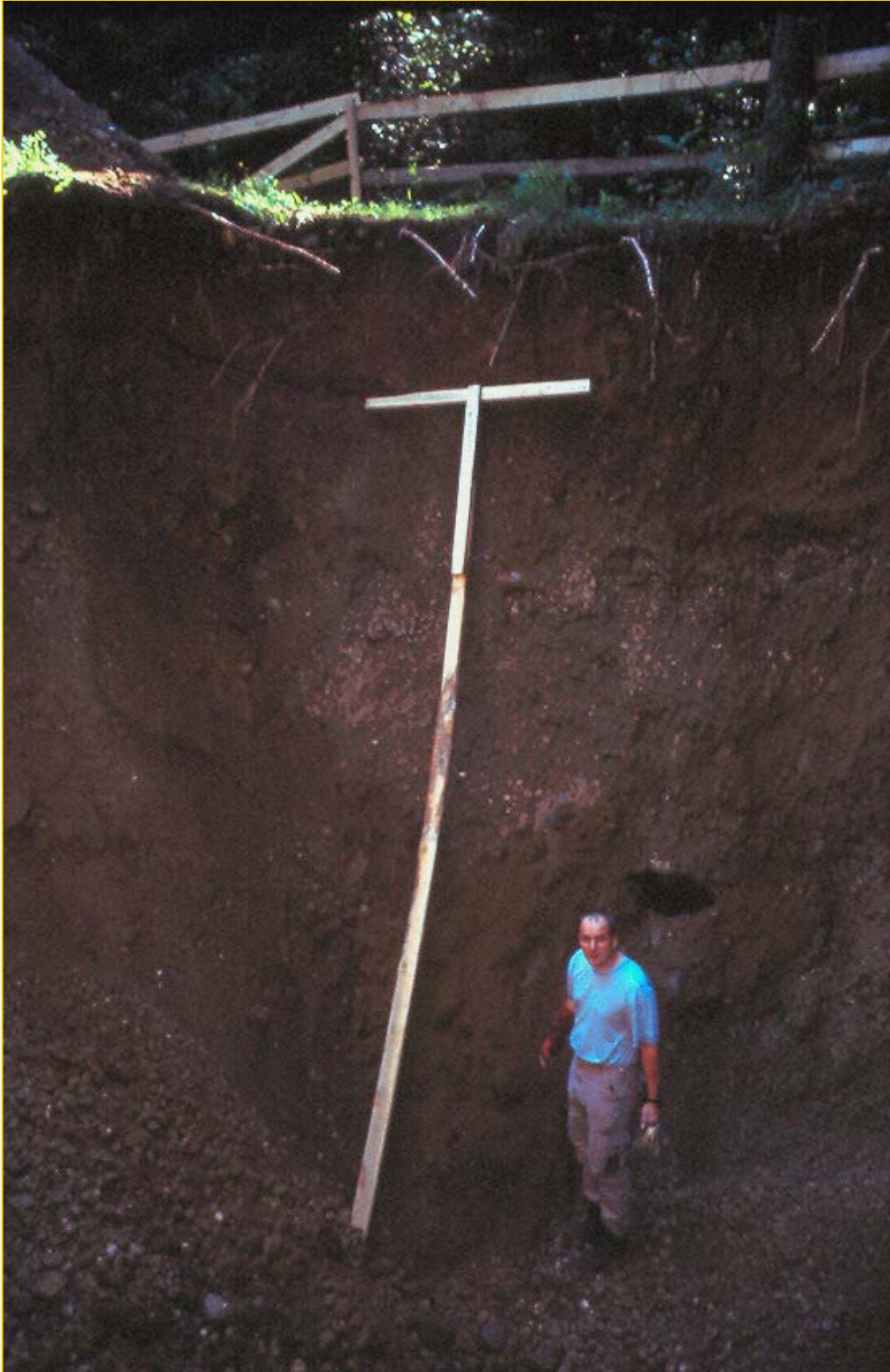


Figure 14: *Unsaturated zone profile*

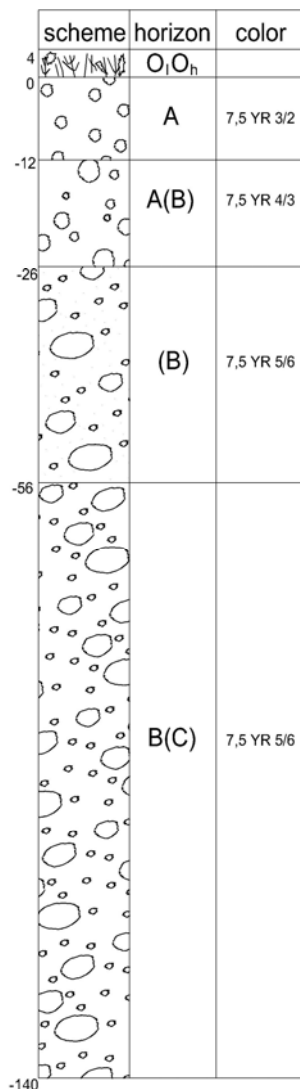


Figure 15: Pedological profile

Table 4: Results of pedological analysis

Horizons	Depth (cm)	Description		
O ₁ O _h	5-0 cm	Remnants of moss, grass and little roots		
A	0-12 cm	Dark-brown coloured (7.5 YR 3/2) on account of a large quantity of organic matter, structure is scattered with 2-3 mm structural aggregates.		
A(B)	12-26 cm	Passage from organic-matter colored horizon A into horizon (B). The color changed into bright dark brown (7.5 YR 4/3). The structure is lumped with aggregates somewhat longer than in the upper horizon A. Skeleton – gravel up to 30%.		
(B)	26-56 cm	Mineral cambic horizon, strong brown colored with an orange cast (7.5 YR 5/6). The quantity of gravel is high, estimated to 50%		
(B)C	56-140 cm	Continuation of upper (B) horizon, the amount of gravel reaches 60-70%		
Sample	pH (KCl)	Texture	Org. matter	Saturation with basic cations (V) %
PS-5 A	4.38	PI	6.96	17.75
PS-5 A(B)	4.49	PI	6.28	15.19
PS-5 (B)	4.72	PI	1.3	17.33
PS-5 (B)C	4.29	PI	0.09	36.41

3.4.3 Hydraulic properties

Hydraulic characteristics of the field site were estimated by granulometric analyses and by infiltration tests performed by double ring method.

3.4.3.1 Methods for characterizing hydraulic properties

Granulometric analyses

Gravel samples for granulometric analyses were taken during construction at 1.5m, 3.30m (two samples) and 6 m depth. The samples were screened at sieves with openings 0.1; 0.2; 0.5; 1, 2, 5, 10, 20, 30, 40, 60 or 100 mm. Necessary amount of sample was obtained by successive quartering of cuts at the same sieves. For each granulation a weighted percentage was calculated. Based on granulometric analyses, the granulometric curves were constructed. Gravel samples were analysed by Geoinženiring d.o.o.

Based on granulometric analyses, sorting coefficient and hydraulic conductivity were estimated. For the calculation of hydraulic conductivity parameter, the USBR and Hazen empirical equations were used (Aljovski, 1973; Vuković and Soro, 1984).

$$\text{Sorting coefficient} \quad \frac{d_{60}}{d_{10}} \quad (31)$$

d_{60} - grain size diameter the contents of which in the sample is lower than 60%

d_{10} - effective grain size diameter the contents of which in the sample is lower than 10%

USBR :

$$k = 0,36 \cdot d_{20}^{2,3} \text{ (cm/s)} \quad (32)$$

k - hydraulic conductivity

d_{20} - effective grain size diameter the contents of which in the sample is lower than 20%

Hazen:

$$k = C \cdot d_{ef}^2 (0,7 + 0,03T) \text{ (m/day)} \quad (33)$$

C -empirical coefficient, it is 800-1200 for pure and homogeneous sand and 400-800 for unhomogenous, loam sand

k - hydraulic conductivity

d_{ef} - effective grain size diameter

T – water temperature effective °C

For Selniška Dobrava location the next parameters were taken:

C – 1000

d_{10} - effective grain size diameter

T – 10°C

And the Eq. 33 becomes

$$k = 0,0116 \cdot d_{ef}^2 \text{ (m/s)} \quad (34)$$

Conditions for equation validation are:

- if $d_{10} = 0.1-0.3$
- $d_{60}/d_{10} > 5$

Double ring measurements

The double ring infiltrometer enables to approximate the infiltration and field-saturated hydraulic conductivity of low-permeable materials. The set of the double ring infiltrometer consists of two stainless steel rings of different diameters (32 cm, 57 cm) inserted at a shallow depth into the material to be tested (*Figure 16*). Water is allowed to infiltrate between the two rings and within the inner ring. As vertically infiltrated water runs away to the sides, the outer ring of the infiltrometer serves as a separation. The water infiltrating between the two rings provides a barrier which constrains the water from the inner ring to infiltrate vertically downwards. The measurements exclusively take place in the inner ring through which the water runs virtually vertical; in the outer ring the steady-state flow is sustained.



Figure 16: Set-up of double ring measurements

The rate of infiltration is determined as the amount of water per surface area and the time unit in which it penetrates the soil. The solution for vertical, field-saturated hydraulic conductivity (k) follows directly from

$$k = \frac{Q}{\pi \cdot r^2} \quad (35)$$

Q - flow rate into the inner ring during measured time
 r - radius of the inner ring.

Base on measured results of the double-ring the conductivity coefficient of the soil was calculated using the Hvorslev equation.

Hvorslev equation:

$$k = \frac{A}{\Delta t \times F} \times \ln \frac{h_1}{h_2} \quad (36)$$

F is shape factor and is 2.75 D for a cylinder:

$$F = 2.75D \quad (37)$$

k- hydraulic conductivity
A – cross-section of flow
F - shape factor
D- diameter
Δt – time change
h₁, h₂ – water level

The double ring measurements were performed twice on 3 locations near and over lysimeter site. The water level fall in the inner ring was electronically measured.

3.4.3.2 Site hydraulic properties

In *Table 5* estimations of hydraulic properties parameters are given.

Table 5: Hydraulic property parameters

	JAZ 1,5	JAZ 3,3/1	JAZ 3,3/2	JAZ 6	Mean	Min	Max
d60/d10	84.0	175.0	55.8	60.0	93.7	55.8	175.0
k - USBR (m/s)	1.5E-01	7.8E-03	1.1E-01	1.3E-02	6.9E-02	7.8E-03	1.5E-01
k-Hazane (m/s)	6.5E-03	1.2E-04	2.1E-03	2.9E-03	2.9E-03	1.2E-04	6.5E-03

Double ring	P1	P2	P3	Mean	Min	Max
k (m/s)	3.5E-05	1.5E-05	4.5E-05	3.2E-05	1.5E-05	4.5E-05
infiltration (m/s)	2.0E-05	5.4E-06	1.8E-05	1.4E-05	5.4E-06	2.0E-05

The granulometric analyses showed that more than 20% of grains are classified as gravel material (*Annex A, Figure 17*). Sorting coefficient of the coarse gravel shows that the material is not well sorted. In the research report of the Selniška dobrava coarse gravel aquifer the hydraulic conductivity of aquifer was estimated to 5.10⁻³ m/s by pumping tests (Mali, 1996; Mali and Janža, 2005). Based on granulometric analyses the hydraulic conductivity of the coarse gravel was estimated to 2.9x10⁻³-6.8x10⁻² m/s. The infiltration tests showed that hydraulic conductivity of the soil is in the range of 1.5x10⁻⁵-4.5x10⁻⁵m/s defined by the double ring method.



Figure 17: Coarse gravel at the Selniška Dobrava lysimeter location

4 METHODOLOGY

This chapter describes the experimental site and the sampling and experimental procedure used in this work. The first part describes in situ investigations for site property descriptions and the lysimeter construction with a description of the sampling sites, and at the end the isotope and chemical sampling design and measurements that were applied are presented.

4.1 Research plan

Experimental work is the main tool of my research to investigate the characteristics, groundwater flow and transport in the unsaturated zone of a coarse gravel aquifer. One part of the work was the setting up of a monitoring system with measuring equipment. The construction was designed based on literature study and our field experiences. The equipment was installed over a period of several years, and at the time of lysimeter operation the equipment was also being tested. To put the lysimeter into operation, the following steps were carried out:

- lysimeter construction design
- equipment selection
- equipment testing

Other investigations in the field laboratory – lysimeter in Selniška Dobrava were classified in a research plan (sampling design) which is presented in *Figure 18*. The investigations were carried out on the following subjects:

- experimental site characterization
- isotope and geochemical investigations
- tracing experiment

For each topic the following sampling-measuring points were defined in *Table 6*:

Table 6: List of sampling and measuring points

SUBJECT	Type of investigation; sampling domain	Sampling-measuring points
SITE CHARACTERIZATION	Petrographic analyses Pedological analyses Double ring infiltration tests Granulometric analyses	JA-1, JA-2 A, A(B), (B), (B)C P-1, P-2, P-3 1,5; 3,3 (1,2); 6
GEOCHEMICAL AND ISOTOPE INVESTIGATIONS	Unsaturated zone -water -CO ₂ , T, moisture Groundwater Precipitation	JV-1 to JV-10 JV-1 to JV-10 PS-5 P-1
TRACING	Unsaturated zone -water	JV-1 to JV-10

4.1.1 Experimental site characterization

The site characteristics were estimated by pedological, petrographical, granulometrical analyses and hydraulic tests. During the time of lysimeter construction samples of gravel for granulometrical and petrographical analyses were taken. At the same time also a pedological

list of soil types was compiled. All researches for site characterization are described in chapter 3.4.

4.1.2 Isotope and geochemical investigations

The main method used to study the flow and transport processes is the isotope method. The isotope and geochemical investigations are classified into two groups, long- and short-term investigations.

Long-term investigations - Over a long hydrological period, samples of groundwater in the unsaturated zone have been collected monthly at different depths in the lysimeter. The content of $\delta^{18}\text{O}$ and $\delta^2\text{H}$ stable isotopes in the water was determined. The principal physico-chemical characteristics in the water and outflow water were measured in the field. Periodically in some water samples also chemical composition and $\delta^{13}\text{C}$ isotope content were determined. At some points in the lysimeter, the temperature and partial pressure of CO_2 were measured for a period in-situ in the gravel. Periodically also samples of gas for $\delta^{13}\text{C}$ isotope determination were collected.

Short-term investigations were used to precisely identify the reaction of the coarse gravel unsaturated zone system to special events like snow melting and storm events. At that time of soil and gravel saturation, preferential flow occurs. After special events (snow melting and storm event) daily sampling was performed for several days, and after that time weekly samplings were done. The principal physico-chemical characteristics in the water and outflow water were measured at the same time.

4.1.3 Tracing experiment

To better understand the movement and transport of water and pollution through the coarse gravel unsaturated zone, a tracing experiment was conducted to estimate water flow and transport processes in a field laboratory – in lysimeter. A combined tracing experiment was performed with deuterated water and fluorescent dye – uranine on April 21, 2004. Samples of unsaturated water were collected daily for the first few days, afterwards weekly or every two weeks until October 2005. At the time of sampling also the volume of outflow water, temperature and conductivity were measured.

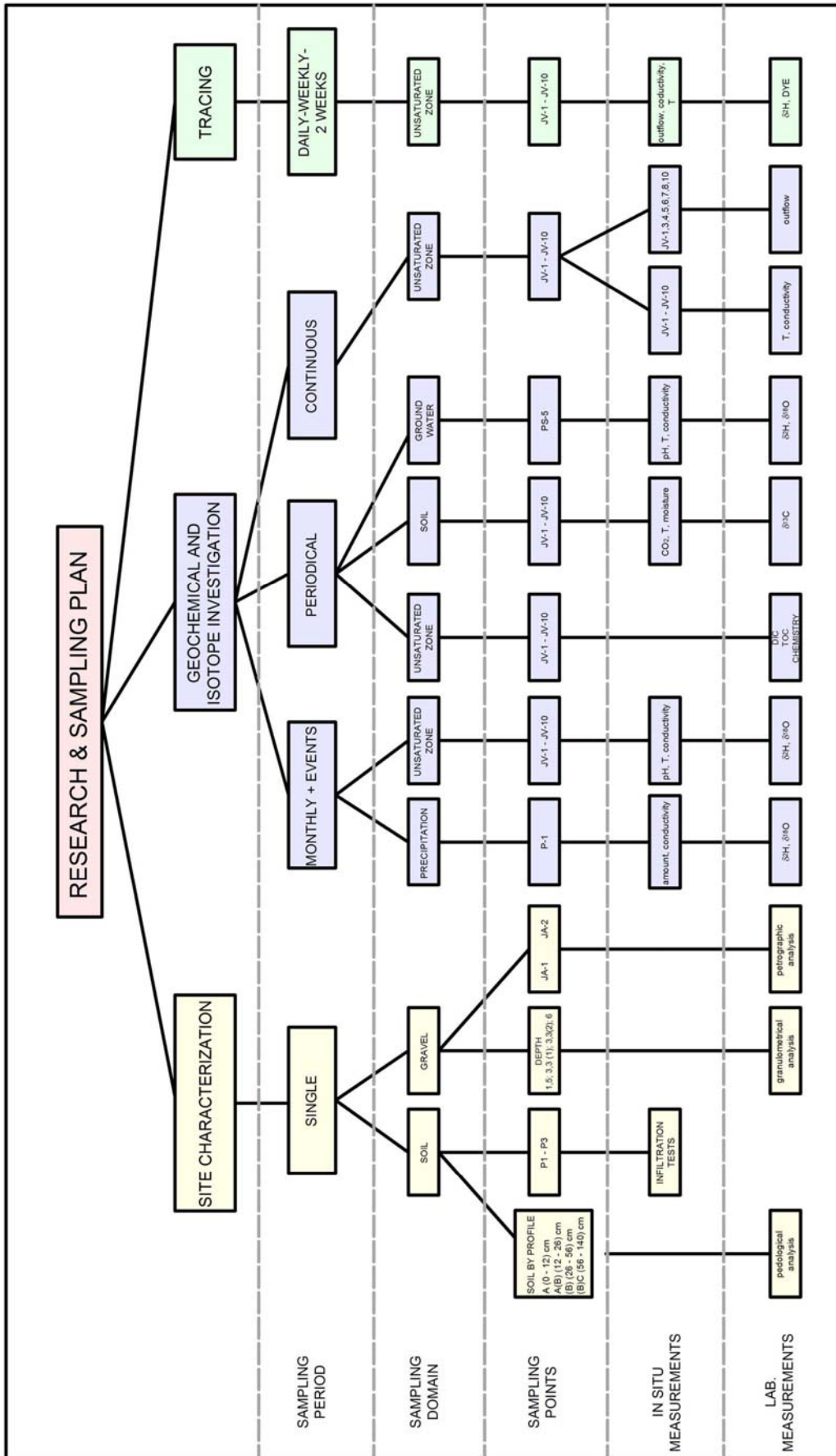


Figure 18: Research sampling plan

4.2 Experimental set-up

4.2.1 Lysimeter construction

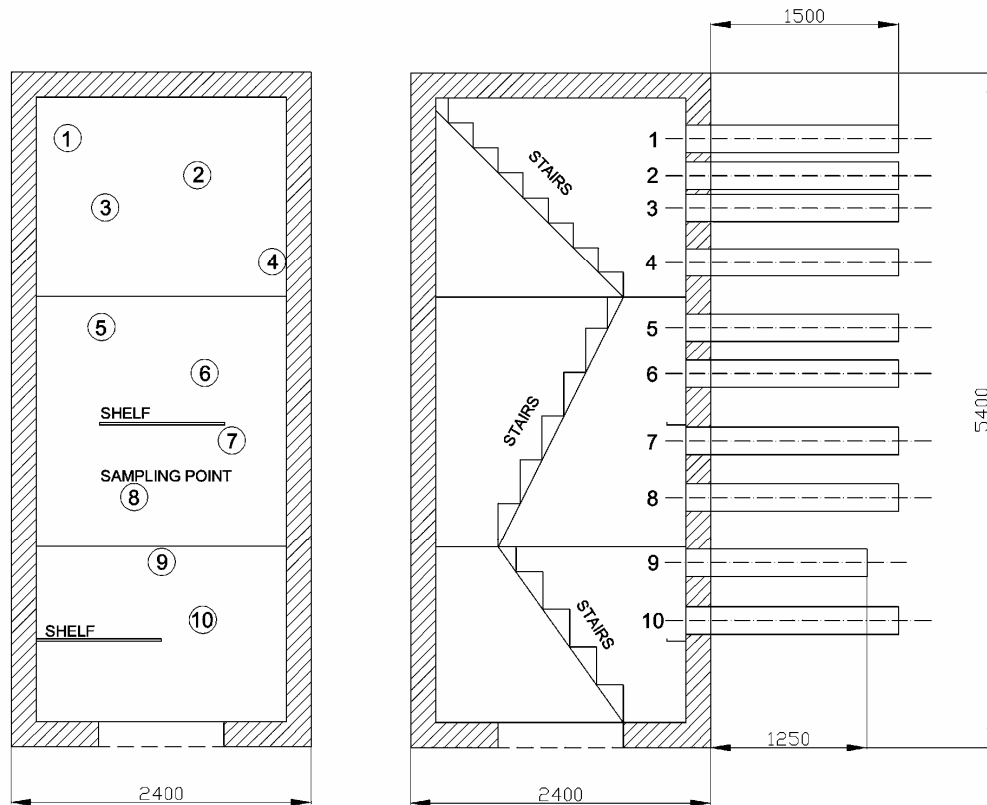


Figure 19: Lysimeter cross-section; Locations of sampling points from JV-1 to JV-10

Lysimeter design is presented in *Figure 19*. The basic idea was to construct a lysimeter to define unsaturated zone properties and to predict the possibility of contamination from nearby agriculture and urban areas. The lysimeter was designed as a concrete box, dimensions 2x2m, 5m deep, with walls 0.2m thick. The lysimeter was constructed so that gravel was excavated, and a concrete box with openings for equipment installation was inserted (*Figure 20*). To provide for an undisturbed wall of the unsaturated zone, wood bars protected the block to prevent stress relief of gravel during excavation. *Figure 21* shows the entrance and the inside of lysimeter.



Figure 20: Lysimeter construction



Figure 21: Entrance and the inside of lysimeter

Unsaturated zone water sampling system

There are 10 sampling and measuring points at different depths (JV-1 to JV-10, *Figure 19*). Sampling point position followed a randomized design by lysimeter width but at approximately equal distances by depth. Drainage samplers were installed for sampling groundwater in the unsaturated zone. The stainless steel drains are profiles 10cm X 10cm, 1.7 m long, with inverse inner perforated profiles (5x5 cm) and with a collection system on the end. The steel drains were inserted horizontally into the undisturbed wall using a hydraulic press. Drains of 1.5m length were installed in the unsaturated zone. Each sampling point was equipped with water collection system (*Figure 22*). The closed system was made up of one 400 ml glass bottle and collecting containers. Drains, both conductivity and outflow volume measuring systems installed before water collectors, and bottles were linked with small silicone tubes. The collecting system enables the sampling of outflow water at a fixed time, following the volume of outflow, and collecting the entire outflow water for a defined period.

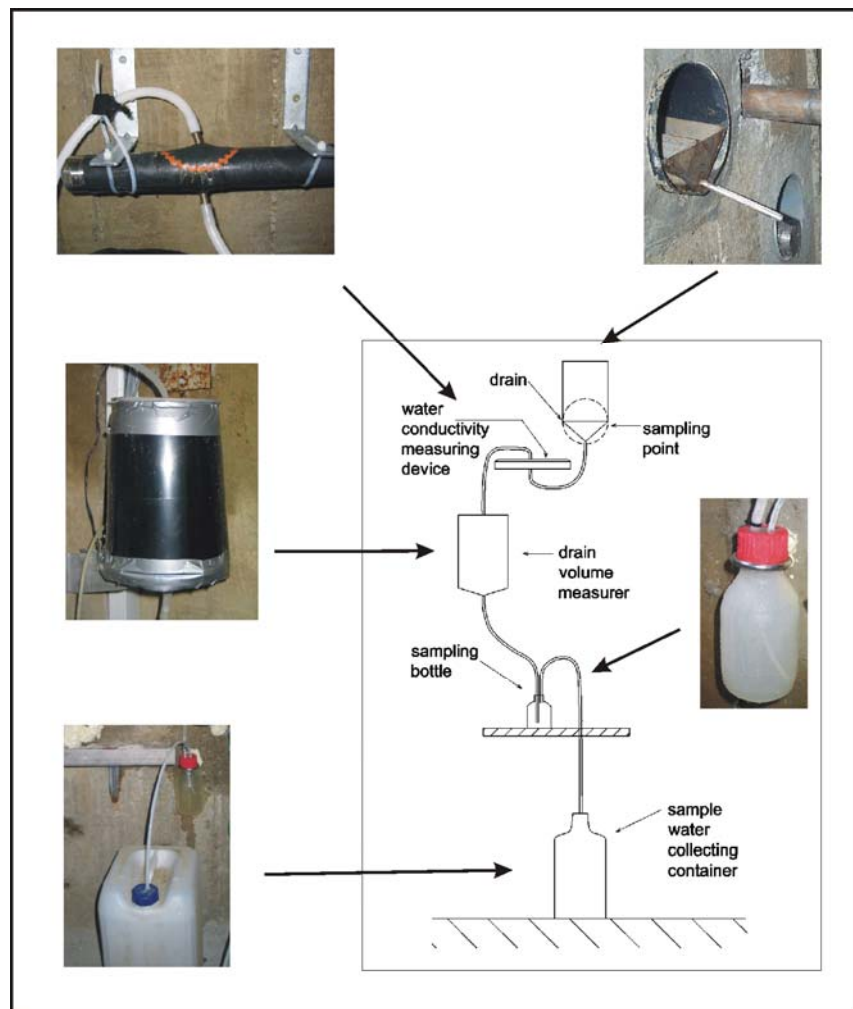


Figure 22: Sampling point set-up

Water conductivity, temperature and outflow volume measuring system

In all sampler exits (JV-1 till JV-10) conductivity and temperature of water are measured with automated conductivity and temperature probes PS-100 (ELTRA). In sampling points JV-1, JV-3, JV-4, JV-5, JV-6, JV-7, JV-8 and JV-10, the quantity of outflow (discharge) is measured also with automated rain gauges. All automated measurements were recorded on a 10 min basis.

Soil measurement system

Near each sampling point, measuring equipment for temperature, soil moisture and gas sampling was installed (*Figure 23*). All three components were inserted 1.5 m deep horizontally in the unsaturated zone at a time.



Figure 23: Soil measurement system

For measuring soil temperature the PS-100 sensors were used.

The same points were equipped with soil moisture meters. In coarse gravel it is almost impossible to measure water content. We chose equipment, which had adequate characteristics and predicted successful results. Soil moisture sensors that measure the moisture tension in the soil are read by the soil moisture meter Watermark. The measuring principle is similar to that of the gypsum block system. The special sensors, however, do not dissolve in the soil and have a more consistent distribution of pores thus enabling more accurate measurements. The meter internally converts the electrical resistance reading of the sensors to the tension or suction values. The soil moisture sensors can be used as a replacement for tensiometers. The soil moisture sensors have a measuring range of 0-200 kPa.

To sample gas in soil, copper tubes with airtight caps were inserted, which prevent air exchange between lysimeter and soil.

Precipitation

Precipitation rate was measured near lysimeter entrance using an automatic tipping bucket gauge set to record measurements every 5 min (*Figure 21*). The rain gauge system is used also for precipitation collecting for water sampling. The exit of rain gauge is connected by a tube to a glass bottle for precipitation collection.

4.2.2 Evaluation of experimental set-up

Lysimeter construction and most equipment testing were completed during the time of study. The results of investigations on lysimeter Selniška Dobrava showed that lysimeter design, both equipment selection and construction, were appropriate to research water flow in the unsaturated zone in a coarse gravel aquifer. The results show that the drainage samplers are suitable for groundwater collection in the unsaturated zone especially in a coarse gravel unsaturated zone. The measurements of the conductivity and temperature in outflow water indicate some disturbances in measurements. Nevertheless the data are already now useful to detect water flow dynamics in the unsaturated zone and recognize the differences in water composition during different seasons. The water outflow and the soil measuring systems are well constructed. The soil measuring system enables the sampling of gas and measuring of temperature and $p\text{CO}_2$ in the soil. But the selected Watermark sensors for moisture measuring are not appropriate to measure moisture in a coarse gravel environment. The purpose of these sensors is the control of irrigation in agriculture (also in coarse sand) but they are not useful for measuring moisture in the coarse gravel unsaturated zone. Yet this is the first equipment with which the differences of moisture content in such material were detected at all.

4.3 Sampling

Oxygen-18 and deuterium

Over a period of 3 years samples of groundwater in the unsaturated zone were collected monthly in containers at all ten sampling points (JV-1 till JV-10) at different depths in lysimeter to determine $\delta^{18}\text{O}$ isotope composition. A few times a year also a sample of groundwater in the monitoring well PS-5 was taken. Also precipitation was sampled monthly.

For a short time during the investigation, an extreme event of snow melting was studied. At the time of fast snow melting, a short-term daily sampling was performed for a few days. At the same time samples of precipitation and snow were collected.

The water was sampled in plastic bottles of 120 ml volume. Until the tracing experiment with deuterium, both $\delta^{18}\text{O}$ and $\delta^2\text{H}$ had been analyzed, and after April 2004 only $\delta^{18}\text{O}$ was measured in this study.

Carbon-13

Four times a year we performed the sampling of DIC in the unsaturated zone water and of CO_2 in the soil gas for $\delta^{13}\text{C}$ measurements. The water samples were taken from the first bottle, which is in the closed system, with 3ml syringes. We have used a gas evolution method that (a) avoids the use of toxic additives to prevent microbial activity, (b) requires only small sample volumes, and (c) works reliably and quickly even under difficult field conditions (e.g., lysimeters). 10 ml septum-capped Na-glass vials (Labco exetainer) are preloaded with a few droplets of phosphoric acid, capped, and the head space is flushed with He. In the field, the sample was injected into the exetainer using a needle syringe.

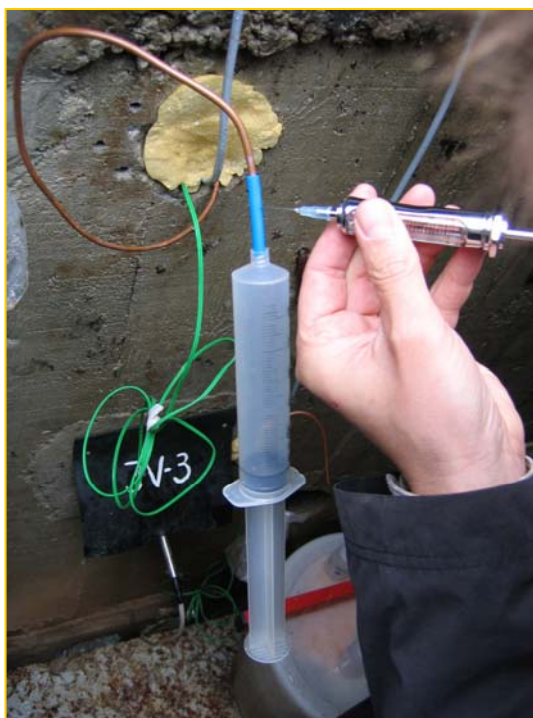


Figure 24: CO₂ carbon ($\delta^{13}\text{C}$) sampling

The samples for determination $\delta^{13}\text{C}$ content in the soil gas were taken with a preinstalled copper tube. A 50ml plastic syringe was connected to the soil gas probe (*Figure 24*). After flushing the volume of the probe with three strokes of the syringe an aliquot of soil gas was extracted using a gastight 5ml needle syringe. This aliquot was injected into a 10 ml autosampler glass vial (Labco exetainer) which has been flushed with He 6.0 prior to going into the field and which is sealed by a pierceable butyl rubber septum. One aliquot of soil gas was injected into the exetainer. During the injection the septum was briefly penetrated using a second hollow needle in order to allow for excess gas to escape and to avoid overpressure inside the exetainer. Extracting and subsequent injection of gas aliquots are performed slowly to minimize possible fractionation as a result of rapid gas transfer.

Tracers

The tracing test was performed on April 21, 2004. Deuterium and uranine were used as artificial tracers. After the tracing experiment, water was sampled in all outflow sampling points twice on the first day, then every day for one week, afterwards sampling has been performed weekly up to the present. Both tracers were detected in the same samples. As soon as possible they were delivered to the laboratory of JOANNEUM RESEARCH, Institute of Water Resources Management, Hydrogeology and Geophysics.

Geochemical investigations

Several times during the entire study period the sampling of outflow water to measure the concentrations of major anions and cations was performed. The samples were stored in plastic bottles of 250 ml volume.

At the beginning of the year 2004 a periodical sampling of outflow water to measure total organic carbon (TOC) was started. The water was collected in a 120 ml plastic bottle.

4.4 Measurements

4.4.1 Field measurements

Table 7 presents the list of in-situ measurement instruments and measuring period.

Table 7: In-situ measurement instruments

WATER	<i>Instruments</i>	<i>Measuring period</i>	<i>Automated measurements</i>
Temperature	WTW pH/Cond 340i; ELTRA	2001-2005	2005
pH	WTW pH/Cond 340i	2001-2005	
Conductivity (SEC)	WTW pH/Cond 340i; ELTRA	2001-2005	2005
Outflow volume/ Discharge	Wilmers precipitation sensors	2001-2005	2005
SOIL	<i>Instruments</i>	<i>Measuring period</i>	<i>Automated measurements</i>
Temperature	PT-1000 ELTRA	2005	JV-5; 2005
Partial pressure CO2	Draeger Pac III	2004 - 2005	
Moisture	Watermark	2005 - 2005	
PRECIPITATION	<i>Instruments</i>	<i>Measuring period</i>	<i>Automated measurements</i>
Quantity	Wilmers precipitation sensors	2002-2005	2005

Precipitation measurements

Precipitation was measured by Wilmers Precipitation sensor with a simple tipping bucket sensing element with an accuracy of +/- 4%. The catchment area and resolution meet the recommendations of the WMO (World Meteorological Organisation).

Outflow measurements

For mass balance calculations and transport modelling also the quantity of outflow water was measured weekly at the sampling points of unsaturated water. Wilmers Precipitation sensor was used as outflow quantity meter with an accuracy of +/- 4%. From the spring 2005 on the sampling points JV-1, JV-3, JV-4, JV-5, JV-6, JV-7, JV-8, JV-10 automated measurements were recorded on a 10 min basis with ELTRA datalogger.

Physico-chemical measurements in the water

In situ water measurements were performed on the outflow water in the first bottle of the sampling system at the time of sampling. The temperature, pH and conductivity (SEC) were measured. During the last year (period) of investigation also on-line combined temperature/conductivity in outflow water and temperature in soil were registered.

Temperature measurements

Water temperature in outflow water was determined by a temperature probe that was part of a pH/conductivity meter (WTW Multi-parameter instrument pH/Cond 340i) and has an accuracy of +/- 0.1 degrees Celsius.

In situ on-line water temperature was measured by combined temperature/conductivity ELTRA measuring system with data logger and temperature probe (sensor PT 1000) accuracy ± 0.3 degrees Celsius.

Soil temperature was measured using an ELTRA reader and sensor PT 1000 set up in the soil, accuracy ± 0.3 degrees Celsius.

Conductivity measurements

Electrical conductivity in water samples was measured using portable WTW Multi-parameter instrument pH/Cond 340i with standard conductivity cell TetraCon 325 and an accuracy of $\pm 1\%$ of values.

Conductivity measurements in the combined temperature/conductivity ELTRA system were determined with a conductivity probe range 10-2000 μS and with an accuracy of $\pm 2\%$.

pH measurements

The pH measurements were performed by using portable WTW Multi-parameter instrument pH/Cond 340i with SenTix 21 electrode with a measurement error of ± 0.01 . The instrument was calibrated each time with technical buffers (with pH 7.0 and 10.0 buffer solutions).

Partial pressure of CO₂

Regularly the percentage of CO₂ content in the soil gas was measured at the same location as the $\delta^{13}\text{C}$ samples were taken. Three volumes of 20 ml were pumped by a syringe from the copper tubes through the system CO₂ meter. Partial pressure of CO₂ was measured by the Drager single gas instrument Pac III with CO₂ Electrochemical Drager Sensor in the range 0-5% volume of CO₂.

Soil moisture measurements

Water content in the unsaturated zone was measured every time we sampled unsaturated zone groundwater. The Watermarks readings reflect soil water tension or suction. The meter internally converts the electric resistance reading of the sensors to these tension or suction values. The value of the moisture was read with soil moisture meter Watermark in centibars (kPa).

4.4.2 Stable isotope analysis

All stable isotope analyses were performed in the laboratory of JOANNEUM RESEARCH Forschungsgesellschaft mbH, Institute of Water Resources Management, Hydrogeology and Geophysics.

Deuterium

Deuterium was measured in continuous flow mode by chromium reduction using a ceramic reactor slightly modified from Morrison et al. (2001). A high temperature oven (HEKAtech, Germany) was fitted with an EuroAS 300 liquid auto sampler (EuroVector, Italy). The elemental analyzer (EA) was configured with a Cr packed reactor held isothermally at 1050 °C. Water samples contained in 2-ml capacity septa-sealed vials were placed onto the carousel of the

liquid auto sampler which was fitted with a 10µl injection syringe (SGE Europe). A sequence of one wash cycle of 3.5 µl volume was carried out for each sample prior to injection into the Cr reactor. Water samples were injected into septa-sealed injector port. The resulting water vapour was flushed into the reactor by the carrier helium gas via a 1-mm-i.d. stainless steel probe extending into the ceramic reactor tube (Al₂O₃). A sample size of 1.4 µl of water was used for the analysis. Water injected into the reactor was reduced by the Cr, resulting in the quantitative conversion to hydrogen gas according to Eq. 38.



The H₂ generated in the Cr reactor was carried in the He stream through the GC column to an open split sampling capillary and into the source of a Finnigan DELTA^{plus} continuous flow stable isotope ratio mass spectrometer.

Oxygen-18

Oxygen-18 was measured with a fully automated device for the classical CO₂ equilibration technique coupled to a Finnigan DELTA plus light stable isotope ratio mass spectrometer working in dual inlet mode (Avak and Brand, 1995).

Carbon-13

Carbon-13 in Dissolved Inorganic Carbon (DIC) was measured using a DeltaplusXP isotope ratio mass spectrometer operating in continuous-flow mode coupled to a GasBench II. More details of this method are given in Spötl (2005). The CO₂ in the headspace of the extainer was analyzed within few days.

Carbon-13 in Soil Air was measured using a DeltaplusXP isotope ratio mass spectrometer operating in continuous-flow mode coupled to a GasBench II. More details of this method are given in Spötl 2004. The samples are usually analyzed within 1–3 days.

4.4.3 Chemical analyses

Chemical analyses of major anions and cations were performed in the laboratory of JOANNEUM RESEARCH Forschungsgesellschaft mbH, Institute of Water Resources Management, Hydrogeology and Geophysics. TOC was measured in the laboratory of Ljubljana Waterworks.

The concentrations of major **anions** (Cl⁻, NO₃⁻, and SO₄²⁻) and **cations** (Na⁺, K⁺, Ca²⁺, and Mg²⁺) were measured by ion chromatography using a 2-channel Dionex DX-500 ion chromatography system. The alkalinity was estimated by using Metrohm 716 DMS titrino autotitrator system.

TOC was measured by SIST ISO 8245 standard testing method (Water quality – guidance for the determination of total organic carbon (TOC) and dissolved organic carbon (DOC)).

4.4.4 Tracers

Deuterium measurements are described above in chapter 4.4.2.

Uranine

The measurements of the fluorescent dye uranine were carried out with a Shimadzu RF-5000 spectrofluorophotometer. The dye was quantitatively measured using a synchron-scan method (Behrens, 1970) where the excitation and emission wavelengths are varied with a constant wavelength separation.

4.4.5 Overview of chemical and isotope analyses

Table 8 gives a list of analysed parameters with the sampling period.

Table 8: Analysed parameters with the measuring period

WATER	Compounds	Measuring time	Measuring period	Laboratory
Ions	Ca ²⁺ , Mg ²⁺ , Na ⁺ , K ⁺ , HCO ₃ ⁻ , Cl ⁻ , SO ₄ ²⁻ , NO ₃ ⁻	periodical	2004	JOANNEUM RESEARCH
	TOC	periodical	2004-2005	VO-KA
Stable isotopes	δ ¹⁸ O, δ ² H,	monthly, events	2001-2005	JOANNEUM RESEARCH
	δ ² H	weekly	2004-2005	JOANNEUM RESEARCH
Fluorescent dye	δ ¹³ C, DIC	periodical	2004-2005	JOANNEUM RESEARCH
	Uranine	weekly	2004-2005	JOANNEUM RESEARCH
SOIL GAS	Compounds	Measuring time	Laboratory	
Stable isotopes	CO ₂ Carbon-13C	periodical	2004-2005	JOANNEUM RESEARCH

4.5 Chemical data presentation

4.5.1 Water typology determination

For easier water typology determination some typical graphical plots for water composition presentation were used. The cations and anions ratios are presented on Piper and Stiff plots. For graphical presentation of analytical results also D'Amore et al. (1983) plots were used. Parameters represent relations between basic chemical components. Six parameters (A-F) represent values without units in a -+100 interval range.

$$\begin{aligned}
 A &= 100 \frac{HCO_3^- - SO_4^{2-}}{(-)} & B &= 100 \left(\frac{SO_4^{2-}}{(-)} - \frac{Na^+}{(+)} \right) \\
 C &= 100 \left(\frac{Na^+}{(+)} - \frac{Cl^-}{(-)} \right) & D &= 100 \frac{Na^+ - Mg^{2+}}{(+)} \\
 E &= 100 \left(\frac{Ca^{2+} + Mg^{2+}}{(+)} - \frac{HCO_3^-}{(-)} \right) & F &= 100 \frac{Ca^{2+} - Na^+ - K^+}{(+)} \quad (39)
 \end{aligned}$$

D'Amore classified four principal water types by the squared plots which are valid for standards. In *Figure 25* the comparison of principal water types in D'Amore and Piper plots is presented. Four principal water types are defined by CaSO_4 , CaCO_3 , NaCl and Na_2CO_3 in the plots.

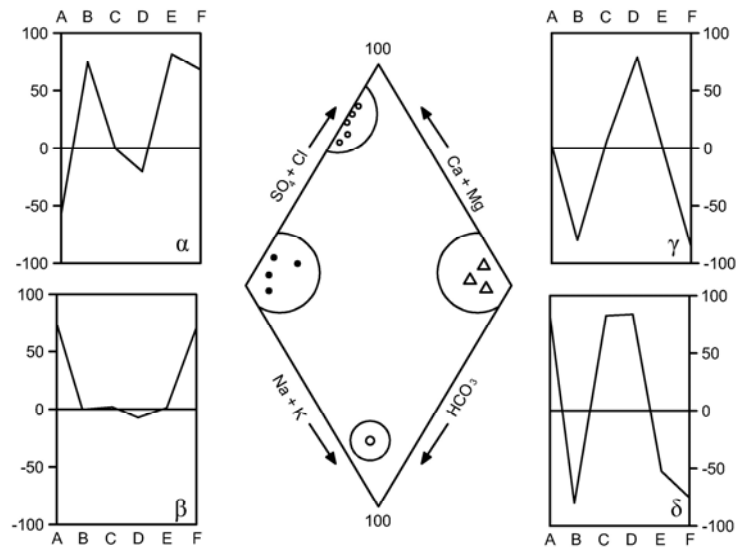


Figure 25: Principal water types in D'Amore plots (D'Amore et al., 1983)

- α – Water from anhydride series
- β – Water from carbonate aquifers
- γ – Water which circulates in deep aquifers, probably in metamorphic rocks.
- δ – Water from schists

D'Amore plots enable the determination of mixing of different water types.

4.5.2 Statistics

In data analyses only descriptive statistics were used to represent a set of data measurements.

Median – is the value midway in the frequency distribution

Mean – arithmetic average is defined as the sum of all observations divided by the number of observations.

The different geochemical and isotope data are presented by boxplots, which are a very useful and concise graphical display for summarizing the distribution of data set (Helsel and Hirsch, 1992). Boxplots provide visual summaries of

- the center of the data (the median - the center line of the box),
- the variation or spread (interquartile range - the box height)
- the skewness (quartile skew- the relative size of the box halves)
- presence or absence of the unusual values (“outside” or “far outside” values)

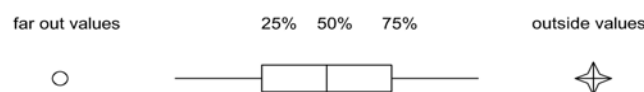


Figure 26: Boxplot presentation

Boxplot consists of the center line (mediana) splitting a rectangle defined by the upper and lower hinges (*Figure 26*). The whiskers are extended to the last observation within one step beyond either end of the box (adjacent values). One step equals 1.5 times the height of the box. Observations between one and two steps from the box in either direction, if present, are plotted individually with an asterisk (outside values). Outside values occur fewer than once in 100 times for data from normal distribution. Observations farther than two steps beyond the box are distinguished with a small circle (far-out values). These occur fewer than once in 300.000 times for normal distribution. The occurrence of outside or far out values more frequently than expected gives a quick visual indication that data may not originate from a normal distribution.

5 RESULTS AND DISCUSION

5.1 In- situ measurements

In 2004 the measurements of the soil and usaturated zone characteristics were started. For this reason one additional measuring point JV-0 was constructed 20 cm deep in the soil. In the *Annex B* the measurements of soil temperature, moisture and partial pressure are given.

Moisture

From the agricultural point of view, the moisture measurements show the following ranges:

-0-10 kPa	-Saturated soil
-10-20 kPa	-Correct soil moisture
-30-60 kPa	-Irrigation required (except loam soil)
-60-100 kPa	-Irrigation required also for loam soil
-100-200 kPa	-Dried-up soil

There were some problems with moisture measurements. The Watermarks's sensitivity was too low for coarse gravel detailed moisture measurements. The entire profile showed a very high field capacity for the whole time, which was presented by very low soil water tension. Irrespective of this, the measurements (Figure 27) indicated the drying of the profile in winter time. We assume that the unsaturated zone in Selniška Dobrava is very wet almost all the time. Only at measuring point JV-7 the water tension measurements never fell to zero which is attributed to local conditions. The maximum value 33 kPa was measured at JV-0. With the depth also the oscillation of water tension measurements decreased and the unsaturated zone became less dependent on drying and wetting. The conditions became more constant with the depth.

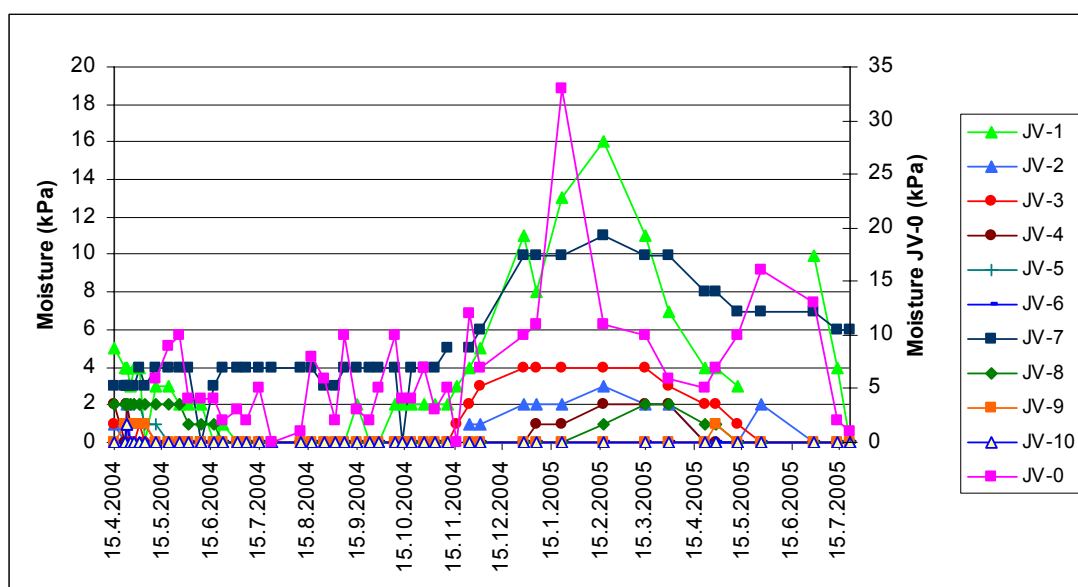


Figure 27: Moisture content by the time

CO₂ partial pressure

CO₂ partial pressure measurements are shown by boxplots and in the time plot (Figure 28, Figure 29), the statistics are in Table 9. Because of the instrument measuring limit (the highest level 5%), the maximum CO₂ partial pressure was recognized at that value. Maximum values (5%) and the largest range of measurements were detected at measuring point JV-6, where CO₂ partial pressure never fell to 0%. The ranges at JV-5, JV-7 and JV-8 followed it. The mean value at JV-6 was 2.24%, at JV-5, JV-7 and JV-8 the means were in the range from 1.31-1.58% Table 9. The mean values at other measuring points were sorted out to 1.02%. The largest values were recognized in summer time, in winter time the CO₂ partial pressure in all measuring points, except JV-6, fell to 0%. The profile (Figure 30) shows the increase of partial pressure with the depth up to JV-6, at greater depths values started decreasing. This phenomenon can be explained by local structure and organic matter content or by processes linked to the carbon cycle in the unsaturated zone described in chapter 2.4.

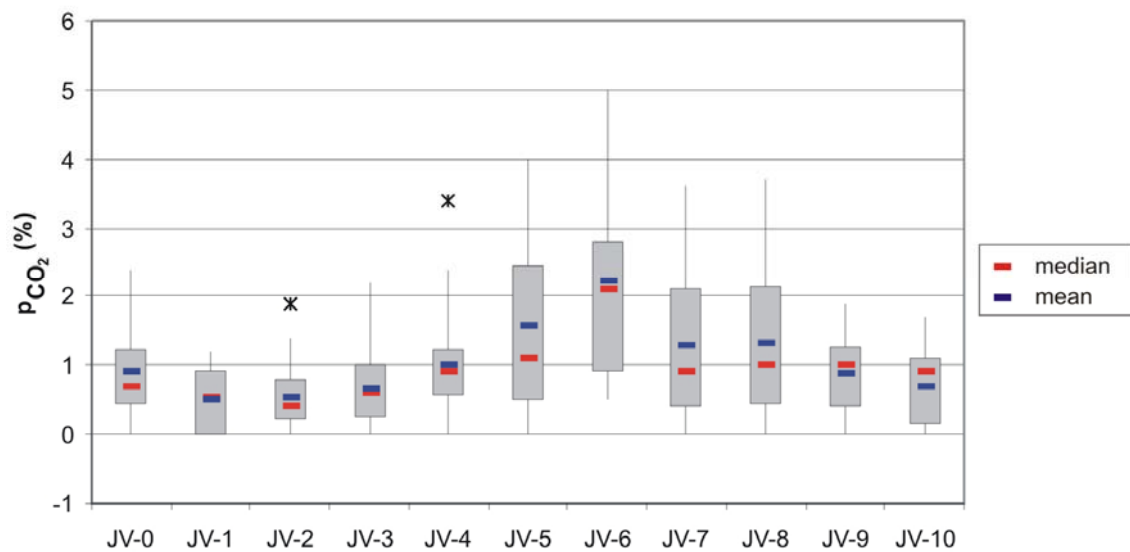


Figure 28: Boxplot of p_{CO_2} measurements

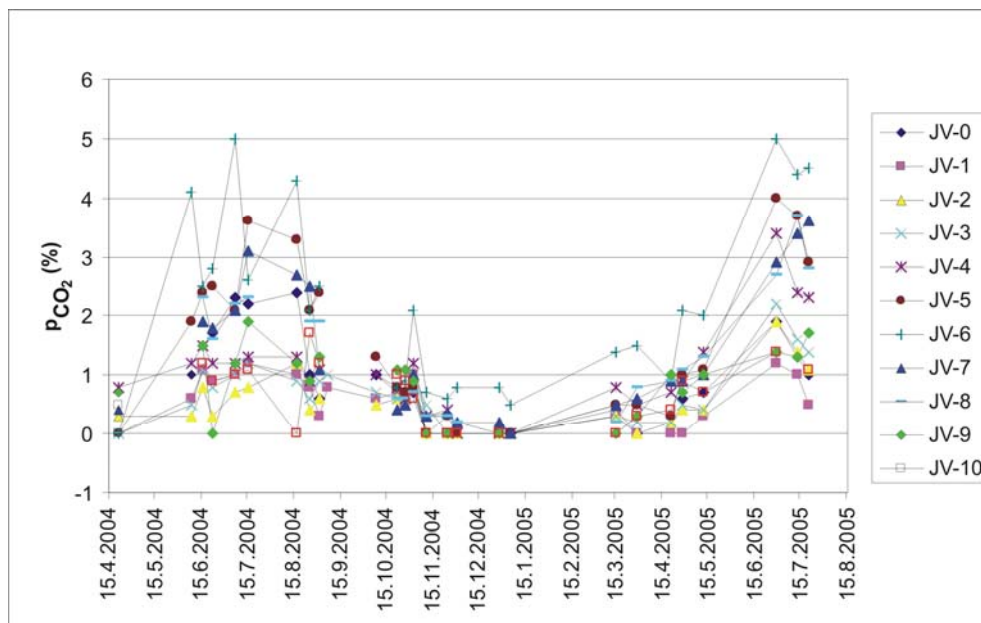


Figure 29: Time plot of p_{CO_2} measurements

Table 9: Statistics of p_{CO_2} measurements

CO ₂	JV-0	JV-1	JV-2	JV-3	JV-4	JV-5	JV-6	JV-7	JV-8	JV-9	JV-10
n	22	28	26	27	28	27	25	25	22	22	23
max.	2.4	1.2	1.9	2.2	3.4	4	5	3.6	3.7	1.9	1.7
min.	0	0	0	0	0	0	0.5	0	0	0	0
mean	0.91	0.52	0.52	0.67	1.02	1.58	2.24	1.31	1.31	0.88	0.70
st. dv.	0.77	0.44	0.48	0.54	0.74	1.34	1.50	1.14	1.03	0.58	0.53

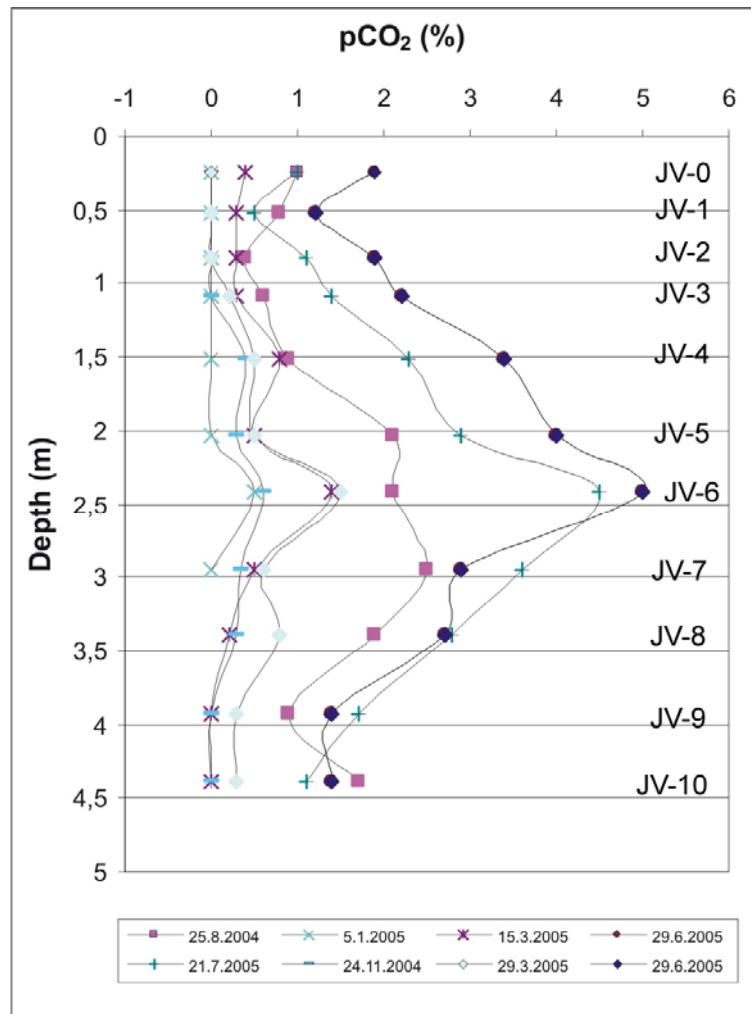


Figure 30: Profiles of p_{CO_2} measurements

Soil temperature

Measurements of soil (unsaturated zone) temperature are presented in boxplot (Figure 31), statistics are given in Table 10. Near the surface the measured values were more spread than at deeper measuring points. Temperature range decreased with the depth (Figure 32). Maximum and minimum values were reached at JV-0 (17.4°C and -3.8 °C), values at the deepest point JV-10 ranged from 2.5 °C to 11°C. Values below 0 °C were found up to JV-6 at a depth of 2.4 m. Figure 33 presents the temperature oscillations. Compared to air temperatures, the temperature values of the unsaturated zone are delayed. Extreme temperatures appeared at a later time at the deepest measuring points, for example in winter the temperature at JV-10 reached the lowest values in March, but at JV-1 already in January and February. Also the

temperature oscillations diminished with the depth. The mean value of temperature was 8.58 °C at the shallow point JV-0, and 7.25 °C at the deepest point JV-10.

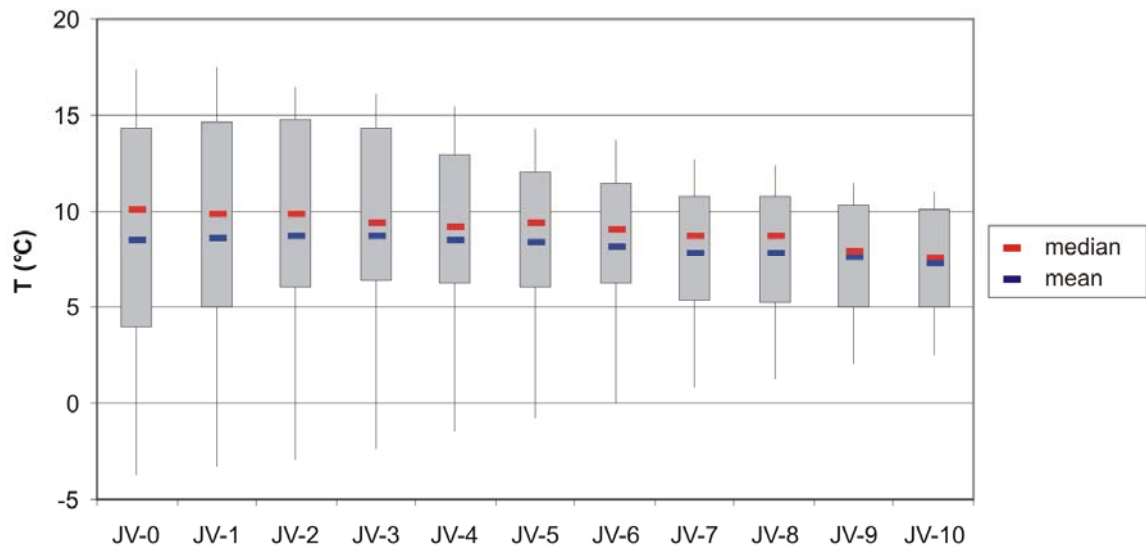


Figure 31: Boxplot of soil and unsaturated zone temperature measurements

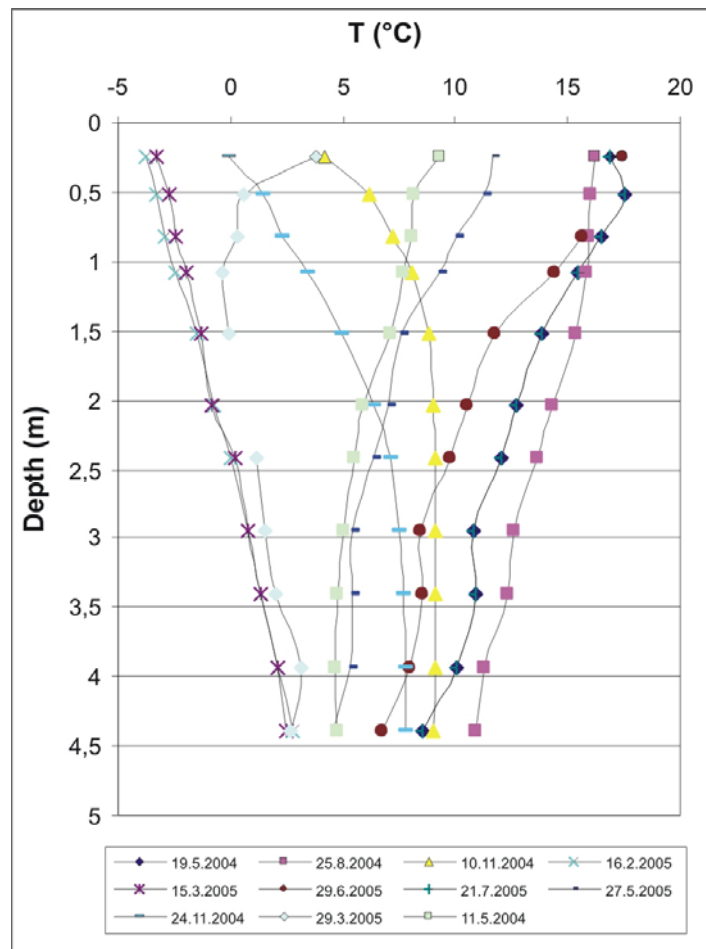


Figure 32: Profiles of soil and unsaturated zone temperature

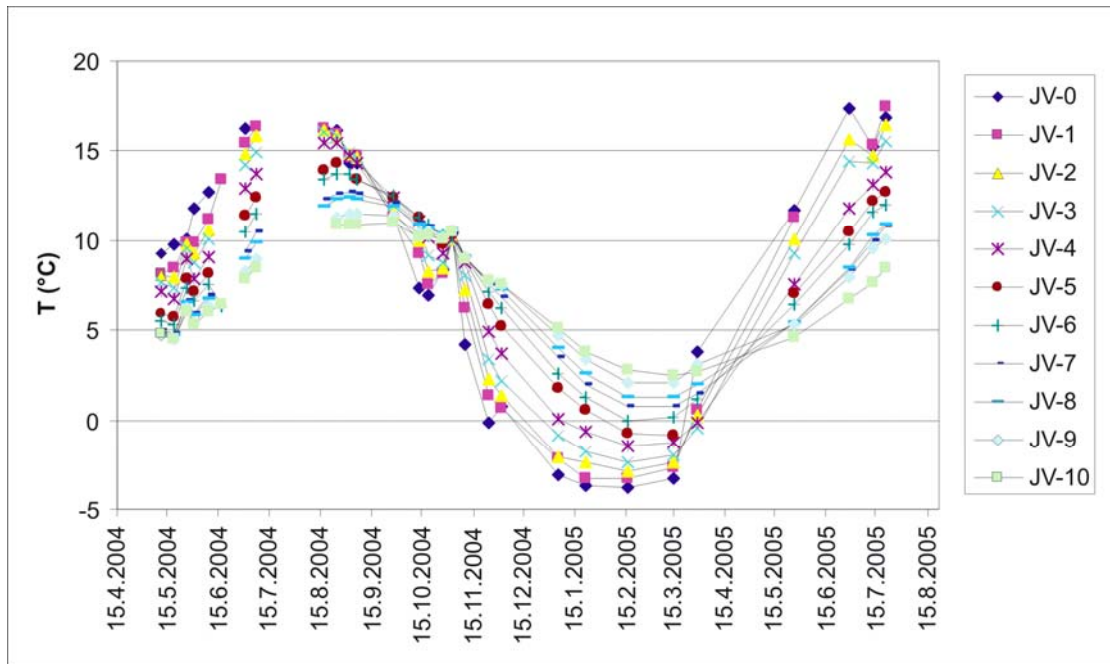


Figure 33: Time plot of soil and unsaturated zone temperature measurements

Table 10: Statistics of soil and unsaturated zone temperature measurements

<i>T</i>	<i>JV-0</i>	<i>JV-1</i>	<i>JV-2</i>	<i>JV-3</i>	<i>JV-4</i>	<i>JV-5</i>	<i>JV-6</i>	<i>JV-7</i>	<i>JV-8</i>	<i>JV-9</i>	<i>JV-10</i>
n	27	28	28	28	28	26	29	28	28	27	28
max.	17.4	17.5	16.5	16.1	15.4	14.3	13.7	12.7	12.4	11.5	11
min.	-3.8	-3.3	-2.9	-2.4	-1.5	-0.8	0	0.8	1.3	2.1	2.5
mean	8.58	8.65	8.74	8.73	8.56	8.40	8.19	7.88	7.90	7.58	7.25
st. dv.	6.94	6.62	6.37	6.01	5.33	4.43	4.20	3.78	3.56	3.07	2.76

Water

All results of conductivity, temperature and pH in-situ measurements in the outflow water of the unsaturated zone are presented in *Annex C*.

Boxplot of pH values (*Figure 34*) clearly shows the lowest values of precipitation (range 4.09-8.36; mean 6.02). The pH values of groundwater were in the range of oscillation values of groundwater in the unsaturated zone between 6.42 and 8.69, the range of means was between 7.44 and 7.65. In general the means of pH values at upper sampling points were slightly higher than at lower points.

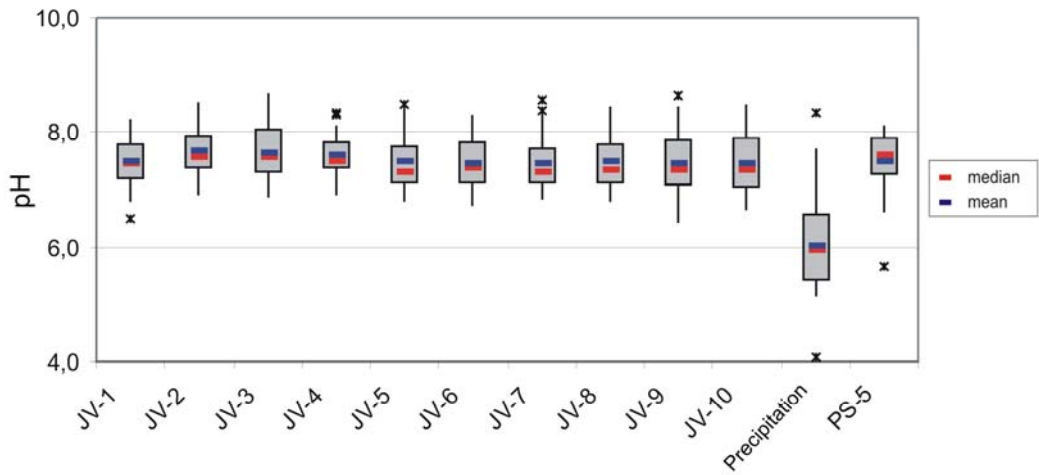


Figure 34: Results of in-situ measurements of pH

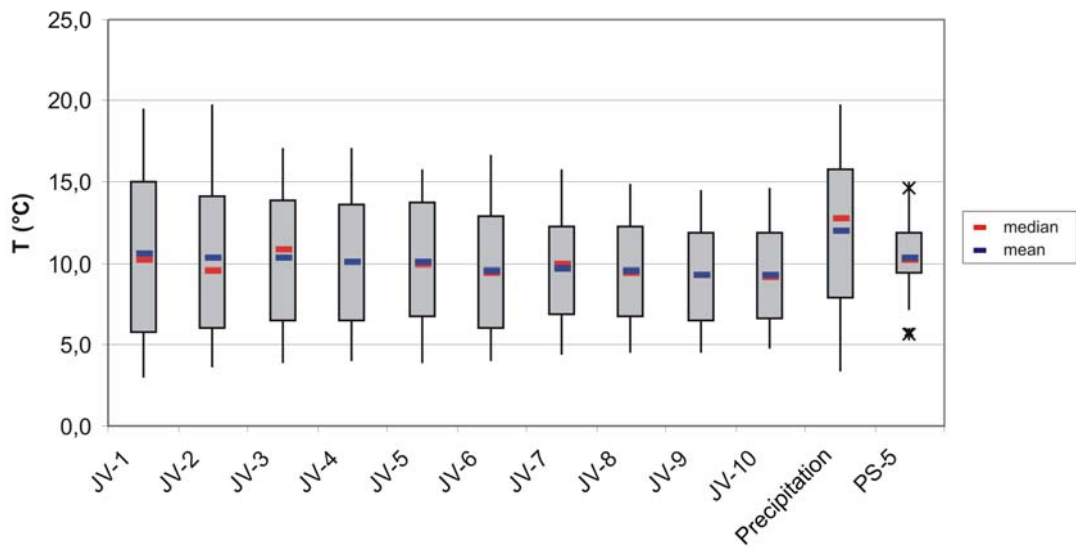


Figure 35: Results of in-situ water temperature measurements

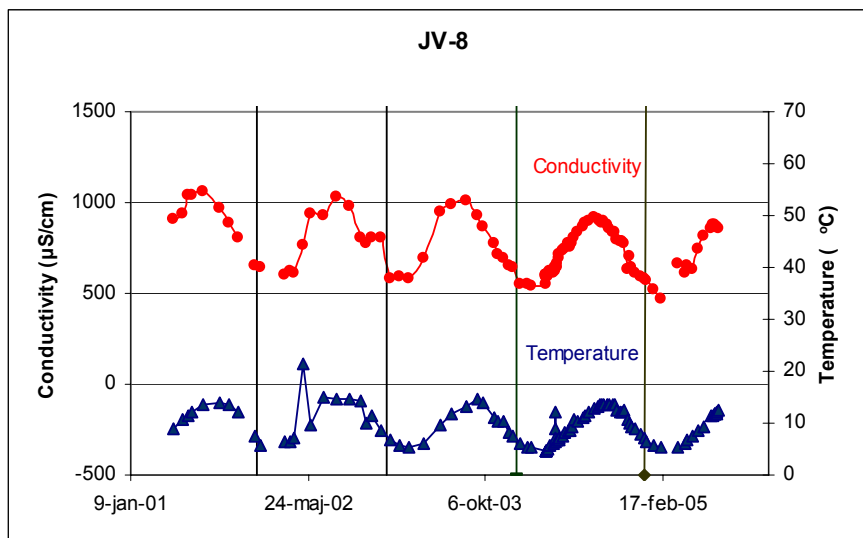


Figure 36: In-situ water conductivity and temperature measurement

Water temperature was measured in sampling bottles at the time of sampling. The boxplot of water temperature (*Figure 35*) shows higher values than the measurements in the soil of the unsaturated zone. This is due to higher temperatures in the lysimeter where the bottles were located. The mean temperature values of the samples were in the range 9.26-10.53, the precipitation temperature mean was 12.02 and groundwater's mean was 10.39 (*Table 11*). The plot shows no special characteristics in a particular range of measurements. From the diagram in *Figure 36*, where the conductivity and temperature of the water are presented at the same time, the seasonal effect can be observed for both parameters. The temperature oscillation at a particular point was between 10°C at the bottom of the lysimeter up to 15°C at upper points. The conductivity measurements oscillated approximately 500µS/cm in the year. The trend of conductivity values for the whole research period decreased. It can be assumed that the dissolution effect of the concrete in the construction is present. The plots in *Annex D* show that the increasing of conductivity values passed with the increase of temperature values. It is assumed that increasing conductivity depends mostly on organic matter and organism activity which correlated with temperature and have impact on the presence of CO₂ and indirectly on carbonate dissolution and water conductivity. These processes are described more in detail in the next chapter.

Table 11: Statistics of pH, temperature and conductivity measurements

pH	JV-1	JV-2	JV-3	JV-4	JV-5	JV-6	JV-7	JV-8	JV-9	JV-10	Precipitation	PS-5
n	30	49	40	66	66	45	57	83	86	86	55	39
max.	8.22	8.52	8.69	8.35	8.50	8.29	8.55	8.45	8.63	8.49	8.36	8.12
min.	6.50	6.89	6.87	6.91	6.80	6.72	6.83	6.79	6.42	6.64	4.09	5.65
Median	7.46	7.58	7.56	7.52	7.32	7.40	7.30	7.35	7.36	7.34	5.95	7.59
Mean	7.50	7.68	7.65	7.62	7.50	7.44	7.46	7.50	7.47	7.47	6.02	7.51
st.dev.	0.44	0.42	0.50	0.36	0.47	0.42	0.45	0.45	0.50	0.51	0.83	0.49

T-Water	JV-1	JV-2	JV-3	JV-4	JV-5	JV-6	JV-7	JV-8	JV-9	JV-10	Precipitation	PS-5
N	32	57	51	81	83	56	73	101	105	103	67	40
max.	19.5	19.8	17.1	17.1	15.8	16.7	15.8	14.9	14.6	14.7	19.8	14.7
min.	2.9	3.6	3.8	4	3.8	4	4.3	4.5	4.5	4.7	3.3	5.6
Median	10.15	9.6	10.8	10.1	10	9.4	10	9.5	9.3	9.2	12.8	10.2
Mean	10.53	10.28	10.35	10.07	10.14	9.56	9.66	9.55	9.34	9.26	12.02	10.39
st.dev.	5.44	4.69	4.06	3.84	3.82	3.84	3.36	3.12	3.08	3.00	4.87	2.10

Conductivity	JV-1	JV-2	JV-3	JV-4	JV-5	JV-6	JV-7	JV-8	JV-9	JV-10	Precipitation	PS-5
N	32	58	51	81	84	57	74	102	106	104	67	39
max.	1064	1281	1651	1398	982	1154	1269	1060	1277	1341	282	543
median	443	738	729	911	600	726	830	770	775	819	31	373
min.	189	412	355	610	437	547	636	473	363	463	9	312
mean	502	767	830	933	633	758	872	756	760	832	51	379
st.dev.	217	259	267	207	127	148	146	143	228	240	55	31

The situations in *Figure 37*, where the conductivity measurements are presented, show quite a different range and mean values of conductivity at particular points. The highest conductivity was measured at JV-3, the lowest at JV-1. At the sampling points in the upper part of the lysimeter the oscillation of the measurements was higher than in the middle and lower part. The mean values showed differences (*Table 11*). It could be concluded on different retention times, different dynamics conditions and mixing processes of the ground water in the unsaturated zone at a particular part of the lysimeter. The highest mean values were measured at JV-4 (933 µS/cm). Beside JV-1 (502 µS/cm) the lowest mean values (633 µS/cm) were detected at JV-5. At sampling points JV-6, JV-8, JV-9 and JV-10 the mean values moved from 756 to 832 µS/cm. In the same range were also the mean values of JV-2 and JV-3 but at those sampling points

the standard deviations were higher. The explanation of the higher conductivity values as were expected is in chapter 5.2.

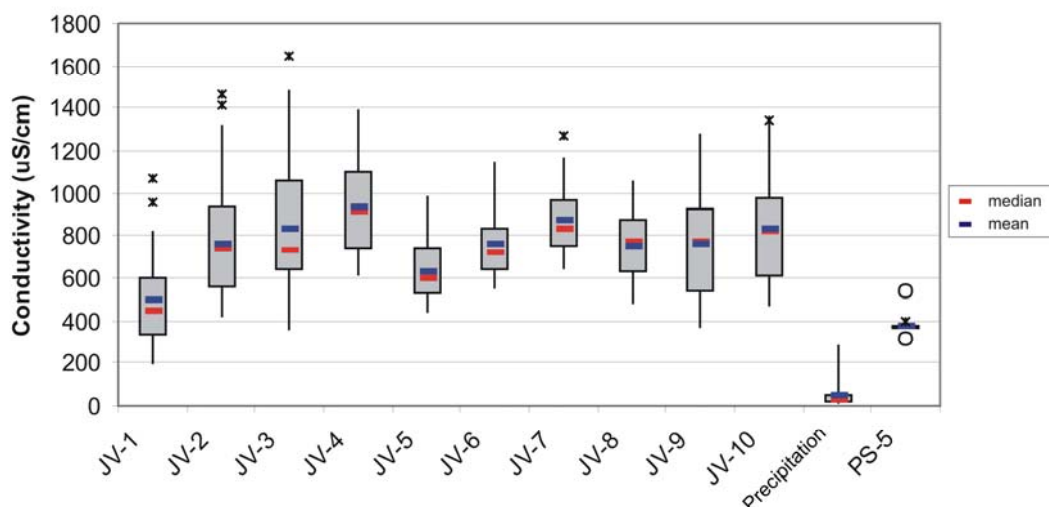


Figure 37: Results of in-situ conductivity measurements

5.2 Geochemical characteristics of the unsaturated water

The chemical analyses during the first period of lysimeter's operation showed oscillations in sulfate concentrations. Concrete leaching was assumed to be taking place. So the sampling of the unsaturated water was then performed in 2004 at different seasons. Results of chemical analyses are given in *Annex E*. To define the influence of the rock (gravel) on groundwater composition in the unsaturated zone, the chemical composition was studied. For the individual sampling points, the mean anion and cation values were calculated for the whole sampling period (*Table 12*). Based on the calculated relation of the ions, the plots for typological diagrams were constructed. The results are presented in Piper and D'Amore plots (*Figure 38*, *Figure 39*) and in Stiff plots enclosed in *Annex F*. The calculated part of individual cations and anions in per cent are presented in *Table 13* and *Figure 40*.

Table 12: Mean values of chemical analyses results

Sampl. points	n	pH	SEC	NO₃⁻	SO₄²⁻	Cl	Ca²⁺	Mg²⁺	Na⁺	K⁺	HCO₃³⁻
	Cl(n-1)		uS/cm	mg/l	mg/l	mg/l	mg/l	mg/l	mg/l	mg/l	mg/l
JV-1	2	7.80	510	12.0	9.3	1.32	102.8	6.8	3.6	10.8	348.0
JV-2	3	7.83	630	9.3	13.4	0.94	99.2	10.5	5.0	11.9	361.0
JV-3	2	8.07	892	21.7	25.9	0.68	170.0	14.1	6.3	17.7	569.2
JV-4	3	7.76	873	5.9	10.4	1.04	159.2	13.5	5.0	24.9	594.8
JV-5	3	7.73	636	16.9	24.2	0.75	97.5	11.6	10.8	18.9	356.1
JV-6	3	7.55	676	31.3	47.4	0.88	94.1	16.6	30.9	8.5	360.9
JV-7	3	7.60	826	24.4	54.3	0.76	111.5	18.8	33.9	5.0	397.5
JV-8	3	7.64	743	18.3	46.4	0.95	118.2	16.5	15.4	2.4	396.0
JV-9	3	7.63	788	18.2	39.7	0.78	127.5	19.1	14.3	10.5	455.3
JV-10	4	7.68	870	28.6	53.9	2.07	134.4	24.8	16.1	4.0	377.5

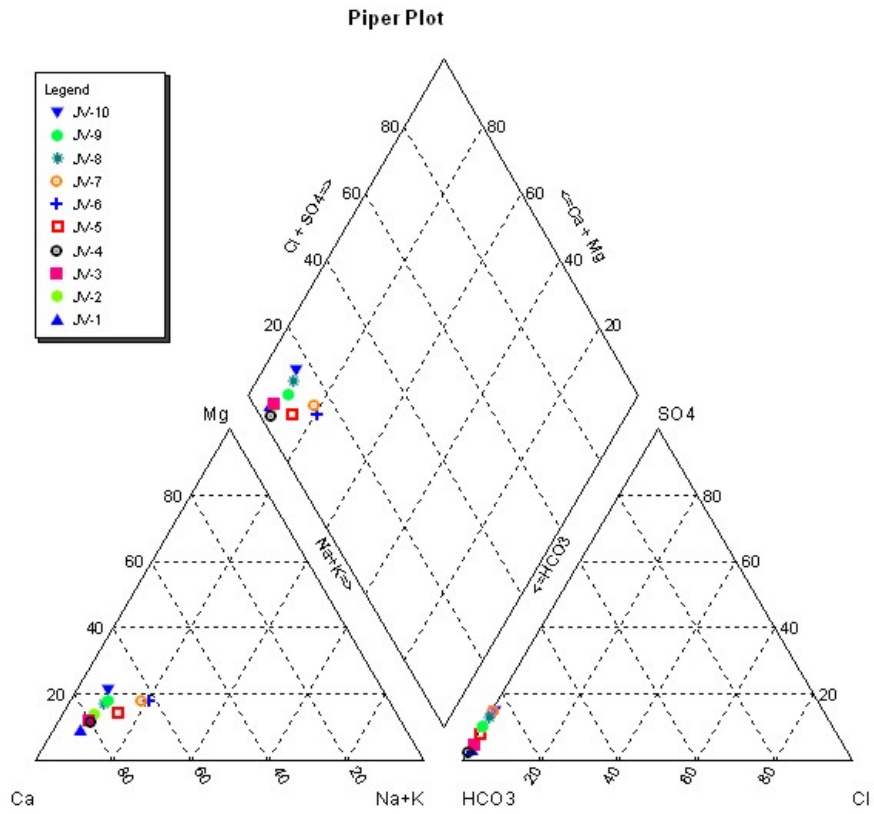


Figure 38: Piper plot

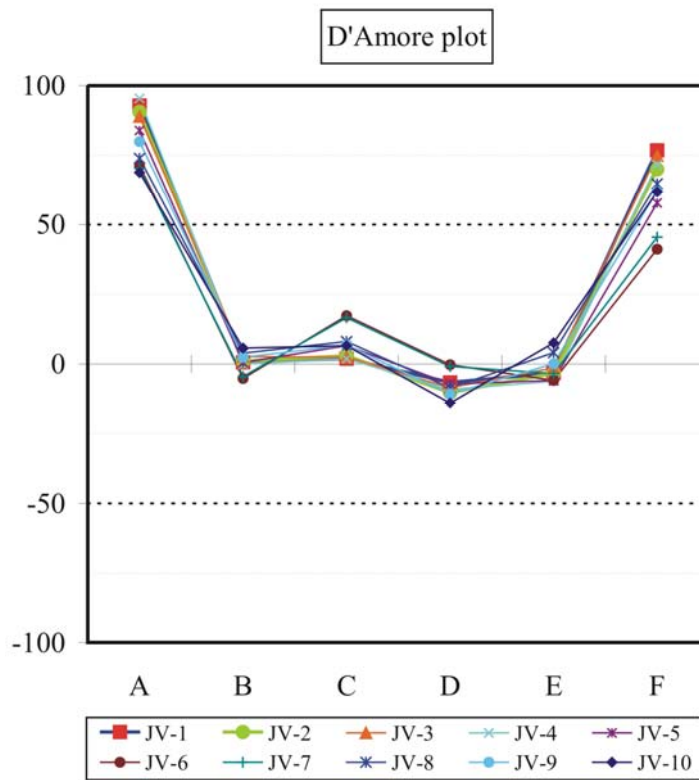


Figure 39: D'Amore plot

Table 13: Percentage of cations and anions

%	Ca ²⁺	Mg ²⁺	Na ⁺	K ⁺	Cl	HCO ³⁻	SO ₄ ²⁻
JV-1	83.80	9.13	2.58	4.49	0.63	96.12	3.26
JV-2	78.09	13.67	3.42	4.82	0.42	95.08	4.50
JV-3	81.83	11.15	2.66	4.36	0.19	94.35	5.45
JV-4	80.16	11.23	2.18	6.43	0.29	97.54	2.16
JV-5	71.83	14.08	6.94	7.15	0.33	91.75	7.92
JV-6	61.63	17.89	17.64	2.84	0.36	85.39	14.25
JV-7	63.84	17.78	16.91	1.47	0.28	84.97	14.75
JV-8	73.84	16.97	8.41	0.77	0.36	86.73	12.91
JV-9	72.07	17.83	7.06	3.05	0.26	89.79	9.94
JV-10	70.20	21.39	7.34	1.07	0.79	83.97	15.24

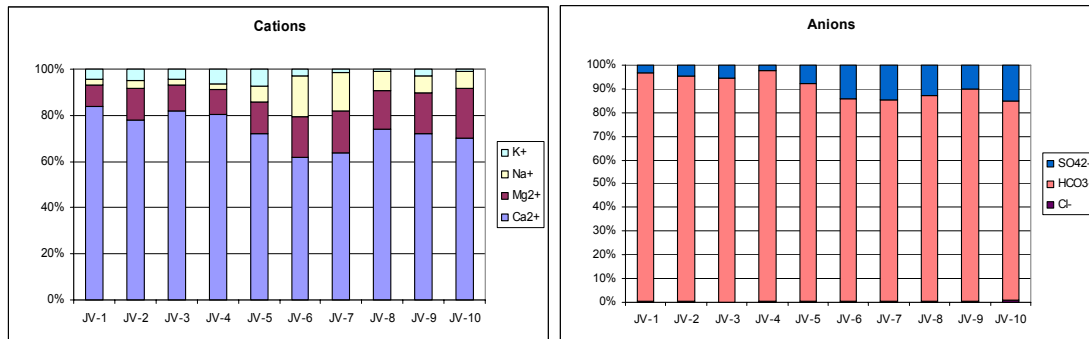


Figure 40: Bar plots of principal cations and anions

The results show that the water is Ca-HCO₃ type of water except JV-10 which is defined as Ca-Mg-HCO₃ water, because Mg concentrations exceed 20% of the total cations. With the depth of the sampling point also the share of carbonate, calcium and potassium declined, on the other hand the share of sodium, magnesium and sulfate rose. The mineralization of water in the unsaturated zone was relatively high. The diagrams of relations between ions and conductivity in *Annex G* show that there are some linear correlations between HCO₃⁻, Ca²⁺ and conductivity and also between Na⁺ and SO₄²⁻. Based on these results and correlations (*Table 14*) it was inferred that calcite dissolution is the main mineralization source. Sulfate was connected with sodium and the influence of concrete leaching was presumed.

To study the geochemical processes in the coarse gravel unsaturated zone, several samplings of isotope δ¹³C were performed in unsaturated zone air, δ¹³C-DIC and TOC in outflow water. The samples were taken in one-year period with all four seasons included. The measurements were compared with in-situ measurements of both pCO₂ and T in the unsaturated zone and water conductivity measured at approximately the same time. *Annex H* and *Table 15* present measurements with the mean values. All parameters are shown in the same plot in *Figure 41*. A comparison of value profiles by the depth made on the basis of mean values is presented in *Figure 42*. TOC was measured in outflow water to detect the presence of organic matter. During 2005 the TOC values increased due to unknown reason.

Table 14: Correlation coefficients of principal water components and conductivity

n		pH	Cond.	NO3	SO4	Cl	Ca	Mg	Na	K	HCO3
28	pH	1.000									
28	SEC	-0.689	1.000								
26	NO ₃ ⁻	-0.621	0.550	1.000							
28	SO ₄ ²⁻	-0.122	0.200	0.479	1.000						
18	Cl ⁻	0.300	-0.242	-0.375	-0.062	1.000					
28	Ca ²⁺	-0.571	<u>0.890</u>	0.434	-0.085	-0.157	1.000				
28	Mg ²⁺	-0.707	0.734	0.648	0.603	-0.019	0.520	1.000			
28	Na ⁺	-0.080	0.117	0.480	<u>0.862</u>	-0.279	-0.167	0.402	1.000		
28	K ⁺	-0.052	0.350	0.050	-0.474	-0.356	0.498	-0.209	-0.280	1.000	
28	HCO ₃ ⁻	-0.657	<u>0.901</u>	0.403	-0.121	-0.183	<u>0.977</u>	0.554	-0.168	0.519	1.000

Table 15: Mean values of geochemical measurements in the period 2004-2005

MEAN	JV-1	JV-2	JV-3	JV-4	JV-5	JV-6	JV-7	JV-8	JV-9	JV-10
pCO2	0.58	0.73	0.90	1.38	1.78	2.48	1.70	1.70	1.25	1.05
13C	-25.05	-26.06	-27.65	-25.03	-25.93	-25.39	-24.34	-24.48	-25.50	-25.42
DIC	-17.10	-16.86	-16.64	-16.74	-16.62	-16.92	-16.30	-16.34	-16.29	-16.90
Conduct.	744	789	980	952	675	740	870	776	755	786
TOC		39.35	25.53	49.55	30.28	26.35	35.78	25.13	28.08	33.25

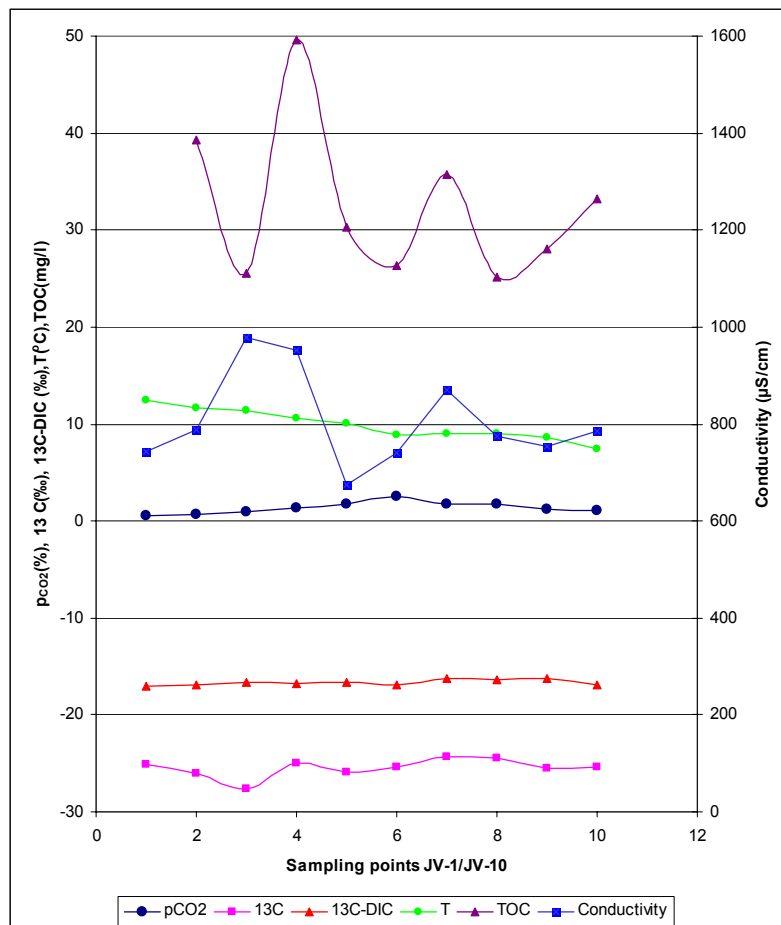


Figure 41: Mean values of geochemical parameters in unsaturated zone

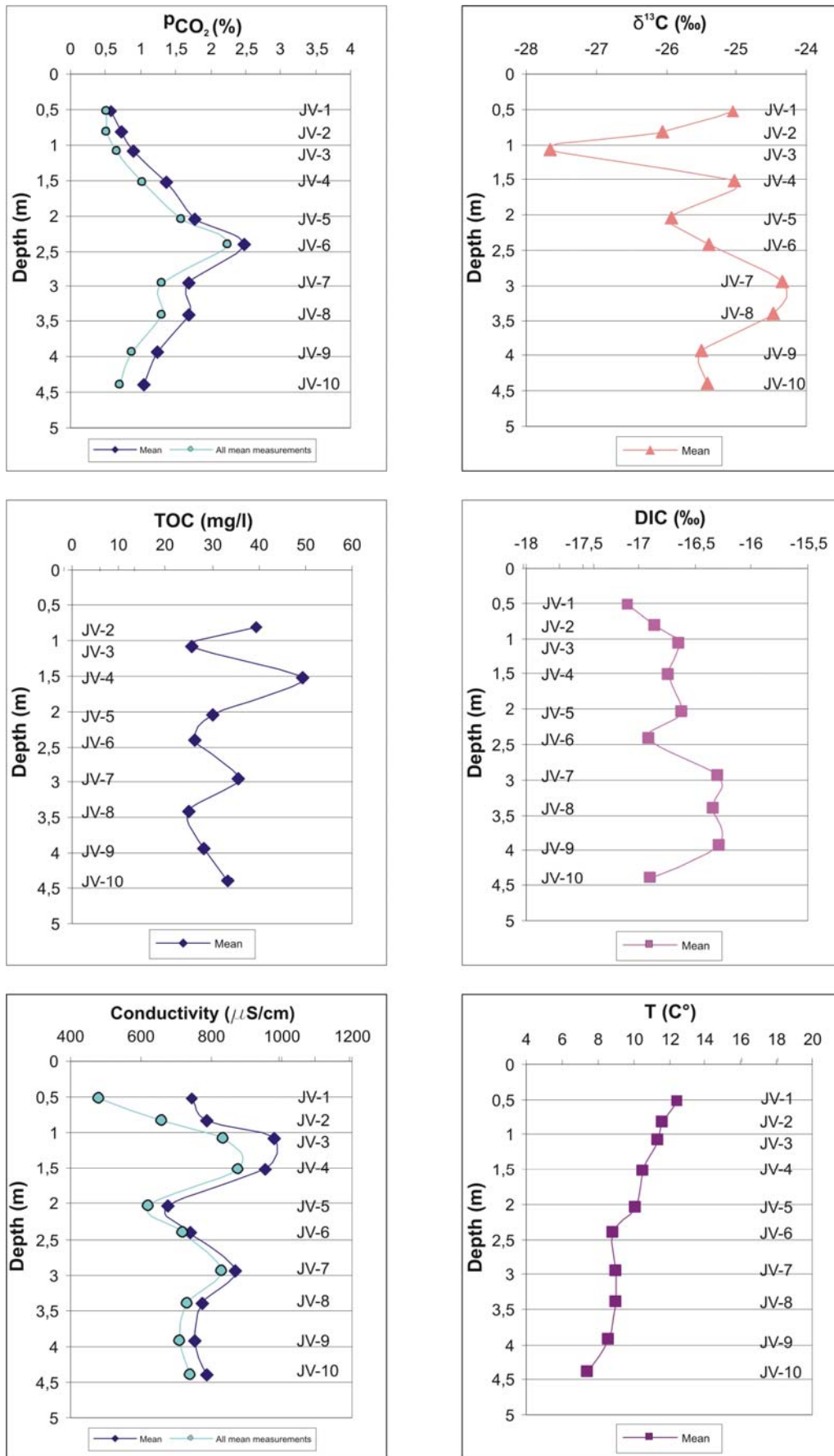


Figure 42: Profiles of mean values of geochemical measurements in the period 2004-2005

The results show that, as it was found out in the previous chapter, the annual mean temperature of the unsaturated zone air decreases with depth and the partial pressure of CO₂ increases up to sampling point JV-6 and then starts decreasing. The δ¹³C values of CO₂ oscillated between -27.65‰ and -24.34‰, which values indicate an organic source of CO₂ from plant breathing, decay and microorganism activity. The results correspond with the TOC values the means of which are in the range between 25mg/l and 50 mg/l, indicating the presence of organic matter. The δ¹³C – DIC values in the water ranged between -17.1‰ and -16.3‰.

5.2.1 Geochemical processes in the unsaturated zone

The main subject of this discussion is a description of the geochemical processes in coarse gravel unsaturated zone which causes surprisingly high values of water conductivity which oscillate with seasons. There is the question of the high mineralization source. Correlations among chemical components in the water and conductivity (*Figure 43, Annex G*) show that carbonate is the principal source of mineralization. CO₂ plays an important role in the control of chemical and biological processes which are the source of mineralization. The TOC measurements in the unsaturated water showed the presence of organic matter which directly influenced the production of CO₂ and carbonate dissolution in the entire lysimeter profile. Also ¹³C values of CO₂ indicate an organic source of CO₂. When the water came in contact with carbonate rocks, the dissolution of calcite, connected with the consumption of CO₂, was started. It took some time until the chemical-isotopic equilibrium was reached. Calcite dissolution also resulted in higher water mineralization. The oscillations of conductivity measurements (*Annex D*) at different seasons showed the connections between seasonal temperature variations, CO₂ production and carbonate dissolution. The highest p_{CO2} was in the area of sampling point JV-6. The lower conductivity and increase of sodium and sulfate parts in mineralization at this level led to the conclusion that part of the CO₂ is consumed in reactions with concrete or that there is locally a layer with clay minerals which caused ion exchange between water and rock.

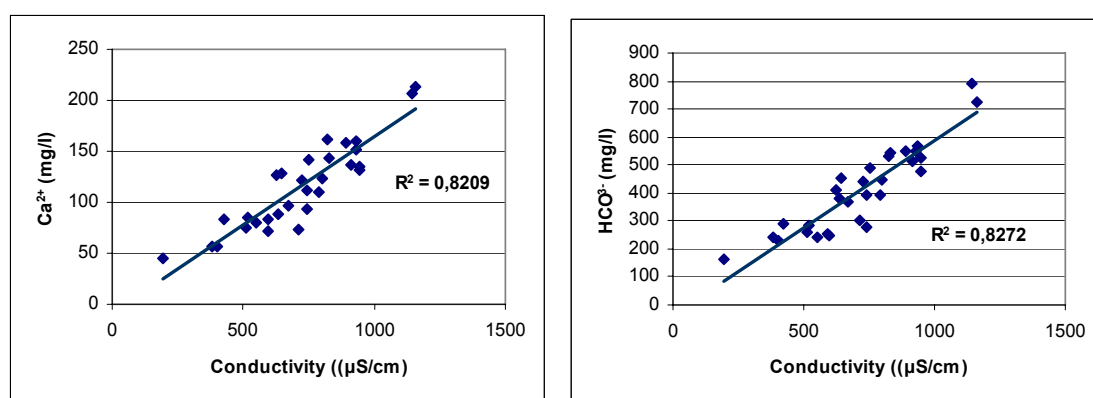


Figure 43: Regressions among Ca²⁺, HCO₃⁻ and conductivity

Miotke (1972) explains that CO₂ originates in the upper part of the soil and moves downwards. The precipitation acts as a kind of plug which pushes the gas. It is evident from previous research and literature that the concentration of CO₂ usually increases with soil depth (Miotke 1972). Heavy precipitation washes out CO₂ from the soil and it takes some time before the partial pressure reaches the earlier value. This interpretation can explain the increase of p_{CO2} with depth and the increase of p_{CO2}-related water mineralization. When the values of p_{CO2} decreased deeper from JV-6 location also the conductivity oscillations became less expressive.

Correlations between conductivity, CO₂ and temperature in all sampling points (*Table 16*) showed a higher correlation between p_{CO2} and temperature in the upper part of the lysimeter, while the correlation between conductivity and p_{CO2} became more expressive in the lower part. This can be explained by the assumption that CO₂ originates in the upper part of the unsaturated zone and moves downwards where, in equilibrium with carbonate, it causes water

mineralization. Seasonal occurring of CO₂ explains the correlation with temperature in the upper part of the lysimeter; in the lower part the temperature is more constant and seasonal oscillations of water mineralization depend more distinctly on p_{CO2} values.

Table 16: Correlations between conductivity, CO₂ and temperature

	JV-1	JV-2	JV-3	JV-4	JV-5	JV-6	JV-7	JV-8	JV-9	JV-10
Conductivity/CO2	0,274	0,553	0,576	0,455	0,794	0,830	0,862	0,808	0,913	0,921
Conductivity/T	-0,414	0,656	0,693	0,900	0,566	0,504	0,713	0,796	0,584	0,410
T/CO2	0,749	0,730	0,742	0,545	0,647	0,472	0,497	0,481	0,598	0,482

n	JV-1	JV-2	JV-3	JV-4	JV-5	JV-6	JV-7	JV-8	JV-9	JV-10
Conductivity/CO2	6	13	15	18	17	11	17	17	18	16
Conductivity/T	6	13	15	18	17	11	17	18	19	20
T/CO2	20	20	20	20	18	19	18	17	18	16

5.3 Isotope composition results of the long term monitoring

Results of isotope composition measurements of the $\delta^{18}\text{O}$ and $\delta^2\text{H}$ are added in *Annex I*. In *Figure 44*, *Figure 45* the results are presented in boxplots. The statistics are given in *Table 17*. Because of the tracing experiment with deuterated water in April 2004, the measurements of $\delta^2\text{H}$ isotope composition in monthly collected water in the unsaturated zone were performed only until this date.

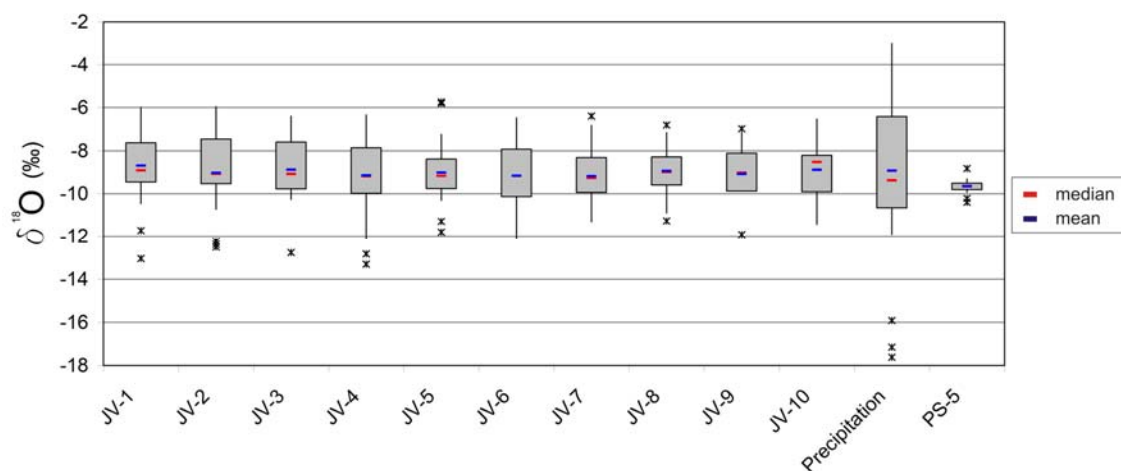


Figure 44: $\delta^{18}\text{O}$ isotope composition results of the monthly sampled water

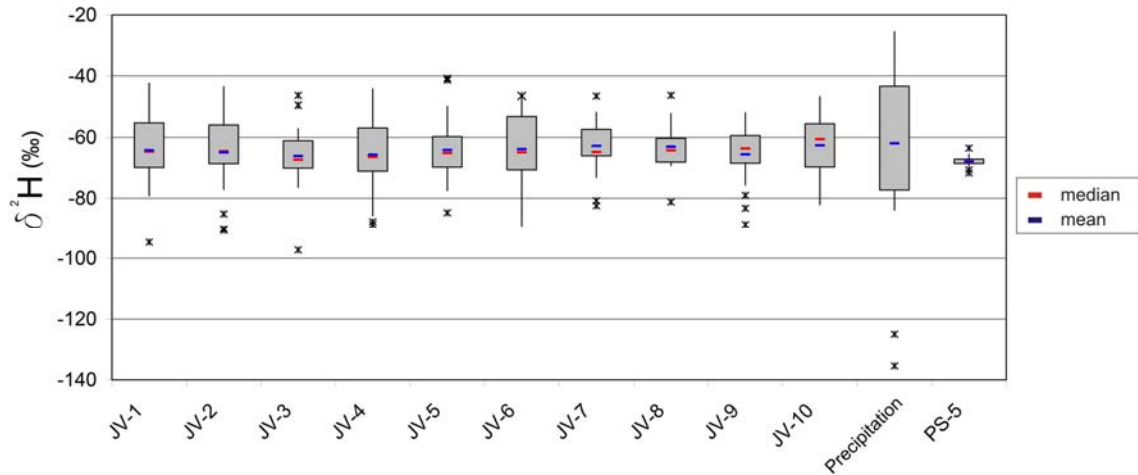


Figure 45: $\delta^2\text{H}$ isotope composition results of the monthly sampled water

Table 17: Statistics of $\delta^{18}\text{O}$ and $\delta^2\text{H}$ isotope composition results of the monthly sampled water

18O	JV-1	JV-2	JV-3	JV-4	JV-5	JV-6	JV-7	JV-8	JV-9	JV-10	Precipitation	PS-5
n	21	32	29	42	45	28	36	50	46	51	39	35
max.	-5.99	-5.96	-6.40	-6.34	-5.74	-6.48	-6.43	-6.79	-6.96	-6.54	-3.00	-8.82
min.	-13.04	-12.93	-12.76	-13.30	-11.81	-12.10	-11.32	-11.28	-11.92	-11.44	-17.62	-10.44
median	-8.91	-9.07	-9.08	-9.185	-9.17	-9.165	-9.265	-8.985	-9.02	-8.52	-9.38	-9.64
mean	-8.69	-9.03	-8.87	-9.15	-9.01	-9.16	-9.19	-8.94	-9.08	-8.88	-8.93	-9.65
st.dv.	1.82	1.91	1.55	1.82	1.26	1.57	1.27	1.02	1.22	1.17	3.54	0.28

2H	JV-1	JV-2	JV-3	JV-4	JV-5	JV-6	JV-7	JV-8	JV-9	JV-10	Precipitation	PS-5
n	14	20	16	27	31	19	21	35	30	34	31	30
max.	-42.40	-43.50	-46.38	-44.18	-40.79	-46.55	-44.56	-46.38	-51.86	-46.84	-25.43	-63.53
min.	-94.66	-90.75	-97.20	-88.68	-84.78	-89.19	-82.46	-81.23	-88.70	-82.10	135.37	-71.67
mediana	-64.71	-64.58	-67.33	-66.44	-65.14	-64.91	-64.8	-64.28	-63.65	-60.59	-61.92	-68.06
mean	-64.25	-64.98	-66.14	-65.72	-64.15	-63.85	-62.81	-63.10	-65.60	-62.62	-61.97	-67.89
st.dv.	13.31	13.31	11.86	11.74	9.49	11.78	9.75	7.82	8.55	8.87	26.06	1.54

Both isotopes were symmetrically arranged in the precipitation, groundwater (PS-5) and in all sampling points in the unsaturated zone. The precipitation has the highest variation of the $\delta^{18}\text{O}$ values. The least oscillations were found in the groundwater. The distant values in the unsaturated zone measurements were due also to the seasonal effect, snow or a special event influence at the time of sampling. The range of $\delta^{18}\text{O}$ isotope composition in the precipitation, snow measurements included, was between -17.62‰ and -3.00‰, the mean value was -8.93‰. The range of $\delta^2\text{H}$ values was -135.37‰ and -25.43‰, mean was -61.97‰. In groundwater the $\delta^{18}\text{O}$ isotope composition was between -10.44‰ to -8.82‰, mean was -9.65‰. $\delta^2\text{H}$ values oscillated between -71.67‰ and -63.53‰, mean was -67.89‰.

Unsaturated zone

The data of $\delta^{18}\text{O}$ and $\delta^2\text{H}$ isotope composition of unsaturated zone groundwater had a similar range of measurements. There were no significant differences between measuring points and the range of $\delta^{18}\text{O}$ values was between -13.04‰ (JV-1) and -5.7‰ (JV-5), the mean values were between -9.19‰ and -8.69‰. The most dispersed values in lysimeter were detected in

the sampling points JV-1, JV-2 and JV-6. The $\delta^2\text{H}$ values moved from -97.20‰ (JV-3) to -40.79‰ (JV-5), the range of mean values was -66.14‰ and -62.62‰.

5.3.1 Seasonal oscillation of $\delta^{18}\text{O}$ isotope composition

The long-term isotope investigation gave an insight into the unsaturated zone system. More information about the water movement could be obtained from seasonal variations in $\delta^{18}\text{O}$ isotope composition at particular sampling points. In the *Annex J* the plots of $\delta^{18}\text{O}$ monthly measurements and the monthly amount of precipitation for the whole period of the investigation are provided. The typical diagram in *Figure 46* shows the time series of $\delta^{18}\text{O}$ isotopic composition of both precipitation and unsaturated zone groundwater for sampling point JV-5. Also in these results the seasonal effects on $\delta^{18}\text{O}$ isotopic composition in precipitation were recognized. The same effect could be traced in the samples at different depths of sampling points.

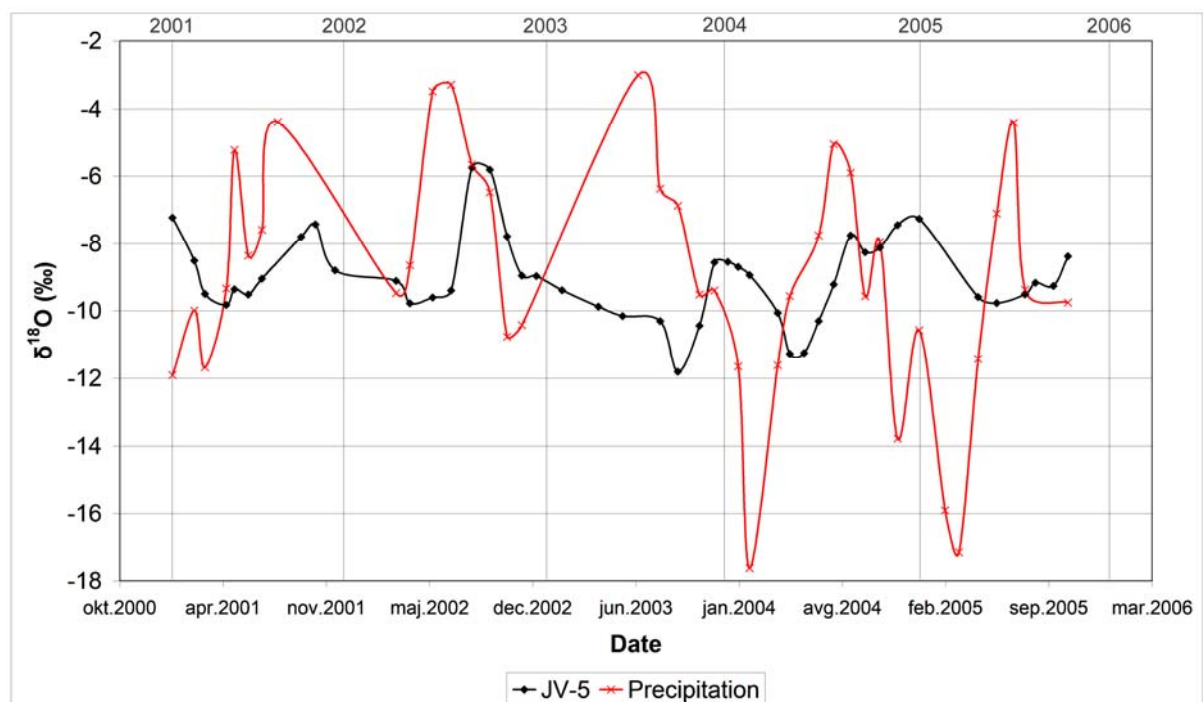


Figure 46: $\delta^{18}\text{O}$ isotope composition for JV-5

Figure 47 presents $\delta^{18}\text{O}$ isotope composition for the year 2002 in detail for sampling points JV-5, JV-7, JV-10 and precipitation. It is indicated that peak precipitation values (summer signal) were detected in unsaturated sampling point measurements in reduced amplitude with depth. With the depth also the moving of peak values was observed.

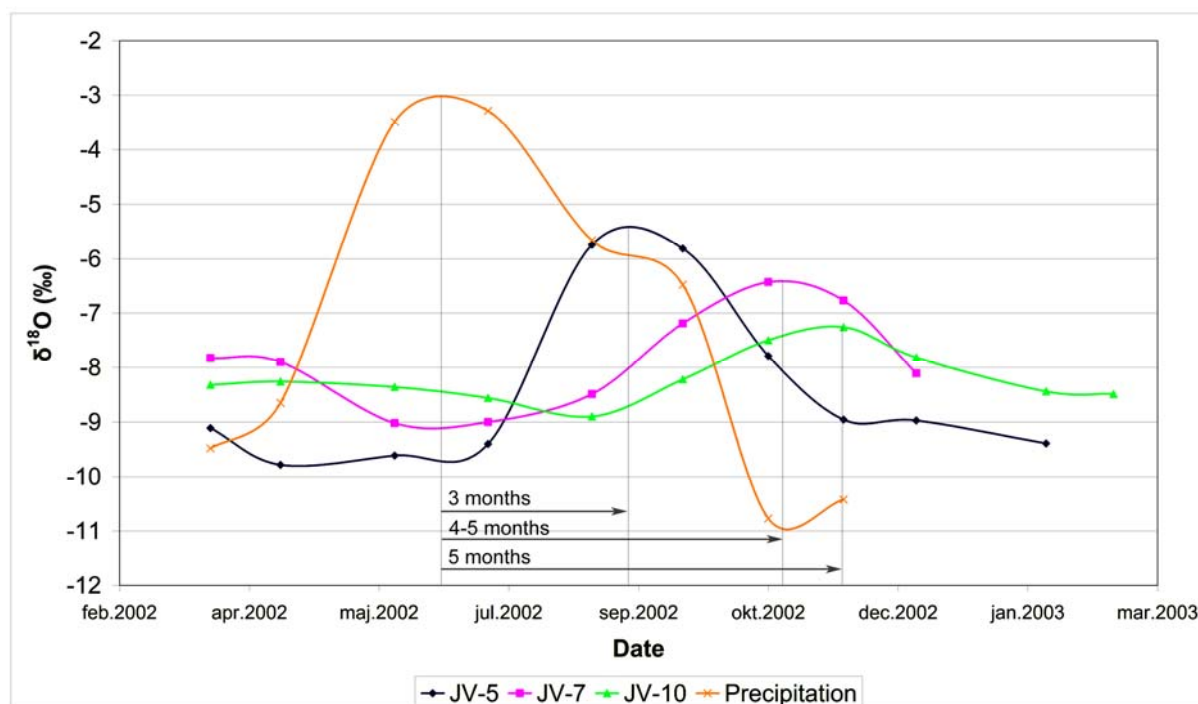


Figure 47: $\delta^{18}\text{O}$ isotope composition for the year 2002

Both phenomena diminish oscillation and the moving peak values could be followed in all sampling points (*Annex J*). The measurements at sampling points JV-1 showed a fast reaction to the precipitation signal. With the depth reaction times became longer. During the first period of the investigation at higher measuring points some difficulties were encountered in the sampling of groundwater in the unsaturated zone, so an estimation of the behaviour at different hydrological periods was not possible. The amplitudes of $\delta^{18}\text{O}$ isotope composition curves were significantly reduced with depth. At JV-7, JV-8, JV-9 and JV-10 the curves became slightly undulating.

The long-term data series enabled the observation of differences between hydrological periods. In 2002, the summer signal was well detected at all observation points in 3-5 months. In the year 2003 the $\delta^{18}\text{O}$ values decreased significantly from the winter almost until September. This was the consequence of the extremely dry period in spring and summer time. There was no fresh water to supply the unsaturated zone and the result was a negative trend (decline) of average $\delta^{18}\text{O}$ isotope composition in the water of the unsaturated zone. On the contrary, the year 2004 had a lot of precipitation already in the winter and spring. The $\delta^{18}\text{O}$ values in the unsaturated zone groundwater rose faster after the precipitation signal than could be recognized in other years. *Table 18* lists mean values of $\delta^{18}\text{O}$ isotope composition for a particular year by observation points. *Figure 48* shows the decline in average $\delta^{18}\text{O}$ values in the year 2003.

Table 18: Mean values of $\delta^{18}\text{O}$ isotope composition by particular year

	<i>JV-1</i>	<i>JV-2</i>	<i>JV-3</i>	<i>JV-4</i>	<i>JV-5</i>	<i>JV-6</i>	<i>JV-7</i>	<i>JV-8</i>	<i>JV-9</i>	<i>JV-10</i>
2001		-7.28	-8.54	-8.57	-8.70	-6.98	-8.30	-8.14	-7.63	-7.74
2002	-8.47	-7.91	-8.48	-8.12	-8.35	-7.53	-7.86	-8.48	-8.33	-8.13
2003	-8.95	-9.93	-10.22	-10.17	-9.89	-10.49	-10.31	-9.71	-10.32	-10.03
2004	-8.82	-9.50	-9.02	-9.44	-9.05	-9.97	-10.20	-9.45	-9.30	-9.76
2005	-8.42	-9.51	-8.43	-9.36	-9.28	-8.73	-9.00	-8.89	-8.84	-8.85

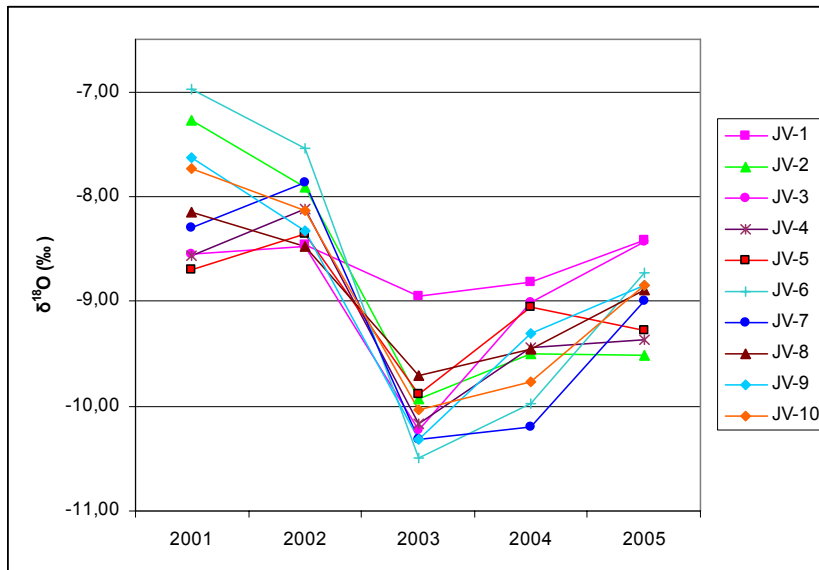


Figure 48: Average values of $\delta^{18}\text{O}$ isotope composition of the monthly sampled water

5.3.2 Depth profiles of $\delta^{18}\text{O}$ signal - groundwater dynamics based on $\delta^{18}\text{O}$ signal

For a detailed observation of water movement based on $\delta^{18}\text{O}$ measurements, the hydrological year 2004-2005 was chosen because of the possible comparison with the tracing experiment results. The profile of $\delta^{18}\text{O}$ values by the depth at the typical season times is shown in *Figure 49*. The diagrams show the movement of the $\delta^{18}\text{O}$ signal. The signal of the negative values (winter) was first reversed in sampling points JV-1, JV-2, JV-4 and JV-5 in May 2004. As late at that time the negative influence decreased $\delta^{18}\text{O}$ values at sampling point JV-7. Next turning points were recognised at sampling points JV-3, JV-6, JV-8, JV-9 and JV-10 (June 2004). In September the JV-7 measurements reached the lowest values and almost at the same time in November 2004 the $\delta^{18}\text{O}$ values reached the highest values at sampling points JV-1, JV-4 and JV-9. In winter (December 2004, January 2005) the $\delta^{18}\text{O}$ values started to decline in observation points JV-2, JV-5, JV-10, JV-7 and JV-8 followed in April 2005.

The groundwater dynamics in the unsaturated zone is highly dependent on precipitation rate (which directly influences the parameters connected to unsaturated flow) which is also evident from long term investigations of isotope composition. From the results it could be concluded:

- Each hydrological year has its own characteristics in groundwater dynamics in the unsaturated zone
- Based on $\delta^{18}\text{O}$ signal the tracing of water movement is possible
- Based on several years of observation results, the sampling points can be classified into the following groups:
 - o JV-1 directly reacts on the precipitation.
 - o JV-2, JV-4, JV-5, JV-6, JV-8, JV-9, JV-10 ; appearance time of the signal is related with depth
 - o JV-3, JV-7 the slowest reaction of the system is observed. Conclusions about longer residence time could be made because of a locally different structure of the unsaturated zone.
- Based on the reaction time, residence time of the water in unsaturated zone can be estimated.

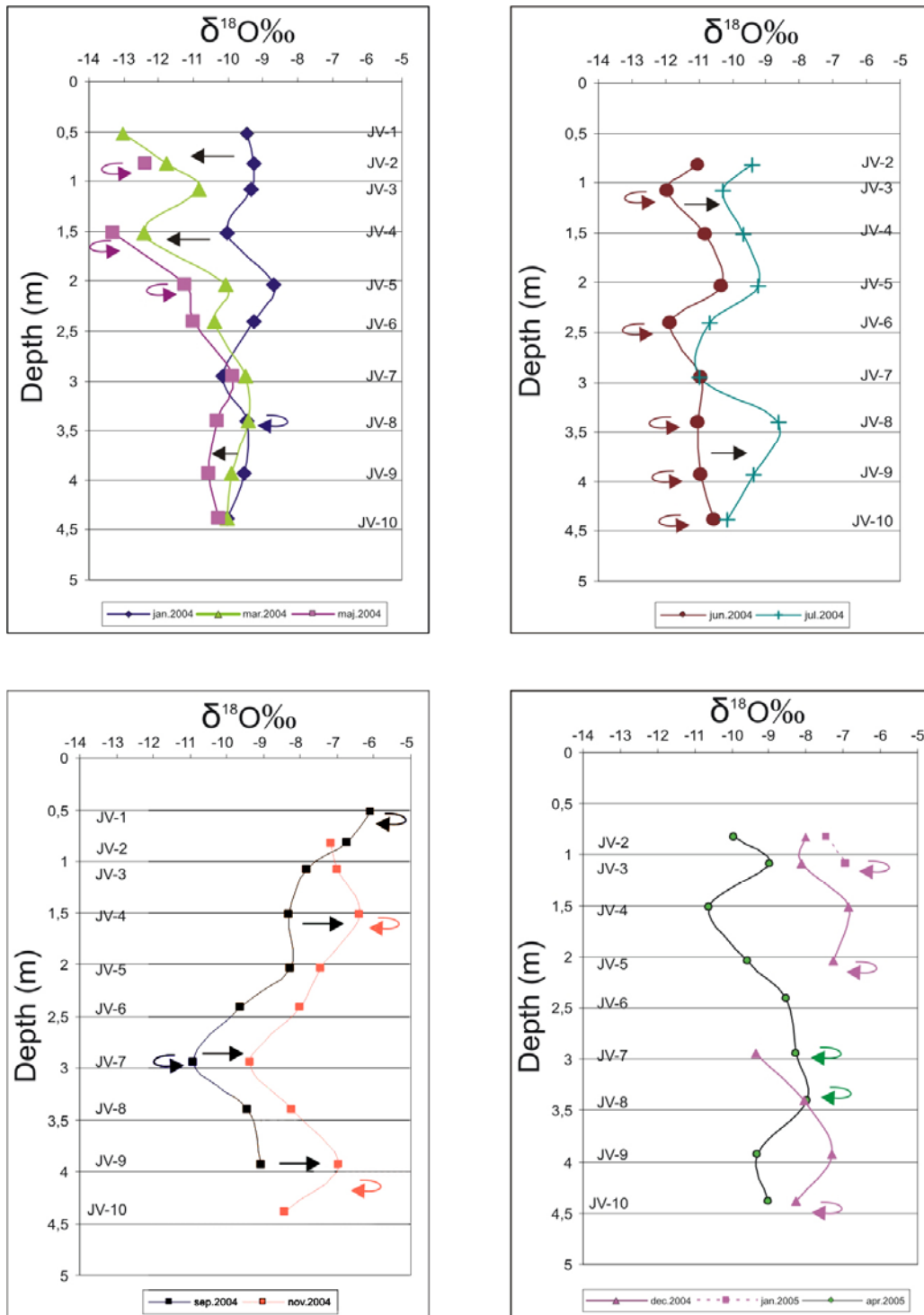


Figure 49: The profile of $\delta^{18}\text{O}$ values by the depth at the typical seasons

5.3.3 Lumped parameter modelling

One of the aims of this study was also the estimation of mean residence time (MRT) in the unsaturated zone based on isotopic investigations. The long term $\delta^{18}\text{O}$ data set of monthly water sampling in the unsaturated zone was suitable for the estimation of MRT by using lumped parameter models. The models included in the FLOWPC 3.1 program (Maloszewski, 1996)

were applied. Detailed description of the models can be found in chapter 2.5. The models were run for all measuring points except JV-1 where the data were not adequate.

To trace water movement in the unsaturated zone, it is necessary to know the precipitation isotope composition as input signal. In long-term investigations also the precipitation defining the isotope composition was sampled. Because of some difficulties in acquiring the complete data series which is needed for modelling, the comparison with precipitation data of Ljubljana and Klagenfurt were made. The source of data is IAEA, GNIP data base, and the "Institute Jožef Stefan" data base. Based on the results of comparison the precipitation data series of Selniška Dobrava were supplemented.

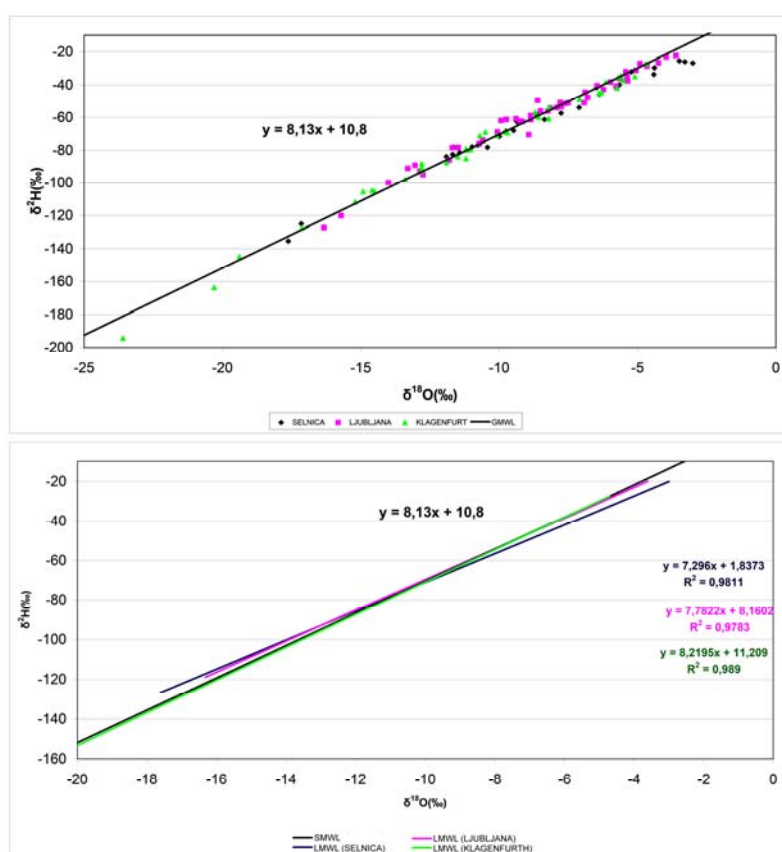


Figure 50: Comparison of the $\delta^{18}\text{O}$ isotope composition of Selnica, Ljubljana and Klagenfurt precipitation with GMWL

In Figure 50 the results of precipitation composition of all three locations are presented with global meteoric water line (GMWL). In general all data fall in the region of the GMWL. Comparison of local meteoric water lines LMWL, calculated only from observed period data, regressions between $\delta^{18}\text{O}$ and $\delta^2\text{H}$, and correlation coefficients of $\delta^{18}\text{O}$ (Table 19) show the similarity between Selnica, Ljubljana and Klagenfurt precipitation isotope composition. Because the Ljubljana data series is more complete, it was chosen to complement the data for modeling. In Figure 51a comparison of $\delta^{18}\text{O}$ values for all three stations is made.

Table 19: Correlation coefficient of the precipitation

	Sel-K	LJ-K	LJ-Sel
$\delta^{18}\text{O}$ (‰)	0.71	0.93	0.71
$\delta^2\text{H}$ (‰)	0.69	0.93	0.61

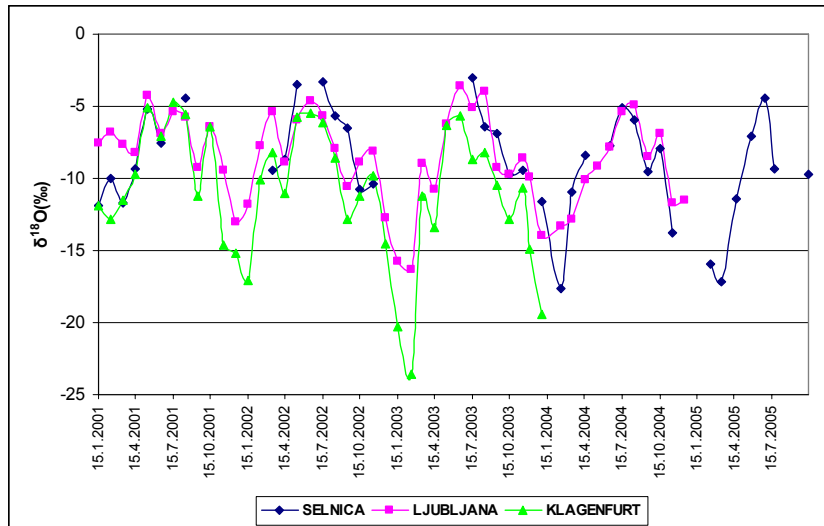


Figure 51: $\delta^{18}\text{O}$ values of Ljubljana, Selniška Dobrava and Klagenfurt precipitation

Beside $\delta^{18}\text{O}$ values of precipitation as input signal also the percentage of infiltration by the months was considered in the input function. With the estimation of infiltration a correction of the input signal power was made. The infiltration was adopted from the mathematical model of the Selniška Dobrava gravel aquifer (Mali and Janža, 2005). *Table 20* gives estimated values of average percentage of infiltration for forest surface in Selniška Dobrava by months, which were included in input functions.

Table 20: Average percentage of infiltration used in input functions

	Jan.	Feb.	Mar.	April	May	June	July	Aug.	Sept.	Okt.	Nov.	Dec.
Infiltration	1	1	1	0.5	0.5	0.5	0.5	0.5	0.5	1	1	1

Data set was run on linear (LM), linear-piston-flow (LPM), exponential (EM), exponential-piston-flow (EPM) and dispersion model (DM). Observed and fitted $\delta^{18}\text{O}$ output functions for all observed sampling points in the unsaturated zone are presented in *Annex K*. The typical modelled output functions for sampling point JV-5 are presented in *Figure 52*. The modelled data comprise a period of more than three hydrological cycles (almost four). As it is described, there were different hydrological years. The year 2003 was abnormally dry, thus causing a weaker input signal. Model calibrations were made on the basis of usual hydrological years (2001-2002 and 2004-2005), because the aim was the estimation of the general MRT. Where a type of applied model was recognized as unsuitable, it was excluded from farther modelling at a particular observing point. The calculated MRT by each model for all considered sampling points are in *Table 21*. The MRT results and shape of the curves showed that the estimations by different model types are of comparable values. On the basis of results it could be concluded that MRT became longer with depth. In the entire system with regard to sampling point depth JV-3 and JV-7 MRT was recognisable longer than at others. This is a consequence of local structural conditions. This could possibly be attributed to a less permeable layer of silt, sand or cemented gravel (conglomerate).

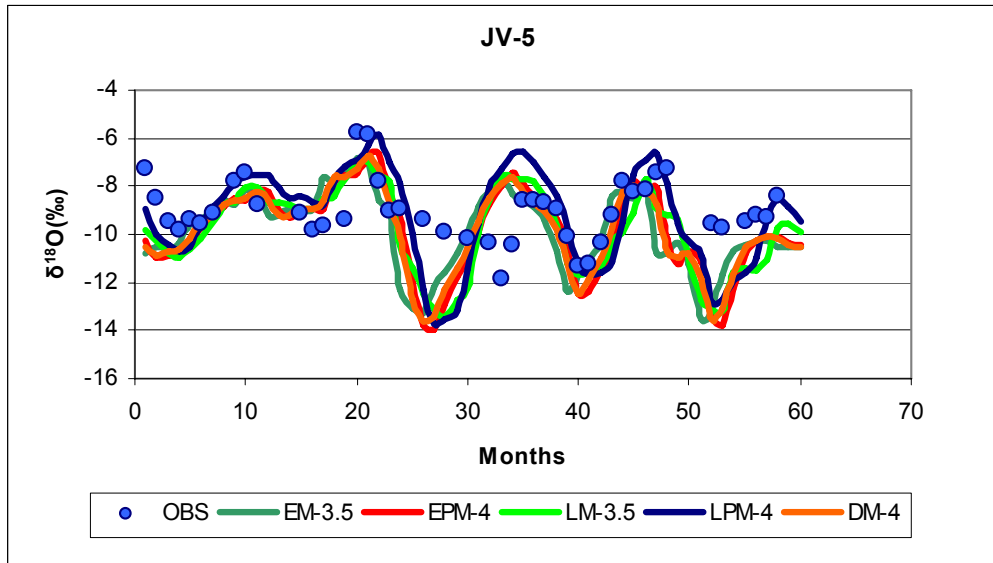


Figure 52: Observed and fitted $\delta^{18}\text{O}$ output functions for sampling point JV-5 (model numbers present MRT in months)

Table 21: Mean values of MRT modelled by different models and compared with results of the tracing experiment (MRT is expressed in months)

Model	JV-2	JV-3	JV-4	JV-5	JV-6	JV-7	JV-8	JV-9	JV-10
LM	2.5		3.5	3.5	3.5				
LPM	3	4	4	4	4.5		8.6		11
EM	3	3.5	4	3.5		8		7	
EPM	2.5	5	3.5	4	4.5	8	7	7	9
DM	2.2	5.5	3	4	4	7	6	6	9
Mean	2.6	4.5	3.6	3.8	4.1	7.7	7.2	6.7	9.7
Tracing-04	1.9	4.5	3.5	4	4.7	8.9	7.5	7.7	9.1
Best fit M	LM.LPM	LPM	LPM	LM.LPM	LM.LPM		DM.EPM	DM.EPM	EPM.DM

Based on MRT also the average velocity was calculated (Table 22). The results showed that the water flow in the unsaturated zone is not unique. The fastest flow velocity was recognized at sampling points JV-5, JV-6 and JV-9 (range 0.018-0.02 m/d). The slowest flow velocity was observed at JV-3 and JV-1 (0.008-0.010 m/d). The velocity at the other sampling points was in the range 0.013-0.016 m/d. It could be concluded that the average velocity of water flow in the coarse gravel unsaturated zone of Selniška Dobrava estimated by lumped parameter models is 0.015 m/d.

Table 22: Average MRT and estimated flow velocities

	JV-2	JV-3	JV-4	JV-5	JV-6	JV-7	JV-8	JV-9	JV-10
Depth	0.82	1.08	1.52	2.04	2.41	2.95	3.4	3.93	4.39
MRT (month)	2.6	4.5	3.6	3.8	4.1	7.7	7.2	6.7	9.7
f.velocity (m/month)	0.3	0.2	0.4	0.5	0.6	0.4	0.5	0.6	0.5
f.velocity (m/d)	0.010	0.008	0.014	0.018	0.019	0.013	0.016	0.020	0.015

Based on best fitted output functions the applicability of a single model at a particular sampling point was evaluated. In Table 21 the types of best models at each sampling point are presented. It could be concluded that up to sampling point JV-6 at a depth of 2.4 m, LM and LPM reflected better the real transport processes than the other models. Deeper in the unsaturated zone the description of unsaturated water flow was better by using EPM, EM and DM. In the first few meters in the unsaturated zone the mixing and dispersion processes were

not so explicit. Surprising results showed that the piston flow in combination with other processes plays an important role in water dynamics in the coarse gravel unsaturated zone.

5.4 Combined uranine and deuterium tracing experiment

A tracing experiment was performed on April 21, 2004, using deuterated water and uranine as artificial tracers (*Figure 53*). The period before tracer injection was a period of intense snow melting. The saturation of the soil profile was near the field capacity. Before tracer injection irrigation with groundwater was performed to reach good field capacity. 75g of uranine and 1100 ml D₂O (55%) were dissolved in 50 l of groundwater and injected by sprinkler irrigation. After injection the tracer was again splashed by irrigated groundwater. The area of irrigation was 9.5 m². The complete injection was done during 5 hours. The distribution of the artificial rainfall was controlled by ten precipitation measuring points. The average amount of irrigated water 107 mm corresponds to a summer thunderstorm event.



Figure 53: Tracing experiment

5.4.1 Results of deuterium tracing experiment

Deuterium tracer was detected in all ten sampling points (*Figure 54*). The maximum concentration of tracer at each single measuring point does not depend on the depth or distance from the lysimeter surface, but on the connection of preferential flow paths. The highest values of $\delta^2\text{H}$ (3100 ‰) were recognized in the first sampling point JV-1 immediately after tracer injection. This can result from the consequences of intense irrigation in time of tracing injection or its contamination. Beside at JV-1, the next maximum values were detected at sampling points JV-5 (572.94 ‰) and JV-8 (315.7 ‰). At the other observation points measured maximum values were below 200 ‰. Based on the analytical results, breakthrough curves for all observation points were constructed. Breakthrough curves with the precipitation amount at the time of tracing experiment are presented in *Figure 54*. Graphs show that the clear recognition of tracer effect in the samples started at the end of May 2005 at sampling points JV-2, JV-5 and JV-4. There was a period of high precipitation from May until the middle of July. At that time the changes of $\delta^2\text{H}$ values at all other sampling points were also observed. From the plot of precipitation and $\delta^2\text{H}$ values it is evident that the high intensity and amount of precipitation forced the occurrence of the tracer at different observation points at the same time. Sampling point JV-7 reacted the last. Amplitude peaks and lengths of breakthrough curves are different. In some higher sampling points (JV-1, JV-2, JV-3, JV-4) in spring time 2005 there was no tracing signal any more, in August 2005 no tracer effect was recognized in all sampling points.

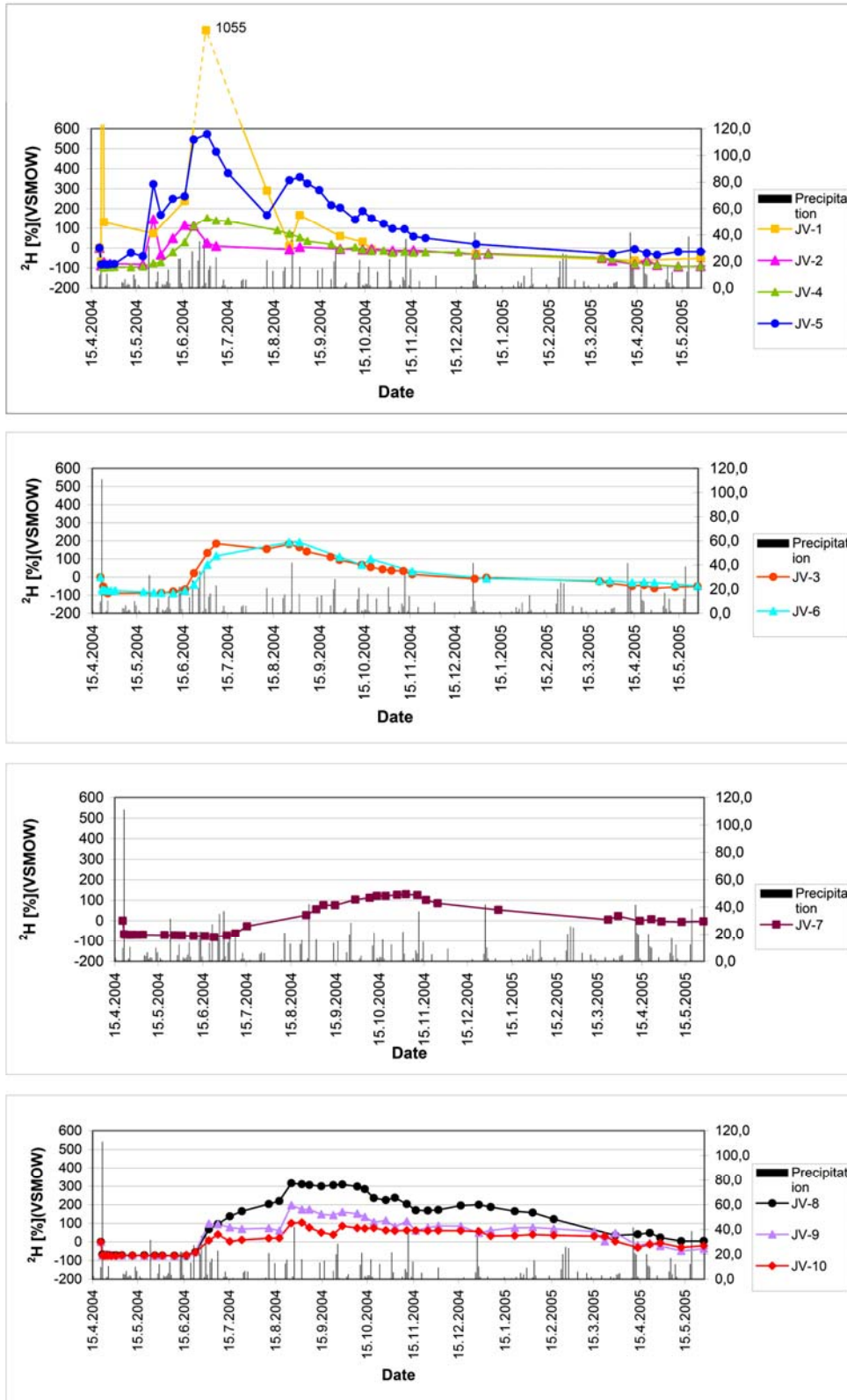


Figure 54: Deuterium breakthrough curves and precipitations during the tracing experiment

More information about the tracer movement in time can be obtained from the profiles in Figure 55. In June 2004 the upper sampling points except JV-3 already reacted (Figure 55a). At that time the values at JV-2 reached the peak. In July the increase in deuterium values was

observed in all sampling point except in JV-7 (*Figure 55b*). The peak values were registered in sampling points JV-1, JV-4 and JV-5. In the end of August (*Figure 55c*), the peaks of tracer values were reached deeper in lysimeter at JV-3, JV-6, JV-8, JV-9 and JV-10. At other upper points the values had already decreased. The reduction of tracer signal was recognized in October 2004 (*Figure 55d*), but at that time also JV-7, which was delayed, reached the peak value. After that time all values of deuterium decreased. These profiles show that the water flow through sampling points JV-3 and JV-7 is slower than through other points.

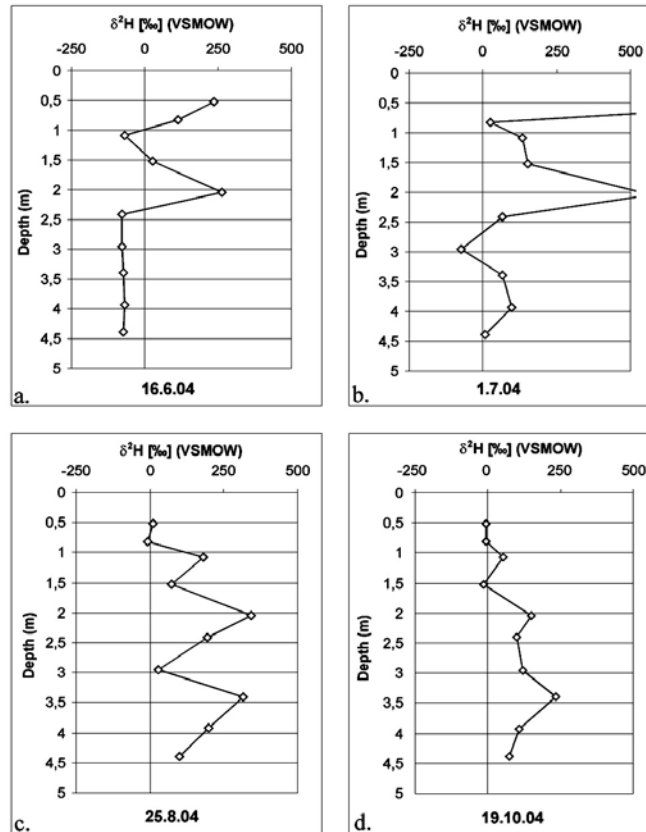


Figure 55: Vertical reviews of δ^2H values of water in unsaturated zone
a. Perception of the tracer signal in June 2004
b. Strengthening of the tracing signal (July 2004)
c. Moving of the tracing signal downwards in lysimeter (August 2004)
d. Diminution of the tracing signal (October 2004)

On the basis of methods described in the previous chapter the same water flow and transport properties were estimated. Regarding the injection time, the first tracer appearance time and the highest concentration time, the fastest flow velocity and dominant flow velocity were calculated (*Table 23*). Based on tracing experiment results, estimations of mean flow velocity and vertical dispersion (*Table 23*) were made by the analytical best-fit method. One dimensional convection-dispersion-model with standardising values for single porosity was used (see chapter 2.6.2). In case JV-2 the application of the Multi-Peak-Modus was used. For all sampling points except JV-1 best fit curves (*Figure 56*) were plotted.

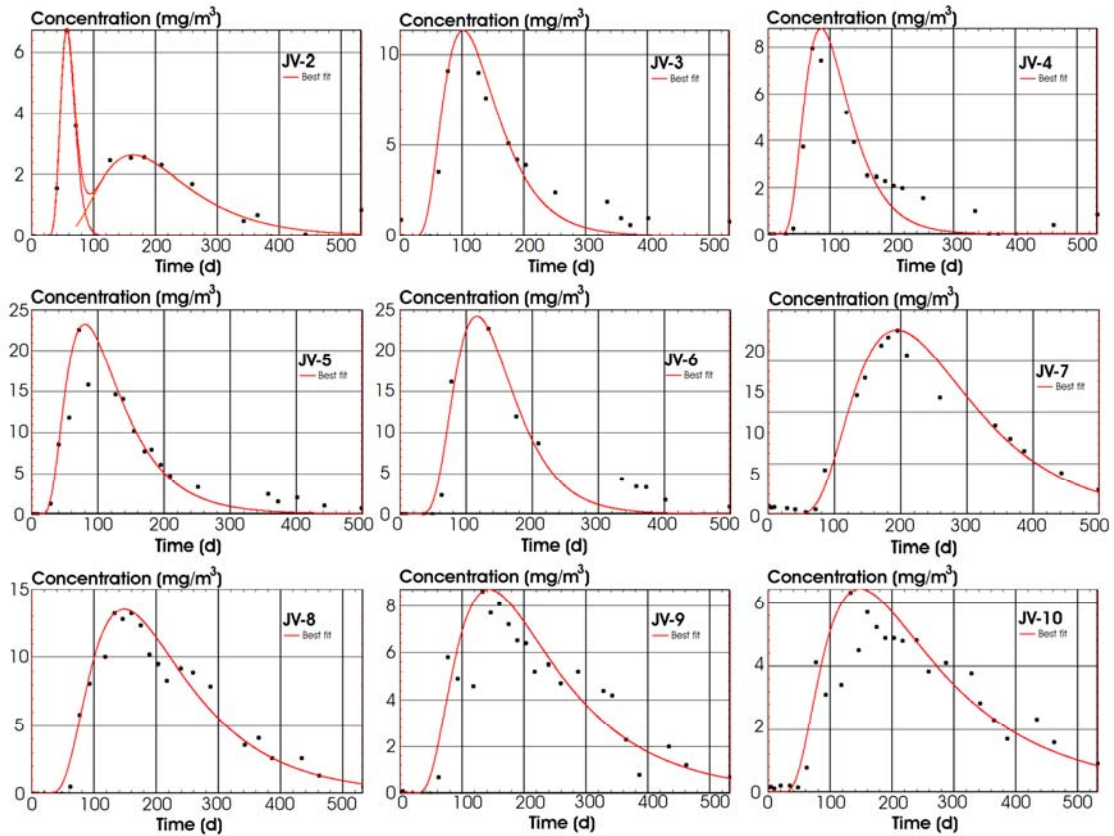


Figure 56: Best fit curves for deuterium concentrations by convection-dispersion model for all sampling points in lysimeter

The fastest flow velocity shows an extremely fast connection of sampling point JV-5 with surface (0.102 m/d). Other values of fastest flow velocity rise with depth from 0.023 m/d to 0.071 m/d, but this is only apparent. From breakthrough curves, precipitation and the first detection time of tracer it can be observed that the influence of a strong rain event on the tracer is reflected in the measuring points. In the rain period in June 2004, in the deepest sampling points from JV-6 to JV-10 (except JV-7) the recognition of tracer occurred almost at once. Because of the different depth position of sampling points and because of the recognition of tracer at the same sampling time it seems that velocity increases with depth. Irrespective of this, it is important for the estimation of the fastest flow velocity to assess the probability of the fastest pollution effect on aquifer through the unsaturated zone.

Dominant flow velocity is related with the time of the highest concentration. The graph of precipitation and $\delta^2\text{H}$ values shows that also the occurrence of the highest $\delta^2\text{H}$ values coincides with the stronger precipitation event. The lowest values of dominant velocity are in sampling points JV-3 and JV-7 (0.014-0.015 m/d), JV-6 has a dominant flow velocity of 0.19 m/d, in other sampling points the dominant flow velocity ranges from 0.21 to 0.33 m/d (Table 23).

Table 23: Calculated fastest, dominant and mean flow velocities of deuterium tracer

		JV-1	JV-2	JV-3	JV-4	JV-5	JV-6	JV-7	JV-8	JV-9	JV-10
Distance	m	0.52	0.82	1.08	1.52	2.04	2.41	2.95	3.4	3.93	4.39
Fastest f.	m/d	0.520	0.023	0.023	0.043	0.102	0.043	0.042	0.055	0.070	0.071
Dom. f.	m/d	0.520	0.023	0.014	0.021	0.029	0.019	0.015	0.027	0.031	0.033
Mean f.	m/d	-	0.014	0.008	0.014	0.017	0.017	0.011	0.015	0.017	0.016
Dispersion	m ² /s	0.488	0	0.001	0.002	0.005	0.003	0.004	0.007	0.011	0.015

The best evaluation of the matrix water flow is the mean flow velocity (*Table 23*). Through the entire lysimeter the estimation of the mean flow velocity based on $\delta^2\text{H}$ concentrations is 0.014-0.017 m/d, except in sampling points JV-3 and JV-7, where it is 0.008 m/d to 0.011 m/d. Dispersion increased from the top of lysimeter to the bottom. If the first measuring point is omitted, the highest dispersion coefficient is reached in JV-10 (0.015 m²/d).

The discharge volume of water in drain systems was measured between two samplings as water volume in the water collector. In the winter time from January 2005 until snow melting in March 2005 there was no outflow water from JV-1 up to sampling point JV-7 included. Because of snow cover and frozen soil there were no conditions for water flow in the unsaturated zone. At different periods at different sampling points there were also some short blockings of the tubes and the measuring of outflow water volume is not correct. But from cumulative values of outflow water volume (*Table 24*) the discharge dynamic can be evaluated. At the time of the tracing experiment till 21.7.2005 at the deepest sampling point the outflow volume of the water was about 400 l. The next most productive drain was JV-8 with 258 l. The deepest sampling point drains discharge more groundwater from the unsaturated zone (JV-10, JV-9, JV-8) than the upper sampling points (JV-1, JV-2, JV-3). In the gravel deposit deeper than 3m from the ground (JV-8, JV-9, JV-10) the field capacity was all the time very high, so vertical water flow existed all the time. Other points were more affected by the drying up in the time of less precipitation and during the time of frozen ground.

Table 24: Cumulative outflow water volume and recovery amount of deuterium tracer

		JV-1	JV-2	JV-3	JV-4	JV-5	JV-6	JV-7	JV-8	JV-9	JV-10	Cumulative
outflow water volume	l	4.93	18.35	23.92	96.47	105.39	35.93	82.75	258.13	161.22	398.62	
amount of recovery tracer	mg	221.49	32.44	58.77	153.47	678.11	49.24	136.79	1297.89	618.24	947.75	4194.20
% of recovery tracer amount	%	5.28	0.77	1.40	3.66	16.17	1.17	3.26	30.94	14.74	22.60	100.00
%of whole amount of tracer	%	0.18	0.03	0.05	0.13	0.56	0.04	0.11	1.07	0.51	0.78	3.47

Tracer recovery was estimated based on outflow water volume and ^2H concentrations. In *Table 24* the quantities, percentages of recovered and injected deuterium tracer by the sampling points are presented. Until the end of July 2005, 4573 mg of ^2H were calculated in collected outflow water which presents 3.78% of the total injected tracer. The largest quantities of deuterium tracer were coming out at sampling points JV-8 and JV-10, 1297 mg and 947 mg, which present 30% and 22% of all recovered tracer and 0.8-1% of the total injected tracer each. In each of the other sampling points tracer recovery values were in the range between 32 mg and 678 mg which represent 0.77-16 % of all recovered tracer and 0.03-0.6% of the total injected tracer. In point JV-1 almost all recovered tracer came out in the first day after injection. If this amount of tracer is not considered, 30 mg of ^2H is recovered in this point.

5.4.2 Results of uranine tracer

Uranine was detected in all sampling points. In the first two days after injection of the tracers very high uranine concentrations were found in several sampling points (JV-1, JV-3, JV-5, JV-7, JV-8, JV-9, JV-10), after that time concentrations decline. In sampling point JV-7 there was no more uranine detected until the end of the tracing experiment. It can not be excluded that the contamination of some sampling points happened at the time of tracer injection. Breakthrough curves of uranine (*Figure 57*) show that higher concentrations of uranine appear impulsively, depending on the quantity and intensity of precipitation. A comparison of deuterium and uranine breakthrough curves shows that the results of deuterium tracing give a more regular distribution of tracer than uranine which shows a strong, impulsive tracer appearance (*Figure 57*). If the increase of uranine concentration during the first two days is not considered, a delay of uranine tracer compared to deuterium is recognized. At sampling point JV-1 breakthrough curves of deuterium and uranine tracer have the same shape at the same time. A maximum concentration of uranine at sampling point JV-5 is covered with the first higher

increase in deuterium values at the time of high precipitation in May 2004. At other sampling points maximum concentrations of uranium lag behind maximum values of deuterium. At the deepest points (JV-8, JV-9, JV-10) plots indicate that the real uranium occurrence must have happened after the end of tracing experiment.

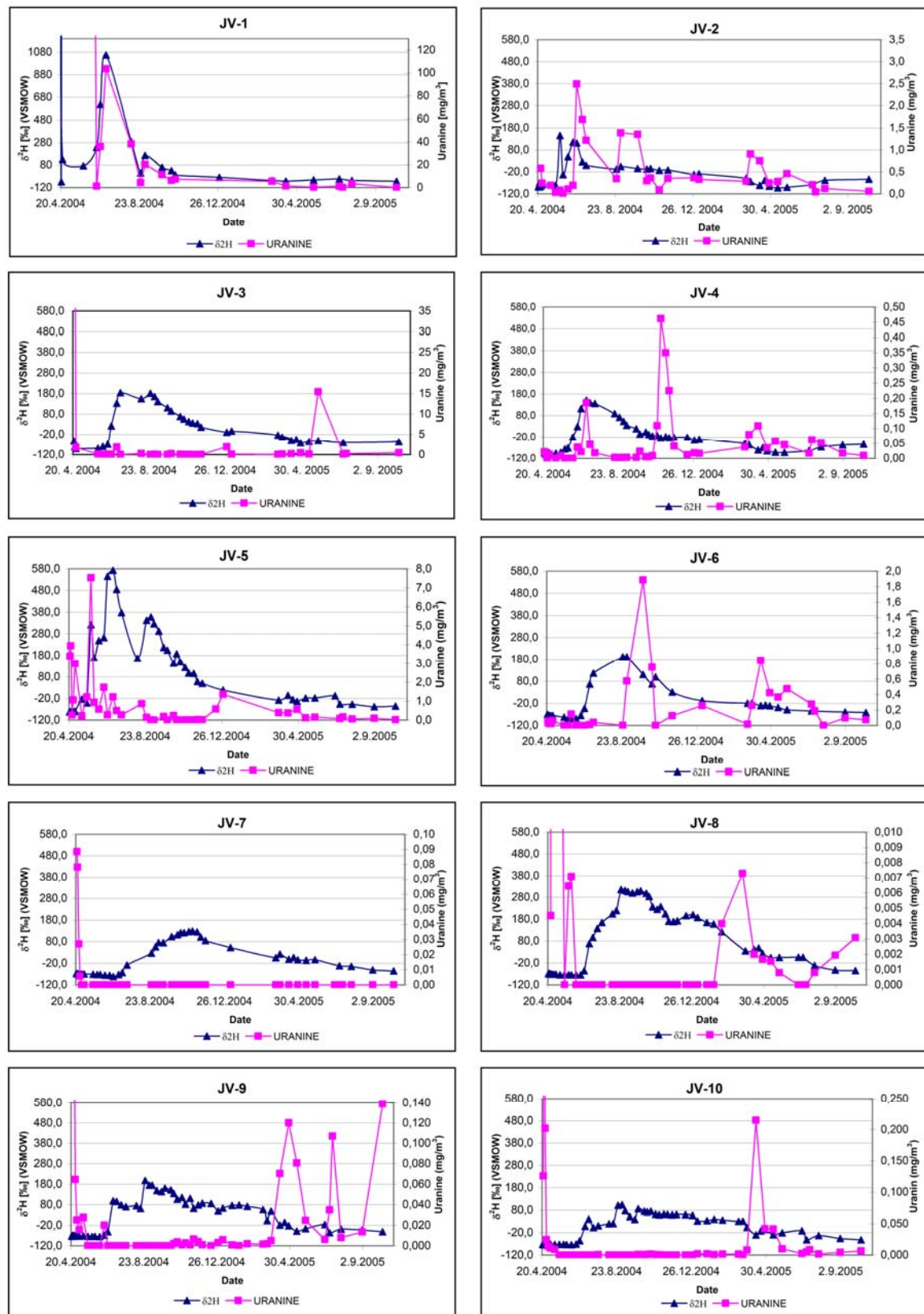


Figure 57: Comparison of deuterium and uranium breakthrough curves

Table 25: Calculated dominant, mean flow velocity and retardation factor of uranine

		<i>JV-1</i>	<i>JV-2</i>	<i>JV-3</i>	<i>JV-4</i>	<i>JV-5</i>	<i>JV-6</i>	<i>JV-7</i>	<i>JV-8</i>	<i>JV-9</i>	<i>JV-10</i>
Distance	m	0.52	0.82	1.08	1.52	2.04	2.41	2.95	3.4	3.93	4.39
Dom. f.	m/d	-	0.013	-	0.008	0.058	0.015	-	0.010	0.011	0.012
Mean f.	m/d	-	0.012	-	0.008	-	0.015	-	0.012	0.01	0.012
R _d -mean flow		-	1.167	-	1.750	-	1.133	-	1.250	1.700	1.333

An estimation of water flow velocity was done also on the basis of uranine tracing results (*Table 25*). Because the uranine tracer appeared in the sampling point almost immediately after the injection on a count of contamination, the maximum velocity hasn't been determined. Based on the knowledge of the aquifer and water flow properties in the lysimeter system, the concentrations of the first few days were not considered for the calculation of dominant velocity. The maximum concentrations of uranine tracer after that period were taken in account. For sampling points *JV-3* and *JV-7* no typical breakthrough curves were found. Lower dominant velocity is established at sampling points *JV-1* and *JV-4* (0.007-0.008 m/d). The highest dominant flow velocity 0.058 m/d is found at *JV-5*. The dominant velocity for other sampling points moves from 0.010 m/d to 0.013 m/d. The analytical best-fit method with the computer program TRACI'95 was used to estimate the mean flow velocity with uranine concentration breakthrough curves for sampling points *JV-2*, *JV-4*, *JV-6*, *JV-8*, *JV-9* and *JV-10*. The calculation was made for typical signals. Among these sampling points the lowest mean flow velocity 0.008 m/d was established at sampling point *JV-4*. The mean flow velocity at other points is between 0.010 m/d and 0.015 m/d. The uranine tracer recovery was very poor and it reached only 0.001% of the total injected tracer.

5.4.3 Comparison of deuterium and uranine tracer

Breakthrough curves of both tracers show retardation in maximum values of dye compared to deuterium. It is presumed that the retardation and impulsive increase of dye tracer concentrations are the result of sorption-desorption processes. With sorption the immobilization of substance dissolved in water on the surface of grains in the aquifer occurs, desorption releases the substance back into the solution. A portion of the tracer is always unavailable for transport, since it is fixed to the rock, mostly organic material in the sediments.. Only the part of the tracer dissolved in the water can be transported away. As soon as the portion of the originally adsorbed dye tracer dissolves, it can also be transported. These processes slow down the transport, since large parts of the tracer are immobilized on the solid phase for part of the time.

The calculation of retardation factor for the dye was made using results of convection-dispersion model for the estimation of mean flow velocity. Only sampling points *JV-2*, *JV-4*, *JV-6*, *JV-8*, *JV-9* and *JV-10* were included because for these points analytical approaches to calculate mean flow velocity for uranine data could be performed. The retardation factor *R* was calculated by Eq. 26.

The range of retardation factor (*Table 25*) is from 1.133 (*JV-6*) to 1.75 (*JV-4*). Usually retardation factors for different tracers are determined by laboratory tests. Our results correspond to the published retardation factors for uranine in gravel media determined in laboratory. Based on column tests Klotz (1982) reported the uranine retardation factor 1.13 (0.99-1.22) in gravely sand. Values obtained from modelling tests were slightly higher but less than 2.

Based on $\delta^2\text{H}$ value profiles, breakthrough curves of both tracers, calculations of different flow velocity parameters and recovery curves of deuterium as a tracer, strong preferential flow is assumed at sampling point *JV-5*. Recovery amounts of the deuterium tracer show that a higher

amount of the tracer came out through sampling points JV-8 (30% of recovered tracer). Beside JV-5, the highest values of $\delta^2\text{H}$ were found at JV-8, and JV-8 sampling point location is below JV-5. On the basis of these reasons conclusions about preferential flow appearance on the left (north) side of lysimeter observation wall can be made (see profil in *Figure 19*).

5.4.4 Evaluation of tracing method (tracing experiment)

A lysimeter tracing experiment showed that deuterated water is a more suitable tracer than uranine for the study of water flow properties in the unsaturated zone. Both tracers appeared at sampling points and their arrival to individual sampling points was in both cases related to the intensity and amount of precipitation. Uranine came in sight very impulsively (*Figure 57*) and its breakthrough curves show several peaks, among which it is difficult to recognize one significant breakthrough curve. On the other hand, the results of deuterium tracer show a typical breakthrough curve (*Figure 54*). The retardation factor of the dye as compared to deuterium was 1.13-1.75, which is in agreement with previously published results. Deuterated water is thus a useful tracer to detect water movement, while the use of uranine may reflect organic compounds transport. In this study deuterium was confirmed as an ideal conservative tracer for tracer studies in the unsaturated zone.

On the basis of tracing experiment results some properties of coarse gravel unsaturated zone at the location of the lysimeter could be described. Tracer concentration diagrams generally show an increasing dispersion effect with the depth. The peaks of different breakthrough curves are delayed with sampling point depth. The travelling of the tracer by depth could be recognized on the typical profiles of deuterium values (*Figure 55*). Also the volumes of outflow water in the drain system (*Table 24*) and dispersion coefficient for deuterium (*Table 23*) increase with the depth. The estimation of mean flow velocity of matrix flow is between 0.014-0.017 m/d (*Table 23*).

Tracing with artificial tracers, especially with deuterated water, was found a very useful tool to assess properties and differences in water flow also in the unsaturated zone of a coarse gravel aquifer. On the basis of the determined range of water flow properties the estimations of groundwater recharge, pollution influence on aquifer and groundwater protection measures can be provided.

5.5 Analyses of precipitation events

The aim of long time isotope observations was the description of matrix flow properties. With the study of unsaturated zone behavior in the time of special weather events, which produced a significant tracing signal, the preferential flow processes were described. The effects of snow melting in March 2004 and two summer storms between July and August 2005 were studied. The isotope results of snow melting were analyzed by two-component hydrograph separation method (chapter 2.7). In the time of summer storms the lysimeter on-line measuring equipment for water outflow, conductivity and amount of precipitation had already been tested and the analysis of data was done.

5.5.1 Snow melting 2004

In March 2004 occurred a special weather condition for this period. In the week between 15.3.2004 and 23.3.2004 the day air temperature exceeded 20°C, causing forced snow melting. In the *Figure 58* maximum, minimum and mean air temperature values for Maribor meteorological station are presented (ARSO, 2004). Location of the lysimeter is in the middle of the mixed forest and the air temperature is lower than on the weather station. The snow melting on the location was late compared to meteorological data. Before the warming there was 40 cm

of snow cover, which was also sampled. The intensive water flow in the unsaturated zone was detected at 23.3.2004 and at that time the water in the unsaturated zone was sampled for isotope analyses. Volume and conductivity of water outflow were measured at the time of sampling. On 24.3.2004 the day precipitation was 70 mm. All the weather conditions cause extreme water flow in the unsaturated zone.

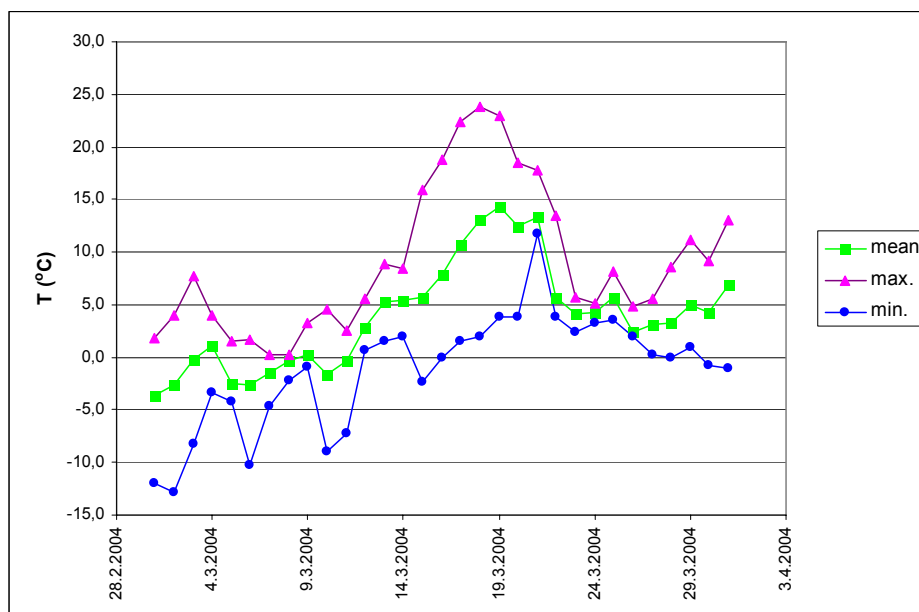


Figure 58: Maximum, minimum and mean day temperature for Maribor meteorological station

The $\delta^{18}\text{O}$ isotope results of the event-influence study are in Table 26. The statistics of $\delta^{18}\text{O}$ results (Table 27) show that the most negative values were reached at JV-1, JV-4 and JV-2. In the following group are JV-5, JV-3 and JV-6. At deeper sampling points the change in $\delta^{18}\text{O}$ isotope composition is insignificant. The ranges between minimal $\delta^{18}\text{O}$ values at the time of sampling and pre-event values give the same results.

Table 26: $\delta^{18}\text{O}$ values of unsaturated water in time of snow melting

	JV-1	JV-2	JV-3	JV-4	JV-5	JV-6	JV-7	JV-8	JV-9	JV-10	Precipitation	PS-5
13.2.2004 12:00	-10.46	-9.38	-9.34	-9.93	-8.94	-9.24	-10.14	-9.36	-9.51	-10.00	-17.62	-9.46
24.3.2004 0:00	-13.10	-10.88	-10.46	-11.54	-9.61			-9.44	-9.91	-9.69	-10.98	-9.56
24.3.2004 12:00	-12.52	-11.28	-10.21	-12.29	-10.23	-9.75	-9.63	-9.52	-9.79	-9.78		
24.3.2004 18:00	-12.97	-12.66	-10.66	-12.62	-10.17	-10.45	-9.47	-9.52	-9.72	-9.98		
25.3.2004 12:00	-11.82	-12.57	-11.04	-12.36	-10.15	-9.72	-9.33	-9.30	-10.06	-10.12	-12.26	
26.3.2004 12:00		-11.88	-11.38	-13.06	-10.11	-10.33	-9.56	-9.24	-10.06	-10.31		
28.3.2004 12:00		-11.43	-11.03	-12.60	-10.11	-9.82	-9.50	-9.55	-10.03	-10.26		
30.3.2004 12:00				-12.08	-10.23		-9.49	-9.43	-10.06	-10.26		
8.4.2004 12:00	-11.58	-12.84	-11.36	-12.83	-10.69	-10.59	-9.57	-9.75	-10.08	-10.32	-10.06	
21.4.2004	-9.1	-12.27			-11.58	-10.06	-9.7	-9.9	-10.5	-10.44	-8.36	-9.66

Table 27: $\delta^{18}\text{O}$ statistics of unsaturated water at the time of snow melting

	JV-1	JV-2	JV-3	JV-4	JV-5	JV-6	JV-7	JV-8	JV-9	JV-10	Precipitation	PS-5
n	6	8	7	8	9	7	8	9	9	9	4	2
mean	-11.85	-11.98	-10.88	-12.42	-10.32	-10.10	-9.53	-9.52	-10.02	-10.13	-10.42	-9.61
max	-9.10	-10.88	-10.21	-11.54	-9.61	-9.72	-9.33	-9.24	-9.72	-9.69	-8.36	-9.56
min	-13.10	-12.84	-11.38	-13.06	-11.58	-10.59	-9.70	-9.90	-10.50	-10.44	-12.26	-9.66
range	-4.00	-1.96	-1.17	-1.52	-1.97	-0.87	-0.37	-0.66	-0.78	-0.75	-3.90	-0.10
event min	-10.46	-9.38	-9.34	-9.93	-8.94	-9.24	-9.33	-9.24	-9.51	-9.69	-8.36	-9.46
event range	-2.64	-3.46	-2.04	-3.13	-2.64	-1.35	-0.37	-0.66	-0.99	-0.75	-3.90	-0.20

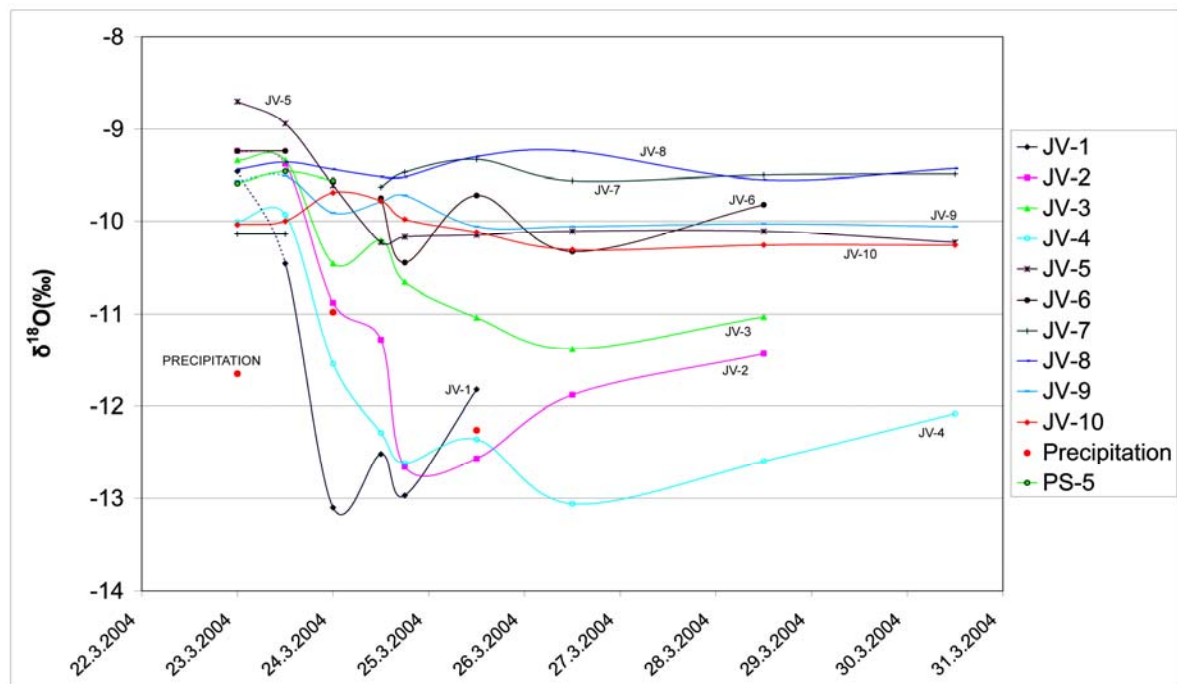


Figure 59: $\delta^{18}\text{O}$ values at the time of snow melting

Figure 59 graphically presents the influence of snow melting on the change of $\delta^{18}\text{O}$ isotope composition. The curves show the different reaction times to the event. The most distinct signals are in sampling points JV-1, JV-2, JV-4, and JV-3. A significant oscillation is identified also at JV-6. At JV-8, JV-9, JV-10 and JV-7 the signal is reduced. From the water discharge data (Figure 60, Table 28) the two types of sampling points can be defined. The group JV-9, JV-5, JV-10 and less JV-8 reacted fast on the snow melting with increased outflow and a clearly recognizable double signal which is caused by effective precipitation at 24.4.2004. The highest outflow is at JV-10 (833 ml/h). JV-4 has a similar discharge as JV-8 but not such a clear double signal. JV-6, JV-2 and JV-7 have a minor discharge and a less clear double signal. The signal at JV-7 lags behind the others. If we link both plots together, we assume that at a deeper part of the lysimeter the piston flow provokes higher outflow with the pushing of old water stored in the unsaturated zone. There was almost no share of new water determined. On the other hand the upper sampling points point at the high influence of the snow melting on both the sampling point discharge and share of fresh water. The share of fresh water continues growing also after the discharge already decreases. This can be a result of the increase of the part of new water in the share of matrix flow. The large amount of fresh water pushes the old water farther and replaces it in a large part in the matrix flow.

Table 28: Water discharge in time of snow melting observation

Q (ml/h)	JV-1	JV-2	JV-3	JV-4	JV-5	JV-6	JV-7	JV-8	JV-9	JV-10
23.3.2004 0:00	0.20	0.00	0.00	3.21	1.25	0.00	0.00	2.67	4.28	17.29
24.3.2004 0:00	59.67	25.42	50.42	17.00	4.17	29.17	22.92	0.00	0.00	0.00
24.3.2004 12:00	180.42	100.83	58.33	107.50	416.67	100.83	0.00	256.50	416.67	833.33
24.3.2004 18:00	403.33	51.00	11.67	226.67	0.00	135.00	48.33	39.33	140.00	138.33
25.3.2004 12:00	30.00	27.22	17.22	152.78	90.56	121.67	78.33	44.44	235.00	187.22
26.3.2004 12:00	0.00	5.33	8.33	126.67	30.00	42.83	35.00	21.88	122.92	122.29
28.3.2004 12:00	0.00	0.54	1.38	35.21	19.79	11.25	21.79	17.92	61.67	96.67
30.3.2004 12:00	0.00	0.00	0.00	5.00	22.08	0.00	5.21	11.46	29.58	65.42
8.4.2004 12:00	1.30	2.57	1.60	10.14	24.77	6.37	9.65	19.26	6.94	49.86
21.4.2004 12:00	0.07	1.94	0.04	4.10	45.51	1.08	28.53	61.89	13.01	38.60

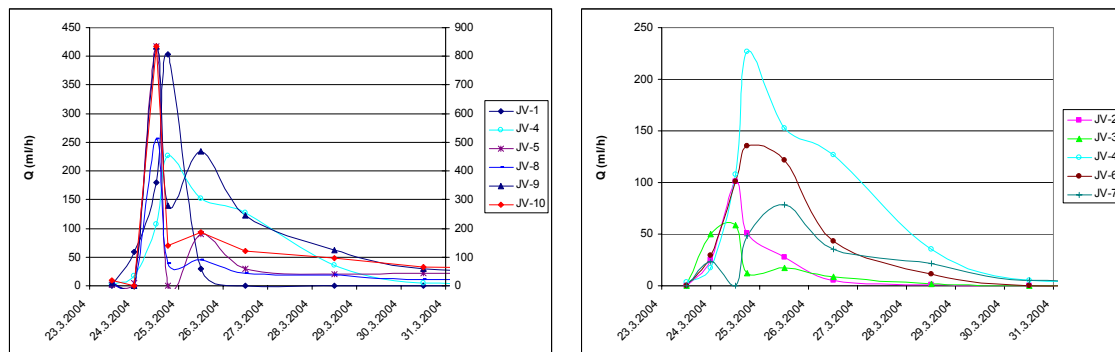


Figure 60: Discharge of the water in unsaturated zone in time of snow melting.

On the basis of $\delta^{18}\text{O}$ values (Table 26) the hydrograph separation was done. The part of new water which moved because of snow melting was estimated. For the pre-snow melting $\delta^{18}\text{O}$ values the last measurements in February were taken (Table 26). The sampled snow $\delta^{18}\text{O}$ value -18.06‰ (16.3.2004) was taken for the input signal. Calculations of the matrix flow shares are in Table 29. The hydrograph separations by each sampling point are added in Annex L. In Figure 61 the typical hydrograph separation of JV-4 is presented. Only the data until 30.3.2004 are considered in the interpretation, because only so far a clear snow melting signal is assumed in the discharge volume. The higher part of the new water is determined in JV-1 (33%), JV-2 (38%), JV-4(38%) and JV-3(28%). The new water share has the longest influence in JV-4. In JV-5 the share of fresh water increased and stayed constant, in JV-6 the part of fresh water reached 14% once. The highest percentage of fresh water correlates with peak $\delta^{18}\text{O}$ values on 24.3.2004. Preferential flow is assumed. Deeper than JV-6, except for the piston flow effect on the discharge, the influence of new water shares are not recognized. The calculations over 100% shares of the old water at deepest points are results of high $\delta^{18}\text{O}$ values in matrix flow and no influence of fresh water.

Table 29: Matrix flow shares in discharge water

Matrix flow shares	JV-1	JV-2	JV-3	JV-4	JV-5	JV-6	JV-7	JV-8	JV-9	JV-10
24.3.2004 0:00	0.65	0.83	0.87	0.80	0.93			0.99	0.95	1.04
24.3.2004 12:00	0.73	0.78	0.90	0.71	0.86	0.94	1.06	0.98	0.97	1.03
24.3.2004 18:00	0.67	0.62	0.85	0.67	0.87	0.86	1.08	0.98	0.98	1.00
25.3.2004 12:00	0.82	0.63	0.81	0.70	0.87	0.95	1.10	1.01	0.94	0.99
26.3.2004 12:00		0.71	0.77	0.62	0.87	0.88	1.07	1.01	0.94	0.96
28.3.2004 12:00		0.76	0.81	0.67	0.87	0.93	1.08	0.98	0.94	0.97
30.3.2004 12:00				0.74	0.86		1.08	0.99	0.94	0.97
8.4.2004 12:00	0.85	0.60	0.77	0.64	0.81	0.85	1.07	0.96	0.93	0.96
21.4.2004 12:00	1.18	0.67			0.71	0.91	1.06	0.94	0.88	0.95

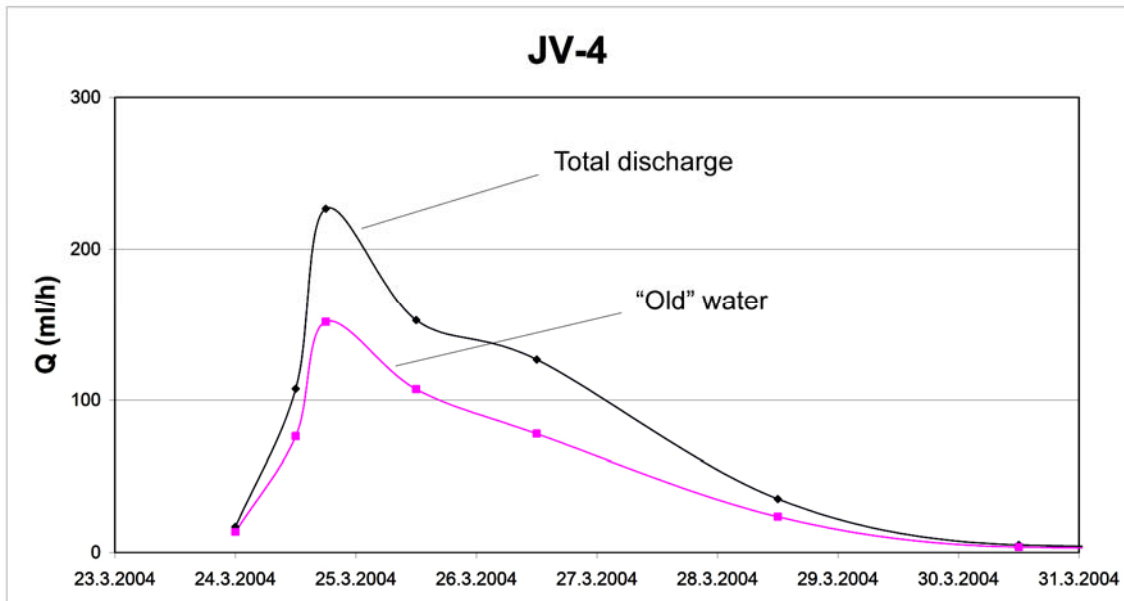


Figure 61: Snow melting component

5.5.2 Summer storm events

Setting up the equipments for measuring discharge, precipitation amount and conductivity in 2005, the monitoring of the water dynamic system in coarse gravel unsaturated zone was made possible. At JV-2 and JV-9 there was no discharge measuring facility, at JV-10 the conductivity measurement was missing. July 2005 was a period with high frequency of summer storms. After some rainy days at the beginning of July, the field capacity of the unsaturated zone was quite high, the real thunderstorm with 90 mm of precipitation occurred. The storm started 10.7.2004 at 23.00. In the first hour there was almost 20 mm of precipitation, and in ten hours the precipitation amounted to 79 mm.

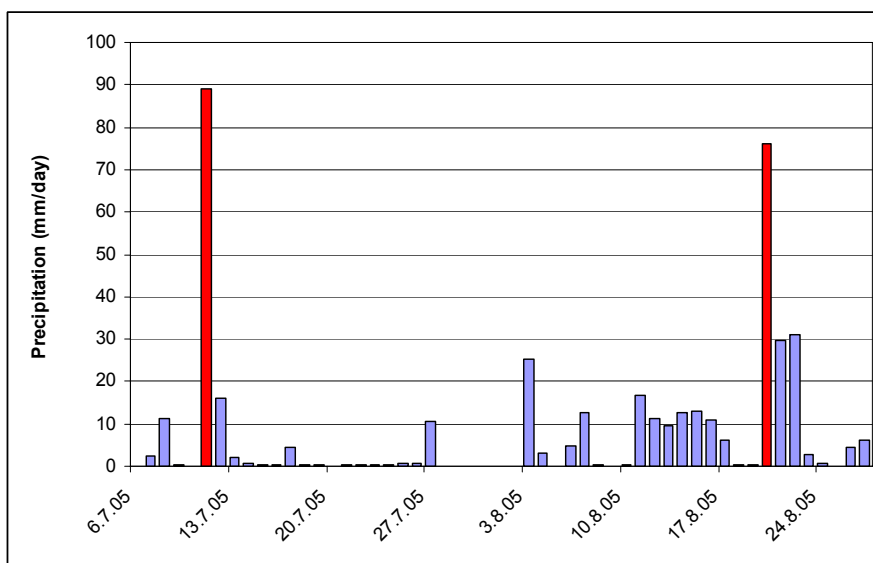


Figure 62: Thunderstorm precipitation

The next measured event occurred in August. On 20.8.2005 there was a thunderstorm with 76 mm of precipitation in four hours and with 54 mm of precipitation in the second hour. In the next two days there were two more thunderstorms with 30 mm of precipitation. *Figure 62* shows the amount of precipitation near the meteorological station for the period 2004-2005 with marked observed special events.

In the diagrams in *Annex M* the measurements of precipitation, conductivity and discharge by each sampling point are performed for both events. Because of deficient data quality the JV-1 sampling point is excluded from the analysis. In the July event changes in discharge caused by thunderstorm were behind the first precipitation wave, but conductivity reacted faster. A possible explanation is that the soil and unsaturated zone need to enrich field capacity which is a condition for exposing water movement in the unsaturated zone. In August the discharge in the upper part of unsaturated zone reacted fast after the storm because a rainy period preceded the storm and possibly the field capacity was very high. Two phenomena in conductivity measurements can be observed. In one group of sampling points the conductivity scarcely arises at all after heavy precipitation and then the conductivity decreases with the intensity of precipitation. With the end of precipitation also the conductivity returns to the prior values. Points JV-2, JV-3 and JV-4 are in this group. At other points conductivity increases with the discharge but both are behindhand compared with precipitation occurring. With the depth and local unsaturated zone structure conditions both signals are diminished and the shape peaks move farther in time scale from the event. This can be explained by the fact that in the upper part of the unsaturated zone new water first pushes the old water but, afterwards there is the effect of preferential flows where the new water takes a big share of water flow and conductivity decreases. When preferential flows stop, the matrix flow starts again and values of conductivity return to normality. The opposite change of conductivity at lower sampling points can be explained with concentrations. If CO₂ is provided, precipitation pushes downward from the upper part of the layer as a plug, in the lower part CO₂ tries to be in equilibrium and dissolves carbonate and water mineralization is increased. When the CO₂ is consumed, the conductivity returns to normality. *Figure 63* shows the diagrams of typical representatives of both groups.

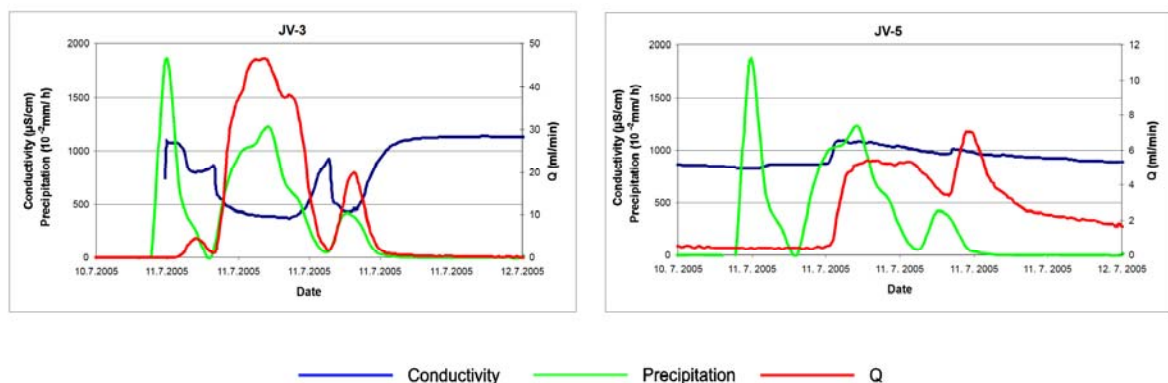


Figure 63: Diagrams of typical reaction of conductivity, precipitation amount and discharge on storm event

5.5.3 Preferential flows

The short time investigations include analysis of data measured in two different special time events. In the first case of snow melting, the watering of the unsaturated zone took longer compared with the time of thunderstorm, and the large amount of water passed through the soil and the unsaturated zone. The snow melting signal was very strong. Beside preferential flow also the recharge and the dynamics of matrix flow could be studied. At the time of storm events, the reactions of the unsaturated systems were studied in a very short period. Based on data analyses the following conclusions are made:

- The increase in discharge does not indicate the presence of preferential flow or its intensity. This could be the consequence of the piston effect from the upper part of the unsaturated zone. With watering of the upper part of the unsaturated zone new water increases the hydraulic pressure and pushes the old water downwards. This is confirmed by the increased conductivity and discharge at the same time (storm event), and a high discharge and low $\delta^{18}\text{O}$ isotope signal in time of snow melting.
- The shapes of $\delta^{18}\text{O}$, conductivity and outflow curves confirm that with the depth in the unsaturated zone the homogenization of differently aged water arises.
- Based on snow melting, the preferential flows are recognized at JV-1, JV-2, JV-3, JV-4, JV-5 and JV-6. The occurrence and intensity of preferential flow depends on the quantity of recharge water, on pre-event moisture conditions of the soil and unsaturated zone and on heterogeneous matrix on micro scale in a lysimeter.
- Based on $\delta^{18}\text{O}$ isotope results at the time of snow melting, the recharge water shares for different locations in the lysimeter are defined. In the upper part of the lysimeter (up to JV-4) the new water takes a 38% share of water discharge. At JV-5 the new water share reached 28%, at JV-6 14%, deep new water share was 5%.

5.6 Water dynamics in a coarse gravel unsaturated zone

The main goal of the dissertation was the description of water movement in a coarse gravel unsaturated zone. If the results of long and short term investigations are summarized, some conclusions about water dynamics in a coarse gravel unsaturated zone could be done.

All results showed that the piston flow has an important role on water flow in the unsaturated zone of an intergranular aquifer. It was noticed that at the time of high quantities of water entering into the aquifer, e.g. snow melting, storm precipitation or tracer injection, the discharge increase did not mean the increase of new water share in the discharge. It was concluded that the piston effect from the upper part of the unsaturated zone pushed the old water downward. Also the comparison of LPM modelling results shows that the mixing and dispersion processes are not so expressive in the first few meters in the unsaturated zone. The preferential flows which occurred at the time of strong precipitation in the intergranular unsaturated zone do not by-pass a larger part of the new water downwards to groundwater. The quantity of water conducted by the preferential flow does not represent a characteristic part of recharge water at a defined time, but the preferential flows have an important role in pollutant transport.

On the basis of isotope investigations and tracing experiments the estimation of several dynamic parameters was done. The lumped parameter models (LPM) for $\delta^{18}\text{O}$ data and one dimensional convection-dispersion model (CDM) for tracing experiment data were used to define MRT and mean flow velocity (chapters 5.3.3, 5.4). Comparisons of both results are in *Table 30*.

Table 30: Comparison of LPM and CDM modelling results

		<i>JV-2</i>	<i>JV-3</i>	<i>JV-4</i>	<i>JV-5</i>	<i>JV-6</i>	<i>JV-7</i>	<i>JV-8</i>	<i>JV-9</i>	<i>JV-10</i>
Depth	m	0.82	1.08	1.52	2.04	2.41	2.95	3.4	3.93	4.39
MRT-LPM	month	2.6	4.5	3.6	3.8	4.1	7.7	7.2	6.7	9.7
m.flow velocity-LPM	m/d	0.010	0.008	0.014	0.018	0.019	0.013	0.016	0.020	0.015
MRT-CDM	month	1.9	4.5	3.6	4.0	4.7	8.9	7.6	7.7	9.1
m.flow velocity-CDM	m/d	0.014	0.008	0.014	0.017	0.017	0.011	0.015	0.017	0.016
MRT-difference	month	0.7	0.0	0.0	-0.2	-0.6	-1.2	-0.4	-1.0	0.5
m.flow velocity-difference	m/d	-0.004	0.000	0.000	0.001	0.002	0.002	0.001	0.003	-0.001

Although the modelling by lumped parameter models was for the observed period 2001-2004, and the evaluation of tracing experiment data was for the hydrological period 2004-2005, MRT estimations are comparable. Generally the MRT calculated by lumped parameters model takes

less time than the MRT calculated by tracing experiment. The biggest differences are noticed at sampling points JV-7 (1.2 months) and JV-9 (1 month). Regarding the position of sampling points also the difference at sampling point JV-1 is not neglected. Comparison of calculated mean flow velocities shows the differences in range 0-0.004 m/d.

Table 31: Estimation of MRT of the water in the coarse gravel unsaturated zone in Selniška Dobrava

Method - Model	m.f.velocity m/d	MRT day	MRT year	velocity range m/d	MRT-range day	MRT-range year
Lumped parameter m.	0.015	1860	5.09	0.008-0.02	1375-3438	3.77-9.42
Convection-dispersion m.	0.0143	1919	5.26	0.008-0.017	1618-3438	4.43-9.42

If it is assumed that the ground water level is 27.5 m deep, it could be concluded that the mean residence time through the unsaturated zone in the Selniška Dobrava coarse gravel aquifer is in the range of 1860-1919 days, i.e. 5-5.3 years. The range of MRT at lysimeter location is estimated at 1375-3435 days, i.e. 3.8-9.4 years (Table 31).

For groundwater protection and for measures performed because of this protection, the first arrival of the tracer through the unsaturated zone is important. The pollution of groundwater depends on pollutant and aquifer properties. If it is adopted that the pollutant behaves like a conservative tracer, and with the estimation of the fastest flow velocity in the lysimeter ranging between 0.1 and 0.07 m/d (Table 23), the pollutant can reach groundwater in 9-12 months. Based on the dominant flow velocity 0.03 m/d the percolation time is 2.5 years.

Even if the aquifer of Selniška Dobrava is treated as homogeneous, there are some differences in results between single observation points which show distinctions in the local unsaturated zone structure. The heterogeneous matrix in micro scale causes the differences in water flow. Results (in-situ measurements, long term isotope investigations, tracing experiment and event analyses) show that on the north side of the lysimeter observation wall more preferential flows occur. It can be concluded, that also in unsaturated zone, especially in the high- permeable coarse gravel aquifer the local structure of the unsaturated zone has a great influence on water flow properties. Regarding the results of dynamic study, the sampling points in lysimeter could be classified in three groups. The sampling points JV-1, JV-5, JV-8 are more subject to the preferential flow influence. The sampling points JV-3 and JV-7 show longer MRT and could be inferred on local less impermeable structure. Others sampling points could be treated as average representative sampling points of the unsaturated zone.

6 CONCLUSIONS

The research was focused on the development and application of an unsaturated zone monitoring network and lysimeter construction in a high-permeable aquifer. Attention was given to the implementation of in-situ measuring of some unsaturated zone characteristics. On the basis of isotope results conclusions about some principal water flow characteristics in the unsaturated zone were made. The mean residence time of the water in the unsaturated zone was estimated by lumped parameter models and compared with results of the tracing experiment. The impact of snow melting and thunderstorms on the preferential flow and on geochemical processes connected with these events were also studied.

6.1 Results summary

The results presented in the thesis and the conclusions thus derived are summarized below.

1. Experimental site characteristics:

- The lysimeter is located in the area of the principal aquifer of Selniška Dobrava downstream from the pumping station GV-1, at an altitude of 295 m. The thickness of the gravel deposit in this area is 37.5m, the water table is at 27.5 m, and the saturated layer is 10 m thick. The larger area of the lower aquifer is covered by mixed forest.
- The soil on lysimeter location was defined as distric cambisol.
- The hydraulic conductivity of the soil was estimated on $1.5-4.5 \times 10^{-5}$ m/s by double ring method.
- Based on granulometric analyses the hydraulic conductivity of the coarse gravel was estimated on $2.9 \times 10^{-3}-6.9 \times 10^{-2}$ m/s.
- The gravel at lysimeter location consists metamorphic rock and carbonates (limestone, marble-sandstone, marble and agglutinated carbonate gravel). Here and there the gravel is incrustated by calcite.
- Average annual rainfall was between 900 mm and 1200 mm in the time of investigations (ARSO, 2005).
- The average yearly air temperature was between 8 and 12 °C.

2. Experimental set-up was constructed and equipment was tested. The following conclusions were made:

- The lysimeter design, both equipment selection and construction, were appropriate in order to research water flow in the unsaturated zone in a coarse gravel aquifer.
- The sampling point set-up enables water sampling in a highly permeable gravel unsaturated zone. Drainage samplers are suitable for groundwater collection in the unsaturated zone, especially in a coarse gravel unsaturated zone, because by means of them much larger quantities of sample water can be obtained than with other sampling methods. The samples remain intact and are less subject to changes in pressure, temperature etc.
- Values of conductivity and temperature in the outflow water indicated some disturbances in measurements and should be improved.
- The soil measuring system was properly constructed. It enables the sampling of gas and measuring of temperature and $p\text{CO}_2$ in the soil.
- Selected Watermark sensors for moisture measuring are not suitable for measuring moisture in a coarse gravel environment.

3. In- situ measurements performed and the conclusions obtained:

- The entire lysimeter profile showed a very high field capacity all the time, which was indicated by very low soil water tension. With depth, the amplitude of water tension measurements decreased and the unsaturated zone become less dependent on drying and wetting. The conditions with depth become more stable.

- The partial pressure CO₂ increased up to sampling point JV-6 and then started decreasing. At measuring point JV-6 partial pressure CO₂ never fell to 0%. The highest values were measured in summer time; in winter time the partial pressure CO₂ in all measuring points, except JV-6, fell to almost 0%. The phenomenon of increase and amplitudes of the partial pressure of CO₂ can be explained by local structure, organic matter content and by processes linked to the carbon cycle in the unsaturated zone.
- There were no special characteristics in particular ranges of pH measurements in the water from unsaturated zone.
- With the depth the annual mean temperature of the unsaturated zone decreased and seasonal oscillations of temperature diminished. The mean value of temperature at the shallowest point JV-0 was 8.58 °C, and at the deepest JV-10 it was 7.25 °C. The values below 0 °C were obtained up to JV-6 at depth 2.4 m.
- Water conductivity and temperature measurements show a seasonal effect. It was assumed that conductivity increase does not depend only on the change in temperature, but it depends mostly on organic matter and organisms activity which have impact on the presence of CO₂ and indirectly on carbonate dissolution and water conductivity.
- The range of water conductivity seasonal amplitude was 500 µS/cm.
- Based on conductivity measurements conclusions about different retention times, different dynamics conditions and mixing processes of the groundwater in the unsaturated zone at a particular part of the lysimeter could be made.

4. Geochemical characteristics and processes in the unsaturated zone:

- Water from the unsaturated zone is declared as Ca-HCO₃ type of water except JV-10 which is declared as Ca-Mg-HCO₃. The mineralization of water in the unsaturated zone is relatively high and its source is mostly carbonate.
- The amplitude of δ¹³C values of CO₂ was between -27.65‰ and -24.34‰. These values indicate an organic source of CO₂ from plant breathing, decay and microorganism activity. The results corresponded with TOC values which showed a presence of dissolved organic substances. The δ¹³C – DIC values in the water were in the range between -17.1‰ and -16.3‰.
- The source of water mineralization is carbonate. CO₂ plays the most important role in the control of chemical and biological processes which are the source of mineralization. The TOC measurements in the unsaturated water showed that along the entire lysimeter profile organic matter is present, which indirectly influences the production of CO₂ and carbonate dissolution. Also the values of δ¹³C in CO₂ indicate a organic source of CO₂. When the water saturated with CO₂ comes into contact with carbonate rocks, the dissolution of calcite is started, which is connected with the consumption of CO₂. Calcite dissolution also increases water mineralization.
- There is a connection between seasonal temperature variations, CO₂ production and carbonate concentration in water.
- A stronger correlation of pCO₂ and temperature is found in the upper part of the lysimeter, in the lower part the correlation between conductivity and pCO₂ becomes more pronounced. This can be explained with theory that CO₂ originates in the upper part of the unsaturated zone and moves downwards where, in equilibrium with carbonate, it influences water mineralization. The seasonal occurrence of CO₂ explains the correlation with temperature in the upper part of the lysimeter, in the lower part the temperature is more constant and seasonal amplitudes of water mineralization are more reflected on pCO₂ values.

5. Long-term isotope investigations gave the following conclusions:

- Environmental isotopes deuterium and oxygen-18 are a suitable tool for the quantification of recharge water movement in the unsaturated zone
- Based on δ¹⁸O signal the tracing of the water movement in coarse gravel unsaturated zone is possible. The δ¹⁸O isotopic composition signal can be traced in the lysimeter samples with some motion with time and with diminishing amplitudes with depth.
- Based on δ¹⁸O signal moving conclusions about the residence time of the water in the unsaturated zone could be drawn.

- The groundwater dynamics in the unsaturated zone are highly dependent on the precipitation rate. Each hydrological year has its own characteristics in groundwater dynamics in the unsaturated zone.
 - Based on several year observation results the sampling points could be classified into the following groups:
 - o JV-1 reacted directly to precipitation.
 - o JV-2, JV-4, JV-5, JV-6, JV-8, JV-9, JV-10 ; appearance time of the signal was related to depth
 - o JV-3, JV-7: the slowest reaction of the system was observed. It could be concluded that the residence time was longer because of locally different structure of the unsaturated zone.
6. Modelling with lumped parameter models (LPM) yielded the following results.
- The lumped parameter models can be used to estimate MRT of the water in the unsaturated zone
 - Mean residence time (MRT) modelled by a different type of LPM were comparable with results of the tracing experiment.
 - Based on the best fitted output functions, the applicability of a single model was evaluated. It could be concluded that up to sampling point JV-6 at a depth 2.4 m, LM and LPM reflected better the real transport processes than the other models. Deeper in the unsaturated zone the description of unsaturated water flow was better by using EPM, EM and DM. In the first few meters in the unsaturated zone the mixing and dispersion processes were not so expressive.
 - Results showed that the piston effect in combination with other processes plays an important role in water dynamics in coarse gravel unsaturated zone.
7. Tracing experiment showed the following results:
- Deuterated water is a more suitable tracer than uranine for the study of water flow properties in the unsaturated zone of intergranular aquifers. In this study deuterium was confirmed as an ideal conservative tracer for tracer studies in the unsaturated zone.
 - Deuterated water is a very useful tracer to detect water movement, but the use of uranine gives information about organic compounds transport.
 - The retardation factor of the uranine as compared to deuterium was 1.13-1.75, which is in agreement with previously published results (Klotz 1982).
 - It was noticed that the dispersion effect increased with the distance from the surface.
 - The peaks of different breakthrough curves were delayed with sampling point depth and the movement of water could be followed.
8. Based on meteoric events studies the following conclusions were made:
- The Study of snow melting and thunderstorm phenomena is an appropriate methodology to explain flow, transport and geochemical processes in a coarse gravel unsaturated zone. Beside preferential flow also the recharge and the dynamics of matrix flow could be studied.
 - The discharge augmentation does not mean the presence of preferential flow or its intensity. This could be the consequence of the piston effect from the upper part of the unsaturated zone. With watering of the upper part of unsaturated zone, new water increases the hydraulic pressure and pushes the old water downwards.
 - Results of $\delta^{18}\text{O}$, conductivity and outflow curves confirmed that with depth in the unsaturated zone the homogenization of differently aged water arises.
 - The occurrence of preferential flow depends on pre-event moisture conditions of the soil and unsaturated zone and on the quantity of recharge water (precipitation).
 - Based on snow melting, the preferential flows were recognized till 2.4 m depth, at JV-1, JV-2, JV-3, JV-4, JV-5 and JV-6.
 - Based on $\delta^{18}\text{O}$ isotope results at the time of snow melting, the recharge water shares for different locations in the lysimeter were defined. In the upper part of the lysimeter (till JV-4) the new water took a 38% share of water discharge, with the depth the share of new water fell to 5%.

9. Conclusions about water dynamics in a coarse gravel unsaturated zone:

- All results showed that the piston effect has an important role on water flow in the unsaturated zone of an intergranular aquifer.
- With the depth the mixing and dispersion processes become more expressive.
- The quantity of water conduct by preferential flow does not represent a characteristic part of recharge water at a defined time, but the preferential flows have an important role in pollutant transfer.
- The MRT results modelled by LPM on $\delta^{18}\text{O}$ data and CDM on tracing experiment data were comparable. Both methods are suitable tools to estimate MRT of water in unsaturated zone.
- For lysimeter location in Selniška Dobrava coarse gravel aquifer, with a 27.5 m thick unsaturated zone, the recharge water MRT from surface to groundwater was estimated to 5-5.3 years.
- The estimation of mean flow velocity of matrix flow was between 0.014-0.015 m/d.
- If it is adopted that the pollutant behaves like a conservative tracer, and with the estimation of the fastest flow velocity in lysimeter in range 0.1-0.07 m/d (Table 1), the pollutant can reach groundwater in 9-12 months. Based on dominant flow velocity 0.03 m/d the percolation time is 2.5 years.
- Some differences in results between single observation points showed distinctions in the local unsaturated zone structure which had a great influence on water flow properties. The heterogeneous matrix in microscale causes the differences in water flow. Results showed that on the left (north) side of lysimeter observation wall more preferential flows occur.

6.2 Research conclusions

Water flow and transport processes in the coarse gravel unsaturated zone are complex and they develop quite differently from those in aquifers with finer unsaturated zone granulation. It is difficult to understand and describe these processes because in such material in-situ parameter measuring is difficult. The research with experimental work, by means of isotope methods and a tracing experiment using a lysimeter in the Selniška Dobrava aquifer, contribute significantly to our knowledge about water flow and transport processes in a high-permeable coarse gravel unsaturated zone. The conclusions can be summarized as follows:

Setting up of the experimental field

An important contribution of this research is the setting up of experimental field in a coarse gravel unsaturated zone. As was mentioned, the sampling of water in a coarse gravel unsaturated zone is very difficult. In the frame of the research, the measuring and sampling system of the coarse gravel unsaturated zone water was developed. Especially constructed drainage samplers prove successful for groundwater collection, because by means of them much larger quantities of sample water can be obtained than with other sampling methods. The large quantity of unsaturated water enables also to carry out different researches (tests, analyses) on the water samples which contribute to the study of unsaturated zone water dynamics. The constructed measuring system enables beside water temperature, conductivity and discharge also the measuring of soil (unsaturated zone) temperature, CO_2 partial pressure and also gas sampling.

Applicability of the different research methods

All methods applied in the doctoral work (environmental isotope hydrology and geochemistry, tracing with artificial tracers, lumped parameter (LP) modelling, hydrograph separations) were found as very useful tools to assess properties and differences in water flow also in the unsaturated zone of a coarse gravel aquifer.

- Water conductivity was proved as a significant parameter on the basis of which conclusions about different retention times, different dynamics conditions and mixing processes of the groundwater in the unsaturated zone of the lysimeter could be made.
- Environmental isotopes deuterium and oxygen-18 are suitable tools for the quantification of recharge water movement in the unsaturated zone. Based on $\delta^{18}\text{O}$

- signal the tracing of the water movement in coarse gravel unsaturated zone is possible with some motion among sampling points and with diminishing amplitudes with depth.
- The lumped parameter models (LPM) can be used to estimate mean residence time (MRT) of the water in the unsaturated zone. Based on the best fitted output functions, the applicability of a single model was evaluated. It could be concluded that up to a depth of 2.4 m, linear model (LM) and linear-piston-flow model (LPM) reflected better the real transport processes than the other models. Deeper in the unsaturated zone the description of unsaturated water flow was better by using exponential-piston-flow model (EPM), exponential (EM) and dispersion model (DM).
 - Deuterated water is a more suitable tracer than uranine for the study of water flow properties in the unsaturated zone of intergranular aquifers. The retardation factor of the uranine as compared to deuterium was 1.13-1.75, which is in agreement with previously published results.
 - The MRT results modelled by LPM on $\delta^{18}\text{O}$ data and convection-dispersion-model (CDM) on tracing experiment data were comparable. Both methods are suitable tools to estimate MRT of water in unsaturated zone.
 - The study of snow melting and thunderstorm phenomena is an appropriate methodology to explain the flow, transport and geochemical processes in a coarse gravel unsaturated zone. Beside preferential flow also the recharge and the dynamics of matrix flow could be studied.

New findings of the Selniška Dobrava coarse gravel unsaturated zone

Even if the aquifer of Selniška Dobrava is treated as homogeneous, there are some differences in results between single observation points which show distinctions in the local unsaturated zone structure. The heterogeneous matrix in micro scale (lysimeter scale) causes the differences in water flow. Although the results of lysimeter investigations indicate the heterogeneous matrix on the lysimeter scale, the conclusions of the research can be up-scaled on the coarse gravel unsaturated zone properties of the entire aquifer. Results show that also in the unsaturated zone, especially in the high-permeable coarse gravel aquifer, the local structure of the unsaturated zone has a great influence on water flow properties, especially on the occurrence of the preferential flow.

Water flow characteristics

Researches confirmed some presumptions about water flow in the unsaturated zone:

- Results of $\delta^{18}\text{O}$, conductivity and outflow curves confirmed that with depth in the unsaturated zone the homogenization of differently aged water arises.
- The occurrence of preferential flow depends on pre-event moisture conditions of the soil and unsaturated zone and on the quantity of recharge water (precipitation).

Based on the investigation results the following conclusions about the water flow in the coarse gravel unsaturated zone at Selniška Dobrava aquifer were made:

- Results showed that at the time of high quantities of water entering into the aquifer, e.g. snow melting, storm precipitation or tracer injection, the discharge increase did not mean the increase of new water share in the discharge. It was concluded that the piston effect from the upper part of the unsaturated zone pushed the old water downward. The quantity of water conducted by the preferential flow does not represent a characteristic part of recharge water at a defined time, but the preferential flows have an important role in pollutant transport.
- Investigations showed that at the time of snow melting the recharge water in the upper part of the unsaturated zone (up to 1.5 m) took a 38% share of water discharge, with the depth the share of new water fell to 5%. It could be concluded that with depth the influence of the preferential flow is reduced.
- Regarding the results of dynamic study, the sampling points in lysimeter could be classified in three groups. The first group (JV-1, JV-5, and JV-8) is more subject to higher mean flow velocity. The second group of sampling points (JV-3 and JV-7) shows longer MRT and could be inferred on local less impermeable structure. Other sampling points could be treated as average representative sampling points of the unsaturated zone.

Geochemical characteristics and processes in the unsaturated zone

Water from the unsaturated zone is declared as Ca-HCO₃ type of water. The mineralization of water in the unsaturated zone is relatively high and its source is mostly carbonate. Researches show that CO₂ plays the most important role in the control of chemical and biological processes which are the source of mineralization. The TOC measurements in the unsaturated water showed that along the entire lysimeter profile organic matter is present, which indirectly influences the production of CO₂ and carbonate dissolution. Also the values of $\delta^{13}\text{C}$ in CO₂ (-27.65‰ to -24.34‰) indicate an organic source of CO₂. When the water saturated with CO₂ comes into contact with carbonate rocks, the dissolution of calcite is started, which is connected with the consumption of CO₂. Calcite dissolution increases water mineralization. The $\delta^{13}\text{C}$ – DIC values in the water were in the range between -17.1‰ and -16.3‰. The CO₂ partial pressure increased up to 2.4 m and then started decreasing. The phenomenon of increase and seasonal amplitudes of the partial pressure of CO₂ can be explained by local structure, organic matter content and by processes linked to the carbon cycle in the unsaturated zone. Water conductivity and temperature measurements show a seasonal effect too. It was assumed that conductivity increase depends mostly on the presence of CO₂ and its influence on carbonate dissolution. The range of water conductivity seasonal amplitude was 500 $\mu\text{S}/\text{cm}$.

Applicability of the results

The question of water supply with quality water and water resources protection have become important concern. Water resources protection demand preventive measures on large areas which causes numerous contradictions among land users. For the optimization of water protection areas and for continued activity development, the knowledge of the aquifer and its unsaturated zone properties is necessary. The Selniška Dobrava gravel aquifer will become an important water resource for Maribor and its surroundings. On the basis of determined range of water flow properties by investigations the estimations of groundwater recharge, much more detailed information about pollution influence on aquifer, and groundwater protection measures can be provided. The following calculations present the basis for water resource protection and land use restrictions.

- For lysimeter location in Selniška Dobrava coarse gravel aquifer, with a 27.5 m thick unsaturated zone, the recharge water MRT from surface to groundwater was estimated to 5-5.3 years.
- The estimation of mean flow velocity of matrix flow was between 0.014-0.015 m/d.
- For groundwater protection the first arrival of the tracer (pollutant) through the unsaturated zone is important. If it is adopted that the pollutant behaves like a conservative tracer, and with the estimation of the fastest flow velocity in lysimeter in the range 0.1-0.07 m/d, the pollutant can reach groundwater in 9-12 months. Based on dominant flow velocity 0.03 m/d the percolation time is 2.5 years.

Future work

The lysimeter investigations improved importance of the field experimental work. The research should be continued on various topics:

- Improvements of the lysimeter with special emphasis on moisture measurements
- Performing of new tracing experiments with different tracers and comparison the results with previous investigations
- The results of tracing experiments will be used to set the mathematical model of the Selniška dobrava coarse gravel unsaturated zone
- With continued isotope investigations some differences among several hydrological periods should be studied
- The more detailed studies of preferential flow in time of precipitation events should be done
- More attention should be given to the detailed study of the CO₂ cycle in the coarse gravel unsaturated zone
- Some statistical methods (time series, multivariate statistics) should be used for data analyses.

7 REFERENCES

- Aeby P., Schultze U., Braichotte D., Bundt M., Moser – Boroumand F., Wydler H., Fluhler H., 2001. Fluorescence imaging of tracer distributions in soil profiles. *Environ. Sci. technol.*, 35: 753-760.
- Aljtoovski M.E. 1974. Hidrogeološki priručnik. Beograd, Građevinska knjiga: 616 p.
- Avak H., Brand W.A. 1995. The Finning MAT HDO-Equilibration - A Fully Automated H₂O/Gas Phase Equilibration System for Hydrogen and Oxygen Isotope Analyses. Thermo Electronic Corporation, Application News No.11: 1-13.
- Bayari C.S. 2002. TRACER: an Excel workbook to calculate mean residence time in groundwater by use of tracer CFC-11, CFC-12 and tritium. *Computer & Geoscience*, 28 (5): 621- 630.
- Bear J. 1972. *Dynamics of Fluids in Porous Media*. New York-London- Amsterdam, Elsevier: 764 p.
- Bear J., Verruijt A. 1992. *Modeling groundwater flow and Pollution*. 3th edition. Dordrecht, D. Reidel Publishing Company: 414 p.
- Becker M.W., Coplen T.B. 2001. Use of deuterated water as a conservative artificial groundwater tracer. *Hydrogeological Journal* , 9: 512-516
- Behrens H. 1970. Zur Messung von Fluoreszenzfarbstoffen.- *Inst. f. Radiohydrometrie, Jahresbericht 1969, GSF-Bericht, R 25: 92-96*
- Berg W., Čenčur Curk B., Fank J., Feichtinger F., Nutzmann G., Papesch W., Rajner V., Rank D., Schneider S., Seiler K.P., Steiner K.H., Stenitzer E., Stichler W., Trček B., Vargay Z., Veselič M., Zojer H. 2001. Tracers in the Unsaturated Zone. *Beiträge zur Hydrogeologie* 52: 1-102.
- Biggar, J.W., Nielsen, D.R. 1976. Spatial variability of the leaching characteristics of a field soil. *Water Resour. Res.* 12: 78-84.
- Corcho Alvarado, J.A., Purtschert, R., Barbecot, F., Chabault, C., Rüedi, J., Schneider, V., Aeschabach-Hertig, W., Kipfer, R. & Loosli, H.H., 2004: Tracer transport in the unsaturated zone of the Fontainebleau sands aquifer. *International workshop on the application of isotope techniques in hydrological and environmental studies, Proc.*, 65, Paris.
- Clark I., Fritz P. 2000. *Environmental Isotopes in hydrogeology*. 2nd edition. Boca Raton, Lewis publishers; 328 p.
- D'Amore F., Scandiffio G., Panichi C. 1983. Some observations on chemical classification on ground waters. *Geothermics*, 2/3: 141-148.
- De Marsily G 1986. *Groundwater hydrology for Engineers*. London, Academic Press Inc.: 440 p.
- Fank J., Berg W. 2001. Results from experimental site – Test site Leibnitz, Styria, Austria. In: *Tracers in the Unsaturated Zone*. Berg et.al., *Beiträge zur Hydrogeologie* 52: 25-38
- Fank J., Seiler K.P., Berg W. 2001. Flow Systems In: *Tracers in the Unsaturated Zone*. Berg et.al., *Beiträge zur Hydrogeologie* 52: 15-19
- Fetter C.W. 1993. *Contaminant Hydrogeology*. New York, Macmillan Publishing Company: 458 p.

- Fitts C.R. 2002. Groundwater science. London, San Diego, (Academic Press) Elsevier Science Ltd.: 450 p.
- Flury, M., Fluhler H. 1995: Tracer characteristics of brilliant blue FCF. – Sci. Soc. Am. J., 59, 22-27.
- Fritz P., Fontes J.Ch. 1980. Handbook of Environmental Isotope Geochemistry. Amsterdam, Elsevier: 546 p.
- Gosar M. 2000: Poročilo o preiskavi talnega profila PS-5 pri Selnici ob Dravi. Ljubljana, GeoZS Report: 6p.
- Grisack G.E., Pickens J.F. 1980. Solute transport through fractured media. Water Resource Research, 16/4: 719-730
- Helsel D.R., Hirsch R.M. 1992. Statistical methods in water resources. Amsterdam, Elsevier 522p. (24-26)
- IAEA 1983. Isotope Hydrology. Vienna, IAEA: 873 p.
- IAEA 2000 a. Environmental Isotopes in the Hydrological Cycle – Principle and Applications. Mook W.G. (ed). Volume IV: Groundwater – Saturated and Unsaturated zone. Geyh M. (ed). Vienna/Paris, IAEA: 196 p.
<http://www.iaea.org/programmes/ripc/ih/volumes/volume4.htm>
- IAEA 2000 b. Environmental Isotopes in the Hydrological Cycle – Principle and Applications. Mook W.G. (ed). Volume VI: Modelling. Yurtsever Y. (ed). Vienna/Paris, IAEA: 127 p.
<http://www.iaea.org/programmes/ripc/ih/volumes/volume6.htm>
- Jabro J.D., Lotse E.G., Fritton D.D., Baker D.E. 1994. Estimation of preferential movement of bromide tracer under field conditions. Journal of Hydrology, 156: 61-71.
- Jury W.A. 1982. Simulation of solute transport using a transfer function model. Water Resour. Res., 18: 363-368
- Kasnavia T., Vu D., Sabatini D.A. 1999. Fluorescent dye and media properties affecting sorption and tracer selection. Ground Water, 37: 376-381
- Käss W. 1998. Tracing techniques in Geohydrology. Rotterdam, A.A. Balkema: 581 p.
- Kendall C., McDonnell J.J. 1998. Isotope Tracers in Catchment Hydrology. Amsterdam, Elsevier: 805 p.
- Ketelen H., Meyer-Windel S. 1999. Adsorption of brilliant blue FCF by soils. Geoderma, 90: 131-145.
- Klotz D. 1982. Verhalten hydrologischer Tracer in ausgewählten Sanden und Kiesen. GSF-Bericht, 290:17-29
- Kogovšek J., Šebela S. 2004. Water tracing through the vadose zone above Postonjska Jama, Slovenia. Environmental Geology, 45: 992-1001
- Kreft A., Zuber A. 1978. On the physical meaning of the dispersion equation and its solutions for different initial and boundary conditions. Chem. Eng. Sci., 33: 1471-1480.
- Kung K.-J.S., Steenhuis T.S. Klavivko E.J., Gish T.J., Bubbenzer G., Helling C.S. 2000. Impact of preferential flow on the transport of adsorbing and non-adsorbing tracers. Soil Sci. Soc. Am. J., 64:1290-1296

Lege T., Kolditz O., Zilke W. 1996. Strömungs- und transportmodellierung. Handbuch zur Erkundung des Untergrundes von deponien und Altlasten. Berlin, Springer: 418 p.

Leis A., Benischke R. 2004. Comparison of different stable hydrogen isotope-ratio measurement techniques for tracer studies with deuterated water in the unsaturated zone in groundwater. Paper presented at the 7th Workshop of European Society for Isotope Research (ESIR), Berichte des Institutes für Erdwissenschaften Karl-Franzes-UniversitätGraz, Seggauberg, 27 June-1 July 2004

Lenda A., Zuber A. 1970. Tracer dispersion in groundwater experiments. Proc. Isotope Hydrology. Vienna, IAEA: 619-641

Levenspiel O. 1962. Mixed models to represent flow of fluids through vessels. The Canadian Journal of Chemical Engineering, 8: 135-138

Levenspiel O. 1999. Chemical Reaction Engineering. 3rd Edition. New York, Wiley: 578 p.

Maciejewski S., Maloszewski P., Stumpp C., Klotz D. 2006. Modelling of water flow through typical Bavarian Soils (Germany) based on lysimeter experiments: 1. Estimation of hydraulic characteristics of the unsaturated zone. Hydrological Sciences Journal, 51(2): 285-297

MacKay D.M., Freyberg D.L., Roberts P.V., Cherry J.A. 1986. A natural gradient experiment on solute transport in a sand aquifer, 1. Approach and overview of plume movement. Water Resource Research, 22/13: 2017-2029

Mali N. 1996. Določitev varstvenih območij in vodnih zalog podtalnice kvartarnega zasipa Selniške Dobrave. Ljubljana, GeoZS: 22 p., 13 app. (GeoZS Archive)

Mali N., Janža M. 2005. Ocena možnosti zajema podzemne vode z uporabo MIKE SHE programskega orodja za hidrogeološko modeliranje. Geologija, 48/2: 281-294

Mali N., Janža M., Rikanovič R., Marinko M., Herič J., Levičnik L., Mozetič S. 2005. Raziskave selniške dobrove – Raziskovalna dela z določitvijo lokacij vodnjakov in ogroženosti vodnega vira na Selniški Dobravi. Ljubljana, GeoZS: 48 p., 16 app. (GeoZS Archive)

Maloszewski P. 1996. LP models for the interpretation of environmental tracer data. In: Manual On Mathematical Models in Isotope Hydrology. Vienna, Austria, IAEA-TECDOC-910: 9-58

Maloszewski P., Maciejewski S., Stumpp C., Stichler W., Trimborn P., Klotz D. 2006. Modelling of water flow through typical Bavarian Soils (Germany) based on lysimeter experiments: 2. Environmental deuterium transport. Hydrological Sciences Journal, 51(2): 298-313

Maloszewski P., Zuber A. 1982. Determining the turnover time of groundwater systems with the aid of environmental tracers – 1. Models and their applicability. Journal of Hydrology, 57: 207-231.

Maloszewski P., Zuber A. 1985. On the theory of tracer experiments in fissured rocks with a porous matrix. Journal of Hydrology, 79: 333-358

Maloszewski P., Zuber A. 1993. Tracer experiments in fractured rock: matrix diffusion and the validity of models. Water Resource Research, 29: 2723-2735

Maloszewski P., Zuber A. 1996. Lumped parameter models for interpretation of environmental tracer data. Manual on Mathematical Models in Isotope Hydrogeology, Vienna: IAEA: 9-58.

Mazor E. 1997. Chemical and isotopic groundwater hydrology. New York, Marcel Dekker Inc.: 413 p.

Mioč P., Žnidarčič M. 1976. OGK SFRJ 1: 100 000, Tolmač za list Slovenj Gradec. Beograd, Zvezni geološki zavod.

- Miotke F.D. 1972. Die Messung des CO₂ Gehaltes der Bodenluft mit dem Dräger-Gerät und die beschleunigte Kalklösung durch höhere Fließgeschwindigkeiten. *Geomorphology*, 16: 93-102.
- Mortensen A.P., Jensen K.H., Nilsson B., Juhler R.K. 2004. Multiple tracing experiments in unsaturated fractured clayey till. *Vadose Zone Journal*, 3: 634-644.
- Morrison J, Brockwell T, Merren T, Fourel F, Philips A.M. 2001. On-line High-Precision Stable Hydrogen isotopic Analyses on Nanoliter Water Samples. *Analytical Chemistry*, 73: 3570-3575
- Moser H., Rauert W. 1980. Isothopenmethoden in der hydrologie. Berlin-Stuttgart, Lehrbuch der Hydrogeologie 8, Gebr. Borntrager: 400 p.
- Mualem Y. 1976. A new model for predicting the hydraulic conductivity of unsaturated porous media. *Water Resources Research*, 12/3: 513-522.
- Nir A. 1986. Role of tracer methods in hydrology as a source of a physical information . Basic concepts and definitions. Time relationship in dynamics system. Vienna, Austria, IAEA-TECDOC-381: 7-44.
- Nützmann G., Stichler W. 2001. Results from Experimental Sites - Berlin Test Site. In: Tracers in the Unsaturated Zone. Berg et.al., Beiträge zur Hydrogeologie 52: 19-25
- Ozyurt N.N., Bayari C.S. 2003. LUMPED: a Visual Basic code of lumped-parameter models for mean residence time analyses of groundwater system. *Computers & Geoscience*, 29: 79-90.
- Öhrström P., Hamed Y., Persson M., Berndtsson R., 2004. Characterizing unsaturated solute transport by simultaneous use of dye and bromide. *Journal of Hydrology*, 289: 23-35.
- Pezdič J. 1999. Izotopi in geokemijski procesi. Ljubljana, Univerza v Ljubljani, Naravoslovnotehniška fakulteta, Oddelek za geologijo: 269 p.
- Rank D., Papesch W., Rajner V., Steiner K.H., Vargay Z. 2001. Results from experimental Sites - Lysimeter Study on Infiltration Processes in the Sandy Soil of the Great Hungarian Plain. In: Tracers in the Unsaturated Zone. Berg et.al., Beiträge zur Hydrogeologie 52: 60-73
- Sauty, J.-P., 1980: An analysis of hydrodispersive transfer in aquifers. *Water Resource Reserch* , 16: 145-158
- Schoen R., Gaudet J.P., Bariac T. 1999. Preferential flow and solute transport in a large lysimeter, under controlled boundary conditions. *Journal of Hydrology*, 215: 70-81
- Seiler K.P., Zoejer H. 2001. Role of tracers in the unsaturated zone. In: Tracers in the Unsaturated Zone. Berg et.al., Beiträge zur Hydrogeologie 52: 11-15
- Shulz H.D. 1998. Evaluation of breakthrough curves. in: Tracing Techniques in Geohydrology. Kass W. (ed). Rotterdam ,A.A. Balkema, , p.366-375.
- Sklash M.G., Farvolden R.N. 1982. The use of environmental isotopes in the study of high-runoff episodes in streams. In: Isotope studies of hydrologic processes. Perry E.C. Jr., Montgomery C.W. (Eds.). Dekalb, IL, Northern Illinois University Press: 65-73
- Spötl C. 2004. A simple method of soil gas stabile carbon isotope analysis. *Rapid communications in mass spectrometry*, 18: 1-4
- Spötl C. 2005. A robust and fast method of sampling and analysis of ¹³C of dissolved inorganic carbon in ground waters. *Isotopes in Environmental and Health studies*, Vol. 41/3: 217-221
- Stephens D.B. 1996. Vadose zone hydrology. Boca Raton, Lewis Publishers: 339 p.

- TRACI'95 1998. Computer program. In: Tracing techniques in Geohydrology. Kass W (ed).Rotterdam, A.A. Balkema
- Trajanova M. 2004. Poročilo o preiskavi vzorcev prodnate usedline iz doline Drave pri Selnici. Ljubljana, GeoZS Report. 12 p.
- Trček B. 1997. Izotopska sestava ogljika v podzemnih vodah Trnovsko –Banjške planote. Master's degree dissertation. Ljubljana,University of Ljubljana, NTF: 108 p.
- Trček B. 2001. Spremljanje prenosa snovi v nezasičeni coni kraškega vodonosnika z naravnimi sledili. Doctoral teases, Ljubljana, University of Ljubljana, NTF: 125 p.
- Trček B., Veselič M., Pezdič J. 2003. The vulnerability of karst springs – a cave study of the Hubelj spring (SW Slovenia). Materials and geoenvironment, Vol. 50.: 385-388
- Urbanc J. 1989. Izotopska sestava ogljika v počasi iztekajočih kraških vodah. Master's degree dissertation. Ljubljana, University of Ljubljana, NTF: 121 p.
- How groundwater occurs. 2003. USGS (Aug.2003)
http://capp.water.usgs.gov/GIP/gw_gip/how_a.html (28.Sept.2005)
- Isotope tracers project. Recources on isotopes. 2001. USGS (Jan. 2001)
http://wwwrcamnl.wr.usgs.gov/isoig/period/o_iig.html (27.Oct.2005)
- Unsaturated zone. 2003. USGS (6.Jun.2003)
<http://water.usgs.gov/ogw/unsaturated.html> (28.Sept. 2005)
- Unsaturated zone flow projects. Unsaturated zone flow: definitions and details. 2001. USGS (13.Mar.2001)
<http://wwwrcamnl.wr.usgs.gov/uzf/> (27.Oct.2005)
- Van der Hoven S.J., Solomon D.K., Moline G.R. 2002. Numerical simulation of unsaturated flow along preferential pathways: implications for the use of mass balance calculations for isotope storm hydrograph separation. Journal of Hydrology, 268: 214-233.
- Van Genuchten M.Th. 1980. A closed-form equation for predicting the hydraulic conductivity of unsaturated soils. Soil. Sci. Soc. Am. J., 44: 892-898.
- Veselič M., Čenčur-Curk B. 2001: Test studies of flow and solute transport in the unsaturated fractured and karstified rock on the experimental field site Sinji Vrh, Slovenia.-in. New Approches Characterizing Groundwater Flow, Proceed. XXXI. IAH Congress, Munich, 10-14 September 2001, p. 211-214, A.A.Balkema, Lisse.
- Veselič M., Čenčur-Curk B., Trček B. 2001. Resualts from experimental site – experimental field site Sinji Vrh. In: Tracers in the Unsaturated Zone. Berg et.al., Beiträge zur Hydrogeologie 52: 45-60
- Vuković M., Soro A. 1984. Dinamika podzemnih voda. Beograd, Institut za odoprivredu "Jaroslav Černi": 500 p.
- Wild A., Babiker I.A., 1976. The asymmetric leaching pattern of nitrate and chloride in loamy sand under field conditions. – Journal of Soil Science, 27: 460-466.
- Zoellemann, Aeschbach-Hertig 2001. Evaluation of environmental tracer data by boxmodel approach. Institute of Hydromechanics and Water Resource Menegemant.
<http://www.baum.ethz.ch/ihw>
- Zuber A. 1886 a. Mathematical models for the interpretation of environmental radioisotopes in groundwater system. In: Handbook of Environmental Isotope Geochemistry, Fritz P., Fontes J Ch. (eds); Amsterdam, Elsevier: 1-59

Zuber A. 1886 b. On the interpretation of tracer data in variable flow system. *Journal of Hydrology*, 86 (1-2): 45-57

Zuber A., Maloszewski P. 2000. Lumped parameter models. In: *Environmental Isotopes in the Hydrological Cycle – Principle and Applications*. Mook W.G. (ed). Volume VI: Modelling. Yurtsever Y. (ed). Vienna/Paris, IAEA: 5-35
<http://www.iaea.org/programmes/ripc/ih/volumes/volume6.htm>

Yasuda H., Berndtsson R., Persson H., Bahri A., Takuma K. 2001. Characterizing preferential transport during flood irrigation of a heavy clay soil using the dye Vitasyn Blau. *Geoderma*, 100: 49-66

ACKNOWLEDGMENT

I would like to thank my advisers Dr. Janko Urbanc and Doc. Dr. Mihael Brenčič from the Geological Survey of Slovenia for their guidance and help with this work.

My thanks go also to Dr. Albrecht Leis from JOANNEUM RESEARCH, Institute of Water Resources Management, Hydrogeology and Geophysics in Graz for his advices on isotope investigations and tracing experiment performance.

I am also very grateful to Jože Herič from the Geological Survey of Slovenia, without him the field research would not be so successful.

This dissertation was supported by the Geological Survey of Slovenia and I would like to thank all my co-workers for their patience and especially to Simon Mozetič for graphic contribution.

The research was carried out within the project Urban Hydrogeology – The impact of Infrastructures on Groundwater, financed by the Ministry of Higher Education, Science and Technology of the Republic of Slovenia (project no. L-1-6670-0215). I would like to thank also to the Maribor Waterworks for their cooperation with the surveys.

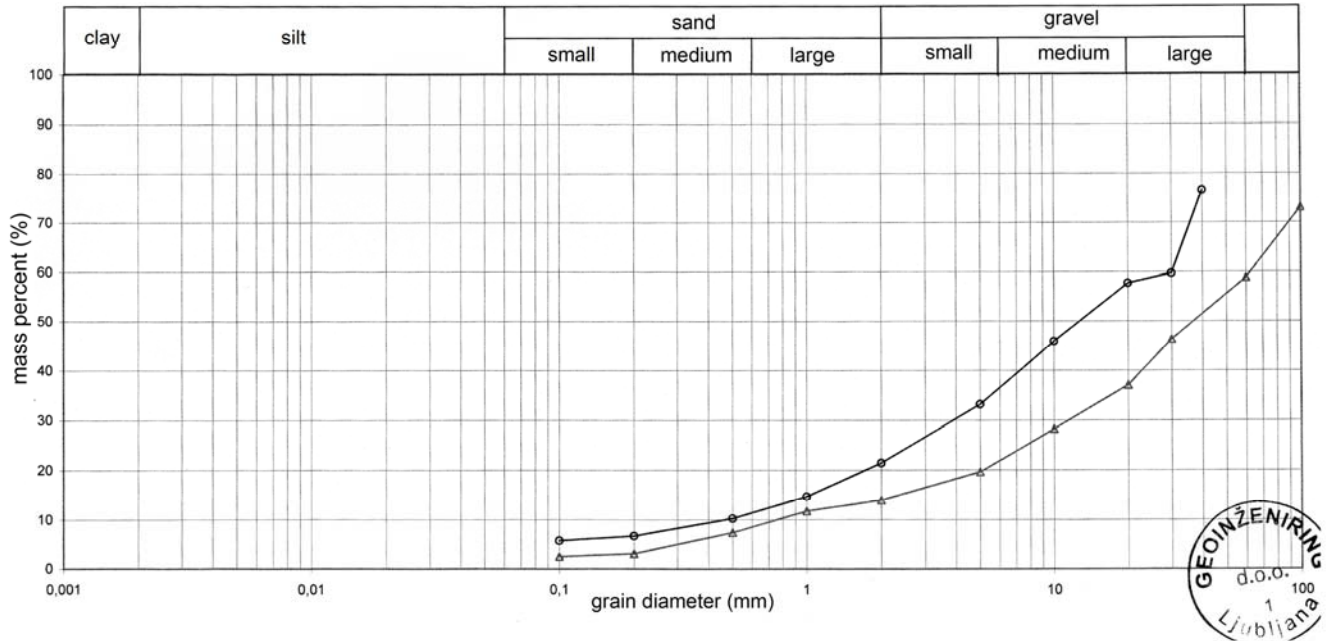
Finally, I would like to give my special thanks and love to my whole family for all their support, in the first place to my husband and son for their patience with this intellectual adventure.

Annexes

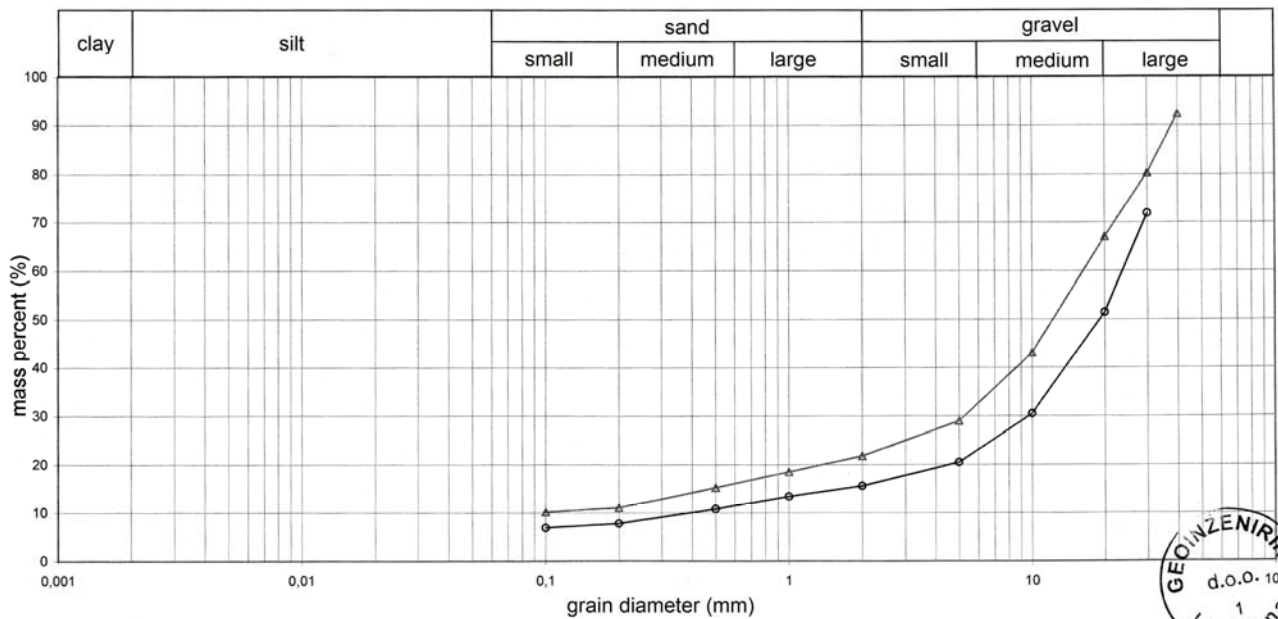
- Annex A:** *Granulometric analyses of a coarse gravel in Selniška Dobrava*
- Annex B:** *Soil and unsaturated zone moisture, temperature and pCO₂ measurements*
- Annex C:** *Water conductivity, temperature and pH measurements*
- Annex D:** *Plots of water conductivity and temperature measurements*
- Annex E:** *Chemical analyses*
- Annex F:** *Stiff plots*
- Annex G:** *Diagrams of relations between conductivity and principal chemical components*
- Annex H:** *Geochemical measurements*
- Annex I:** *$\delta^2\text{H}$ and $\delta^{18}\text{O}$ isotope composition data in the monthly sampled water*
- Annex J:** *$\delta^{18}\text{O}$ isotope composition plots of the monthly sampled water*
- Annex K:** *Results of lumped parameter modelling*
- Annex L:** *Hydrograph separation*
- Annex M:** *Measurements of precipitations, conductivity and discharge for events in July and August 2005*

Annex A: Granulometric analyses of coarse gravel in Selniška Dobrava

object	curve	borehole	depth	d_{60}/d_{10}	type of soil
Selnica	—△—	PS-5	1,50		GW – GP
	—○—	PS-5	6.00		GW – GP



object	curve	borehole	depth	d_{60}/d_{10}	type of soil
Selnica	—△—	PS-5	3,30 vz.1		GP – GM
	—○—	PS-5	3,30 vz.2		GP – GM



Annex B: Soil and unsaturated zone moisture, temperature and p_{CO_2}

Soil and unsaturated zone moisture measurements

Moisture (kPa)

<i>Date</i>	<i>JV-0</i>	<i>JV-1</i>	<i>JV-2</i>	<i>JV-3</i>	<i>JV-4</i>	<i>JV-5</i>	<i>JV-6</i>	<i>JV-7</i>	<i>JV-8</i>	<i>JV-9</i>	<i>JV-10</i>
15.4.2004		5	1	1	2	2	0	3	2	0-1	0
27.4.2004		4	0	0	1	2	0	3	2	1	0
21.4.2004		4	0	1	1-2.	2	0	3	2	1	0-1
22.4.2004		4	0	1	2	2	0	3	2	1	1
23.4.2004		4	2	1	2	2	0	3	2	1	1
25.4.2004		3	0	0	1	2	0	3	2	1	0
30.4.2004		4	0	1	1	2	0	4	2	1	0
4.5.2004		3-4.	0	0	1	1	0	3	2	1	0
11.5.2004	6	3	0	0	0	1	0	4	2	0	0
19.5.2004	9	3	0	0	0	0	0	4	2	0	0
26.5.2004	10	2	0	0	0	0	0	4	2	0	0
31.5.2004	4	2	0	0	0	0	0	4	1	0	0
8.6.2004	4	2	0	0	0	0	0	3-4.	1	0	0
16.6.2004	4	0	0	0	0	0	0	3	1	0	0
22.6.2004	2	1	0	0	0	0	0	4	0	0	0
1.7.2004	3	0	0	0	0	0	0	4	0	0	0
7.7.2004	2	0	0	0	0	0	0	4	0	0	0
23.7.2004	0	0	0	0	0	0	0	4	0	0	0
15.7.2004	5	0	0	0	0	0	0	4	0	0	0
10.8.2004	1	0	0	0	0	0	0	4	0	0	0
17.8.2004	8		0	0	0	0	0	4	0	0	0
25.8.2004	6	0	0	0	0	0	0	3	0	0	0
1.9.2004	2	0	0	0	0	0	0	3	0	0	0
6.9.2004	10	0	0	0	0	0	0	4	0	0	0
14.9.2004	3	2	0	0	0	0	0	4	0	0	0
22.9.2004	2	0	0	0	0	0	0	4	0	0	0
28.9.2004	5	0	0	0	0	0	0	4	0	0	0
8.10.2004	10	2	0	0	0	0	0	4	0	0	0
13.10.2004	4	2	0	0	0	0	0	0	0	0	0
19.10.2004	4	2	0	0	0	0	0	4	0	0	0
27.10.2004	7	2	0	0	0	0	0	4	0	0	0
2.11.2004	3	2	0	0	0	0	0	4	0	0	0
10.11.2004	5	2	0	0	0	0	0	5	0	0	0
16.11.2004	0	3		1							
24.11.2004	12	4	1	2	0	0	0	5	0	0	0
1.12.2004	7	5	1	3	0	0	0	6	0	0	0
28.12.2004	10	11	2	4	0	0	0	10	0	0	0
5.1.2005	11	8	2	4	1	0	0	10	0	0	0
21.1.2005	33	13	2	4	1	0	0	10	0	0	0
16.2.2005	11	16	3	4	2	0	0	11	1	0	0
15.3.2005	10	11	2	4	2	0	0	10	2	0	0
29.3.2005	6	7	2	3	2	0	0	10	2	0	0
21.4.2005	5	4	0	2	0	0	0	8	1	0	0
28.4.2005	7	4	0	2	0	0	0	8	1	1	0
12.5.2005	10	3	0	1	0	0	0	7	0	0	0
27.5.2005	16		2	0	0	0	0	7	0	0	0
29.6.2005	13	10	0	0	0	0	0	7	0	0	0
13.7.2005	2	4	0	0	0	0	0	6	0	0	0
21.7.2005	1	0	0	0	0	0	0	6	0	0	0

Soil and unsaturated zone temperature measurements

T (°C)

<i>datum</i>	<i>JV-0</i>	<i>JV-1</i>	<i>JV-2</i>	<i>JV-3</i>	<i>JV-4</i>	<i>JV-5</i>	<i>JV-6</i>	<i>JV-7</i>	<i>JV-8</i>	<i>JV-9</i>	<i>JV-10</i>
11.5.2004	9.3	8.2	8.1	7.7	7.1	5.9	5.5	5	4.8	4.7	4.8
19.5.2004	9.8	8.5	8	7.3	6.7	5.7	5.3	4.8	4.7	4.5	4.5
26.5.2004	10.1	9.9	9.8	9.6	9	7.9	7.3	6.6	6.5	6.2	6
31.5.2004	11.8	9.9	9.3	8.8	7.9	7.1	6.6	5.9	5.8	5.4	5.3
8.6.2004	12.7	11.2	10.6	10.1	9.1	8.2	7.6	6.9	6.7	6.3	6
16.6.2004		13.4					6.3				6.4
1.7.2004	16.3	15.4	14.8	14.2	12.9	11.4	10.5	9.4	9	8.3	7.9
7.7.2004		16.4	15.8	14.9	13.7	12.4	11.5	10.5	9.9	9	8.5
17.8.2004	16.3	16.3	16.2	16.1	15.4	13.9	13.4	12.3	11.9		
25.8.2004	16.2	16	15.9	15.8	15.4	14.3	13.7	12.6	12.3	11.3	10.9
1.9.2004	14.3	14.6	14.8	14.9	14.7		13.7	12.7	12.4	11.5	10.9
6.9.2004	14.3	14.7	14.6	14.6	14.3	13.4	13.4	12.6	12.3	11.5	10.9
28.9.2004	11.4	11.3	11.6	12	12.4	12.4	12.5	12.1	11.9	11.4	11
13.10.2004	7.3	9.3	10	10.7	11.1	11.3	11.3	11	10.9	10.4	10.2
19.10.2004	6.9	7.5	8.3	9.2	10.2	10.6	10.9	10.8	10.7	10.5	10.3
27.10.2004	8.4	8.2	8.5	8.8	9.3	9.8	10.3	10.3	10.4	10.2	10.1
2.11.2004	10.5	10	10.1	10	10.1	10.3	10.3	10.4	10.6	10.6	10.5
10.11.2004	4.2	6.2	7.2	8.1	8.8	9	9.1	9.1	9.1	9.1	9
24.11.2004	-0.1	1.4	2.3	3.4	4.9	6.4	7.1	7.5	7.7	7.8	7.8
1.12.2004	0.8	0.7	1.4	2.2	3.7	5.2	6.2	6.8	7.2	7.6	7.6
5.1.2005	-3.1	-2.2	-2.1	-0.9	0.1	1.8	2.6	3.5	4	4.7	5.1
21.1.2005	-3.7	-3.3	-2.4	-1.8	-0.6	0.6	1.3	2	2.6	3.4	3.8
16.2.2005	-3.8	-3.3	-2.9	-2.4	-1.5	-0.7	0	0.8	1.3	2.1	2.8
15.3.2005	-3.3	-2.7	-2.4	-2	-1.3	-0.8	0.2	0.8	1.3	2.1	2.5
29.3.2005	3.8	0.6	0.3	-0.4	-0.1		1.2	1.5	2	3.1	2.7
27.5.2005	11.7	11.3	10.1	9.3	7.6	7	6.4	5.4	5.4	5.3	4.6
29.6.2005	17.4		15.6	14.4	11.8	10.5	9.8	8.4	8.5	8	6.7
13.7.2005	15.2	15.3	14.7	14.3	13.1	12.2	11.6	10	10.3	9.6	7.7
21.7.2005	16.9	17.5	16.5	15.5	13.8	12.7	12	10.8	10.9	10.1	8.5
12.10.2005	9.5	10.7	11.1	11.2	11.6	12.1	11.5	11.6	12	11.8	10.7

Soil and unsaturated zone p_{CO2} measurements

p_{CO2} (‰)

<i>Date</i>	<i>JV-0</i>	<i>JV-1</i>	<i>JV-2</i>	<i>JV-3</i>	<i>JV-4</i>	<i>JV-5</i>	<i>JV-6</i>	<i>JV-7</i>	<i>JV-8</i>	<i>JV-9</i>	<i>JV-10</i>
21.4.2004		0.2-0.3	0.3	0	0.8	0.5-0.6	1.2-1.3	0.4	0.7-0.8	0.7	0.5
8.6.2004	1	0.6	0.3	0.5	1.2	1.9	4.1				
16.6.2004		1.1	0.8	1.1	1.5	2.4	2.5	1.9	2.3	1.5	1.2
22.6.2004	1.7	0.9	0.3	0.8	1.2	2.5	2.8	1.8	1.6	1.0-1.1	0.9
7.7.2004	2.3	1	0.7	1	1.2	2.1	5	2.1	2.2	1.2	1
15.7.2004	2.2	1.2	0.8	1.2	1.3	3.6	2.6	3.1	2.3	1.9	1.1
17.8.2004	2.4	1	1.2	0.9	1.3	3.3	4.3	2.7		1.2	1.2?
25.8.2004	1	0.8	0.4	0.6	0.9	2.1	2.1	2.5	1.9	0.9	1.7
1.9.2004	0.6	0.3	0.6	0.9	1.1	2.4	2.5	1.1	1.9	1.3	1.2
6.9.2004		0.8		1							
8.10.2004	1	0.6	0.5	0.7	1	1.3					
22.10.2004	0.7	0.7	0.6	0.6	0.8	0.8	0.8	0.4	0.6	1.1	1
27.10.2004	0.6	0.5	0.6	0.5	0.6	0.7	0.9	0.5	0.6	1.1	0.9
2.11.2004	0.7	1	0.8	1	1.2	0.8	2.1	1	0.7	0.9	0.6
10.11.2004	0	0	0	0.5	0.3	0	0.7	0.3	0.3	0	0
24.11.2004	0	0	0	0	0.4	0.3	0.6	0.35	0.3	0	0
1.12.2004		0	0	0	0	0	0.8	0.2	0.2		0
28.12.2004	0	0	0	0	0	0	0.8	0.2	0	0	0
5.1.2005	0	0	0	0	0	0	0.5	0			
15.3.2005	0.4	0.3	0.3	0.3	0.8	0.5	1.4	0.5	0.2	0	0
29.3.2005	0	0	0	0.2	0.5	0.5	1.5	0.6	0.8	0.3	0.3
21.4.2005		0	0.2	0.2	0.7	0.3	0.9	0.9	0.9	1	0.4
28.4.2005	0.6	0	0.4	0.5	0.9	1	2.1	0.9	1.1	0.7	0.9
12.5.2005	0.7	0.3	0.4	0.4	1.4	1.1	2	1	1.3	1	0.7
29.6.2005	1.9	1.2	1.9	2.2	3.4	4	5	2.9	2.7	1.4	1.4
13.7.2005	1.3	1	1.4	1.6	2.4	3.7	4.4	3.4	3.7	1.3	
21.7.2005	1	0.5	1.1	1.4	2.3	2.9	4.5	3.6	2.8	1.7	1.1

Annex C: Water conductivity, temperature and pH measurements

Water conductivity measurements

Conductivity ($\mu\text{S}/\text{cm}$)

<i>Date</i>	<i>JV-1</i>	<i>JV-2</i>	<i>JV-3</i>	<i>JV-4</i>	<i>JV-5</i>	<i>JV-6</i>	<i>JV-7</i>	<i>JV-8</i>	<i>JV-9</i>	<i>JV-10</i>	<i>Precipitation</i>	<i>PS-5</i>
11.5.2001			355	978	680			908	1040	1254	35	
7.6.2001			699	1147	741			942	1277	1341	81	370
19.6.2001			582	1193	774		1145	1042	1217	1339	22	370
3.7.2001			639	1234	859			1045	1245	1333	45	386
3.8.2001								1060	1258	1320	46	399
17.9.2001		991	487	1398	459		1198	972	1082	1269		400
15.10.2001		1415	500	1297	602	1154	1168	892	1000	1201		374
8.11.2001					588			804	925	1155		381
27.12.2001								651	671	987		
9.1.2002								643	784	992		543
14.2.2002					437					997		
19.3.2002		1281		1100	499	1065	1104	606	743	1046	160	375
3.4.2002	1064							620	819	1080		381
16.4.2002		1129			501	893	974	617	697	1081	44	373
9.5.2002		1092		856	580	843	808	769	945	1190		
30.5.2002				1048	769	805	959	939	1120	1338	31	
5.7.2002					743		1135	930	1171	1302	65	406
14.8.2002	691	1467	814	1314	835	849	1038	1033		1233	25	393
18.9.2002	634	1043		1287	747	748	1003	982	1113	1118	30	371
21.10.2002	577	1244		1190	647	786	846	811	897	971	18	368
6.11.2002	540	1010		1063	599		835	775	883	913		
19.11.2002	414			992	594			806	911	879		371
17.12.2002	436	766	938	1015	593	639	813	807	626	740		
14.1.2003								579	586	683		
5.2.2003				849	464			590	528	680		312
3.3.2003								586	539	624		367
16.4.2003		614		800	527	665	713	698	572	708		373
2.6.2003				813	665			947	1047	1044		375
2.7.2003								994	1059	1088	239	393
14.8.2003	563	1130	1651		770	980		1007	1059	1096	117	399
17.9.2003	303	1116	1388	1294	982	1126	1269	930	887	1004	60	375
2.10.2003		1036		1263	870	809	907	868	814	921	38	360
29.10.2003	424	1004		1086	742	920	1014	778	668	757	28	373
13.11.2003	471	744	963	884	613	720	962	719	697	757	180	359
27.11.2003				911				695	662	762		
10.12.2003	587	724	912	825	598	703	869	656	618	678		372
23.12.2003								646	491	616		365
12.1.2004	369	470	729	788	533	763	868	554	455	589	14	363
3.2.2004	333	469		787	527			547	474	580	12	368
13.2.2004				809				545	489	582		368
24.3.2004	265	486	655	709	530	726		553	539	574		
24.3.2004	255	484	705	645	525	668	716	598	560	589	25	370
24.3.2004	189	412	713	610	521	613	791	598	531	583		
25.3.2004	196	424	624	646	512	592	742	597	519	552	165	
26.3.2004		467	616	644	499	582	734	596	508	542		
28.3.2004		517	587	644	482	574	733	589	498	528		

<i>Date</i>	<i>JV-1</i>	<i>JV-2</i>	<i>JV-3</i>	<i>JV-4</i>	<i>JV-5</i>	<i>JV-6</i>	<i>JV-7</i>	<i>JV-8</i>	<i>JV-9</i>	<i>JV-10</i>	<i>Precipitation</i>	<i>PS-5</i>
30.3.2004				677	474		740	588	490	541		
8.4.2004	431	448	559	629	537	605	711	623	435	606	60	381
15.4.2004		575		648	514	559	714	614	503	612	113	375
21.4.2004		591			546	576	736	633	645	700	282	392
22.4.2004	314	566	599	672	538	659	736	638	640	704		
22.4.2004	324	551	428	654	550	629	725	626	598	694		
23.4.2004		631	646	711	455	595	738	647	638	725		
25.4.2004		663	797	735	555	617	770	646	733	736	134	
27.4.2004				735	560	646	781	662	754	781		
30.4.2004					605		752	698	812	818		
4.5.2004							713	715	836	847		
11.5.2004				817	556			734	893	876	132	
19.5.2004		713		830	670	636	789	741	913	945	67	
26.5.2004		647		839	626	691	817	771	923	966	31	
31.5.2004			1013	894	736		823	760	950	999	43	
8.6.2004		947	1110	922	733	754	894	780	934	988	32	
15.6.2004		911	1150	923	797	827	877	809	894	940	27	
22.6.2004	590	749	1120	969	788	794	887	837	937	956	28	
7.7.2004		899	1121	1025	801	945	931	867	908	968	27	
15.7.2004				1016	797		882	884	931	961	64	
23.7.2004								897	940	957		
10.8.2004					782			917	978	970		
17.8.2004				1264				908	970	955	20	367
25.8.2004		659	1168	1147	762	778	966	898	937	1085	16	
1.9.2004	824	753	1160	1144	725	800	946	892	932	931	12	
6.9.2004			1044	1117	690		944	897	921	914		
14.9.2004							929	878	912	926	37	
22.9.2004			1108	1193	638			861	908	906	33	
28.9.2004	823	811	1152	1147	609	795	854	839	765	830	12	
8.10.2004				1159	596		860	832	850	815	32	
13.10.2004	795	837	1114	1140	599	761	824	799	662	756	16	377
19.10.2004	951	869	1075	1097	565	702	808	786	663	749	13	
27.10.2004			963	1076	601		823	781	730	768	16	
2.11.2004		821	1081	1049	630		806	777	731	754	18	
10.11.2004			849	925	487		814	631	551	568	27	
16.11.2004		732	826	884	526	547	783	708	535	554	14	
24.11.2004				718	452		777	638	516	532	26	
1.12.2004								614	423	525	32	
16.12.2004				752				593	417	520		
28.12.2004	397	491	677	830	533			577	410	524	10	368
5.1.2005		489	657	752		639	636	574	363	463	21	
21.1.2005								523	384	479	24	
16.2.2005								473	399	465	14	
15.3.2005									410	493	15	
22.3.2005	393	505	682	723		646	711		406	492		
29.3.2005		466	668	731	472	693	663		490	500	18	
31.3.2005		538	679	681	487	645	675	665	532	517	30	
21.4.2005		622	612	738	551	711	806	616	577	589	32	375
28.4.2005		613	714	721	531	690	789	649	550	670	26	
14.5.2005				684	475	643	674		490	508		

<i>Date</i>	<i>JV-1</i>	<i>JV-2</i>	<i>JV-3</i>	<i>JV-4</i>	<i>JV-5</i>	<i>JV-6</i>	<i>JV-7</i>	<i>JV-8</i>	<i>JV-9</i>	<i>JV-10</i>	<i>Precipitation</i>	<i>PS-5</i>
12.5.2005		731		817	679	809	804	636	730	744	135	
27.5.2005	306	763	462	895	727	838	846	742	825	957	64	
14.6.2005								816	922	888	43	
29.6.2005					685				940	907	46	
7.7.2005	450	945	945	1146	827	1074	1144	853	920	866	15	
12.7.2005		855	638	1049	838	962	1143	874	917	856	9	
13.7.2005	620	810	973	1066	836	947	1069	870	918	820	10	
14.7.2005					802	887	1013	866	835	776		
15.7.2005				1047	799	883	1031	874	872			
18.7.2005				989			1024	865	884		48	
21.7.2005							1004	865	905			
27.7.2005	537	763		1067	808		1005	859	912			

Water temperature measurements

T (°C)

Date	JV-1	JV-2	JV-3	JV-4	JV-5	JV-6	JV-7	JV-8	JV-9	JV-10	Precipitation	PS-5
11.5.2001			10.2	9.8	9.8			8.9	8.8	9	10.8	
7.6.2001			12.6	12.3	12.3			10.7	10.4	10.2	12.9	12.9
19.6.2001			13.1	11.8	13.02		11.3	11.6	11.4	10.8	13.4	10.5
3.7.2001			14.4	14.2	14			12.1	11.9	11.9	14.7	12.1
3.8.2001								13.7	12.9	13.2	17.1	12.4
17.9.2001		13.9	14.5	14	14.7		14.4	14.1	14	13.7		10.2
15.10.2001		13.8	13.7	13.9	13.6	13.6	13.5	13.4	13.4	13.6		10.8
8.11.2001					11.7			12	11.9	12.1		10.6
27.12.2001								7.5	7.4	7.3		
9.1.2002								5.6	6	5.7		7.8
19.3.2002		6.3		6.7	6.1	6.1	6.3	6.4	6.3	6.8	6.9	10.7
3.4.2002	7							6.6	6.7	6.9		10.2
16.4.2002		7.3			7	7.1	7.1	7	7.1	7.2	8.4	10.2
9.5.2002		21.4		21.3	21.3	21	21.4	21.4	21.5	21.4		
30.5.2002				11.9	11.6	11.4	10.3	9.7	9.6	9.4	14.9	
5.7.2002					15.2		15.3	14.9	14.6	14.7	16.8	14.7
18.9.2002	15.1	15.1		15.4	15.2	15.2	15	14.6	14.5	14.3	15.3	11.4
21.10.2002	14.2	14.1		14	14.5	14.5	14.2	14.2	14.3	14.3	14.6	14.4
6.11.2002	8.9	11.6		10.8	10		10	10.1	10.7	11.2		
19.11.2002	10.3			11.1	11.1			11.4	11.3	11.4		9.7
17.12.2002	6.4	6.8	8	7.9	7.8	7.8	8.2	8.7	8.6	8.8		
14.1.2003								6.7	6.8	6.6		
5.2.2003				5	4.8			5.8	5.6	5.9		6.1
3.3.2003								5.3	5.2	5.2		8
16.4.2003		6		6.1	5.8	5.9	6.2	6.2	6.2	6.6		10
2.6.2003				11.2	11.1			9.5	9.3	9.3		11.5
2.7.2003								11.8	11.2	11.2	19.4	12.1
14.8.2003	18.7	19	17.1	17.1	15.2	16.7		13.2	14.1	13.4	19.8	12.6
17.9.2003	15	14.8	15.1	15.6	14.9	15.2	15.2	14.7	14.5	14.1	14.8	14.3
2.10.2003		14.3		14.3	14.3	14.3	14.3	14.1	14	13.8	14.8	11.9
29.10.2003	9.1	9.4		10.2	10.4	10.1	10.4	11	10.9	11	9	9.5
13.11.2003	8.9	9.2	9.9	9.9	9.9	9.9	10	10.5	10.5	10.6	9.1	9.7
27.11.2003				9.9				10.2	10.1	10.2		
10.12.2003	6.2	6.4	7.2	7.4	7.4	7.3	7.7	8.3	8.1	8.3		9
23.12.2003								7.51	7.4	7.7		5.6
12.1.2004	3.6	4.2	5	5.3	5.1	5.1	5.6	6.1	6	6.3	3.9	5.7
3.2.2004	3.5	3.9		4.5	4.5			5.5	5.4	5.6	3.8	8.8
13.2.2004				4.2				5.2	5	5.2		9.1
24.3.2004	3.1	3.6	4	4	3.8	4		4.7	4.7	4.7		
24.3.2004	2.9	3.6	3.8	4.1	3.8	4	4.3	4.6	4.5	4.8	3.7	9
24.3.2004	3	3.6	4.2	4.1	4	4.1	4.3	4.5	4.5	4.8		
25.3.2004	3.8	3.8	4	4.3	4	4.4	4.6	4.5	4.7	4.8	4.1	
26.3.2004		4.1	4.1	4.3	4.2	4.1	4.4	4.6	4.8	5.1		
28.3.2004		4.8	4.5	4.3	4.1	4.3	4.4	4.6	4.9	5.2		
30.3.2004				5.1	4.2		4.7	5	5.1	5.2		
8.4.2004	6.1	5.9	5.2	5.3	5.2	5.4	5.5	5.6	5.8	5.8	6.7	9.9
15.4.2004		6.2		6.1	5.7	5.9	5.7	6	6.1	6.2	8.6	10
21.4.2004		8.9			6.4	8.2	6.4	6.3	6.3	6.5	10.3	11.4
22.4.2004	13	13.7	13.3	12.4	10.8	11.8	11.6	12.3	12	13.4		

<i>Date</i>	<i>JV-1</i>	<i>JV-2</i>	<i>JV-3</i>	<i>JV-4</i>	<i>JV-5</i>	<i>JV-6</i>	<i>JV-7</i>	<i>JV-8</i>	<i>JV-9</i>	<i>JV-10</i>	<i>Precipitation</i>	<i>PS-5</i>
23.4.2004		8.6	8.2	7.5	7.2	8.1	7	7.1	7.1	7.2		
25.4.2004		8.7	8.2	7.3	7.9	9.5	6.9	6.8	6.7	6.7	10.3	
27.4.2004				7.3	7.3	7.3	7	6.7	6.8	6.9		
30.4.2004					8.1		7.3	6.9	7	7.2		
4.5.2004							7.9	7.3	7.3	7.3		
11.5.2004				8.5	8.8			7.5	7.5	7.5	11.6	
19.5.2004		10.5		9.2	9.2	9	8.5	8.1	8.1	8.1	12	
26.5.2004		10.8		9.4	9.3	9.3	8.7	8.4	8.3	8.2	13.8	
31.5.2004			10.1	9.8	9.9		9.3	8.7	8.6	8.8	12.4	
8.6.2004		12.3	11	10.7	10.9	10.6	9.9	9.3	9.1	9.3	15.4	
15.6.2004		13.9	12.5	12.3	12.4	12.2	11	10.8	10.3	9.8	16.1	
22.6.2004	14.8	19.8	12.2	12	12.3	12.1	11.4	10.2	10.4	10.1	16.5	
7.7.2004		15.6	13.5	13.3	13.8	13.8	12	11.2	11.4	10.9	18.6	
15.7.2004				13.7	13.8		12.5	11.5	11.7	11	16.8	372
23.7.2004								12.3	12.2	11.6		
10.8.2004					15.4			12.8	12.9	12.3		
17.8.2004				15.2				13.2	13.1	12.8	18.2	11.8
25.8.2004		17.2	15.8	15.3	15.2	15.2	14.4	13.4	13.4	13.3	18.5	
1.9.2004	16.6	16.1	15.4	15.1	15.1	15	14.2	13.6	13.4	13.3	17.6	
6.9.2004			15.4	15.1	15.2		14.4	13.6	13.5	13.3		
14.9.2004							14.2	13.5	13.5	13.4	17.7	
22.9.2004			14.6	14.3	15.1			13.4	13.5	13.2	15.4	
28.9.2004	15	14.6	14.3	14.1	14.4	14.1	13.9	13.5	13.4	13.3	15	
8.10.2004				13.7	14.2		13.7	13.5	13.2	13.2	15.8	
13.10.2004	10	11.2	12.1	12.2	12.4	12	12.4	12.5	12.4	12.4	10.3	9.4
19.10.2004	12	12	12.4	12.4	12.4	12.1	12.2	12.3	12.3	12.2	12.2	
27.10.2004			12.6	12.4	12.5		12.6	12.3	12.3	12.4	12.9	
2.11.2004		13	12.6	12.5	13		12.6	12.4	12.4	12.4	12.8	
10.11.2004			9.4	10.1	9.9		10.2	10.7	10.6	10.4	6.3	
16.11.2004		8.4	9.2	9.4	9.7	9.3	9.5	10.1	9.9	9.9	7.7	
24.11.2004				8.7	9		8.7	9.3	9.3	9.3	5.9	
1.12.2004								9.1	9	9	7.3	9.9
16.12.2004				6.9				7.8	7.8	7.7		
28.12.2004	4.6	5.3	6.3	6.3	6.6			7.2	7.3	7.1	4.9	9.5
5.1.2005		5.2	5.6	5.7		6.1	5.9	6.5	6.5	6.7	4.5	
21.1.2005								5.7	5.8	5.8	4.4	
16.2.2005								5.4	5.2	5.1	3.3	
15.3.2005									5.1	5.2	4.1	
22.3.2005	4.7	4.2	4.6	4.9		4.4	4.6		5.1	5.7		
29.3.2005		5.2	5.4	5.1	5.4	5.1	5.7		5.5	5.9	6.5	
31.3.2005		5.8	5.4	5.4	5.3	5.2	5.5	5.4	5.6	6	6.5	
21.4.2005		7.2	6.6	6.5	6.5	6.4	6.2	6.2	6.4	6.5	8	9.6
28.4.2005		9.6	10	7.3	7.3	7.4	6.9	6.8	7	6.9	10.3	
14.5.2005				5.3	5	5.2	5.7		5.8	6.1		
12.5.2005		9		8.2	8.3	8.1	7.5	7.6	7.5	7.7	10.4	
27.5.2005	13.4	12.1	10.3	9.9	9.8	10	8.6	8.5	8.5	8.8	15.6	
14.6.2005								9.4	9.5	9.2	12.7	
29.6.2005					13.5				10.5	9.9	15.9	
7.7.2005	16.9	16	14	13.4	14.3	12.7	10.8	11.3	11.1	10.9	16.4	
12.7.2005		16.2	14.7	13.7	13.6	13.3	10.9	11.6	11.7	11	15.7	

<i>Date</i>	<i>JV-1</i>	<i>JV-2</i>	<i>JV-3</i>	<i>JV-4</i>	<i>JV-5</i>	<i>JV-6</i>	<i>JV-7</i>	<i>JV-8</i>	<i>JV-9</i>	<i>JV-10</i>	<i>Precipitation</i>	<i>PS-5</i>
13.7.2005	15.6	15.9	14.3	13.6	13.5	12.8	11.2	11.8	11.9	11	17	
14.7.2005					14	13.1	11.3	11.9	11.6	11.4		
15.7.2005				13.9	13.9	12.9	11.3	11.9	11.5			
18.7.2005				14.5			11.3	11.9	11.7		18.5	
21.7.2005							12.2	12.3	12.4			
27.7.2005	16.8	16.9		14.6	14.2		11.3	12.4	12.1			

Water pH measurements

pH

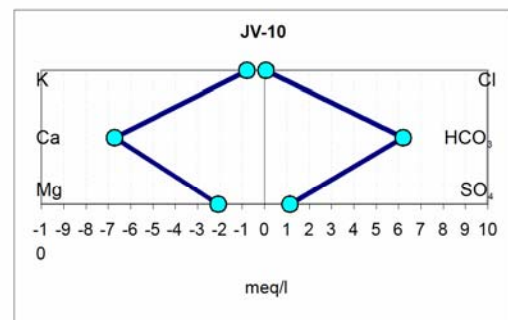
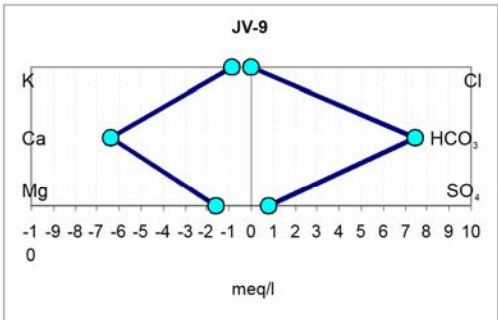
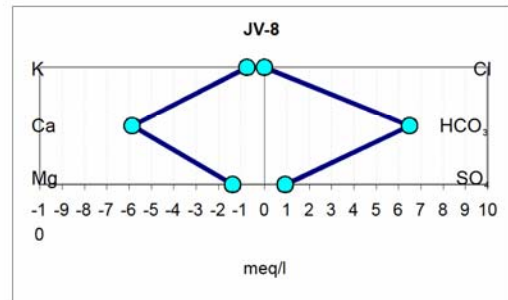
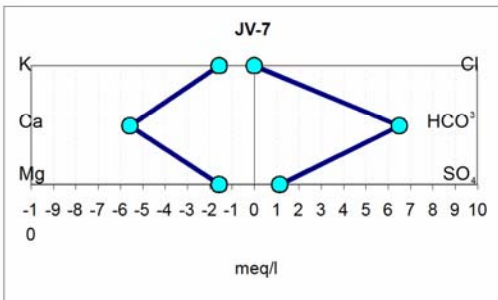
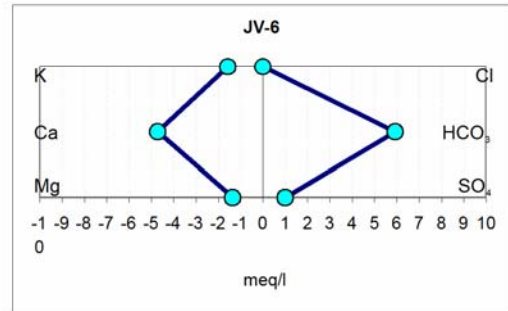
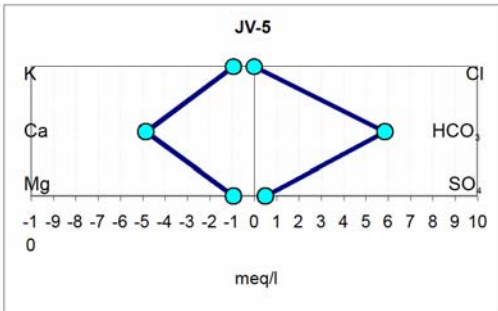
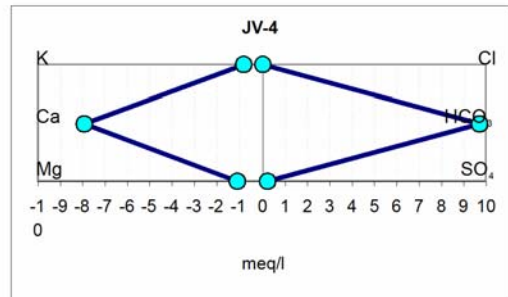
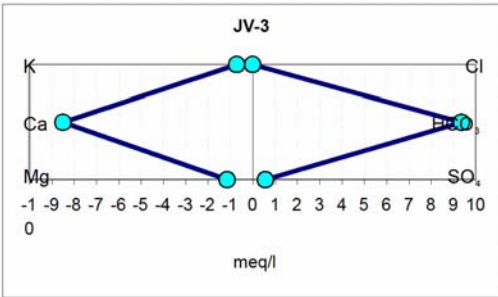
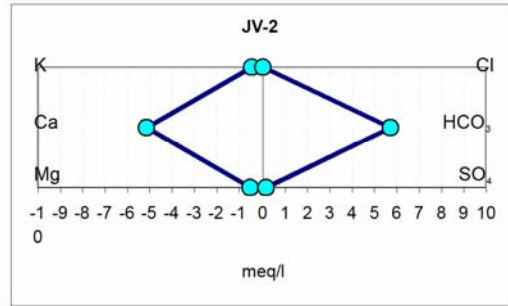
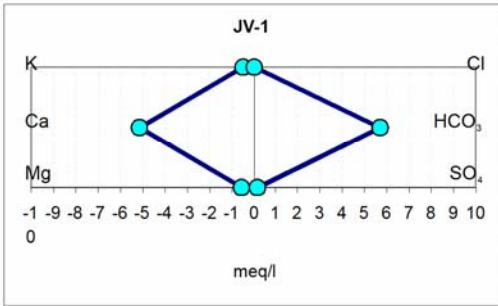
<i>Date</i>	<i>JV-1</i>	<i>JV-2</i>	<i>JV-3</i>	<i>JV-4</i>	<i>JV-5</i>	<i>JV-6</i>	<i>JV-7</i>	<i>JV-8</i>	<i>JV-9</i>	<i>JV-10</i>	<i>Precipitation</i>	<i>PS-5</i>
11.5.2001			7.41	7.18	7.06			7.07	7	6.76	6.23	
7.6.2001			7.32	7.47	7.32			7.05	6.91	6.93	6.17	7
19.6.2001			7.1	7.3	7.04		6.96	6.96	6.93	6.89	5.22	6.59
3.7.2001			7.12	7.21	7.05			7.01	6.97	7.03	6.83	7.24
3.8.2001								6.9	6.83	6.84	6.74	7.2
17.9.2001		7	7.15	7.02	6.99		6.9	6.79	6.76	6.71		7.8
15.10.2001		7.24	6.99	7.12	6.8	6.96	7.08	6.96	6.92	6.95		7.75
27.12.2001								7.68	7.51	7.85		
9.1.2002								7.77	7.54	7.96		7.88
19.3.2002		7.87		7.96	8.13	7.46	7.58	7.95	7.98	7.89	7.77	7.74
3.4.2002	7.42							7.92	7.81	7.88		7.98
16.4.2002		7.8			7.2	7.4	7.6	7.72	7.72	7.54	6.83	7.5
9.5.2002		7.78		7.4	7.3	7.12	7.25	7.24	7.25	7.09		
30.5.2002				7.25	7.19	6.92	7.22	7.21	7.14	7.08	5.47	
5.7.2002					7.11		7.12	7.4	6.98	7.07	5.92	7.48
18.9.2002	7.18	7.18		7.34	6.8	6.75	6.83	7	6.55	6.99	5.7	7.28
21.10.2002	7.29	7.31		7.35	7.29	7.19	7.3	7.21	7.3	7.21	6.9	5.65
6.11.2002	7.83	7.94		7.78	7.73		7.8	7.52	7.57	7.58		
19.11.2002	7.63			7.7	7.41			7.32	7.28	7.21		7.7
17.12.2002	7.7	7.85	7.82	7.48	7.65	7.66	7.74	7.45	7.97	8.01		
14.1.2003								7.77	7.96	7.97		
5.2.2003				7.83	8.1			8.09	8.18	8.22		7.97
3.3.2003								6.93	7.07	6.64		7.28
16.4.2003		7.52		7.4	7.57	7.48	7.53	7.51	7.46	7.36		7.48
2.6.2003				7.26	7.23			7.23	7.13	7.04		7.53
2.7.2003								7.08	7.07	6.87	7	7.08
14.8.2003	6.8	6.89	6.87	7.22	6.9	6.85		7.04	6.94	6.89	6.17	7.62
17.9.2003	6.5	7.2	7.22	7.38	6.99	7.09	7.02	7.11	7.15	7.03	5.56	7.55
2.10.2003		7.34		7.32	7.1	7.09	7.09	7.14	7.15	7.11	6.4	6.8
29.10.2003	7.06	7.4		7.74	7.68	7.3	7.24	7.53	7.66	7.52	5.74	7.92
13.11.2003	7.53	7.51	7.56	7.65	7.74	7.51	7.55	7.62	7.64	7.72	6.88	7.93
27.11.2003				7.75				7.65	7.7	7.52		
10.12.2003	7.48	7.49	7.69	7.76	7.64	7.67	7.82	7.86	7.88	8.01		7.93
23.12.2003								7.75	8	8.03		7.44
12.1.2004	8.2	8.22	8.11	8.13	7.92	7.91	7.95	8.04	8.09	7.87	8.36	7.91
3.2.2004	7.35	7.55		7.51	7.6			7.71	7.78	7.76	5.15	7.6
13.2.2004				7.78				8	8.08	8.03		7.98
24.3.2004	8.17	8.36	8.42	8.16	8.29	7.93		8.33	8.36	8.4		
24.3.2004	8.08	8.36	8.31	8.15	8.4	7.93	8.19	8.31	8.37	8.42	6.66	8.12
24.3.2004	8.22	8.52	8.69	8.25	8.45	8.17	8.13	8.31	8.42	8.49		
25.3.2004	8.15	8.4	8.62	8.13	8.43	8.13	8.33	8.41	8.4	8.42	6.26	
26.3.2004		8.51	8.59	8.32	8.5	8.21	8.36	8.44	8.44	8.39		
28.3.2004		8.26	8.47	8.35	8.45	8.29	8.37	8.41	8.63	8.42		
30.3.2004				8.32	8.48		8.55	8.45	8.46	8.47		
8.4.2004	8.04	7.92	8.14	8.12	8.1	7.95	8.15	8.17	10.4	8.17	7.44	7.9
15.4.2004		8.15		8.2	8.16	8	8.16	8.2	8.28	8.16	7.26	8

<i>Date</i>	<i>JV-1</i>	<i>JV-2</i>	<i>JV-3</i>	<i>JV-4</i>	<i>JV-5</i>	<i>JV-6</i>	<i>JV-7</i>	<i>JV-8</i>	<i>JV-9</i>	<i>JV-10</i>	<i>Precipitation</i>	<i>PS-5</i>
21.4.2004		8.04			7.9	7.9	7.68	7.8	7.86	7.79	7.28	7.87
30.4.2004					7.64		7.54	7.48	7.45	7.48		
19.5.2004		7.67		7.69	7.48	7.45	7.4	7.36	7.42	7.37	6.22	
26.5.2004		7.58		7.78	7.44	7.47	7.31	7.35	7.43	7.4	5.26	
31.5.2004			7.61	7.57	7.31		7.29	7.31	7.36	7.28	5.18	
8.6.2004		7.61	7.64	7.56	7.32	7.18	7.25	7.28	7.38	7.35	5.16	
15.6.2004		7.54	7.63	7.5	7.19	7.25	7.29	7.35	7.39	7.36	5.42	
22.6.2004	7.39	7.52	7.68	7.56	7.28	7.24	7.24	7.34	7.34	7.32	4.74	
7.7.2004		7.64	7.61	7.5	7.1	7.33	7.31	7.36	7.33	7.24	5.4	
15.7.2004				7.41	7.1		7.12	7.21	7.21	7.13	4.09	11.4
23.7.2004								7.19	7.72	7.19		
10.8.2004					7.08			7.2	7.16	7.13		
17.8.2004				7.44				7.25	7.18	7.12	5.58	7.4
25.8.2004		7.3	7.42	7.41	7.09	7	6.99	7.14	7.1	7.07	5.45	
1.9.2004	7.44	7.42	7.51	7.47	7.27	7.07	7.07	7.14	7.06	7.02	5.46	
6.9.2004			7.51	7.5	7.31		7.12	7.14	7.06	7		
14.9.2004							7.15	7.2	7.1	7.1	5.65	
22.9.2004			7.37	7.39	7.32			7.15	7.11	7.01	6.17	
28.9.2004	7.49	7.44	7.54	7.49	7.28	7.16	7.29	7.25	7.25	7.17	5.81	
8.10.2004				7.43	7.23		7.29	7.16	7.17	7.24	5.95	
13.10.2004	7.43	7.44	7.48	7.47	7.23	7.24	7.37	7.45	7.39	7.38	5.38	7.59
19.10.2004	7.73	7.57	7.56	7.52	7.38	7.36	7.45	7.5	7.31	7.22	5.42	
16.12.2004				7.9				8.08	7.08	8.07		
28.12.2004	7.53	8.28	8.16	8.06	8.19			8.1	8.04	8.16	6.21	7.75
5.1.2005		8.06	8.16	7.97		7.82	8.34	8.33	8.27	8.3	6.17	
21.1.2005								8.07	8.02	8.16	5.84	
16.2.2005								6.9	6.9	6.86	6.86	
15.3.2005									6.9	6.91	6.88	
22.3.2005	6.92	6.92	6.91	6.91		6.91	6.9		6.91	6.91		
29.3.2005				6.92			6.92		6.42	6.9		
21.4.2005		7.95	7.93	8.02	7.82	7.68	7.7	7.82	7.82	7.83	6.11	6.65
28.4.2005		8.02	8.03	8.14	7.78	7.82	7.74	7.71	7.87	7.73	6.3	
12.5.2005		7.75		7.83	7.65	7.61	7.58	7.57	7.64	7.6	6.52	
27.5.2005	7.13	7.64	7.37	7.65	7.45	7.51	7.36	7.32	7.4	7.31	5.26	
14.6.2005								7.32	7.35	7.36	5.45	
29.6.2005					7.04				7.12	7.08	4.19	
7.7.2005	6.96	7.37	7.26	7.35	7.18	7.15	7.16	7.09	7.18	7.1	6	
13.7.2005	7.38	7.42	7.27	7.31	7.1	7.11	7.17	7.09	7.19	7.09	5.46	
21.7.2005							7.14	7.14	7.1			
27.7.2005	7.12	7.32		7.77	7.2		7.14	7.09	7.13			

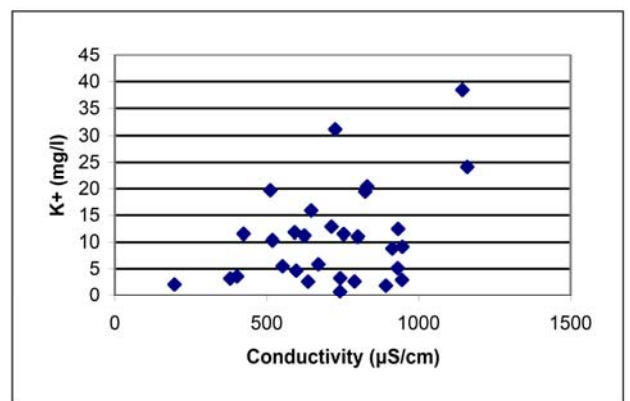
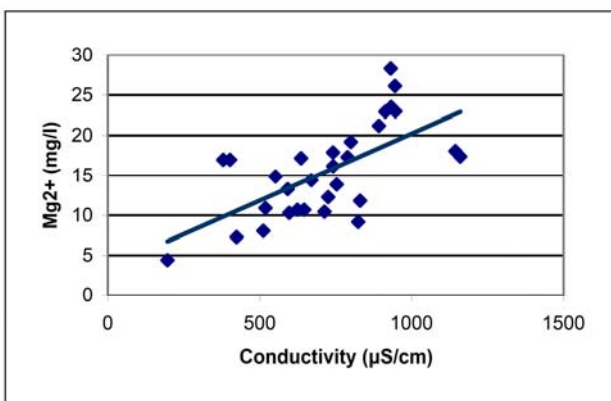
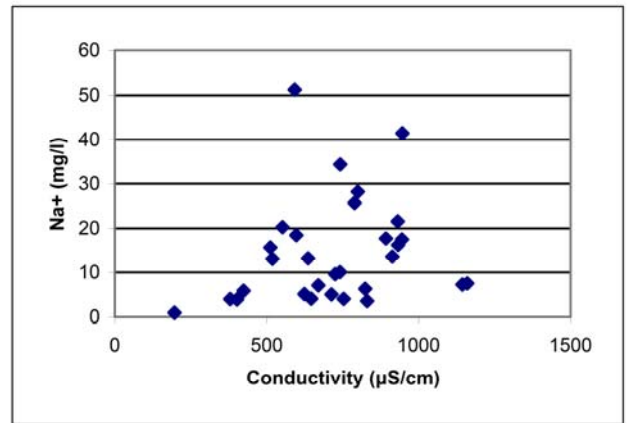
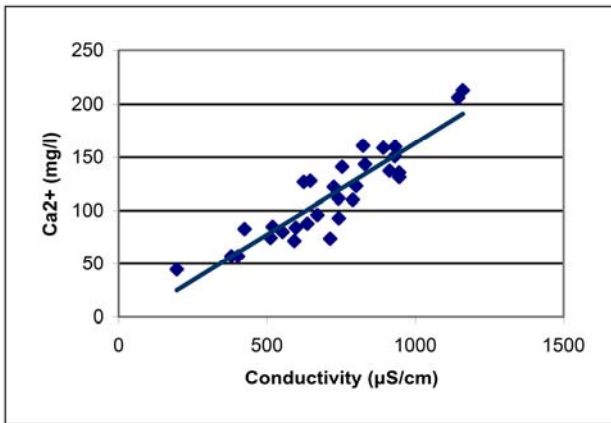
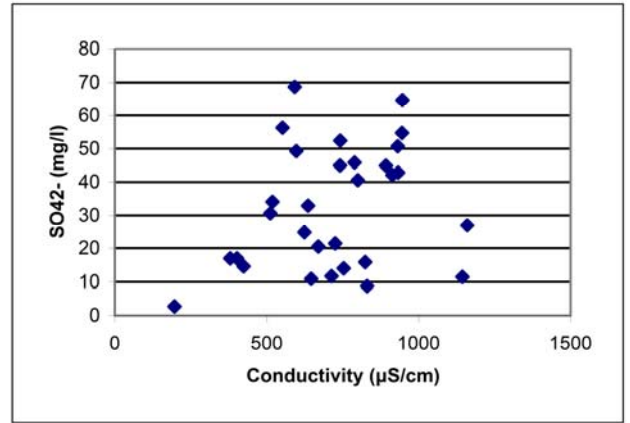
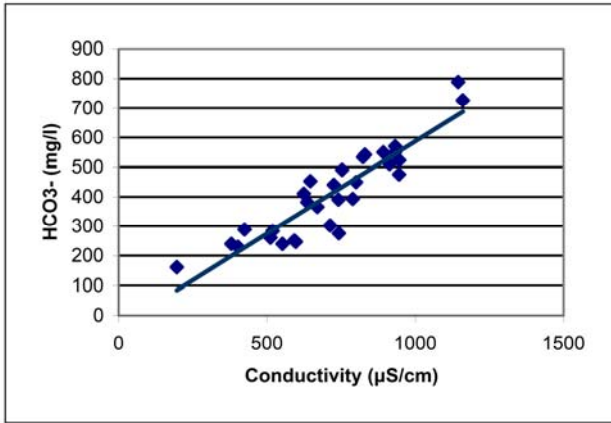
Annex E: Chemical analyses

<i>Sampl.point</i>	<i>Date</i>	<i>pH</i>	<i>SEC</i> <i>µS/cm</i>	<i>NO3</i> <i>mg/l</i>	<i>SO4</i> <i>mg/l</i>	<i>Cl</i> <i>mg/l</i>	<i>Ca</i> <i>mg/l</i>	<i>Mg</i> <i>mg/l</i>	<i>Na</i> <i>mg/l</i>	<i>K</i> <i>mg/l</i>	<i>HCO3</i> <i>mg/l</i>
JV-1	25.3.2004	8.15	196	0.46	2.7		44.5	4.41	0.96	2.07	162
JV-1	1.9.2004	7.44	824	23.5	15.9	1.32	161.0	9.2	6.3	19.4	533.9
JV-2	25.3.2004	8.4	424	2.87	14.6		82.7	7.29	5.89	11.5	289
JV-2	19.5.2004	7.67	713	6.92	11.70	0.75	73.7	10.4	5.03	12.85	303
JV-2	1.9.2004	7.42	753	18.1	14.0	1.12	141.2	13.9	4.0	11.5	491.2
JV-3	25.3.2004	8.62	624	4.62	24.8		126.9	10.7	5.13	11.2	411
JV-3	1.9.2004	7.51	1160	38.7	27.0	0.68	213.2	17.4	7.5	24.2	727.4
JV-4	25.3.2004	8.13	646	1.77	10.9		127.9	10.7	4.09	15.9	453
JV-4	19.5.2004	7.69	830	4.91	8.77	1.40	143.5	11.8	3.57	20.41	542
JV-4	1.9.2004	7.47	1144	10.9	11.5	0.67	206.3	18.1	7.3	38.4	789.0
JV-5	25.3.2004	8.43	512	9.37	30.6		74.5	8.06	15.7	19.7	261
JV-5	19.5.2004	7.48	670	8.37	20.53	1.06	96.0	14.4	7.10	5.88	366
JV-5	1.9.2004	7.27	725	33.1	21.5	0.44	122.0	12.3	9.6	31.2	441.2
JV-6	25.3.2004	8.13	592	25	68.7		71.5	13.3	51.3	11.8	251
JV-6	19.5.2004	7.45	636	16.10	32.93	1.17	87.9	17.2	13.22	2.61	382
JV-6	1.9.2004	7.07	800	52.9	40.6	0.59	123.0	19.2	28.2	11.0	449.7
JV-7	25.3.2004	8.33	742	25.7	52.4		92.9	16.2	34.4	3.27	276
JV-7	19.5.2004	7.4	789	>10	45.88	0.79	110.2	17.3	25.73	2.65	393
JV-7	1.9.2004	7.07	946	23.1	64.7	0.72	131.4	23.0	41.5	9.2	523.6
JV-8	25.3.2004	8.41	597	11.7	49.3		84.1	10.3	18.5	4.68	247
JV-8	19.5.2004	7.36	741	14.43	44.98	1.30	111.4	17.9	10.10	0.68	391
JV-8	1.9.2004	7.14	892	28.8	44.9	0.60	159.0	21.2	17.7	1.9	550.4
JV-9	25.3.2004	8.4	519	7.75	34.1		85	10.9	13.1	10.3	284
JV-9	19.5.2004	7.42	913	15.97	42.13	0.92	137.3	23.0	13.63	8.82	511
JV-9	1.9.2004	7.06	932	30.9	42.9	0.64	160.2	23.5	16.3	12.4	570.5
JV-10	25.3.2004	8.42	552	15.2	56.3		80	14.9	20.3	5.49	240
JV-10	19.5.2004	7.37	945		54.73	1.25	135.7	26.15	17.52	2.92	476
JV-10	1.9.2004	7.02	931	42.0	50.7	1.36	151.0	28.3	21.6	5.1	549.2
PS-5	30.5.2002	7.7	380	2.2	17	1.5	57	17	4	3.2	240
PS-5	5.7.2002		402	7.1	17	2	57	17	3.9	3.6	230

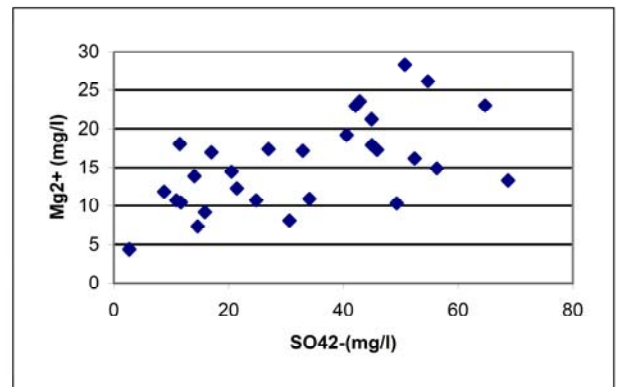
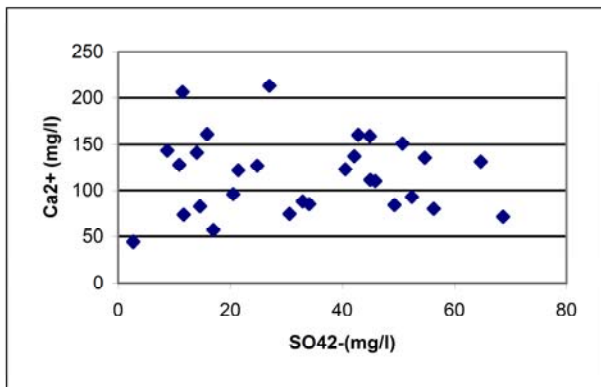
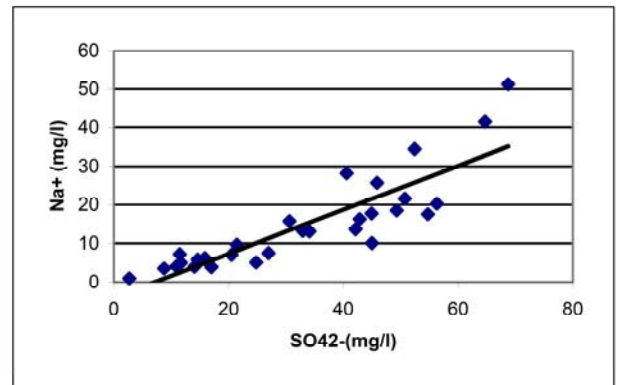
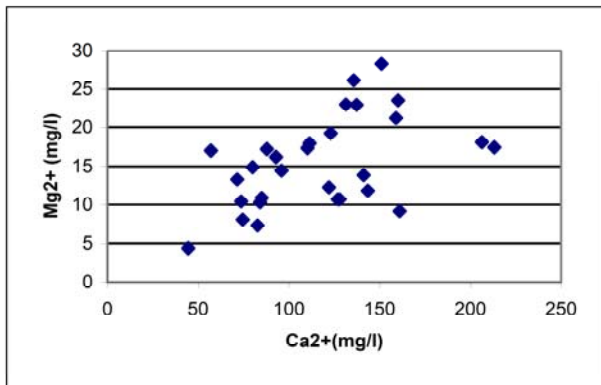
Annex F: Stiff plots



Annex G: Diagrams of relations between conductivity and principal chemical components



Diagrams of relations between conductivity and principal chemical components



Annex H: Geochemical measurements

13C(‰)	JV-1	JV-2	JV-3	JV-4	JV-5	JV-6	JV-7	JV-8	JV-9	JV-10
16.6.2004	-25,45	-25,95	-27,8	-24,7	-25,78				-25,32	-25,65
19.10.2004	-26,36	-26,67	-27,83	-26,13	-26,28	-26,17	-24,32	-24,64	-25,47	-25,64
28.4.2005	-22,51	-24,91	-27,75	-24,2	-26,47	-25,67	-24,67	-24,87	-26,02	-25,53
10.8.2005	-25,87	-26,72	-27,23	-25,08	-25,18	-24,34	-24,04	-23,92	-25,19	-24,85
Mean	-25,05	-26,06	-27,65	-25,03	-25,93	-25,39	-24,34	-24,48	-25,50	-25,42

13C-DIC(‰)	JV-1	JV-2	JV-3	JV-4	JV-5	JV-6	JV-7	JV-8	JV-9	JV-10
16.6.2004		-17,76	-17,89	-17,75	-17,82	-17,8	-17,05	-17,08	-17,07	-17,34
19.10.2004	-16,77	-17,08	-16,65	-16,74	-16,28	-17,02	-15,62	-15,58	-16,11	-17,37
28.4.2005		-14,9	-14,94	-15,67	-15,46	-15,74	-15,85	-15,87	-15,07	-16,06
10.8.2005	-17,43	-17,69	-17,09	-16,78	-16,93	-17,1	-16,66	-16,81	-16,89	-16,83
Mean	-17,10	-16,86	-16,64	-16,74	-16,62	-16,92	-16,30	-16,34	-16,29	-16,90

CO2 (%)	JV-1	JV-2	JV-3	JV-4	JV-5	JV-6	JV-7	JV-8	JV-9	JV-10
16.6.2004	1,1	0,8	1,1	1,5	2,4	2,5	1,9	2,3	1,5	1,2
22.10.2004	0,7	0,6	0,6	0,8	0,8	0,8	0,4	0,6	1,1	1
28.4.2005	0	0,4	0,5	0,9	1	2,1	0,9	1,1	0,7	0,9
21.7.2005	0,5	1,1	1,4	2,3	2,9	4,5	3,6	2,8	1,7	1,1
Mean	0,6	0,7	0,9	1,4	1,8	2,5	1,7	1,7	1,3	1,1

T (°C)	JV-1	JV-2	JV-3	JV-4	JV-5	JV-6	JV-7	JV-8	JV-9	JV-10
15.6.2004	13,4					6,3				6,4
19.10.2004	7,5	8,3	9,2	10,2	10,6	10,9	10,8	10,7	10,5	10,3
27.5.2005	11,3	10,1	9,3	7,6	7	6,4	5,4	5,4	5,3	4,6
21.7.2005	17,5	16,5	15,5	13,8	12,7	12	10,8	10,9	10,1	8,5
Mean	12,4	11,6	11,3	10,5	10,1	8,9	9,0	9,0	8,6	7,5

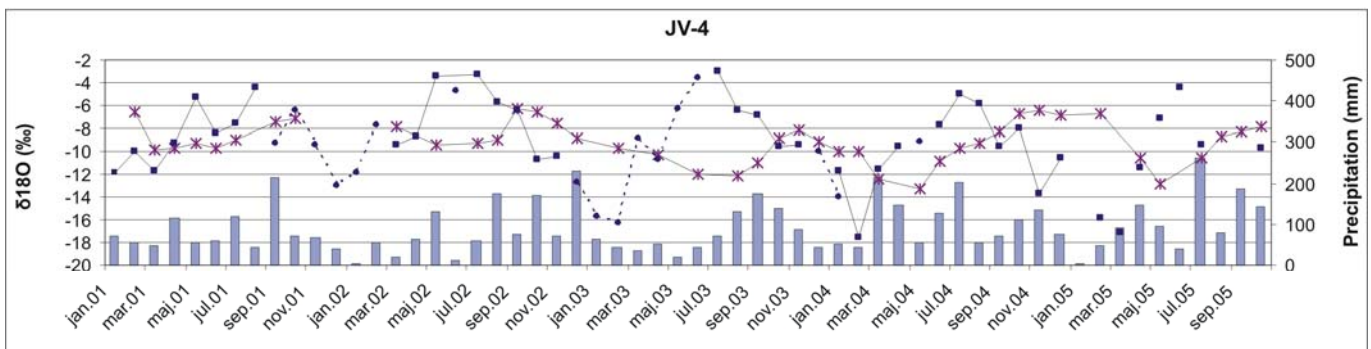
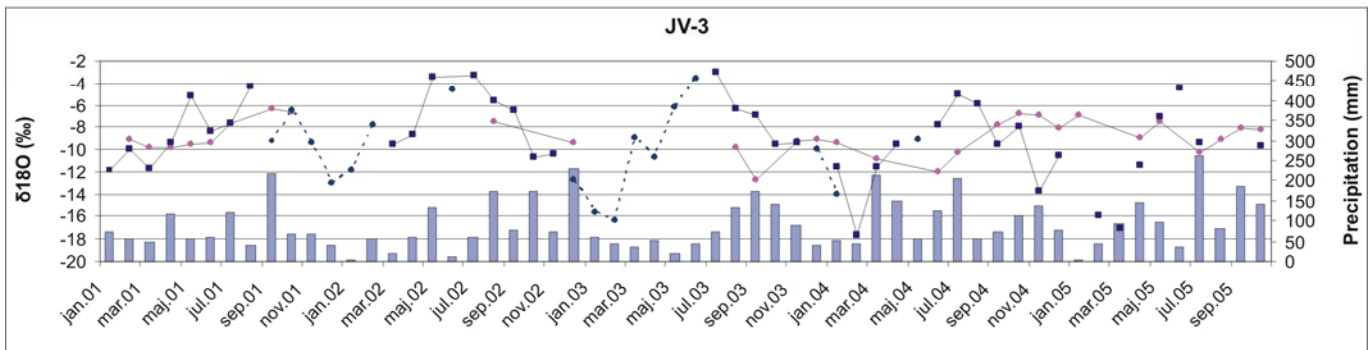
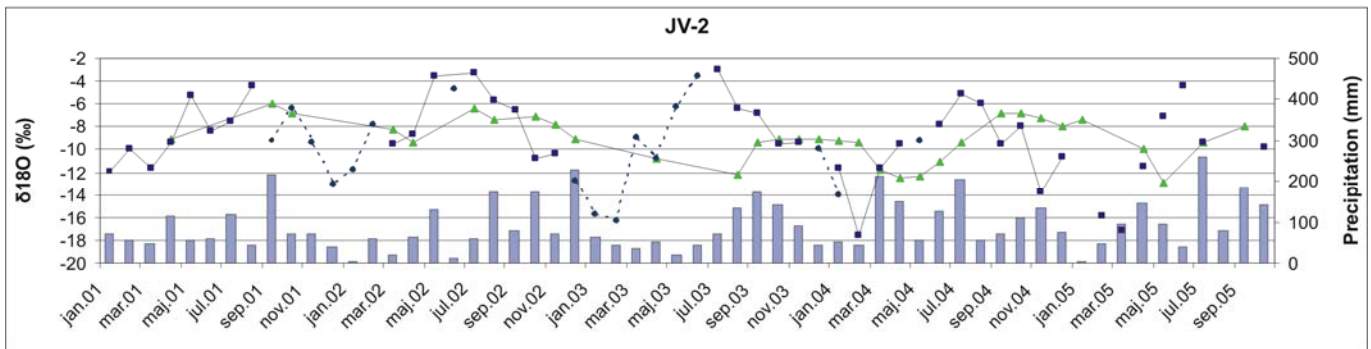
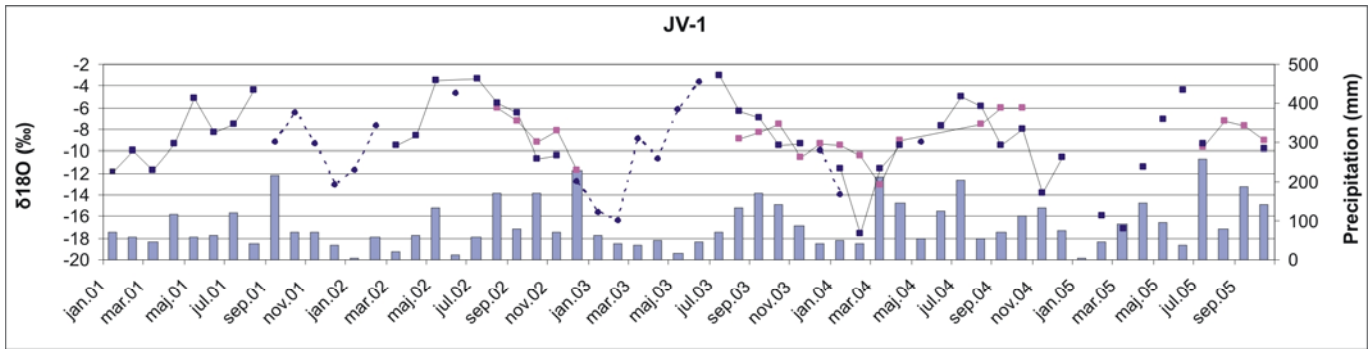
Conductivity (µS/cm)	JV-1	JV-2	JV-3	JV-4	JV-5	JV-6	JV-7	JV-8	JV-9	JV-10
16.6.2004		911	1150	923	797	827	877	809	894	940
19.10.2004	951	869	1075	1097	565	702	808	786	663	749
28.4.2005		613	714	721	531	690	789	649	550	670
27.7.2005	537	763		1067	808		1005	859	912	
Mean	744	789	980	952	675	740	870	776	755	786

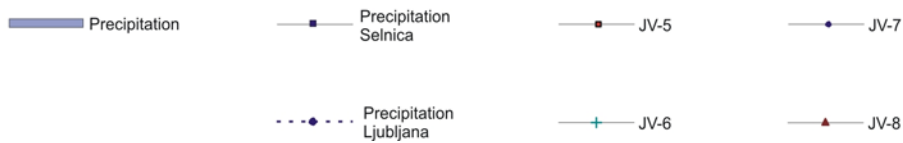
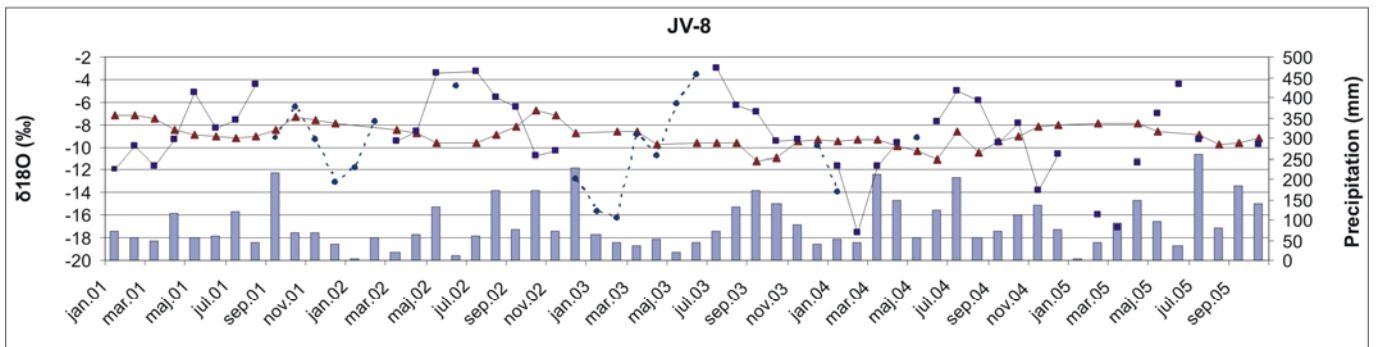
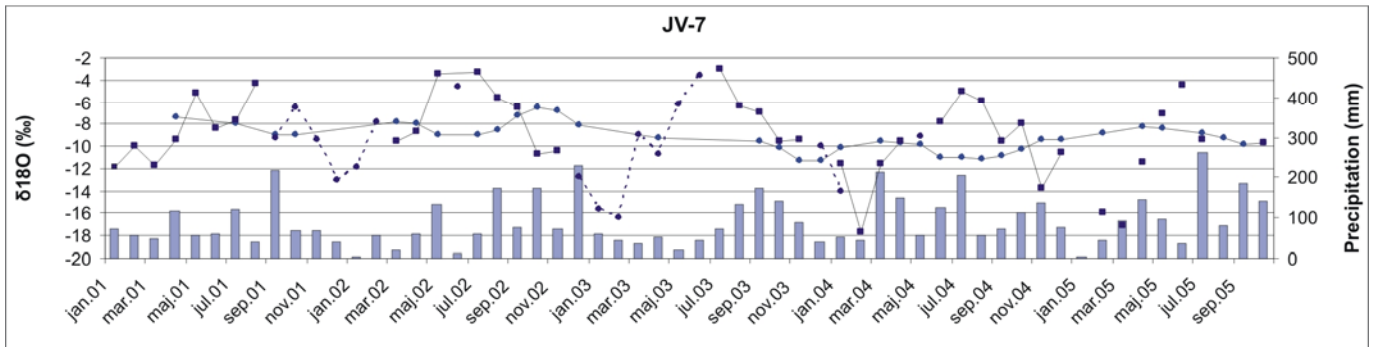
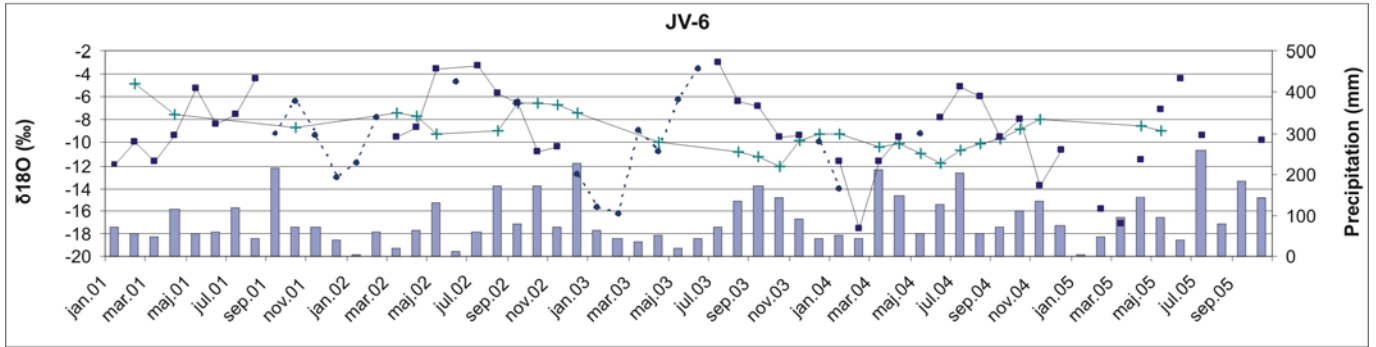
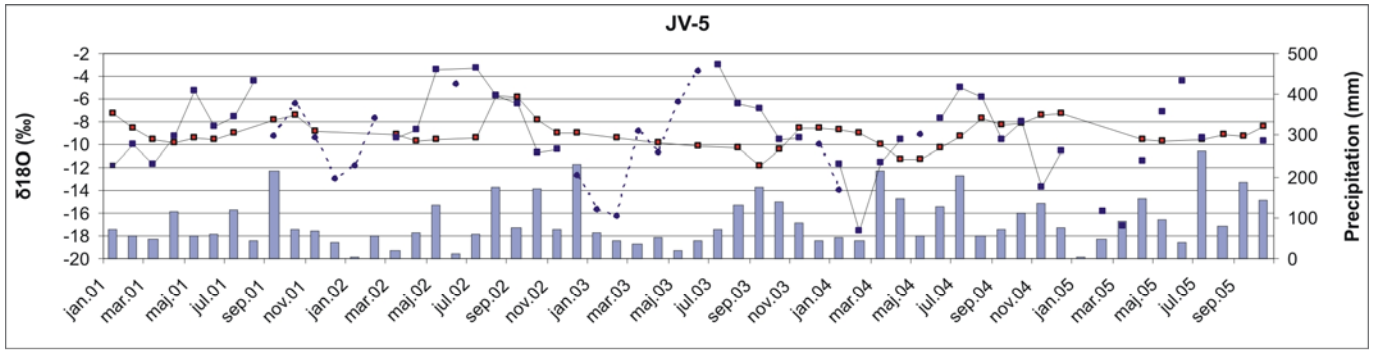
TOC (mg/l)	JV-1	JV-2	JV-3	JV-4	JV-5	JV-6	JV-7	JV-8	JV-9	JV-10
16.6.2004		12,4	18	14,3	7,7	12,1	13,6	8,8	10,2	11,2
25.8.2004		10	17,1	29,9	7,4	8,8	11,5	6,7	6,1	6,8
27.5.2005		86	47	100	63	37,5	70	35	40	72
10.8.2005		49	20	54	43	47	48	50	56	43
Mean		39,35	25,525	49,55	30,275	26,35	35,775	25,125	28,075	33,25

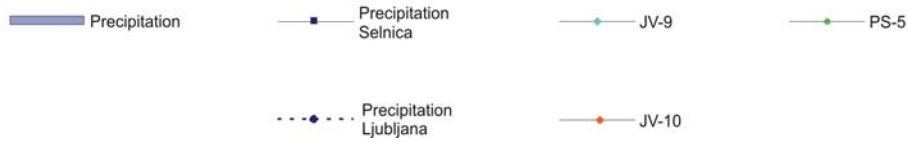
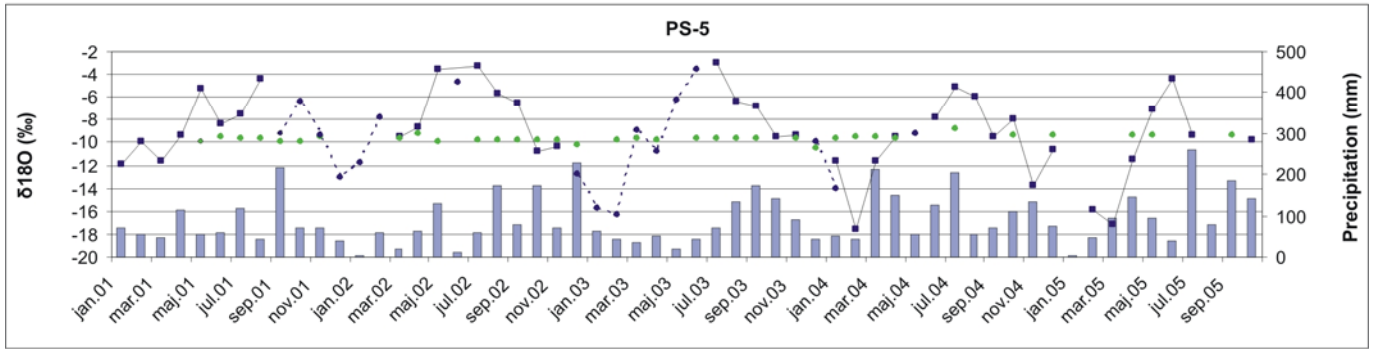
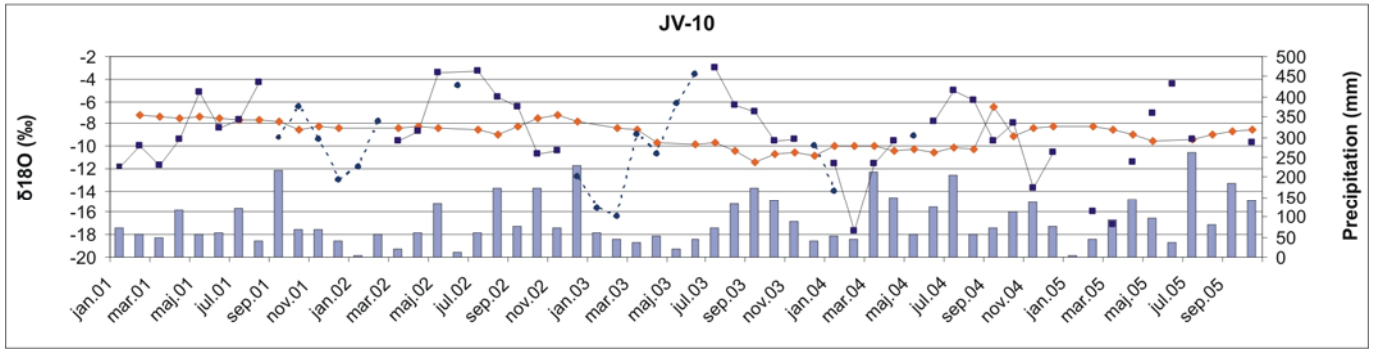
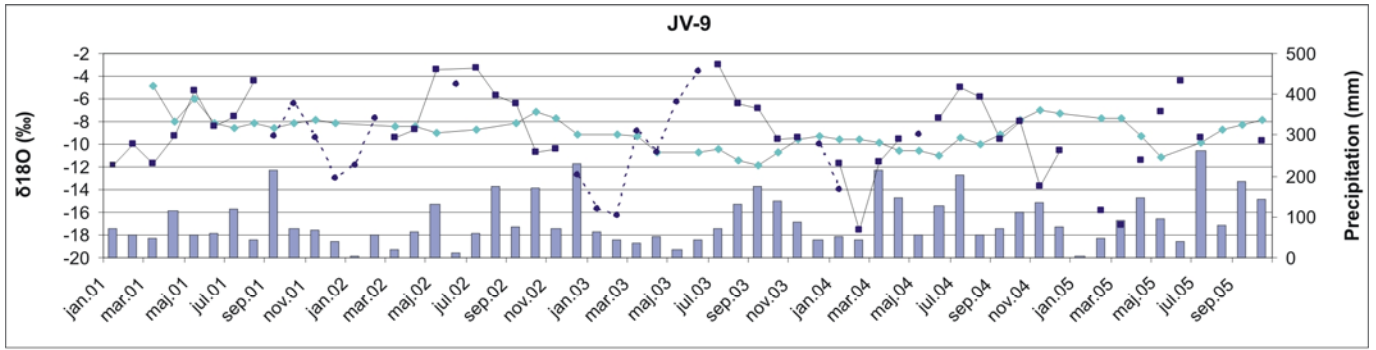
Annex I: δ²H and δ¹⁸O isotope composition data in the monthly sampled water

<i>datum</i>	<i>JV-1</i> 2H	<i>JV-1</i> 18O	<i>JV-2</i> 2H	<i>JV-2</i> 18O	<i>JV-3</i> 2H	<i>JV-3</i> 18O	<i>JV-4</i> 2H	<i>JV-4</i> 18O	<i>JV-5</i> 2H	<i>JV-5</i> 18O	<i>JV-6</i> 2H	<i>JV-6</i> 18O	<i>JV-7</i> 2H	<i>JV-7</i> 18O	<i>JV-8</i> 2H	<i>JV-8</i> 18O	<i>JV-9</i> 2H	<i>JV-9</i> 18O	<i>JV-10</i> 2H	<i>JV-10</i> 18O	<i>Padavine</i> 2H	<i>Padavine</i> 18O	<i>PS-5</i> 2H	<i>PS-5</i> 18O	
jan.2001									-50	-7,23					-49,5	-7,14					-83,9	-11,91			
feb.2001					-62,45	-9,08	-51,66	-6,5	-58,98	-8,51					-48,39	-7,17			-52,68	-7,16	-71,76	-9,99			
mar.2001					-68,7	-9,78	-69,73	-9,89	-66,1	-9,5					-52,14	-7,4			-54,09	-7,43	-82,45	-11,68			
apr.2001			-70,24	-9,05	-72,63	-9,84	-73	-9,73	-70,78	-9,83	-50,57	-7,49	-51,77	-7,35	-59,72	-8,47	-59,4	-7,98	-54,26	-7,47	-62,95	-9,34			
maj.2001					-69,97	-9,6	-70,61	-9,28	-69,28	-9,36					-63,74	-8,86			-53,5	-7,34	-32,03	-5,22	-68,72	-9,93	
jun.2001					-70,79	-9,41	-71,74	-9,67	-70,24	-9,52					-65,81	-9,03	-58,45	-8,12	-52,69	-7,45	-58,88	-8,36	-67,92	-9,52	
jul.2001					-57,11	-7,6	-68,47	-9,0	-65,14	-9,1			-55,58	-8,0	-66,89	-9,2	-61,71	-8,5	-53,31	-7,6	-51,6	-7,6	-66,37	-9,6	
avg.2001															-68,5	-9	-61,03	-8,16	-55,48	-7,66	-29,64	-4,39	-67,11	-9,64	
sep.2001			-43,5	-5,96	-49,52	-6,4	-54,29	-7,38	-58,45	-7,8			-65,15	-8,97	-64,28	-8,52	-64,45	-8,57	-56,36	-7,75			-68,42	-9,91	
okt.2001			-49,7	-6,82	-46,38	-6,64	-51,12	-7,09	-54,18	-7,43	-64,91	-8,61	-65,21	-8,94	-54,2	-7,34	-59,47	-8,11	-60,77	-8,52			-69,38	-9,89	
nov.2001															-55,10	-7,7	-58,75	-7,9	-60,36	-8,3			-68,98	-9,5	
dec.2001															-58,32	-7,91	-59,14	-8,15	-59,7	-8,41					
jan.2002																									
feb.2002																									
mar.2002			-59,08	-8,22			-58,45	-7,92	-64,31	-9,11	-54,59	-7,37	-57,39	-7,83	-61,25	-8,43	-59,5	-8,4	-62,08	-8,32	-68,12	-9,48	-68,46	-9,61	
apr.2002			-67,86	-9,32					-69,67	-9,78	-57,15	-7,68	-57,72	-7,9	-61,9	-8,83	-60,96	-8,47	-61,03	-8,26	-58,24	-8,65	-66,83	-9,25	
maj.2002							-67	-9,47	-68,13	-9,61	-65,56	-9,16	-64,8	-9,02	-69,27	-9,58	-62,84	-8,96	-59,18	-8,36	-25,43	-3,49	-68,46	-9,87	
jun.2002																									
jul.2002			-48,01	-6,46			-65,41	-9,3	-66,41	-9,4			-64	-9	-68,14	-9,61	-62,62	-8,77	-62,09	-8,56	-26,01	-3,29	-68,73	-9,82	
avg.2002	-42,4	-6,07	-54,62	-7,45	-53,31	-7,48	-64,72	-9,07	-40,79	-5,74	-63,42	-8,9	-61,08	-8,49	-62,48	-8,85			-63,66	-8,9	-39,98	-5,66	-68,26	-9,84	
sep.2002	-48,02	-7,2					-44,18	-6,34	-41,36	-5,81	-47,79	-6,56	-54,09	-7,19	-60,98	-8,21	-57,63	-8,11	-58,9	-8,22	-41,68	-6,48	-70,62	-9,84	
okt.2002	-65,1	-9,25	-49,2	-7,09			-45,58	-6,52	-53,56	-7,79	-46,55	-6,48	-46,63	-6,43	-46,38	-6,79	-51,86	-7,09	-52,25	-7,5	-76,78	-10,77	-68,68	-9,8	
nov.2002	-58,53	-8,1	-56,36	-7,8			-53,41	-7,5	-61,88	-9,0	-50,05	-6,7	-44,56	-6,8	-49,78	-7,2	-54,19	-7,7	-46,84	-7,3	-78,2	-10,4	-65,5	-9,8	
dec.2002	-79,16	-11,73	-64,46	-9,03	-67,76	-9,47	-61,93	-8,86	-63,24	-8,97	-51,75	-7,44	-57,88	-8,11	-63,05	-8,81	-66,35	-9,09	-55,73	-7,82			-71,67	-10,22	
jan.2003																									
feb.2003							-66,44	-9,73	-67,57	-9,39					-60,83	-8,65	-58,58	-9,19	-59,91	-8,44			-68,14	-9,73	
mar.2003															-62,05	-8,65	-66,70	-9,25	-60,40	-8,49			-68,42	-9,72	
apr.2003			-77,09	-10,73			-73,34	-10,27	-69,09	-9,88	-71,22	-9,94	-64,93	-9,22	-69,14	-9,79	-75,63	-10,73	-68,09	-9,68			-68,89	-9,79	
maj.2003																									
jun.2003							-85,70	-12,01	-70,80	-10,16					-68,20	-9,63	-75,34	-10,73	-70,02	-9,84			-68,28	-9,72	
jul.2003															-68,51	-9,62	-73,64	-10,48	-69,02	-9,73	-26,73	-3,00	-67,75	-9,64	
avg.2003	-61,70	-8,91	-90,75	-12,24	-69,90	-9,80	-87,77	-12,12	-73,24	-10,31	-77,41	-10,77			-69,03	-9,70	-83,31	-11,38	-76,06	-10,49	-45,72	-6,37	-67,95	-9,61	
sep.2003	-53,26	-8,26	-68,13	-9,38	-97,20	-12,76	-79,47	-11,07	-84,78	-11,81	-79,54	-11,17	-66,10	-9,59	-81,23	-11,28	-88,70	-11,92	-82,10	-11,44	-45,07	-6,88	-67,94	-9,62	
okt.2003	-54,18	-7,6	-66,42	-9,1			-63,26	-8,8	-77,44	-10,4	-89,19	-12,1	-73,13	-10,1	-78,74	-10,9	-79,05	-10,8	-78,78	-10,8	-67,6	-9,5			
nov.2003	-74,10	-10,5	-64,14	-9,0	-66,90	-9,2	-55,36	-8,2	-60,39	-8,6	-70,15	-9,8	-80,82	-11,3	-67,96	-9,5	-66,97	-9,5	-76,72	-10,6	-61,9	-9,4	-67,94	-9,6	
dec.2003	-65,14	-9,4	-63,96	-9,1	-62,95	-9,1	-63,22	-9,1	-59,09	-8,6	-64,58	-9,2	-82,46	-11,3	-64,39	-9,4	-64,80	-9,2	-72,73	-10,9			-65,10	-10,4	
jan.2004	-64,31	-9,46	-64,7	-9,24	-66,19	-9,34	-70,07	-10,01	-60,59	-8,7	-66,02	-9,24	-72,51	-10,14	-66,36	-9,44	-68,2	-9,56	-72,91	-10,04	-77,93	-11,65	-67,97	-9,59	
feb.2004	-70,40	-10,46	-65,72	-9,38			-69,73	-9,93	-63,88	-8,94					-67,51	-9,36	-68,64	-9,51	-73,62	-10,00	-135,37	-17,62	-66,64	-9,46	
mar.2004	-94,66	-13,0	-85,18	-11,8	-76,42	-10,8	-88,68	-12,4	-69,98	-10,1	-73,16	-10,4	-67,82	-9,5	-66,20	-9,4	-67,61	-9,9	-70,21	-10,0	-82,9	-11,6	-66,99	-9,6	
apr.2004	-68,55	-9,1	-90,41	-12,5					-76,15	-11,3	-69,61	-10,1	-65,47	-9,7	-68,40	-9,9	-72,38	-10,5	-63,40	-10,4	-70,45	-9,56	-67,18	-9,7	
maj.2004			-81,51	-12,37			-92,64	-13,3		-11,26	-71,73	-10,99	-68,92	-9,88	-71,18	-10,3		-10,55	-10,28						
jun.2004			91,92	-11,02	-45,32	-11,95	129,55	-10,83	402,96	-10,31	-62,12	-11,85	-76,88	-10,94	-68,42	-11,02	-66,41	-10,95	-62,99	-10,55	-57,41	-7,76			
jul.2004				-9,40			-10,27			-9,67					-10,70			-9,36		-10,17				-5,05	-8,82
avg.2004		-7,62						-9,32		-7,76		-10,05		-11,15		-10,53		-10,00		-10,21				-5,90	
sep.2004		-6,09		-6,75		-7,83		-8,32		-8,26		-9,63		-10,91		-9,45		-9,08		-6,54				-9,57	
okt.2004		-5,99		-6,80		-6,79		-6,77		-8,12		-8,82		-10,25		-9,06		-7,92		-9,05				-7,95	-9,41
nov.2004				-7,19		-7,00		-6,38		-7,45		-8,00		-9,37		-8,24		-6,96		-8,42				-13,78	
dec.2004				-8,01		-8,11		-6,86		-7,27				-9,35		-8,06		-7,32		-8,27				-10,58	-9,39
jan.2005				-7,44		-6,93																			
feb.2005							-6,72						-8,78			-7,975		-7,78		-8,19				-15,91	
mar.2005																		-7,72		-8,52	-124,97	-17,15			
apr.2005				-9,94		-8,99		-10,63		-9,59		-8,52		-8,27		-7,97		-9,30		-9,03	-81,44	-11,43	-63,53	-9,33	
maj.05				-12,93		-7,56		-12,82		-9,77		-8,93		-8,33		-8,64		-11,10		-9,60	-53,90	-7,11		-9,38	
jun.05																					-33,60	-4,41			
jul.05			-9,72		-9,34		-10,25		-10,54		-9,51			-8,78		-8,97		-9,85		-9,36				-9,38	
avg.05		-7,28				-9,08		-8,67		-9,17				-9,31		-9,83		-8,78		-8,92					
sep.05		-7,65		-7,89		-8,03		-8,33		-9,26				-9,78		-9,61		-8,33		-8,62				-9,31	
okt.05		-9,01				-8,18		-7,83		-8,38				-9,75		-9,25		-7,86		-8,52		-68,50	-9,76		

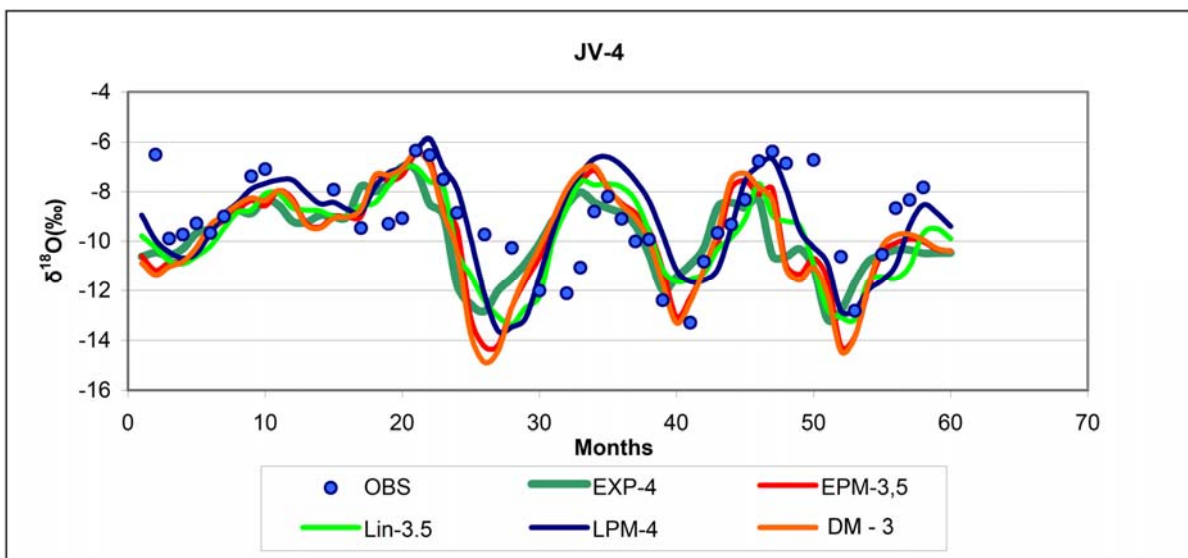
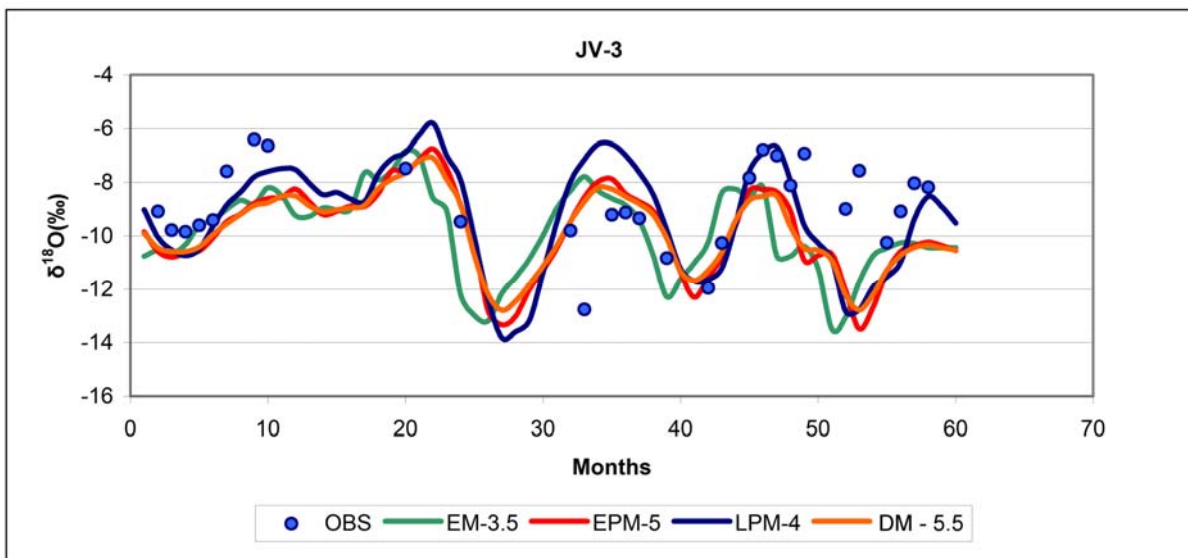
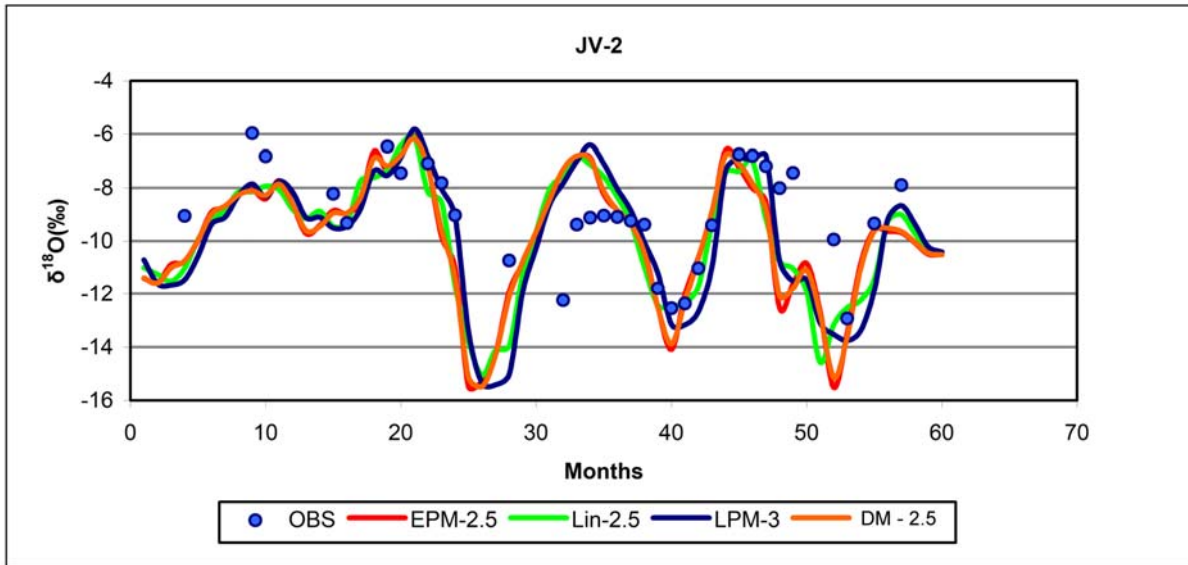
Annex J: $\delta^{18}\text{O}$ isotope composition plots of the monthly sampled water

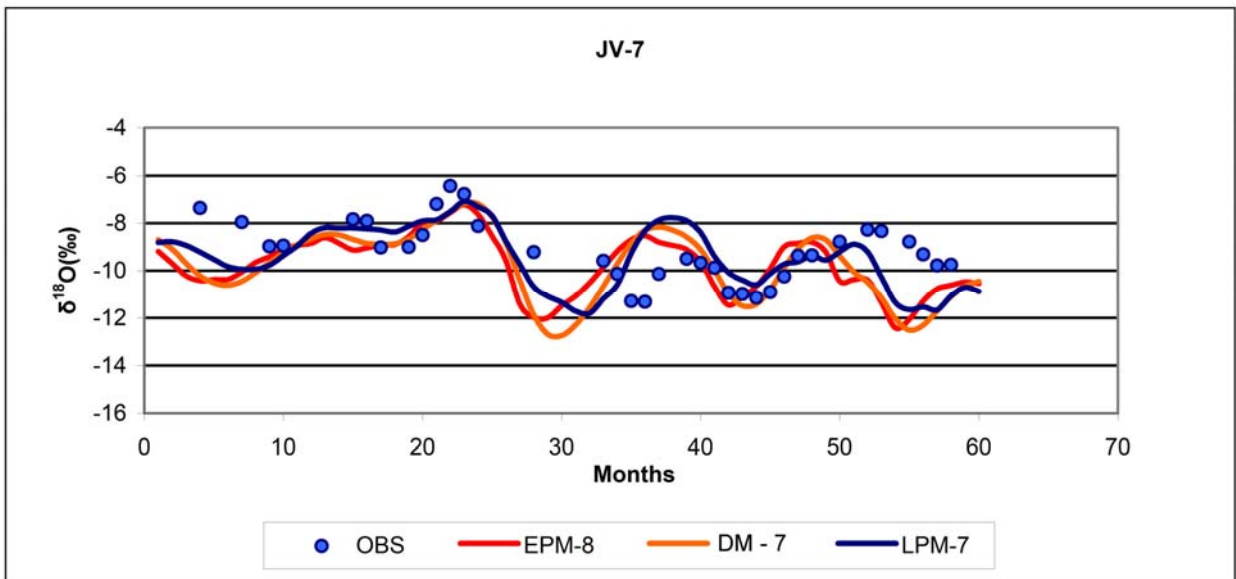
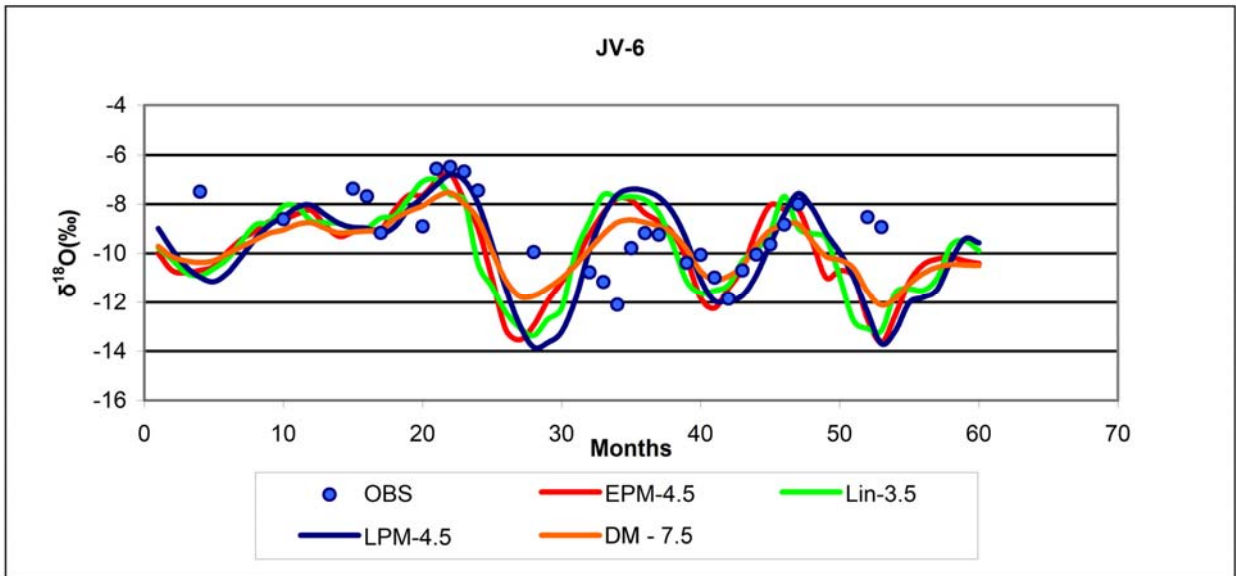
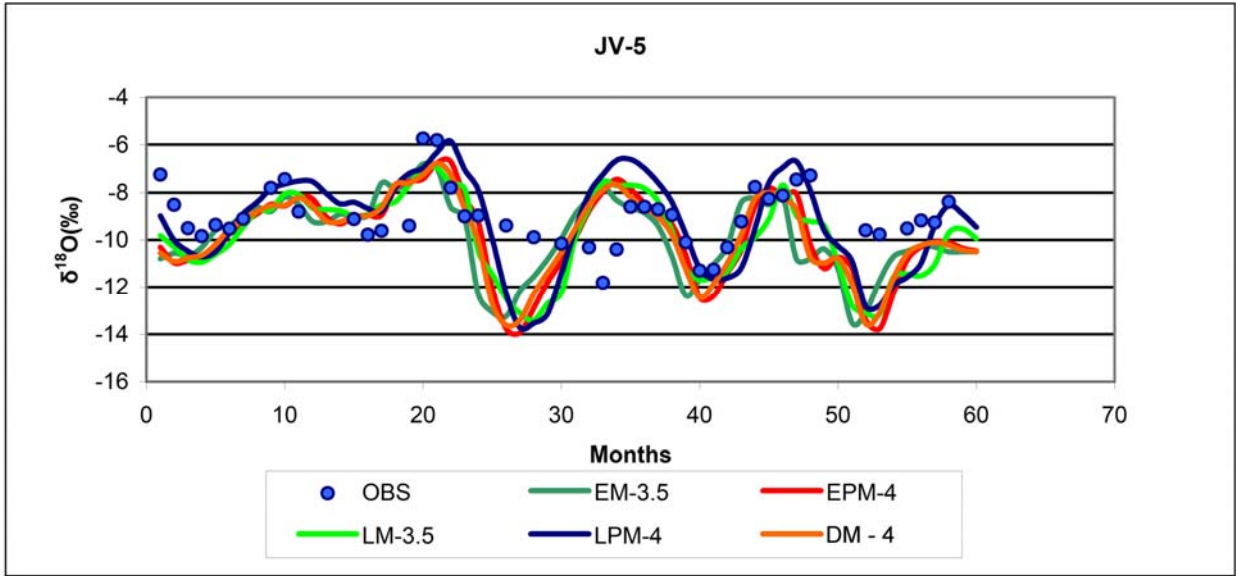


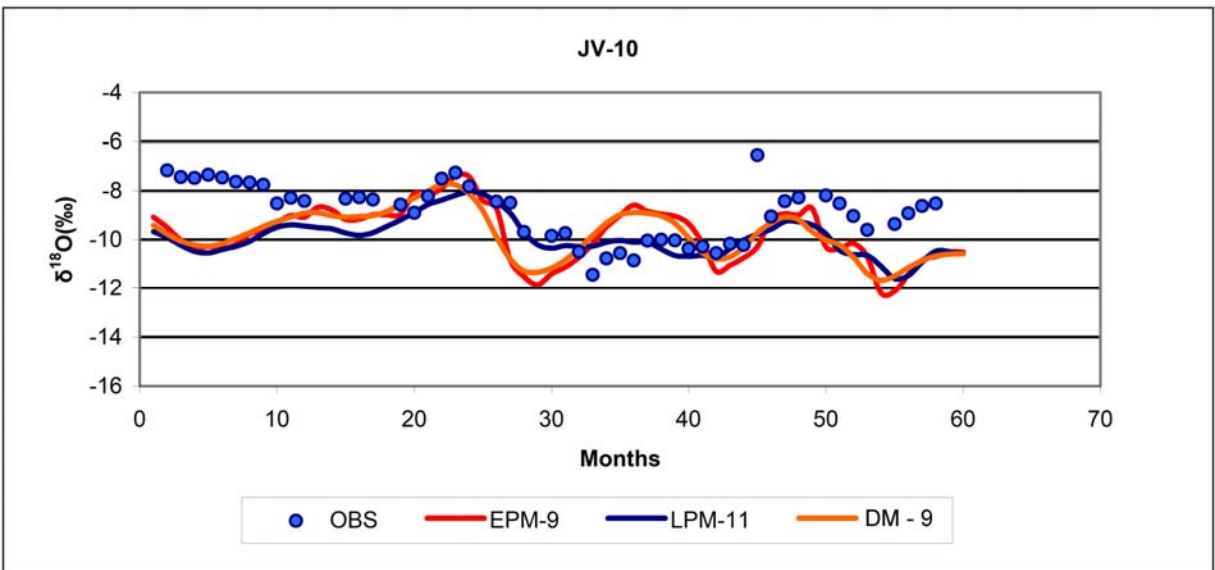
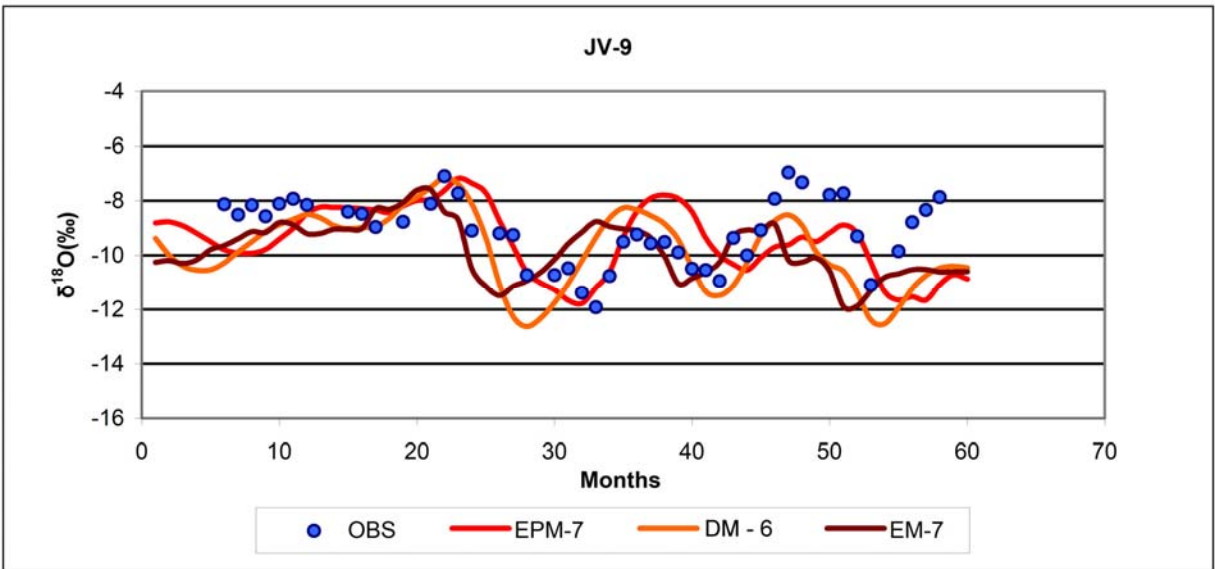
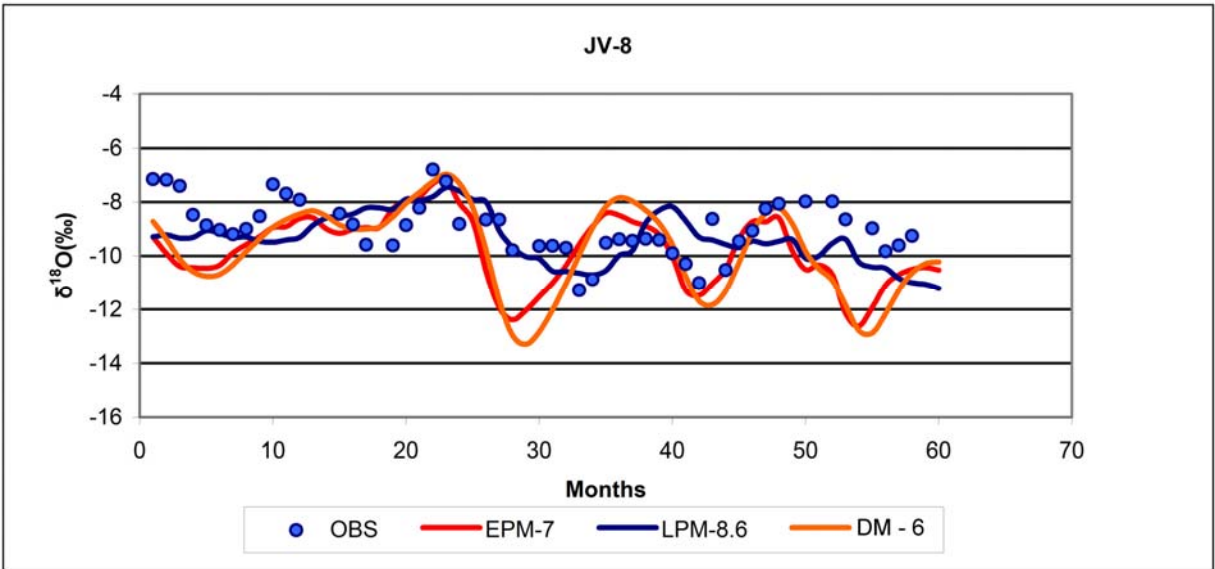




Annex K: Results of lumped parameter modelling

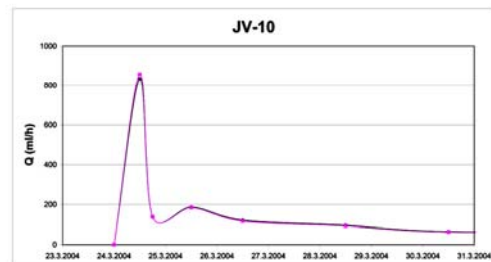
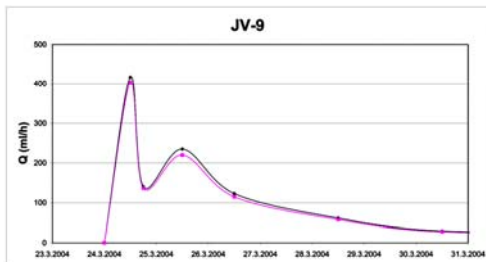
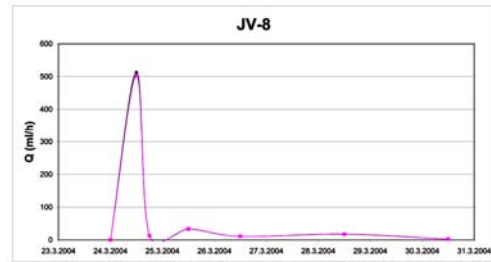
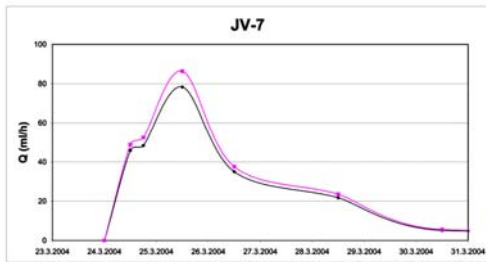
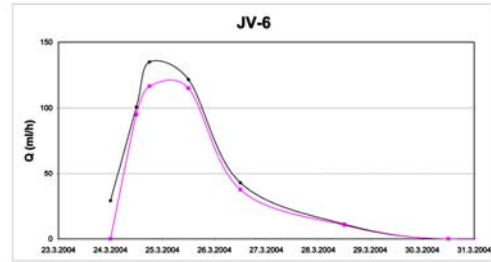
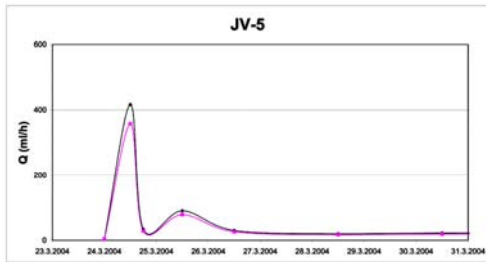
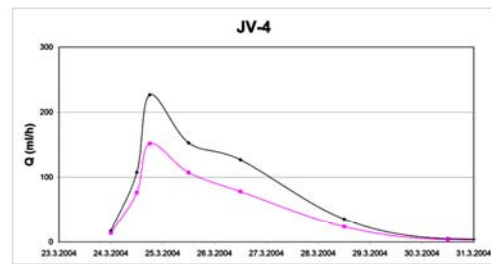
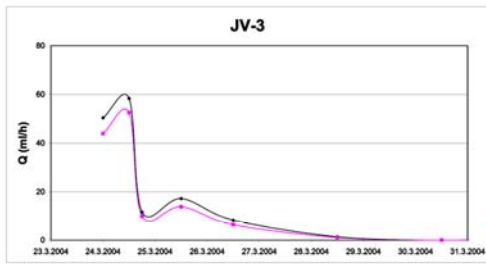
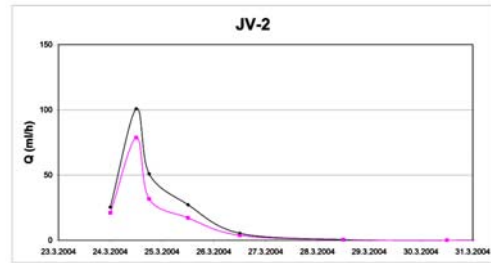
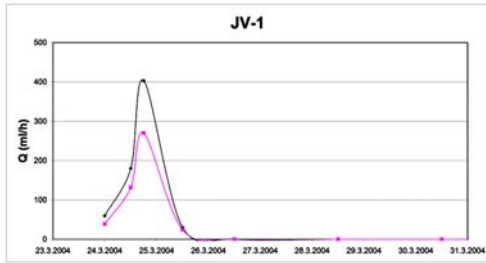






Annex L: Hydrograph separation

Modelled total discharge and old water discharge for the snowmelt event

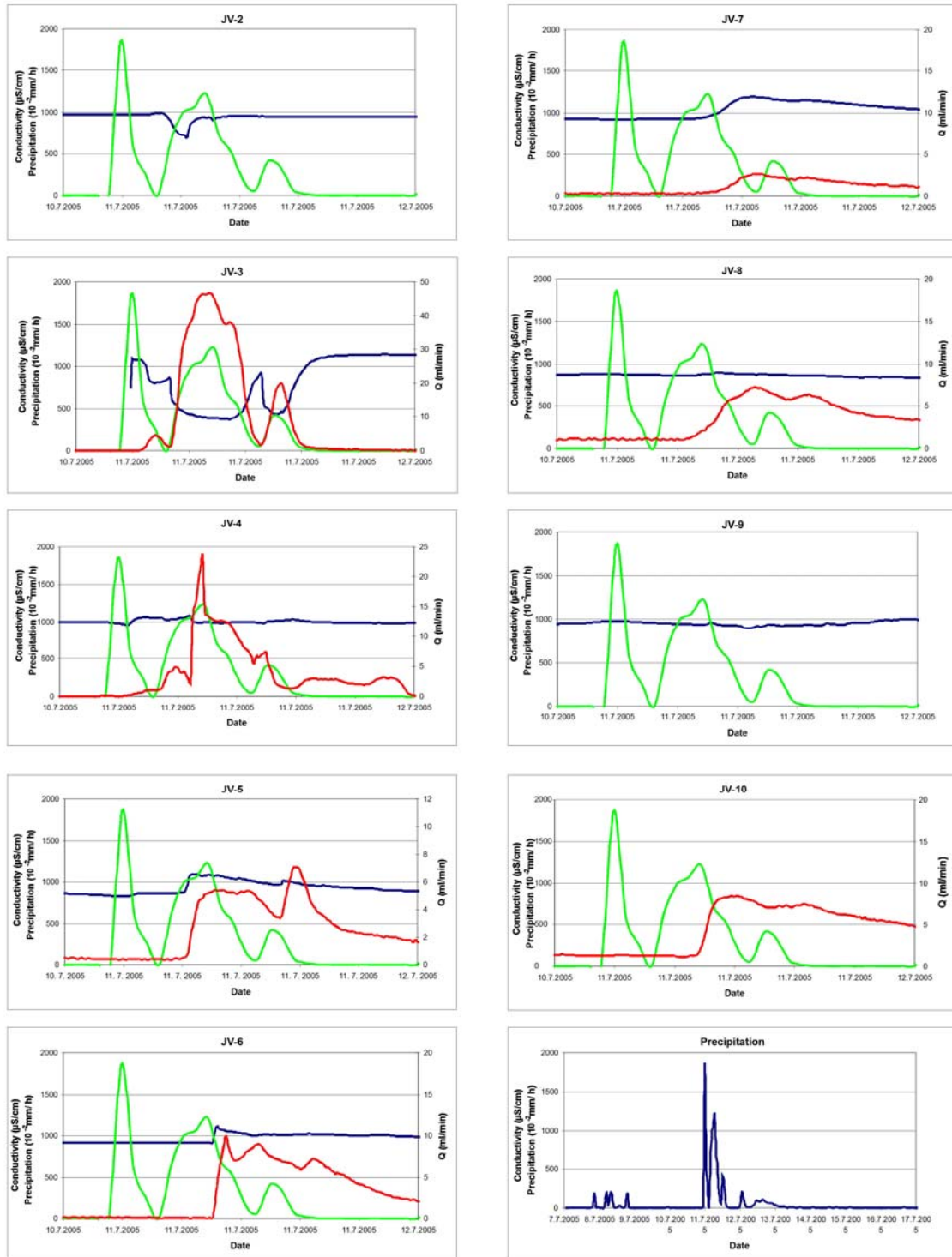


— old water

— total discharge

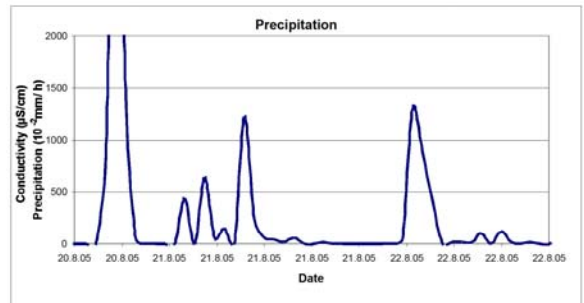
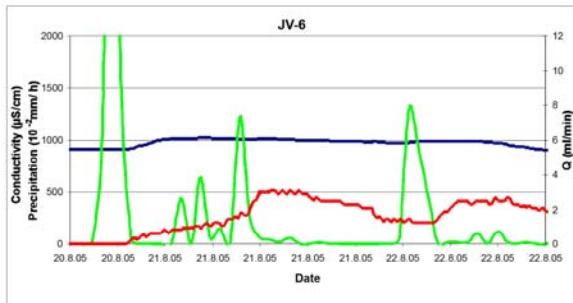
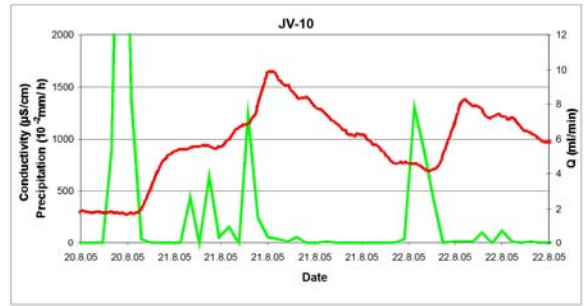
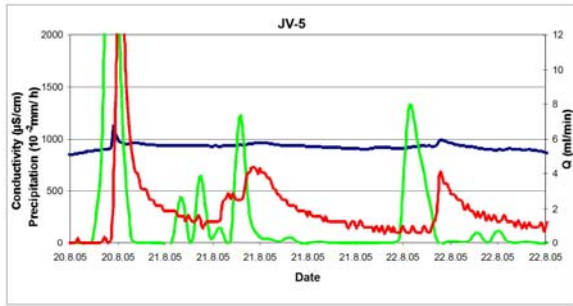
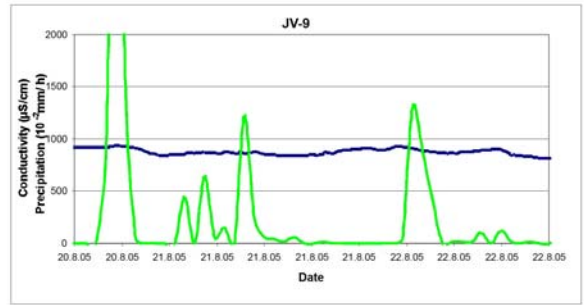
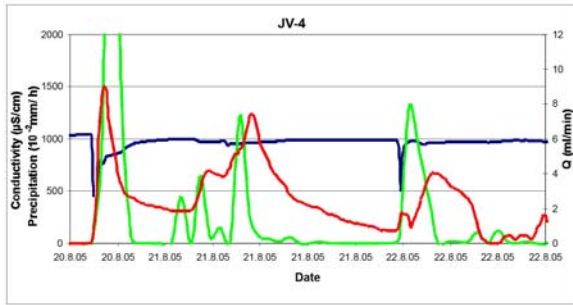
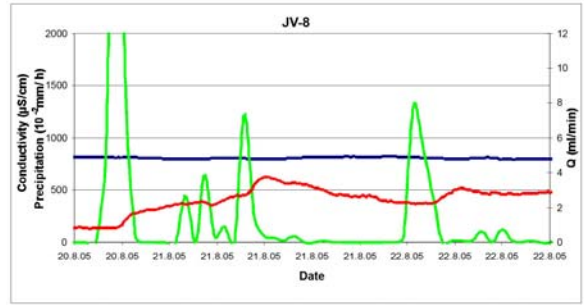
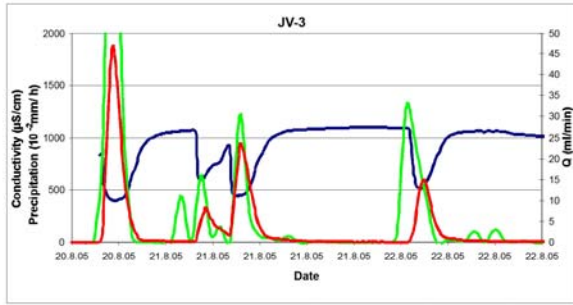
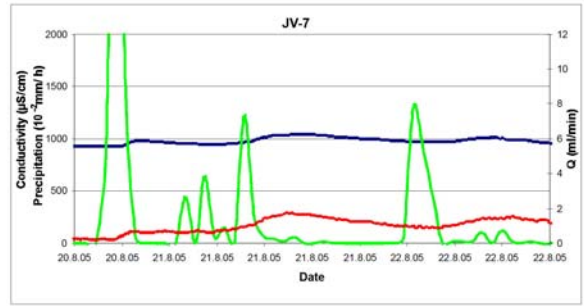
Annex M: Measurements of precipitations, conductivity and discharge for events in July and August 2005

Event 11.7.2005



— Conductivity — Precipitation — Q

Event 20.8.2005



— Conductivity
 — Precipitation
 — Q